Charles University
Second Faculty of Medicine

Doctoral Study Programme: Neurosciences

MUDr. Dmitry Tukmachev

BIOMATERIALS AND STEM CELLS IN SPINAL CORD INJURY
BIOMATERIÁLY A KMENOVÉ BUŇKY PŘI PORANĚNÍ MÍCHY

Dissertation Thesis

Supervisor: prof. MUDr. Eva Syková, DrSc.
Advisor: prof. MUDr. Zdeněk Klézl, CSc.

Prague, 2022

Prohlášení

Prohlašuji, že jsem disertační práci zpracoval samostatně a že jsem řádně uvedl a citoval všechny použité prameny a literaturu. Současně prohlašuji, že práce nebyla využita k získání jiného nebo stejného titulu.

Nesouhlasím s trvalým uložením elektronické verze mé práce v databázi systému meziuniverzitního projektu Theses.cz za účelem soustavné kontroly podobnosti kvalifikačních prací.

V Praze, 02.01.2022

Dmitry Tukmachev

ACKNOWLEDGEMENTS

First, my heartfelt thanks to supervisor prof. Eva Syková for her continuous contribution of time, ideas, support, and guidance to make my PhD productive and stimulating. I would like to thank Dr. Sarka Kubinová gratefully and sincerely who (have always guided me and were ready to discuss experimental design, while also providing invaluable help with their constructive suggestions through the duration of my thesis work. It has been an unforgettable experience for me during the design of all steps of in vitro and in vivo experiments. Without doubt, she is a brilliant, extraordinary, and an inspiringly friendly professor, great mentor, and a genuinely kind advisor. She is always ready to share her valuable intellectual property and expertise to help me complete my PhD. She encouraged me not only to grow as a normal researcher but also as an instructor and an independent thinker. It gives me great pleasure in expressing my thanks to all our lab colleagues for their support and helpful discussions and providing a stimulating and fun-filled environment in making this PhD thesis possible. My warmest thanks go to doc. Pavla Jendelová and prof. Zděnek Klézl for valuable quick help with administrative procedures for consumable and non-consumable items. I am very thankful to Mrs. Elisa Brann who is a wonderful secretary that always helped me to make appointments with prof. Zděnek Klézl for stimulating scientific discussions regarding my PhD work. Big thanks to prof. Stephen F. Badylack who provided me primary extracellular matrix various times for my experiment. Special appreciation goes to prof. Govindan Dyaniti for his valuable suggestions. I express my thanks to prof. Jan Štulík for his technical assistance during the initial stage of my PhD work. Special thanks go to Dr. Serhiy Forostyak and Dr. Yurij Petrenko for technical assistance during the early stage of my experimentation. My special thanks to all lab members of the Institute of Experimental Medicine ASER for their advice. They gave me lots of laughs and relaxing breaks whenever I needed them the most. Special thanks to Dr. Mariia Lunova and Dr. Oleg Lunov for giving the introduction in the fascinating field of confocal microscopy. Thanks, and appreciations go to doc. Vladimír Beneš for his peripheral mentioning during PhD work. Many thanks to doc. Ales Hejčl for a very nice collaboration and for the fantastic image analysis of histological data. I'm extremely grateful to doc. Ondřej Bradáč. The completion of my dissertation would not have been possible without the support and nurturing of doc. Ondřej Bradáč. I must again thank all my research friends for their friendship, support, and all the impressive moments. I also received great help from undergraduate research assistants working in our group.

Lastly, I would like to thank to my parents Irina and Alexej for their love and encouragement. I must specially thank my sweet wife Julia for her always being with me whenever I needed any support. She encourages me and allows me to work over the weekend and late nights. She supports me with her endless love, unlimited support and enormous encouragements that are always with me.

ABSTRACT

Spinal Cord Injury is a very serious trauma which can't be effectively cured at present time. The use of ECM hydrogels as supportive and stimulatory milieu and transplantation of stem cells represent promising approaches for SCI therapy. However, current treatments are limited by inefficient delivery of stem cells into the lesion site. Therefore, the aim of this study was the development of SCI treatment using ECM hydrogels and effective stem cell delivery system. The non-invasive magnetic system was designed and used to accumulate SPION-labelled stem cells at a specific site of a SCI lesion. Decellularized porcine SC and UB tissues, synthetic P(HEMA-AEMA) hydrogel with oriented porosity and modified hyaluronic acid HA-PH-RGD were transplanted into a spinal cord lesion of rats with or without stem cells, followed by histological analysis and gene expression analysis. All types of hydrogels integrated into the lesion and stimulated neovascularization and axonal ingrowth into the lesion. There was no significant difference in the tissue infiltration between the plain hydrogels and those seeded with stem cells. However, a subacute injection HA-PH-RGD/Fibrinogen combined with Wharton's jelly-derived human mesenchymal stem cells enhanced axonal ingrowth into the lesion. Significant down-regulation of genes related to immune response and inflammation was observed in hydrogels. Therefore, combined application of injectable hydrogel scaffolds and effective delivery of stem cells are the key factors for improving survival of cells in lesion site, inhibition of systematic inflammation and *in vivo*-like neural regeneration.

Keywords

Spinal cord injury, injectable extracellular matrix derived hydrogels, hyaluronic acid, mesenchymal stem cells, magnetic field, magnetic stem cell delivery, stem cell transplantation, neuroregeneration, neovascularization, axonal ingrowth.

ABSTRAKT

Poranění míchy (SCI) je velmi vážné trauma, které v současné době nelze účinně léčit. Použití hydrogelů na bázi ECM jako podpůrného a stimulačního prostředí a transplantace kmenových buněk představují slibné přístupy k léčbě SCI. Současné léčebné postupy však limituje neefektivní transport kmenových buněk do místa léze. Cílem této studie byl proto vývoj léčby SCI pomocí hydrogelů na bázi ECM a účinného systému pro transport kmenových buněk. Byl navržen neinvazivní magnetický systém, který byl následně použit k akumulaci kmenových buněk značených SPION na specifickém místě léze SCI. Decelularizované tkáně prasečí SC a UB syntetický hydrogel P(HEMA-AEMA) s orientovanou porozitou a modifikované HA-PH-RGD kyseliny hyaluronové byly transplantovány do míšní léze potkanů, a to buď s kmenovými buňkami nebo bez kmenových buněk. Následovala histologická analýza a analýza genové exprese. Všechny typy hydrogelů se integrovaly do léze a stimulovaly neovaskularizaci a axonální vrůstání do léze. Nebyl zjištěn žádný významný rozdíl v infiltraci tkáně mezi prostými hydrogely a hydrogely s nasazenými kmenovými buňkami. Subakutní injekce HA-PH-RGD/fibrinogenu v kombinaci s lidskými mezenchymálními kmenovými buňkami získanými z Whartonova želé však zesílila axonální vrůstání do léze. V hydrogelech byla pozorována významná down-regulace genů spojených s imunitní odpovědí a zánětem. Kombinovaná aplikace injikovatelných hydrogelových skafoldů a technika neinvazivního magnetického transportu jsou proto klíčovými faktory pro zlepšení přežití buněk v místě léze, inhibici systematického zánětu a *in vivo* podobnou neuroregeneraci.

Klíčová slova

Poranění míchy, injikovatelné hydrogely na bázi extracelulární matrix, kyselina hyaluronová, mezenchymální kmenové buňky, magnetické pole, magnetický transport kmenových buněk, transplantace kmenových buněk, neuroregenerace, neovaskularizace, axonální vrůstání.

LIST OF ABBREVIATIONS

3D	three-dimensional
AEMA	aminoethylmethacrylate
Akt1	serine/threonine-protein kinase 1
Arg1	arginase 1
ATP	adenosine triphosphate
ASIA	American Spinal Injury Association
B-ECM	brain derived extracellular matrix
BBB	blood-brain barrier
BBB test	Basso-Beattie-Bresnahan open field locomotor test
BDNF	brain-derived neurotrophic factor
bFGF	basic fibroblast growth factor
Casp3	caspase 3 (gene)
Ccl3 / MIP -1α	macrophage inflammatory protein-1 alpha
Ccl5 / RANTES	chemokine (C-C motif) ligand 5
CNS	central nervous system
CM	conditioned medium
cPD	cumulative population doubling
CSPG	chondroitin sulphate proteoglican
CXCR4	chemokine (C-X-C motif) receptor type 4
CXCL10 / IP-10	chemokine (C-X-C motif) type 10
cDNA	complementary deoxyribonucleic acid
DRG	dorsal root ganglion
dsDNA	double-strain DNA
ECM	extracellular matrix
EDMA	ethylene dimethacrylate
EDTA	ethylenediaminetetraacetic acid
EGF	epidermal growth factor
FACS	fluorescence activated cell sorting
FBS	fetal bovine serum
G-CSF	granulocyte-colony stimulating factor
GAP43	growth associated protein 43
Gapdh	glyceraldehyde 3-phosphate dehydrogenase (gene)

GDNF	glial cell line-derived neurotrophic factor
GFAP	glial fibrillary acidic protein
GGF	glial growth factor
GlcA	glucuronic acid
GM-CSF	granulocyte-macrophage colony-stimulating factor
H&E	haematoxylin-eosin
HA	hyaluronic acid
hASC	human adipose tissue-derived stem cells
hBMNC	human bone marrow mononuclear cell fraction
hBM-MSCs	human bone marrow mesenchymal stem cells
HEMA	2-hydroxyethyl methacrylate
HGF	hepatocyte growth factor
hMSCs	human mesenchymal stem cells
HuCNS-SC	fetal brain-derived human central nervous system stem cell
hWJ-MSCs	human Wharton´s jelly mesenchymal stem cells
ChABC	chondroitinase ABC
i.m.	intramuscular
i.p.	intraperitoneal
i.t.	intrathecal
i.v.	intravenous
Ig	Immunoglobulin
IDO	indoleamine 2,3-dioxygenase
ICAM-1/CD54	intercellular adhesion molecule 1
IFNγ	interferon gamma
IGF-1	insulin-like growth factor 1
IL	interleukin
IP-10/CXCL10	interferon gamma-induced protein 10
iPSCs	induced pluripotent stem cells
Irf5	interferon regulatory factor 5 (gene)
LC-MS	liquid chromatography–mass spectrometry
LIF	leukemia inhibitory factor
M-CSF	macrophage colony-stimulating factor
MAI	myelin-associated inhibitors
MAG	myelin-associated glycoprotein

MAP2	microtubule-associated protein 2
MCP1	monocyte chemoattractant protein-1
MIP-1α	macrophage inflammatory protein 1α
MPSS	methylprednisolone
Mrc1	mannose receptor C-type 1 (gene)
mRNA	messenger ribonucleic acid
MTCO2	human cytochrome C oxidase subunit II
N/A	not applicable
NCAM	neural-cell adhesion molecule
NCSC	neural crest-derived stem cell
Nestin	type VI intermediate filament (IF) protein
NF 70	neurofilament 70
NF 160	neurofilament 160
NGF	nerve growth factor receptor (NGFR)
CD271/p75	nerve growth factor receptor NgR (Nogo-66 receptor)
NCS	neural stem cells
NO	nitric oxide
Nos2	inducible nitric oxide synthase 2 (gene)
Nrp-1	neuropilin 1
NT3/Sort1	neurotrophin type 3
OEC	olfactory ensheating cell
OPC	oligodendrocyte precursor cell p75
P/S	penicillin/streptomycin
PAN/PVC	polyacrylonitrile/polyvinylchloride
PBS	phosphate-buffered saline
PCL	poly (ε-caprolactone)
PD	population doubling
PEDOT	poly (3, 4-ethylendioxythiopene)
PEG	polyethylene glycol
PGA	poly (glycolic acid)
PGE2	prostaglandin E2
PHEMA	poly(2-hydroxyethylmethacrylate)
PHPMA	poly[N-(2-hydroxypropyl) methacrylate]
PlGF	placental growth factor

PLA	poly (lactic acid)
PLCL	poly (lactic-co-caprolactone)
PLGA	poly (lactic-co-glycolic acid)
PNN	perineural net
Ptgs2	prostaglandin-endoperoxide synthase 2 (gene)
PTFE	poly (tetrafluoroethylene)
PVA	polyvinyl alcohol
PVDF	polyvinylidene fluoride
qRT-PCR	quantitative real-time polymerase chain reaction
RANTES/Ccl5	regulated on activation, normal T-cell expressed and secreted
RECA	anti-endothelial cell antibody
RGD	arginine-glycine-aspartic acid
ROS	Reactive Oxygen Species
s.c.	Subcutaneous
SC-ECM	Spinal Cord-derived Extracellular Matrix
SCF	Stem Cell Factor
SCI	Spinal Cord Injury
SDF-1	Stromal Cell-derived Factor 1
sDNA	single-strain DNA
SEM	Scanning Electron Microscope
SIKVAV	Ser-Ile-Lys-Val-Ala-Val
SVF	Stromal Vascular Fraction
TCP	tissue culture polystyrene
TE	tissue engineering
TNF-α	tumor necrosis factor Alpha
Tn-R	tenascin-R
TGF-α(β)	transforming growth factor-alpha(beta)
TrkA (B, C)	tropomyosin related kinase A (B, C)
UB-ECM	urinary bladder extracellular matrix
UC-ECM	umbilical cord extracellular matrix
VCAM-1 / CD106	vascular cell adhesion molecule
VEGF-A	vascular endothelial growth factor A
Vimentin	type III intermediate filament
Wnt	Wingless/int-1 signaling pathways

CONTENTS

1. INTRODUCTION 14
1.1. Epidemiology of spinal cord injury 16
1.2. Pathology of spinal cord injury 17
1.3. Molecular factors controlling neuroregeneration in spinal cord injury 31
1.4. Stem cell therapy technologies in the treatment of spinal cord injury 35
1.5. Magnetic stem cell delivery strategy for spinal cord injury therapy 47
1.6. Biomaterials as scaffolds for spinal cord injury repair 50
2. AIMS AND HYPOTHESES 63
3. MATERIALS AND METHODS 64
3.1. Hydrogels preparation 64
3.1.1. Preparation of porcine urinary bladder and spinal cord extracellular matrix hydrogels 64
3.1.2. Preparation of poly(2-hydroxyethyl methacrylate-*co*-2-aminoethylmethacrylate) hydrogel with oriented porosity 64
3.1.2.1. Immobilization of HS-CGGASIKVAVS-OH on the P(HEMA-AEMA) discs 66
3.1.2.2. Characterization of P(HEMA-AEMA) discs 67
3.1.3. Hyaluronan RGD modification 67
3.1.3.1. Chemical characterization of HA-PHA-RGD derivative 68
3.1.3.2. HA-PH-RGD hydrogel preparation and crosslinking 68
3.1.3.3. HA-PH-RGD hydrogel characterization 68
3.2. Stem cell cultures 69
3.2.1. GFP-positive rat mesenchymal stem cells preparation 69
3.2.2. GFP-positive rat MSCs labelling with SPIONs 69
3.2.3. Seeding GFP-positive rat MSCs on HEMA hydrogel 70
3.2.4. Human Wharton's jelly mesenchymal stem cells culture preparation 70
3.2.5. Seeding hWJ-MSCs on porcine SC- and UB-ECM hydrogels 71
3.2.6. Seeding hWJ-MSCs on HA-PH-RGD hydrogel 72
3.2.7. *In vitro* hWJ-MSCs growth and viability 72
3.2.8. Rat dorsal root ganglia explant culture preparation 72
3.3. Animal experiments 73
3.3.1. Animal handling and surgery 73
3.3.2. Balloon-induced compression lesion model 73
3.3.3. SPION-labelled GFP-MSCs transplantation 74
3.3.4. Spinal cord transection 76
3.3.5. HEMA hydrogel application into the SCI lesion 76

3.3.6. Spinal cord hemisection ... 77
3.3.7. UB- and SC-ECM hydrogel application into the SCI lesion ... 77
3.3.8. HA-PH-RGD hydrogel application into the SCI lesion ... 78
3.3.9. Analysis of locomotor functions ... 78
3.4. Tissue processing and histology ... 79
3.4.1. Spinal cord lesion processing and histology ... 79
3.4.2. SPION-labelled GFP+ MSCs visualization and quantification in rat spinal cord lesion ... 79
3.4.3. Immunohistochemical staining ... 80
3.4.4. HEMA hydrogel retrograde staining ... 81
3.4.5. Axonal and blood vessel ingrowth analysis ... 81
3.5. Gene expression analysis ... 82
3.6. Mathematical modeling ... 83
3.7. Statistical evaluations ... 84
4. RESULTS AND DISCUSSION ... 85
4.1. ANEFFECTIVE STRATEGY OF MAGNETIC STEM CELL DELIVERY FOR SPINAL CORD INJURY THERAPY ... 85
4.1.1. Design of magnetic system with trapping area ... 85
4.1.2. Evaluation of SPION-labelled MSCs distribution under magnetic field ... 85
4.1.3. Discussion ... 90
4.2. INJECTABLE EXTRACELLULAR MATRIX HYDROGELS FOR SPINAL CORD INJURY REPAIR ... 93
4.2.1. Porcine spinal cord and urinary bladder extracellular matrix hydrogels ... 93
4.2.1.1. Biocompatibility and bioadhesive properties of SC-ECM and UB-ECM hydrogels for hWJ-MSCs ... 93
4.2.1.2. Neurotrophic properties of SC-ECM and UB-ECM hydrogels ... 95
4.2.1.3. Histological evaluation of injected UB-ECM and SC-ECM hydrogels ... 97
4.2.1.4. Histological evaluation of implanted UB-ECM and SC-ECM hydrogels combined with hWJ-MSCs ... 102
4.2.1.5. Gene expression induced by UB-ECM and SC-ECM hydrogels ... 102
4.2.1.6. Evaluation of hind limb motor functions ... 106
4.2.1.7. Discussion ... 106
4.2.2. DYNAMICS OF TISSUE INGROWTH INTO SIKVAV-MODIFIED HIGHLY SUPERPOROUS PHEMA SCAFFOLDS WITH ORIENTED PORES AFTER BRIDGING A SPINAL CORD TRANSECTION ... 110
4.2.2.1. P(HEMA-AEMA) hydrogel scaffold production and characterization ... 110
4.2.2.2. Bridging the post-traumatic cavity with P(HEMA-AEMA) hydrogel ... 111
4.2.2.3. Connective tissue infiltration in P(HEMA-AEMA) hydrogel scaffold ... 112
4.2.2.4. Dynamics of axonal infiltration in P(HEMA-AEMA) hydrogel ... 114

4.2.2.5. Dynamics of blood vessels ingrowth into P(HEMA-AEMA) hydrogel .. 115
4.2.2.6. Long-term effects of implanted MSCs-seeded P(HEMA-AEMA) scaffold hydrogels 116
4.2.2.7. Discussion 116
4.2.3. INJECTABLE HYDROXYPHENYL DERIVATIVE OF HYALURONIC ACID HYDROGEL MODIFIED WITH RGD AS A SCAFFOLD FOR SPINAL CORD INJURY REPAIR 120
4.2.3.1. Characterization of HA-PH-RGD hydrogel 120
4.2.3.2. hWJ-MSCs proliferation *in vitro* on HA-PH and HA-PH-RGD hydrogels 121
4.2.3.3. Evaluation of ingrowth of neurofilaments and blood vessels into HA-PH-RGD hydrogels in acute SCI lesions 122
4.2.3.4. Histological evaluation of HA-PH-RGD hydrogels in subacute SCI lesion 124
4.2.3.5. Gene expression analysis in subacute SCI lesions 128
4.2.3.6. Analysis of locomotor functions in subacute SCI lesions 129
4.2.3.7. Discussion 130
5. GENERAL DISCUSSION 134
6. CONCLUSIONS 139
7. SUMMARY 140
8. LITERATURE REFERENCES 142
9. LIST OF AUTHOR'S PUBLICATIONS 165

1. INTRODUCTION

Spinal Cord Injury (SCI) is a very serious trauma that leads to extensive damage, disability and mortality and presents the global ongoing neurological problem which greatly hampers the financial and social status of patients and caregivers alike. It is estimated that 17,500 traumatic spinal cord injury cases occur each year in USA alone while approximately 285,000 people are living with chronic SCI (Alabama at Birmingham, 2017). Reports indicate that physical trauma due to traffic accidents (50%), falls (22%), violence (16%) and sports injuries (12%) lead to ~90% of the SCI cases. Most victims of SCI (80%) are young males (aged 15-35). In over half of cases, the patients suffer from partial or complete paralysis of the arms, legs and torso, a condition called tetraplegia. Others may be paraplegic wherein there is partial or total paralysis of the legs. Individuals suffering from SCI not only face grave physical impairment, but also have other equally problematic vocational setbacks. Moreover, as compared to individuals without SCI, adults suffering from traumatic SCI face a greater risk of developing mental health ailments.

In addition to motor and sensory impairment, SCI patients also often suffer from chronic pain, spasticity, respiratory and cardiovascular alterations, neurogenic bowel and bladder disorders, and integumentary complications, affecting overall quality of life and life expectancy. Patients suffering from high SCI injuries and those within 1 year of injury have the highest risk of death.

Although the past decade has ushered notable developments in clinically addressing SCI, research exploring possible treatments for the neurological rehabilitation of the patients has not gained much traction. Conventional treatments of SCI have not been efficient enough in healing complex and deep injuries. Therefore, prevention is considered the best medicine for this condition.

However, discoveries of the past decades as well as developing of new promising technologies give many SCI patients new hope for at least facilitating their condition. Using self-regenerating human stem cells as a treatment seems like a promising solution. Stem cells are unspecialized cells that have the ability to differentiate into any cell types. They can differentiate into neurons, replacing damaged cells, or secrete many factors to accelerate growth of the existing cells (Mezey E. et al., 2000b; Tropel P. et al., 2006; Park H.-W.et al., 2012; Taran R. et al., 2014; Ullah I. et al., 2015). In contrast to current treatment strategy, stem cell therapy is considered more promising and may significantly increase the chances for recovery.

However, application of stem cells is limited by inefficient delivery strategies for targeting cells into the injured tissue. The delivery technique of stem cells is a major factor determining the success of the transplantation. This is largely the reason behind the limited use of these therapies at present. It not only has to be efficient and minimally invasive but it should also ensure proper retention and longevity of the cells for *in vivo*-like regeneration (Pluchino A. et al., 2003, Wu S. et al, 2002, Bakshi M. et al., 2004). Treating of SCI with stem cell-based therapies using magnetic nanoparticles for assisted magnetic targeting is an innovative approach which allows to solve these problems.

Highly effective minimally invasive cell transplantation for tissue repair can be achieved through magnetic targeting, using magnetic fields to detect and translocate magnetically labelled cells. Transplantation of bone marrow cells, mesenchymal stem cells (MSCs), neural progenitor cells, blood CD133-positive cells and induced pluripotent stem cells have been successfully performed with this technique (Landazuri N. et al., 2012, Vandergriff A.C. et al., 2014, Cheng K. et al., 2014). Even bone, cartilage, skeletal muscle, and spinal cord regeneration have been successful because this method enables better aggregation and superior adhesion of the cells introduced (Pislaru S.V. et al., 2006, Polyak B. et al., 2008, Riegler J. et al., 2013, Panseri S. et al., 2013, Kamei G. et al., 2013, Yanai A. et al., 2012).

One of the most promising strategies may involve using implants based on natural or synthetic polymers with sufficient biocompatibility and ability to reconstruct the damaged area of the spinal cord. Developed scaffold or matrix materials are made in the form of hydrogels, lyophilized sponges, fibers, powders, as well as combinations of these forms. Matrix implants serve as scaffold, to fill the defect and may have trophic functions supporting the viability of implanted stem cells (Favia P. et al., 2006; Yoshil S. et al., 2009; Wang W.H. et al., 2010). However, it should be noted that none of the huge number of natural and artificial matrix materials show promise as components for spinal cord injury treatment or fully satisfies all the requirements. Among the significant disadvantages of synthetic materials, it is the fact that without additional modifications, they cannot support adhesion, growth of cells and regeneration of axons since they do not carry the appropriate ligands for cell receptors. At present time the most promising direction in the development of treatments of injuries of the nervous system such as spinal cord is to create a micro structured matrix composite implant having a three-dimensional pattern of signaling molecules that regulate cell proliferation and differentiation, stimulate adhesion and cell migration, axonal growth, and recovery of brain function.

A plethora of available scientific literature describes the use of MSCs for treating traumatic SCI (Sykova E. et al., 2021). Using animal models, designed for developing rehabilitative training as well as cellular, molecular, and combinatorial therapies for SCI has yielded some desirable results (Sykova E. et al., 2021). However, more research to verify the safety and efficacy of these treatments in human SCI cases is yet to be performed.

Therefore, the aim of our studies was developing new techniques for stem cell delivery with application of injectable extracellular matrix hydrogels as milieu for neuroregeneration *in vivo*.

1.1. Epidemiology of spinal cord injury

Currently in the European Union there are at least 330 000 people living with spinal cord injuries and about 11 000 new cases every year (Onose G. et al., 2009). According to the National Spinal Cord Injury Statistical Center (NSCISC), the number of people in the United States who were alive in 2010 and have SCI has been estimated to be approximately 265,000 persons, with a range of 232,000 to 316,000 persons, with approximately 12 000 new cases annually. It is estimated that the annual incidence of spinal cord injury in the population, excluding those who died at the scene of an accident, is approximately 40 cases per million (NSCISC, 2010). The above statistics suggest that this is a serious problem that affects countries worldwide with nearly the same frequency of new cases annually. Even though the level of medical care has increased in the last decades and life expectancy for people exposed to traumas and various types of neurodegenerative diseases has significantly grown, there has still been very limited progress in improving the neurological symptoms and defects of the affected patients as there are still large gaps in our understanding of the processes that take place after injury or the onset of degeneration. Due to these gaps in understanding, it remains unclear what kind of treatment approach should be employed and when treatment should be implemented.

According to Edvard C. Benzel (2005) in the United States, each year 150-160 thousand people suffer from spinal cord disorders, 10-30% of them have spinal cord injuries. There are about 256 000 patients with spinal cord injury in the USA and annually registered about 12,000 new cases (Hama A. and Sagen J., 2012). Expected costs of their treatment are over 4 billion dollars yearly (Benzel Edvard C., 2005).

The social significance of spinal cord injury is defined by a high mortality rate (17-23% in acute trauma), severe and persistent effects, drastically altering the social status of the victims. 70-80% of the cases result in disability, with the prevalence I and II groups of disability. Despite significant progress in surgery, anesthesiology and intensive care, mortality due to spinal cord injuries widely ranges from 16% to 64% of cases (Davies S. at al., 1995).

Various rehabilitation activities may significantly improve the conditions of injured persons in some cases and improve their quality of life, but they cannot eliminate the severe neurological deficits and restore lost functions. Surgical treatment is mainly directed to orthopedic correction of the spine and the spinal canal, showing its effectiveness in the acute phase of injury, which in most cases does not lead to an improvement in the neurological status of patients with spinal cord injury with duration of more than 72 hours. It is evident that there is inefficiency of the existing approaches for the treatment of this disease.

1.2. Pathology of spinal cord injury

Spinal cord injury is one of the most severe types of injuries. The severity of spinal cord injury depends on the level of spinal cord lesions. According to the level of spinal cord lesion and its severity, SCI conditions are classified into following types:

Paraplegia is the result of a spinal cord injury in the thoracic or lumbar departments. This leads to a paralysis of both legs and dysfunction of the bladder and rectum.

Tetraplegia is the result of a spinal cord injury in the cervical spine. It is characterized by the loss of muscle strength in all four extremities.

Complete spinal cord injury is characterized by a complete loss of motor function and sensation below the level of spinal cord lesions. The defeat is identical on both sides of the body. Complete intersection and separation are rarely observed even in the full spinal cord injury. More frequently is the loss of function caused by contusion or compression of the spinal cord.

Incomplete spinal cord injury is a type of the injury when some functions of the spinal cord below the level of the lesion are stored. There is a noticeable greater functional response on one side of the body in comparison with another.

The disease onset is pathophysiologically divided into three distinct phases - acute phase (< 48 h), sub-acute (intermediate) phase (48 h to 14 days), and chronic phase (> 6 months). The pathophysiological events in each phase are different.

Acute phase: About 27% of human SCIs are characterized by the direct impact of penetrating objects (rapid flexion/rotation, distortion, laceration or foreign body stabbing). The remaining 73% of clinical cases are caused by temporary compression of the cord due to bone fragments, intervertebral disks etc. Any mechanical deformation of the spinal cord leads to the rupture of neuronal cell membranes with the release of the intracellular contents, hemorrhage, vasospasm, localized edema, breakdown of the blood-brain barrier etc. As a result, a cascade of vascular, biochemical, and cellular processes leads to necrosis and apoptosis, causing the massive death of neuronal, glial and endothelial cells and a shift of metabolism towards anaerobic glycolysis (Katoh H. et al., 1996, Emery E. et al., 1998). Meanwhile, there is also an activation of macroglial cells and ongoing demyelination involving oligodendroglial cells (Beattie M.S. et al., 2000, Farooqui A.A. et al., 2004). Morphologically and clinically, the extent of post-traumatic damage usually correlates with the degree of force and pressure applied on the spinal cord, the time elapsed after the initial damage, and the kinetic energy that was absorbed by the nervous tissue. It is also interesting to note that most of the time, damage to the spinal cord is limited to a single segment, and only rarely does complete damage (transection) to the spinal cord occur. The transection of axons in the adult mammalian CNS also induces the degeneration of the axons separated from the cell bodies (Wallerian degeneration); meanwhile the proximal endings that remain connected to their perikarya, form terminal retraction bulbs. After the initial phase of SCI, axonal dieback occurs up to several millimeters more proximal from the site of the lesion (Seif G.I. et al., 2007).

Intermediate phase: The intermediate phase begins minutes after the initial injury and persists for weeks after SCI. This phase is characterized by secondary damage to the nervous tissue caused by vascular defects with related hypoxia, the release of glutamate from intracellular stores that causes excitotoxicity (Katayama Y. et al., 1990) via an increased influx of Ca^{2+} into the neurons along with a depletion of ATP regeneration (uncoupled mitochondrial electron transport), the production of free radicals with subsequent lipid peroxidation, local inflammation (Taoka Y. et al., 1997, Carlson S.L. et al., 1998) and changes in ionic homeostasis (Figure 2). All these processes trigger a chain of events that are accompanied by an inflammatory reaction leading to secondary necrotic cell death (mainly of oligodendrocytes) at the core of the injury site and

apoptotic cell death in the surrounding areas (Crowe M.J. et al., 1997, Popovich P.G. et al., 1997), reaching its highest levels at about 1 week after injury (Farooqui A.A. et al., 2004). The demyelination (Waxman S.G., 1989, Bunge M.B. et al., 1993) and degeneration of the fiber tracts also leads to neuronal death in areas remote from the primary lesion site, such as the motor cortex in the brain (Lee B.H. et al., 2004). At this stage several oligodendrocytes and astrocytes die in the core of the injury (Crowe M.J. et al., 1997), meanwhile there is an activation of astrocytes at the edge of the primary injury site. These astrocytes display increased metabolism (the number of mitochondria and endoplasmic reticula inside cells is increased), and they start to form long neurites, aiming to prevent the spread of an aggressive environment further in both directions (Nathaniel E.J. and Nathaniel D.R., 1977, Eddleston M. and Mucke L., 1993). These cells are also called gemistocytes, and the peak of tissue infiltration by these cells is reached two to three weeks after injury. Importantly, this infiltration of activated astrocytes subsequently acts to block regeneration after SCI due to the formation of a barrier to axonal sprouting across the lesion (Fawcett J.W., 2006). Another important factor that blocks the regeneration of the injured axons at this stage is the activation of oligodendrocytes, which results in the formation of myelin membranes and the synthesis of oligodendrocyte-myelin glycoprotein (OMG) and myelin-associated glycoprotein (MAG), both of which have neurite growth inhibitory activity (Schwab M.E. and Caroni P., 1988, Domeniconi M. et al., 2002, Oertle T. et al., 2003).

Chronic phase: The chronic phase starts days after injury and can last for years. The main feature of this phase is ongoing demyelination (Bunge M.B. et al., 1993, Schwab M.E. and Bartholdi D., 1996, Totoiu M.O. and Keirstead H.S., 2005), local inflammation and apoptosis (Fleming J.C. et al., 2006), a decrease in the number of activated macrophages, and the formation of a glial scar and pseudocysts (also called syringomyelia) (Windle W.F. and Chambers W.W., 1950, Fawcett J.W. and Asher R.A., 1999, Nielsen O.A. et al., 1999, Perrouin-Verbe B. et al., 1999). This phase of SCI presents a major challenge to doctors and scientists and attracts the greatest research interest, as most SCI patients remain in this phase, to a greater or lesser extent, for the rest of their lives. Targeting the main components of the glial scar in the chronic phase could provide effective therapy for patients in the future.

Since the pathology of SCI is extremely complex and dynamic, each SCI is unique. This makes it even more important for clinicians to evaluate and comprehend the

conditions of SCI and administer the best therapy accordingly. With respect to the different stages and different types of SCI, the treatment types will vary.

A disturbance in the regulation of organs functions is not limited to the injured segment of spinal cord injury and extends below the level of damage and are generally irreversible (Eves F.J., Rivera N., 2010). It happens because after a transection or a contusion of spinal cord, spinal shock occurs (sharp decrease in excitability and inhibition of the activity of all the reflex points, below the injury site (Figure 1)). Skeletal motor and autonomic reflexes disappear. The level of blood pressure decreases, there are no vascular reflexes, acts of defecation or urination. However, centers located above the injury remain active. The duration of the shock is different across the species of animals standing at different stages of the evolutionary ladder. Shock in frogs lasts 3 - 5 minutes, in dogs - 7 - 10 days, in monkeys - more than 1 month. In humans motor reactions to external stimuli gradually reappear systematically over the next days and weeks (Christensen PB, at al., 1990, Ditunno JF, et al., 2004, Ko HY, at al., 1999).

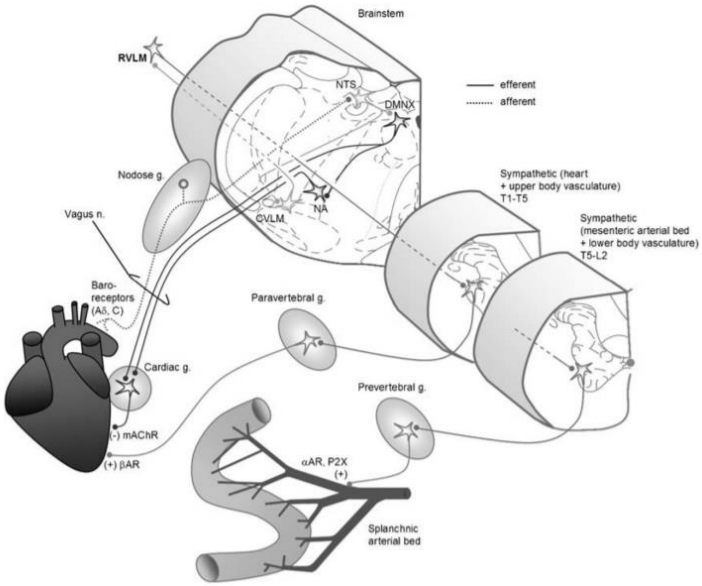

A - the innervation the cardiovascular system

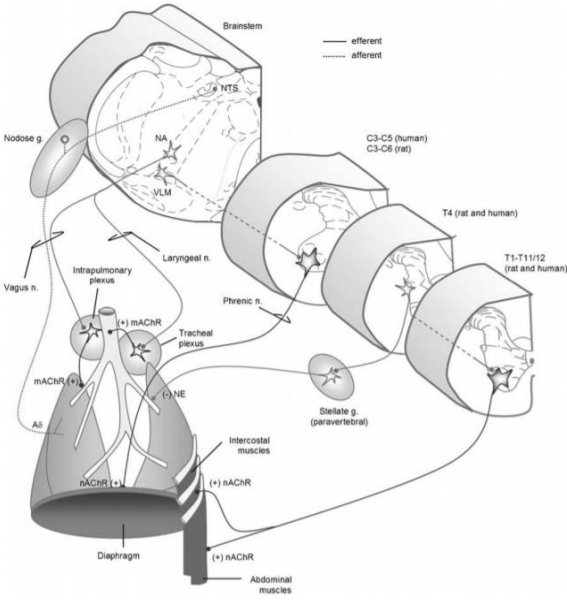

B - the innervation of the respiratory system.

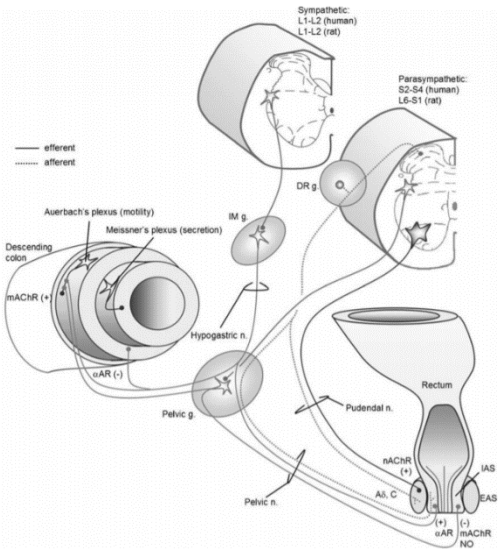

C - the innervation the gastro-intestinal tract.

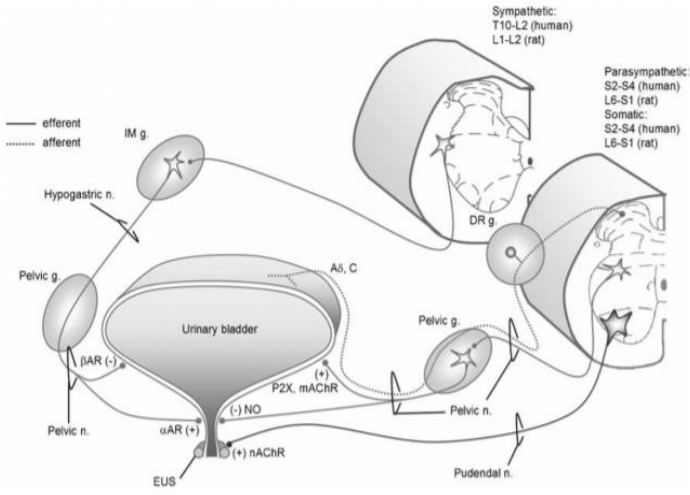

D - the innervation of the urinary system.

Figure 1. Spinal cord injury at the segment level T8-T9 (Inskip J.A., 2009).

According to statistics, the most frequently damaged spinal cord segments are medium thoracic (T5-T8) and inferior thoracic (T9-T12). Figure 1 represents the spinal cord injury at the segment level T8-T9, the most used as a model of injury in experiments that does not lead to a breaking of the cardiovascular system, but it violates the activities of peripheral arterial vessels and abdominal muscles. Dysregulation of functions at this level has a very extensive manifestation (Inskip J.A. at al., 2009). The higher the level of the spinal cord lesion, leads to loss of more motor functions (Benzel Edvard C., 2005).

In case of localization of SCI at medium thoracic and inferior thoracic levels, 65 of 79 patients with disabilities enrolled in the rehabilitation had been diagnosed with lower spastic paraparesis of varying severity, in 8 cases hemiparesis was diagnosed and 12 examinees observed a resistant lower paraplegia with severe muscular atrophy and the complete lack of movement in the legs (Inskip J.A. at al., 2009).

Severe motor defects are aggravated by significant disorders of pelvic organs in all the patients, as well as disorders of the psycho-emotional sphere of varying severity. These complications have occurred after all the victims were operated on in neurosurgical departments as soon as possible after an injury for the purpose of decompression of the spinal cord, revision, and restoration of liquor flow. In 62% of cases orthopedic surgery were produced to restore the stability of the damaged spine using different fixatives.

To clarify the extent of the residual function of spinal cord after injury, the American Spinal Injury Association (ASIA) has developed an International Standards to document remaining Autonomic Function after Spinal Cord Injury (ISAFSCI). It is based on the Frankel scale with several changes (Table 1). This document is recommended as a supplement to International Standards for Neurological Classification of Spinal Cord Injury (ISNCSCI) and is used to determine the localization of damage.

Table 1. American Spinal Injury Association (ASIA) impairment scale

A	Complete: no motor or sensory function is preserved in the sacral segments S4-S5.
B	Incomplete: sensory but not motor function is preserved below the neurological level and includes the sacral segments S4-S5.
C	Incomplete: motor function is preserved below injury level, and more than half of the key muscles below the neurological level have a muscle grade less than 3
D	Incomplete: fair to good motor function below injury level, half of the key muscles below the neurological level have a muscle grade more than 3
E	Normal: motor and sensory functions are normal

Prospects for the rehabilitation of patients with spinal cord injury are determined mainly by the degree of tissue preservation. Existence of minimal motor function immediately after the injury points to incomplete damage. In these cases, timely medical

treatment, including electrical and mechanical stimulation of neuromuscular endings and involuntary muscle movements via activation of robotic systems provide a partial rehabilitation (Nadvornik P. et al., 2014). Psychological help should be provided simultaneously.

In general, in a modern scientific literature there is a certain consensus about the sequence and relationship of pathological processes in spinal cord injury (Ronaghi M. at al., 2010; Borgens R.B., Liu-Snyder P., 2012). As an example, we can mention the scheme proposed by Oyinbo (Oyinbo C.A., 2011), which provides an understanding of the number and the interconditionality of reactions to the trauma of the spinal cord (Table 2), although the relative importance of the factors that control these processes remains a subject of much discussion.

Table 2. The main features that characterize three phases a spinal cord injury (Oyinbo C.A., 2011).

Acute (primary) phase (from seconds to minutes)	Subacute (secondary) phase (from minutes to weeks)	Chronic Phase (months to years)
Systemic hypotension and spinal shock		
Vascular spasm	Vascular spasm	
The death of cells directly from a spinal cord infarction	The death of cells directly from a spinal cord infarction	
Ischemia	Ischemia	
Edema	Edema	
Violation of ion balance	Violation of ion balance	
The release of neurotransmitters	Glutamatergic excitotoxicity	
Violation of the plasma membrane	Violation of the plasma membrane / increase in permeability	
	Production of free radicals	
	Lipid peroxidation	
	Excess of nitric oxide	
	The blockade of the conduction of nerve impulses	
	The excess of noradrenaline	
	Energy deficiency, fall in ATP	
	Invasion of immune cells and cytokine release	
	Cell death as a result of inflammation	
	Production of neurite growth inhibitors	

	Central chromatolysis	
	Intervertebral compression	
	Demyelination of survivor's axons	The ongoing demyelination
	Apoptosis	The ongoing apoptosis
	Beginning of central cavitation	Continued central cavitation
	Launching of the astroglia scar growth	The formation of glial scar
		Changing the mode of ion channels and receptors
		Development of regenerative processes, including and sprouting
		The changes of neural cycles
		Syringomyelia

Pathologies emerged during the spinal cord damage and their development over time are determined by two separate phases: primary (e.g. due to mechanical damage) and secondary, representing a cascade of vascular and biochemical reactions. Primary (acute) phase occurs at the time of injury and lasts from seconds to minutes. Typical associated features in the primary phase are discontinuity and/or compression of the tissue, local hemorrhage, edema, and local ischemia, followed immediately by the death of cells in the lesion. At the same time the following system reactions of an organism usually appear: hypotension, spinal shock, vasospasm, ischemia, impaired ion homeostasis, excess accumulation of neurotransmitters, causing toxic effects. A heavy inflammatory reaction also occurs in the lesion site (Xue et al., 2017). Therefore, administration of anti-inflammatory drugs must be done in the acute phase.

Even though the visible tissue damage in the primary phase localized in the gray matter of the spinal cord (Figure 2) and the white matter looks mechanically more durable, MRI registers swelling in tissues of the white matter at a distance up to 4 mm from the epicenter of injury, which indicates the risk of secondary damage (Narayana P.A. et al., 2004; Simard J.M., 2012).

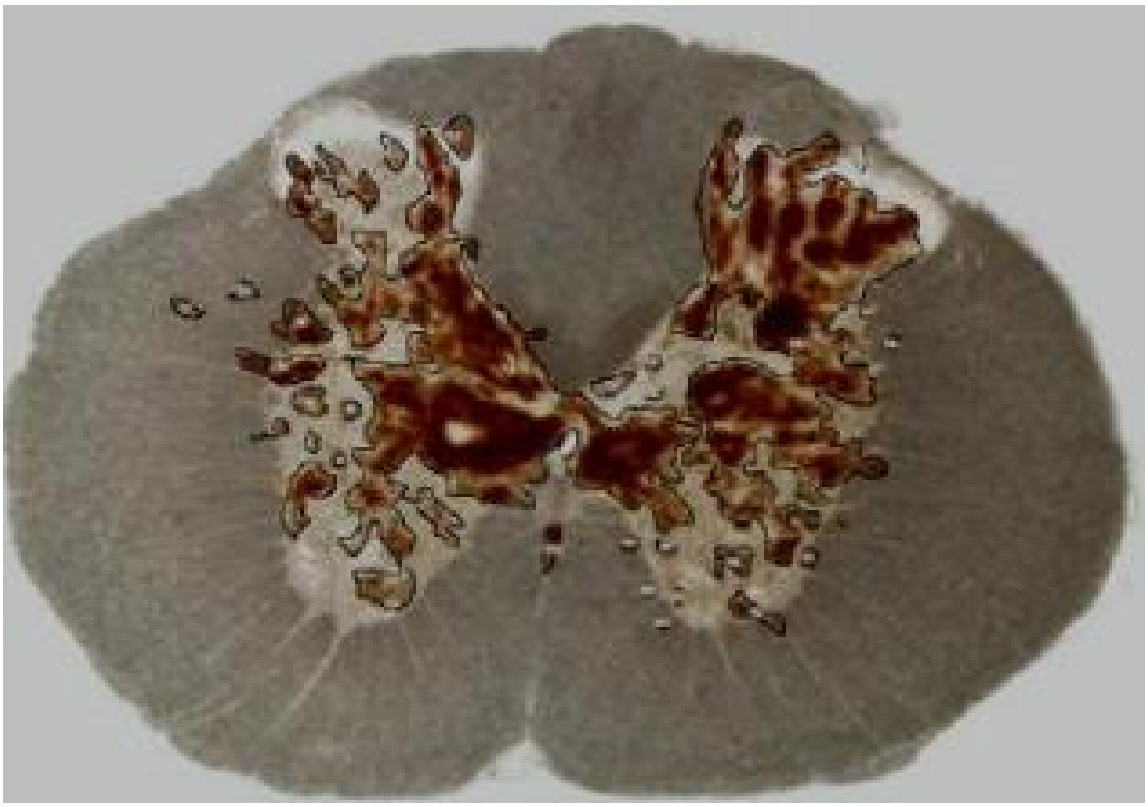

Figure 2. A cross section in spinal cord contusion injury under a light microscope after 15 minutes after a damage. Visible extensive hemorrhages in both halves of the gray matter. White matter looks intact, even though the impact was on the dorsal site of the white matter. The length of the interval: 1 mm. (Ek C.J. at al., 2010)

The secondary phase develops directly behind the primary, it lasts for several weeks or months and is accompanied by a progressive loss of cells not affected by actual primary injury. That leads to a significant increase of the initial lesion site. If the process of neuronal death of gray matter is completed by the end of the first day after the contusion, the death of axons of white matter continues from one to four weeks.

Saving the mechanical integrity of white matter tissue during the contusion indicates the possible preservation of white matter in case of a sufficiently early application of therapeutic methods, preventing development of pathological processes of secondary degeneration. These pathological processes are the extensions of similar processes of the primary phase (ionic imbalance, edema, necrosis), but they also include a wide range of new events: formation of free radicals, delay entry of calcium ions, immune response/inflammation and finally apoptosis. These processes are interrelated, once established, they are mutually reinforcing and develop as a chain reaction. This leads to irreversible changes around the injury throughout the whole organism (Ronaghi M. et al., 2010; Liu W.M. et al., 2011; Varma A.K. et al., 2013).

The secondary damage after SCI is characterized by oxidative responses in addition to the inflammatory responses (Siva X. et al., 2014). Due to the decrease of molecular

oxygen in the mitochondria, very high levels of reactive oxygen species (ROS) are created - this condition is called oxidative stress. Accumulation of ROS can have many deleterious effects including lipid peroxidation, DNA damage, and in some cases, cell death (Sugawara T. et al., 2003). If antioxidant therapy is given at the acute phase, the oxidative stress injury is reduced. Further, this plays an important role in the recovery of neurological function post SCI (Nagoshi N. et al., 2017, Zhang X.Y. et al., 2014). In the phase following the acute phase, i.e., the sub-acute phase, the cystic cavity starts to coalesce, and the axons, that have been denuded or damaged, get retracted or degenerate.

Spinal cord injury gives rise to an auto destructive process called "progressive hemorrhagic necrosis" (PHN), leading to widespread destruction of spinal tissue (Figure 3).

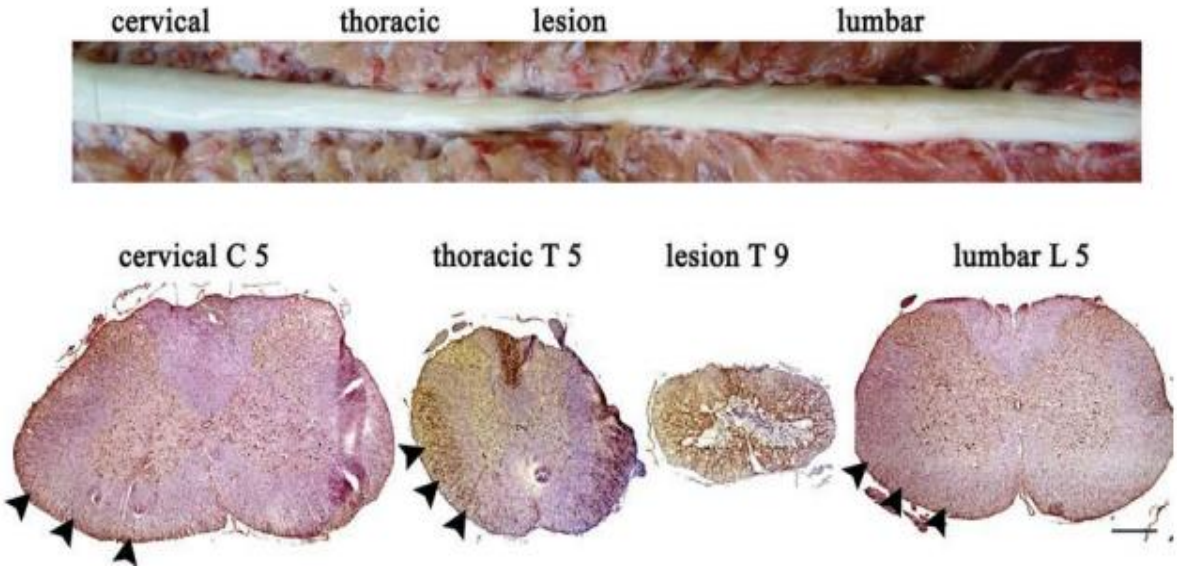

Figure 3. Spinal cord of rat after spinal cord contusion. Due to post-traumatic syringomyelia the spine is typically narrowed at the area of injury. The corresponding cross-sections at different distances from the injury epicenter. The arrows indicate areas of white matter. The length of the interval 500 microns. (Knerlich-Lukoschus F. et al., 2010)

There are two most important components of PHN: progressive secondary hemorrhage and necrosis of cells (Simard J.M. et al., 2012; Simard J.M. et al., 2013). Hemorrhage is an accumulation of blood, extravasated into the surrounding tissue due to vessel damage. Spinal cord injury is accompanied by subarachnoid, subdural, and epidural hemorrhage, leading to compression (Vinay S. et al., 2011; Ishizaka S. et al., 2012; Papanagiotou P., 2012). Compression of the cells causes damage and the violation of their functions. The data obtained by the ultrasound contrast ultrasonography (CEU) indicate

that bleeding occurs after an injury inside the spinal cord parenchyma has occurred, which is amplified within the first hour (Soubeyrand M. et al., 2012). As a result, oxidative stress and inflammation are developed, and contribute to the progress of hemorrhagic necrosis. Capillary endothelial cells, neurons and oligodendrocytes are especially vulnerable to hemorrhages.

Another result of the destruction of vessels during the injury, is ischemia - a decrease in the blood supply of the organ or tissue due to the weakening or interruption of the arterial blood flow and reduction of oxygen supply. Ischemia in spinal cord injury initially occurs from the mechanical destruction of capillaries. And further it is complicated by petechiae, vasogenic edema, excitotoxicity, and reduced blood flow in penumbra due to vasospasm (Benton R.L. et al., 2009). In response to prolonged ischemia, pathological angiogenic processes develop, lasting for days or weeks and leading to neovascularization of damaged spinal cord tissue. Moreover, impaired blood-brain barrier and microvascular changes lead to a decrease in the blood supply of the spinal cord. These changes are hallmarks of secondary damage to the spinal cord, leading to the further deterioration of the patient's condition.

Spinal cord injury is almost always accompanied by local or general swelling. As the scope of edema is strictly limited by the vertebral segments, the development of edema inevitably leads to compression of the spinal cord tissue, cessation of blood flow and exacerbation of ischemia. The causes of swelling can be divided to vasogenic, cytotoxic and osmotic origin.

The cytotoxic edema is characterized by the increase in the content of intracellular water as a result of cellular metabolism violations during hypoxia, the fall of ATP synthesis and the inhibition of ATP-dependent sodium-potassium pump. The cytotoxic edema develops very quickly, within minutes or hours, leading to the swelling of neuronal, glial, and endothelial cells. The conduction activates nonselective Ca-ATP channels resulting in an accumulation of intracellular calcium, activation of phospholipases and the release of arachidonic acid, development of oxidative stress and necrosis. Vascular permeability violation leads to infiltration of high osmotic pressure plasma components in the intracellular space and swelling of the brain tissue. The compression of veins occurs in the areas of trauma and the intravenous pressure increases. This leads to increased extrusion of fluid from the capillaries and further expansion of edema. The result is a complete occlusion of the blood vessels around the edema followed by dying of the nervous tissue (Goldshmit H.S., 2009).

The local compression of nervous tissue, even for short time, is a fatal consequence for the survival of cells. The lack of oxygen and nutrients caused by ischemia leads to accumulation of free radicals and an increase of cell membrane permeability. Restoration of blood flow (reperfusion) in many cases leads to oxidative stress and, consequently, to inflammation and oxidative damage of cells (Smith J.A. et al., 2013).

The immune response of the organism to the spinal cord injury has cellular and molecular aspects that are closely linked. Activation of immune cells and regulatory proteins lead to the development of inflammation. It occurs immediately at the time of injury and lasts for weeks and months (Fehlings M.G. and Nguyen D.H., 2010). Immune cells secrete proinflammatory cytokines (interleukins IL-1β, IL-6 and tumor necrosis factor TNF-α), enhancing the degree of inflammation. Inflammation is intended to clean the lesion from the remains of dead cells and prevent infection. But in the specific conditions of the nervous tissue, the development of inflammation can prevent control, that leads to the death of healthy cells and expansion of the lesion (Rossignol S. et al., 2007).

The proper functioning of the spinal cord depends on the four important types of cells: neurons, astrocytes, oligodendrocytes, and oligodendrocyte progenitors. These cells suffer from the intracellular stress as a consequence of tissue injury of the spinal cord. Disruption of normal metabolism of these cells leads to the accumulation of misfolded proteins. This causes an increase in activity of appropriate chaperones and amplification of ATP consumption in acute phase. This process is mostly expressed in astrocytes. Prolonged stress, which is accompanied by mechanical injury of the spinal cord, leads to the exhaustion of capacity of the cells for protein repair, and includes a mechanism of apoptosis in subacute phase. At the same time the oligodendrocyte precursors are the most susceptible type of cells to apoptosis (Matsuyama D. et al., 2014). The key point is the expression of the apoptosis inductor - the transcription factor CHOP in the nucleus of neurons, oligodendrocytes, and their precursors (Wang Z.Y. et al., 2014), while in astrocytes its expression occurs in the cytoplasm. This suggests the susceptibility of astrocytes to apoptosis in the spinal cord.

Glial barriers formed in the spinal cord injury cavity are represented by two structures: the glial scar and enveloping of the abnormal pathological cavities (cysts). Both structures have a similar structure and contain reactive astrocytes as the predominant cell type. Astrocytes produce inhibitory molecules of axonal growth in the glial scar and enveloping of cysts, the most studied component are chondroitin sulfate proteoglycans (CSPG) (Bradbury E.J. and Carter L.M., 2011; Kawano H. et al., 2012, Danisovic L. et al.,

2009 Sykova E. et al., 2021). When the matrix is already organized it appears as a coat on the neuronal surface and controls the formation of synapses and connections that are important for plasticity. CSPG have been shown to play an important role in axonal guidance during development and regeneration (Kwok et al., Bruckner et al., 2000, Kwok et al., 2008). On the other hand, in vitro and in vivo experiments have shown that after an injury to the spinal cord, CSPG and particularly chondroitin sulphate chains are up-regulated in activated astrocytes, leading to the restriction of anatomical as well as synaptic plasticity and axonal outgrowth into the site of injury (Lin et al., Smith-Thomas et al., 1994, Smith-Thomas et al., 1995, Chung et al., 2000).

Glial barriers play an important role in the suppression of neuroregeneration. There are two basic components causing this negative effect. One of them is the formation glial physical barrier from reactive astrocytes. The other, perhaps more significant, is the production of specific axonal growth inhibitory molecules by reactive astrocytes. However, glial barriers that appeared after spinal cord injury played a positive role by separating the compartments of damaged and normal tissue and contributing to the restoration of the blood-brain barrier. This role has also been associated with the ability of glial barriers to maintain the integrity of the spinal cord, reconstruct damaged tissue, prevent undesirable cell responses and the spread of infectious agents. Formed structure of glial barrier shows a stimulating effect on the processes of neovascularization, which is important for trophic and metabolic support of neuroregeneration.

To the beneficial properties of the glial scar, it is also necessary to name its ability to limit the inflammatory response and to inhibit the degeneration of cells. In addition, the positive role of glial scar includes the fact that many molecules produced by astrocytes have the neurotrophic effect and astrocytes themselves form the potential space for the growth of axons (Tysseling-Mattiace V.M. et al., 2008, Kawano H. at al., 2012).

The process of forming pathological cavities (abnormal cavitation) is mostly expressed in the contusion injury of the spinal cord as a result of primary damage. In the beginning of the pathological process, the cavity occupies a limited area in the epicenter of the trauma and are typically small. Then cavities fuse and form a larger cavity within the gray and white matter, separated from the surrounding tissues by a glial barrier. As a result of progressive cavitation lasting from days to several weeks, the size of the cavity can significantly exceed the size of the original area of damage (Figure 4). Moreover, the process of post-traumatic syringomyelia is running. During the development of inflammation, macrophages actively penetrate the lesion epicenter which causes migration

of astrocytes in the opposite direction, i.e., from the place of focal inflammation to the periphery, which separates the forming cavity from the surrounding spinal cord tissue (Fitch M.T. et al., 1999).

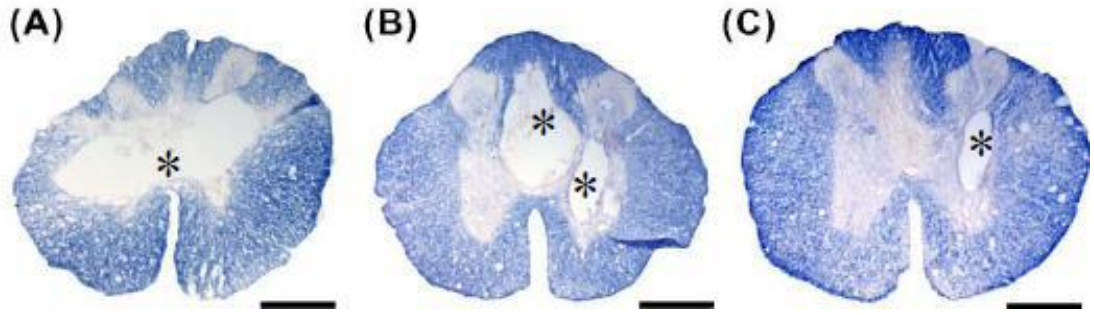

Figure 4. Cavities in cross sections of the rat spinal cord following contusion injury (indicated by asterisks) (Hwang D.H. et al., 2009). The length of segments 500 μm.

However, the causes of pathological cavities have not been studied in detail. As hypotheses for this ischemia, hemorrhage, activation of peptidases, hydrodynamic shock, macrophage infiltration and inflammation are considered (Fitch M.T. et al., 1999; Loy D.N. et al., 2002; Ek C.J. et al., 2010; Miranda T.A. et al., 2012).

Today inflammation is considered to be the main cause of progressive development of pathological cavities in the spinal cord. Activation of macrophages leads to the increase of inflammatory response, cavitation process and the production of axonal growth inhibitory molecules in the white matter, such as proteoglycans (Fitch M.T. et al., 1999; Young W., 2014; Bartus K. et al., 2014). From the above-mentioned hypothetical causes of pathological cavities, the most studied was the significance of molecular and cellular mechanisms of inflammation that induce and maintain specific changes in the phenotype of the most representative and heterogeneous population of glial cells, astrocytes. Glial scars are formed after the violation of the integrity of the blood-brain barrier and penetrating the tissue of the spinal cord by molecules from the internal environment of the body, usually absent in the central nervous system. The barrier remained permeable for these molecules from blood two weeks after injury. There is a direct correlation between the degree of disintegration of the blood-brain barrier, intensity of the formation of glial scar tissue and the degree of activated macrophages infiltration in the epicenter of an injury (Kawano H. et al., 2012).

There is a compact cluster of reactive astrocytes at the spinal cord injury glial scar. They are branched intensively, but shorter compared to intact astrocytes whose area of branching does not overlap (Lukovic D. at al., 2015). Perikaryons of reactive astrocytes,

including proliferating astrocytes along with the dense network of overlapping processes of the adjacent cells associated by slotted contacts form a glial barrier for axon growth. In addition to reactive astrocytes, which are the main cellular component in the composition of the glial scar, there are macroglia predecessors, as well as actively penetrating the scars reactive microglia macrophages. Moreover, in cases of integrity violation of the dura mater, in the composition of the glial scar, fibroblasts and perivascular cells are found.

Implantation of stem cells in the spinal cord may be involved in the replacement of the lost tissue and abnormal cavities filling. In the model of experimentally created pathological cavities in the rat spinal cord by administering quisqualic acid has shown a 20-fold increase in progenitor cells, whose presence is traced until the end of the second month after the injury (Tu J. et al., 2011). Most of these cells were localized in the gray matter along the border between the cavity and the surrounding tissue, and this pool of cells was represented by multipotent neural cells, precursors of oligodendrocytes and astrocytes. The presence of neural progenitor cells can be linked to the possibility of restoring the structure of the spinal cord at the post-traumatic syringomyelia.

1.3. Molecular factors controlling neuroregeneration in spinal cord injury

Myelin proteins. Neurons of corticospinal tract in adults retain the ability to regenerate, but that ability is suppressed by the microenvironment in the affected area. The main factors inhibiting axonal growth are considered following myelin proteins: Nogo, myelin-associated glycoprotein (MAG), and oligodendrocyte-myelin glycoprotein (OMgp). The basis of their actions is a common mechanism: Nogo, MAG and OMgp are associated with Nogo-receptor that interacts with p75 neurotrophic receptor, activating a small protein GTPase RhoA, which directly inhibits the growth of neurites (Wang K.C. et al., 2002; Cafferty W.B. et al., 2010). Blocking specific myelin proteins or their common receptor improves functional recovery after the injury (Schwab M.E. and Bartholdi D., 1996) Nevertheless, only a very small percentage of axons regenerate at the same time (Zheng B. et al., 2003).

The molecules of the extracellular matrix (primarily proteoglycans - chondroitin sulfate), which are part of the glial scar in spinal cord injury, inhibit the growth of axons and prevent regeneration. It is shown that splitting of proteoglycans by matrix-metalloproteinases support the regeneration of nerve fibers and restore the nerve connections (Pizzi M.A. and Crowe M.J., 2006). In spinal cord injury an increase in the

expression of NG2, the main representative of the proteoglycan family was recorded (Jones L.L. et al., 2003).

One easy and convenient way of manipulating the ECM in both the glial scar and PNN in the CNS is by the application of chondroitinase ABC (chaseABC). ChaseABC is a bacterial enzyme isolated from Proteus vulgaris, which digests the chondroitin sulfate chain into its basic disaccharide units, hence removing the glycosaminoglycan chains from the core proteins (Kwok et_al., Yamagata et al., 1968). It has been shown that if CSPG are digested after a trauma to soluble disaccharides with chaseABC, then the axons are able to regenerate and sprout through the glial scar more readily, suggesting that enzymatic digestion of CSPG can reactivate plasticity in the adult CNS (Carulli D. et al., Davies S.J. et al., 1997, Lemons M.L. et al., 1999, Pizzorusso T. et al., 2002, Galtrey C.M. et al., 2007).

Interestingly, chaseABC mono/combined therapy is effective not only in the early post-injury period, but also in the chronic stage after SCI. It has been shown that chaseABC therapy initiated 1 month after injury of the rubrospinal tract not only promoted the sustained rescue of neuronal atrophy, but also partially reduced the already established atrophy of the rubrospinal neuronal cell bodies (Carter L.M. et al., 2011). Moreover, the sustained infusion of chaseABC into the chronically injured spinal cord followed by the application of NPCs promoted the integration and extensive migration of the cells within the host SC (KarimiAbdolrezaee S. et al., 2012). There is also evidence that the application of chaseABC after SCI might also enhance remyelination (Siebert J.R. et al., 2011). However, there are several disadvantages to the use of chaseABC, one of which is that it loses its enzymatic activity rapidly at 37 °C, necessitating the use of repeated injections or local infusions for a period of days to weeks (Bradbury E.J. and Carter L.M., 2011). Recently, it has been reported that this problem can be overcome by the creation of thermostabilized chaseABC, which showed significant differences in CSPG digestion, axonal growth and functional recovery following the sustained local release of thermostabilized chaseABC delivered by a hydrogel-microtube scaffold system versus a single injection of chaseABC (Lee X. et al., 2010). Furthermore, no adverse effects have been noted after the intrathecal or intraspinal application of chaseABC in either rodents or in larger mammals such as cats, rabbits, and pigs, thus making it a potential candidate for clinical trials in human (Bradbury E.J. and Carter L.M.,

2011, Olmarker K. et al., 1991, Olmarker K. et al., 1996, Tester N.J. and Howland D.R., 2008).

Molecules-navigators. Directional cell migration plays a key role in the reconstruction of damaged tissues, including nervous tissue. Intensive investigations revealed the existence of a limited and very conservatively composed set of attraction and repulsion agents, which joint actions guide immature neurons in the desired location. This class of agents consists of a family of netrin, semaphorin, ephrins and various neurotrophic factors (Marin O. et al., 2003).

In recent years, researchers have attracted attention to several signaling molecules located on the surface of cells and involved in the regulation of directed growth of axons in the developing organism. In particular, the tyrosine kinase Eph-receptors, together with its protein ligands - ephrins regulate the direction of the growth of axons, inducing the collapse of parts of the tip of the axon growth when contacted with the membrane of astrocytes (Kullander K. et al., 2001; Ren Z. et al., 2013). Their production is increased in the adult organism during trauma, and this has a negative effect on axonal regeneration directly through the inhibition of growing neurite in the place of contact with astroglial cells, and indirectly, through activation of astrocytes, which form the glial scar. After the spinal cord hemisection in EphA4 deficient mice, it was revealed that a large number of axons successfully sprouting through the damaged area due to decreased formation of glial scar comparing to wild-type mice (Goldshmit Y. et al., 2004). Later it was shown that in normal mice, prolonged administration of EphA4 receptor blockers or ephrins resulted in a significant increase in the number of regenerating axons overcoming the region of glial scar (Goldshmit Y. et al., 2011). Another important result of this work was the determination of a negative correlation between the restoration of damaged blood brain barrier (because of the injury) and effective use of external blockers of Eph-receptors or ephrins. It can be assumed that the temporary disruption of the blood brain barrier in spinal cord injury has adaptive function and is intended to facilitate the delivery of various molecular factors to the damage zone.

Potential neuroregeneration stimulants. Among the endogenous stimulators of neuroregeneration, neurotrophic factors were studied most intensively. In accordance with the definition, they support neuronal survival and axonal growth in the central and peripheral nervous system. The large number of papers were devoted to the role and mechanisms of action of neurotrophic factors in neuroregeneration: neurotrophins - nerve growth factor (NGF) (Chao T. and Gupta R., 2012), brain-derived neurotrophic factor

(BDNF) (Acheson A. at al., 1995, Allen SJ. at al., 2013, Mitsui T. at al., 2005), neurotrophin-3 (NT3) (Shang A.J. et al., 2011), vascular endothelial growth factor (VEGF) (Benton R.L. at al., 2009, Han YF. et al., 2013, Zhang H. at al., 2003), fibroblast growth factor 2 (FGF2), glial-derived neurotrophic factor (GDNF) (Allen S.J. at al., 2013, Chen J. at al., 2010, Deng LX. at al., 2013).

Nerve growth factor (NGF) is a neurotrophic factor primarily involved in the regulation of growth, maintenance, proliferation, and survival of certain target neurons. In fact, NGF is critical for the survival and maintenance of sympathetic and sensory neurons, as they undergo apoptosis in its absence (Freeman R.S. at al., 2004). However, several recent studies suggest that NGF is also involved in other pathways besides those regulating the life cycle of neurons. NGF prevents or reduces neuronal degeneration in animal models of neurodegenerative diseases and these encouraging results in animals have led to several clinical trials in humans (Tuszynski M.H. and Blesch A., 2004). NGF promotes peripheral nerve regeneration in rats (Sun W. at al., 2009). The expression of NGF is increased in inflammatory diseases where it suppresses inflammation (Freund V., 2004). NGF appears to promote myelin repair (Althaus H.H., 2004). Connective tissue cells genetically engineered to synthesize and secrete NGF when implanted in Alzheimer's disease patients' basal forebrains reliably pumped out NGF, which enhanced the cells' size and their ability to sprout new neural fibers (Allen S.J. And Dawbarn D., 2006). Hence NGF may be useful for the treatment of SCI.

Brain-derived neurotrophic factor (BDNF) is a member of the neurotrophin family of growth factors, which are related to the nerve growth factor. BDNF acts on certain neurons of the central nervous system and the peripheral nervous system, helping to support the survival of existing neurons, and encouraging growth and differentiation of new neurons and synapses (Acheson A. at al., 1995, Huang E.J. and Reichardt L.F., 2001).

Neurotrophin-3 (NT3) is a neurotrophic factor in the NGF family of neurotrophins. It is a protein growth factor which affects on certain neurons of the peripheral and central nervous system; it helps to support the survival and differentiation of existing neurons and encourages the growth and differentiation of new neurons and synapses (Mitsui T. at al., 2005, Zhang W. at al., 2010).

Vascular endothelial growth factor (VEGF). In contusion injury, the expression of VEGF and its receptors VEGFR1 and 2 increases during the first days after injury and lasts for at least two weeks. Thus, increased production VEGFR2 occurs primarily in endothelial cells and VEGFR1 in microglial cells, reactive astrocytes, and macrophages

(Choi J.S. et al., 2007). The application of VEGFR2 inhibitor suppresses the proliferation of blood vessels and increases the degeneration of the endothelium, without any effect on the astrogliosis.

Fibroblast growth factor 2 (FGF2) is a key representative of the family of morphogens, which control the induction and specification of tissues during embryogenesis. FGF2 is a growth factor with a pronounced neurotrophic activity and is considered as an obligatory component in the mediums for the directed differentiation of neural cells *in vitro*. In the mature spinal cord FGF2 participates in the proliferation of neural progenitors (Meng X.T. et al., 2008; Lee J.W. et al., 2012). FGF2 is regarded as nodal molecules in the pathophysiology of spinal cord injury. It was shown that in SCI the amount of FGF2 positive cells increased by 15 times (Mutsui T. at al., 2005). The application of FGF2 in combination with transplantation of human mesenchymal stem cells improves functional performance of spinal cord regeneration (Kim K.N. et al., 2006). The application of FGF2 to spinal cord injury significantly reduces the size of pathological cavities and promotes survival of white matter (Jimenez Hamann M.C. et al., 2005). Subcutaneous administration of FGF2 in rats with the motor cortex damage contributes to the reconstruction of neural connections and restoration of functions (Monfils M.H. et al., 2008).

Glial-derived neurotrophic factor (GDNF) is a powerful factor in maintaining the viability of neurons. GDNF is expressed by astrocytes and Schwann cells and was selected as a therapeutic gene. It stimulates the growth of axons and their myelination, decreases apoptosis and tissue degeneration (Allen S.J. et al., 2013). The targets of GDNF action are dopaminergic and motor neurons, both in the peripheral and central nervous system. Application of BDNF promotes sprouting and the collateral organization of both damaged and intact axons, which leads to the improvement of motor functions.

1.4. Stem cell therapy technologies in the treatment of spinal cord injury

One of the leading positions among the few experimental approaches for stimulation of post-traumatic regeneration of the spinal cord belongs to cell therapy (Syková E. et al., 2006; Kubinová S. and Syková E., 2010; Forostyak S. et al., 2013; Sykova E. and Forostyak S., 2013). Today, cell technologies have become an indispensable tool for fundamental studies of structural and functional connections in the spinal cord, embryonic neurogenesis, neuroplasticity, and nerve regeneration (Syková E. and Jendelová P., 2007;

Kubinová S. and Syková E., 2010; Lukovic D. et al., 2015). Experimental studies revealed the benefits of stem cell therapy in comparison with pharmacotherapy:

1. Cell transplants promote anatomical reconstruction of damaged tissue (Bjorklund A. et al., 1981).
2. Cells contained in the graft may form structural links with the tissue of the recipient (Chopp M. and Li Y., 2002).
3. Cells in the graft can secrete many different neurotrophins and growth factors required for regeneration of nerve tissue (Li Y. et al., 2002).
4. Transplanted cells stimulate the production of growth factors and neurotrophins by the recipient's own cells (Li Y., Chen J. et al., 2002).
5. The interaction between neurons and glial cells of the recipient with the transplanted cells is dynamically dependent on the microenvironment.
6. Transplanted cells may migrate into the zone of the injury, and in the case of their successful integration into the tissue of the recipient, may exert beneficial effects for many months and years particularly due to their paracrine actions (Chen X. et al., 2002; Sykova E. and Jendelova P., 2007; Sykova E. and Jendelova P., 2007).

Clinical exploration of cell transplant therapy in acute SCI patients led to the initiation of a 2010 Geron Corporation trial exploring introduction of human ESC–derived oligodendrocyte progenitor cells (OPCs) into the lesion site (Frantz S., 2012). Since then, investigations into cell-based therapies have expanded on multiple frontiers, from the deriving of transplantable cells from neural progenitors to the establishment of a multitude of methods for optimizing transplant delivery. An ongoing phase I/II dose-escalation trial by Asterias Biotherapeutics aims to evaluate human ESC–derived OPC transplants in cervical SCI and was expected to reach completion by December 2018 (Table 3, 4).

Cell therapy involves the activation of endogenous repair mechanisms and the formation of structure-function relationships between the transplanted cells and the cells of the recipient, which should provide a regenerative effect. Transplanted cells are necessary for recovery of tissue matrix and formation of guide paths for axon growth, maintaining survival of neurons and glial cells, neurite elongation, promotion of myelination. They support the survival of neurons and glial cells, neurite elongation, promotion of myelination (Figure 5).

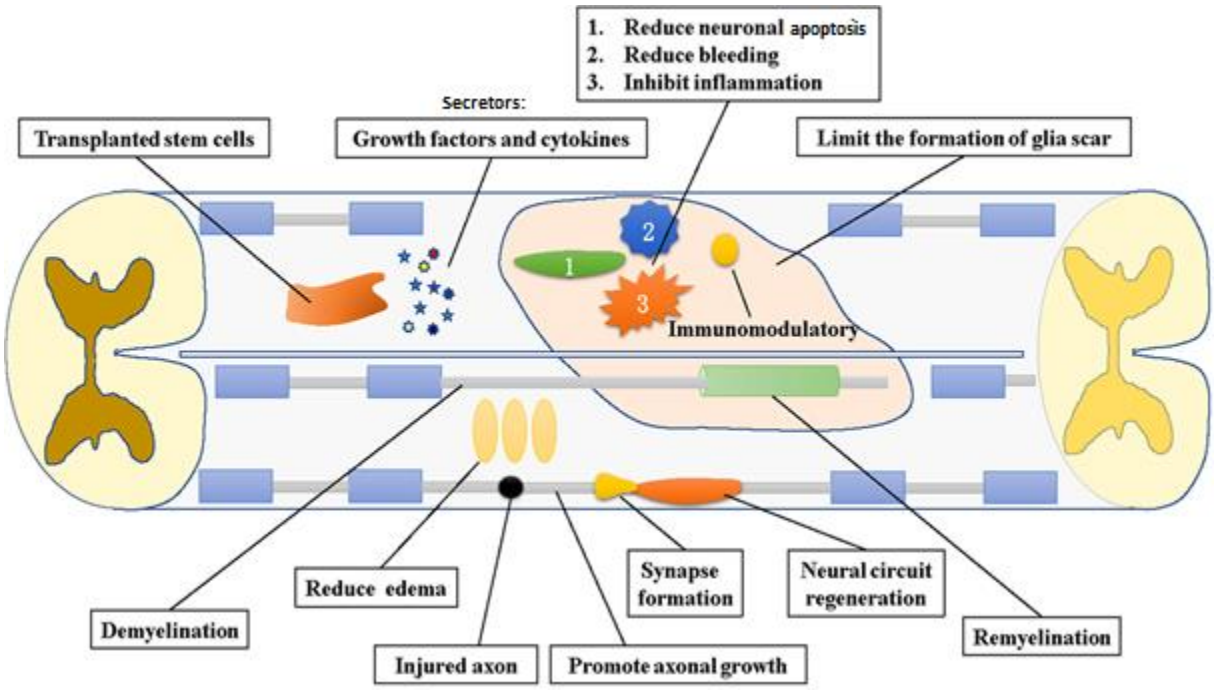

Figure 5. The potential mechanisms of action of stem cells in spinal cord injury (Shao A. at al., 2019).

Several types of cells, used in experimental model of spinal cord injury are studied for these conditions in a different degree. Particularly interesting are studies performed with the transplantation of mesenchymal stem cells, neural olfactory ensheathing cells (OECs) or human umbilical cord blood cells (HUCB) cells. Human OECs can stimulate regeneration and myelination of axons in damaged rat spinal cord and partially restore motor and sensory function (Ramon-Cueto A. et al., 1998). OECs produce a complex of neurotrophic factors, extracellular matrix proteins and neural cell adhesion molecules. The interest to these cells is supported by the possibility of autologous transplantation; the sampling of cells from olfactory area does not lead to a prolonged disruption of the sense of smell. OECs are actively investigated due to their low immunogenicity, availability, simplicity and safety of production and the ability to withstand long-term storage and usability autologous cells (Deng X.Y. et al., 2010; Park D.H. et al., 2011; Han Y.-F. et al., 2013).

Regenerative medicine is a generalized term for a variety of therapeutic and surgical cell technologies (organ regeneration and tissue engineering), aimed at the partial or full compensation of the damaged or lost organs (tissues) functions (Atala A. et al., 2008; Pal'cev M.P., 2009). In regenerative medicine there are two main directions. The first of them is a regenerative cell therapy associated with stimulation of the cell / tissue regeneration (cell-based tissue regeneration) by transplanting stem cells or their secretomes

associates with somatic cells (Kirschstein R. and Skieboll L.R., 2001; Repin V.S. et al., 2002; Stem cell technology, 2008). The second direction consists of restoration of integrity and function of tissues and organs using so-called bioartificial (tissue-engineering) construction (TEC): (biomaterial-based tissue regeneration). That includes the following components (Sevastianov V.I. and Kirpichnikov M.P., 2011): 1) cells capable to form a functional extracellular matrix; 2) suitable biodegradable carrier (matrix) for cell transplantation; 3) bioactive molecules (cytokines, growth factors), which have a bio stimulating effect on cells of the injured tissue. As a cellular component, cells of different types and different origins are used, including embryonic progenitor cells, multipotent mesenchymal stem cells (MSCs) and differentiated (specialized, tissue specific) cells from induced pluripotent stem cells (iPSC) (Kirschstein R. and Skieboll L.R., 2001; Repin V.S. et al., 2002; Pal'cev M.P., 2009; Stem cell technology, 2008). Autologous or allogeneic differentiated cells obtained by biopsy can be cultured *in vitro* and transplanted into the injury site.

Technologies of tissue engineering and regenerative medicine can be divided into three groups:

- bio stimulation of patient's tissue regeneration using bioactive materials.
- cell therapy - the use of stem cells or signal biomolecules for stimulation of tissue regeneration.
- tissue engineering of organs and tissues.

As a criterion of the adequacy of cell therapy for SCI are determined: the principal possibility of neural differentiation, the expression of the phenotype, which produces molecules important for regeneration in the new conditions of the microenvironment in the recipient tissue, the possibility of expansion *ex vivo* to obtain enough cells. It is important that transplanted cells migrate even to the most distant locations from the application site, and the ability for long-term survival into the tissue of the recipient to support the neurons survival and axonal growth. Oncogenic and infectious safety, minimally invasive procedures for the collection of material are also important for cell therapy in connection with the direct clinical implementation of research. Today, one of the criteria for selecting the cells designed for transplantation is the ability to transfect therapeutic genes with a high efficiency of expression in a tissue recipient. Several types of cells transplanted in an experimental model of spinal cord injury are satisfied for these conditions in various degrees.

The stem cells present in the adult nervous system are called the adult endogenous stem cells (AESCs). Ependymal cells, strip cells, and radial glial cells, located near the central canal of the spinal cord, have some stem cell properties. Although normally, these cells are latent/dormant, if there is any damage to the spinal cord, they immediately get triggered to produce more and more glial cells (Nomura T. et al., 2010). In some research projects, these cells have been transplanted into the lesions of animal hemiplegia (caused by SCI) models, where significant motor functional recovery has been observed (Nomura T. et al., 2010). As these endogenous cells can be directly activated without any traumatic cell transplantation, they are being studied as candidates for noninvasive cell therapy.

The olfactory ensheathing cells (OECs). There is significant interest in the study of transplantation of multipotent mesenchymal stem cells and neural (glial) cells of the olfactory structures, especially the olfactory bulb cells and olfactory endothelial cells. These specialized glial cells are like astrocytic pattern, but at the same time express several cytochemical characteristics of the Schwann cells and oligodendrocytes. The neurons of the olfactory epithelium are unique because during their life they are constantly renewed. They also direct the axonal growth from the peripheral nervous system and from the central nervous system (Murrell W. et al., 2005; Higginson J.R. and Barnett S.C., 2011). A composition of OECs obtained from biopsies of the olfactory region of the nasal mucosa contains both the olfactory neural epithelial cells and cells of the basal layer. However, in the culture, these cells form neurospheres; they express neuronal marker nestin as well as neuronal markers of glia and neurons. It is found that the OECs possess multipotency, and their differentiation depends on the presence of tissue-specific factors in the culture medium (Murrell W. et al., 2005). Human OECs are capable to stimulate regeneration and myelination of damaged axons in rat spinal cord and partially restore motor and sensory function. OECs produce a set of neurotrophic factors such as FGF1 (Key B. et al., 1996), FGF2 (Chuah M.I. and Teague R., 1999), NGF, BDNF, GDNF (Woodhall E. et al., 2001) and glial growth factor 2 (GGF2) (Chuah M.I. et al., 2000), extracellular matrix proteins (Treloar H.B. et al., 1996) and neural cell adhesion molecule (Miragall F. et al., 1988).

The mechanism of the positive impact of OECs transplantation in neuroregeneration process remains unclear. There are assumptions about the manifestation of immunocompetent cells properties in OECs and ability to modulate intensity of the processes of inflammation and secondary injury in SCI (Gorrie C.A. et al., 2010; Kalincik T. et al., 2010).

Schwann cells play an important role in the regeneration of the peripheral nervous system, due to the expression of neurotrophic growth factors, cell adhesion molecules, extracellular matrix molecules form a three-dimensional structure directing axonal growth. These properties could be used in the regeneration of the central nervous system. In the models of spinal cord contusion injury in the rat, it was shown that by the end of the second week after SCI in the process of remyelination of axons had participated not only oligodendrocytes but also endogenous Schwann cells (Keirstead H.S., 2005).

Under the normal conditions Schwann cells do not migrate from the peripheral nervous system to the CNS. But they appear in the central nervous system in demyelination foci in the region of traumatic injury. Schwann cells may be involved in myelination of axons in the CNS (Duncan I.D. and Hoffman R.L., 1997; Franklin R.J. and Barnett S.C., 1997). According to most researchers, the appearance of Schwann cells in the spinal cord injury is associated with their migration from peripheral nerve structures due to violation of the integrity of the barrier (Oudega M. and Xu X.M., 2006).

Participation of endogenous Schwann cells in the process of remyelination of central axons stimulated the use of Schwann cells from the various sources (including those obtained by directed differentiation of stem cells of different lineages) for transplantation into the site of spinal cord injury (Chi G.F. et al., 2010). Since differentiated oligodendrocyte precursors obtained from embryonic stem cells after the transplantation into the spinal cord differentiate into Schwann cells, they maintain remyelination and recovery of locomotor function (Totoiu M.O. and Keirstead H.S., 2005).

In January 2013 the United States began the first officially approved clinical trials of autologous Schwann cells transplantation to treat patients in the subacute phase of the thoracic spinal cord injury. Initially, the cells were obtained by biopsy of a sensory nerve of the lower limbs, then cultured, purified, and injected directly into the spinal cord. The preparation procedure takes 3-4 weeks, and this is the reason for the cell's application in the sub-acute phase of injury. Due to the high risk of operation, it was decided in the first stage to limit the transplantation of unmodified Schwann cells. According to the first published data, three months after the surgery, complications have been not identified in all eight patients.

Embryonic stem cells (ESCs) have been intensively studied since their discovery in 1964 (Kleinsmith L.J., and Pierce G.B. Jr., 1964), when it was shown that a single embryo cell can proliferate indefinitely in culture, giving rise to many types of mature cells. Out of all stem cells, embryonic stem cells have the greatest potential for use in substitution

therapy. However, due to the nature of embryonic stem cell research, there are a lot of controversial opinions on the topic. Since harvesting embryonic stem cells necessitates destroying the embryo from which those cells are obtained, the moral status of the embryo comes into question. Some claim that the 5-day old mass of cells is too young to achieve personhood or that the embryo, if donated from an IVF clinic (which is where labs typically acquire embryos from), would otherwise go to medical waste anyway. Opponents of ESC research claim that an embryo is a human life, therefore destroying it is murder and the embryo must be protected under the same ethical view as a more developed human being (King N.M. and Perrin J., 2014).

One of the great advantages of embryonic stem cells over other cell types is their accessibility to genetic manipulation. They can easily undergo genetic modifications while remaining pluripotent and can be selectively propagated, allowing the clonal expansion of genetically altered cells in culture. Since the first isolation of ESC in mice, many effective techniques have been developed for gene delivery and manipulation of ESC. These include transfection, electroporation, and infection protocols, as well as different approaches for inserting, deleting, or changing the expression of genes (Epsztejn-Litman S. and Eiges R., 2010). These methods proved to be extremely useful in mouse ES cells, for monitoring and directing differentiation, discovering unknown genes, and studying their function, which are now being initiated in human ESC.

Embryonic stem cells are derived from the inner cell mass of the blastocyst and then after the direct differentiation into the neural precursors transplanted to stimulate post-injured spinal cord regeneration (Dagci T. et al., 2009). Embryonic stem cells survive, migrate, and differentiate into neurons (10%), oligodendrocytes (60%), and astrocytes (10%) (McDonald J.W., 2004).

Transplanted embryonic stem cells are capable of proliferating and differentiating into the cells of new tissues and migrate and integrate into the existing structures of CNS. Numerous studies have shown that transplantation of embryonic stem cells into the spinal cord improves remyelination and functional recovery, but cardinal function improvement was not achieved (Zhang W. et al., 2010; Erdogan B. et al., 2010). Transplantation of human oligodendrocyte precursors derived from embryonic stem cells in the region of the spinal cord contusion injury of rat improved recovery of motor function (Keirstead H.S., 2005).

The most important problem of transplantation of embryonic stem cells is immunological rejection by the recipient. Essentially, there is a real danger of tumorigenicity.

Neural stem cells (NSC) are a type of progenitor stem cell that is extracted from the brain, spinal cord and optic nerve which are genetically predisposed to differentiate into the nervous tissue. Numerous studies in spinal cord injury showed that newly formed nerve cells migrate over long distances from the zone of injury, forming organized structures along the roads of damaged axonal processes and showing the potential ability to restore the broken relationships (Park D.Y. et al., 2013). Neural stem cells and glial-restricted precursors in experimental transplantation in spinal cord injury were broadly investigated (Hill C.E. et al., 2004; Cao Q. et al., 2005; Cummings B.J. et al., 2005; Mitsui T. et al., 2005; Boido M.D. et al., 2011). In several studies using labelled transplanted cells and myelin proteins as markers, showed that transplanted neural precursors differentiated only into astro- and oligodendroglial lineages (Vroemen M. et al., 2003; Pfeifer K. et al., 2004).

In recent years, special attention by experts in the field of cell therapy has attracted neural precursor cells from the tooth germ. Cells from the tooth pulp (Gronthos S. et al., 2002) and dental sac (Morsczeck C. et al., 2005) third molar (wisdom tooth) in the postnatal period exhibit the properties of mesenchymal stem cells retaining the ability to self-renew and differentiate into different cell types *in vitro* (Kerkis I. et al., 2008). Pulp cells secrete nerve growth factor, BDNF, GDNF and support the survival of sensory neurons *in vitro* and motoneurons *in vivo* (Nosrat I.V. et al., 2001).

Mesenchymal stem cells (MSCs), also called mesenchymal or stromal cells, mostly meet the criteria of minimally invasive cell therapy in the spinal cord injury, because they allow transplantation by administering to the blood or liquor. Due to disturbances of the blood brain barrier, these cells can penetrate the spinal cord injury epicenter, reaching (homing) and integrating into the damaged tissue. Mesenchymal stem cells are present in many tissues - umbilical cord blood, brain, liver, adipose tissue, lung, and amniotic fluid. Therapeutic applicability of mesenchymal stem cells is based on three fundamental features: the ability to differentiate into different types of tissue cells (multipotency), immunomodulatory effects and secrete tissue-specific bioactive factors (paracrine activity) (Lavoie J.R. and Rosu-Myles M., 2013).

However, the ability of MSCs to differentiate into various cell types *in vivo* during transplantation into the body is substantially limited, as well as survival, which in the best case does not exceed several months (Forostyak S. at al., 2013, Qu J. and Zhang H., 2017,

Sykova E. At al., 2021). Results of long-term studies indicate that the therapeutic efficacy of mesenchymal stem cells are caused not by their ability to differentiate, but mainly by anti-inflammatory and paracrine activity (Lavoie J.R. and Rosu-Myles M., 2013). In experimental model of spinal cord injury, the application of following types of mesenchymal cells are examined: mesenchymal stem cells, hematopoietic stem cells, bone marrow stromal cells, the cells of the umbilical cord and cord blood.

Bone marrow mesenchymal cells (BMSCs) were the first cell type used for traumatic injury treatment in experimental and clinical trials alike (Syková E. et al., 2006a). Primary studies based on the thoracic spinal cord contusion and BMSC transplantation in rats showed partial improvements in motor, sensory, and autonomic functions as well as in tissue sparing (Syková E. et al., 2006b). Interestingly, similar beneficial effects were detected when BMSCs were administered locally into the cavity of the spinal cord (Nandoe R.D.S. et al., 2006), intrathecally (Cizkova D. et al., 2011) or systemically (Cízková D. et al., 2006; Osaka M. et al., 2010). In a rat SCI model, as in balloon-induced compression lesion (Vanický I. et al., 2001), BMSCs were grafted intravenously at 1 week after injury. Behavioral testing revealed a significant improvement in motor and sensory tests (Jendelová et al., 2004).

In these studies, magnetic resonance imaging (MRI) was used as a non-invasive method of studying the progress of transplanted cells in SCI *in vivo* (Jendelová P. et al., 2003, 2004; Syková E. and Jendelová P., 2005). Superparamagnetic iron-oxide nanoparticles were inserted into adult BMSCs during their cultivation prior to their transplantation into the animals with SCI. The BMSCs were then visible in the MRI images of SCI as hypointensive signals persisting for more than 4 weeks. *Ex vivo* Prussian blue histological staining for iron confirmed iron-positive cells at the lesion site (Syková E. and Jendelová P., 2005; Sykova E. and Jendelova P., 2007).

These promising preclinical studies initiated a series of I/II clinical trials delivering BMSCs (autologous and allogenic) or mononuclear fractions in patients with acute, sub-acute, or chronic SCI. In summary, the results from these clinical trials demonstrate that BMSCs are safe and without adverse effects. One of the first studies used all mononuclear cells from BM (Syková E. et al., 2006a). Partial improvement in the American Spinal Injury Association (ASIA) score and recovery of motor-evoked potentials and somato-sensory evoked potentials were observed in several patients when treated during the acute or sub-acute phase. Subsequently, a number of phase I/II clinical studies were launched in Korea, Japan, India, Egypt, China, Brazil, Chile, and Switzerland (Forostyak S. et al.,

2013; Muthu S. et al., 2020; Silvestro S. et al., 2020, *clinicaltrials.gov*). The results of these studies are modest but promising. However, regardless of the promising results achieved, larger groups of patients are required before any practical statements can be drawn (Forostyak S. and Sykova E., 2017).

Umbilical cord blood cells are characterized by high immunogenicity, availability, simplicity and safety of production and the ability to withstand long-term storage. Umbilical cord blood mononuclear cells (mononuclear UCBCs) fraction contains an extremely heterogeneous mixture of hematopoietic, mesenchymal stem cells, progenitor endothelial cells and other cell precursors. In addition, there is also a small fraction of non-hematopoietic multipotent stem cells negative for CD34, which express protein SSEA-4, specific for embryonic stem cells, and the transcription factors OCT4, SOX2 and NANOG - markers of pluripotent cells. The ability of these cells to differentiate into the cell types of all three germ layers was proved experimentally. Mesenchymal stem cells isolated from the UCBCs, have a high degree of morphological and molecular homology with MSCs of bone marrow and peripheral blood, including the absence of hematopoietic surface antigens. However, unlike the mesenchymal stem cells from bone marrow, MSCs from umbilical cord blood have a greater ability to reproduce *ex vivo*, a higher proliferation rate and low immunogenicity (Lavoie J.R. and Rosu-Myles M., 2013).

Besides the possibility for substitution of damaged neurons and oligodendrocytes, the mesenchymal stem cells play an important supporting role in the treatment of spinal cord injury by the regulation of immune response, expression of cytokines and growth factors. They also improve vascularization and tissue preservation and suppress the process of cavitation. Entered the bloodstream, mononuclear UCBCs migrate and accumulate in the damaged area of the CNS. Administration of human umbilical cord blood cells into the bloodstream leads to inhibition of the inflammatory response, has neurotrophic effects, stimulates neovascularization (Chen C.T. et al., 2008; Chen M. et al., 2013), reduces the expression of pro-apoptotic genes and supports neuronal survival (Dasari V.R. et al., 2009).

On the model of spinal cord injury in the dog, it was shown the opportunity of human umbilical cord blood cells to amplify remyelination of peripheral-type myelin sheaths formation (Lee J.W. et al., 2012). After the hemisection in rats, the transplantation of CD34+ mononuclear UCSCs led to the improvement of motor functions (Kaner T. et al., 2010). Transplanted cells in the damaged zone immediately after the spinal cord contusion injury in rats undifferentiated human mononuclear UCBCs under

immunosuppression survived for at least six weeks and successfully facilitated functional recovery in comparison to the control group. However, it did not affect the size of the pathological cavity (Rodrigues L.P. et al., 2012).

Despite significant functional improvements it was found that transplantation of mononuclear UCBCs and CD34 positive cells in the spinal cord had not led to their differentiation into neural or glial cells (Rodrigues L.P. et al., 2012; Ning G. et al., 2013). As the mechanism of the impact of hematopoietic stem cells in SCI is considered the weakening of infarction tissue and apoptosis (Park D.H. et al., 2011), as well as secretion of thrombopoietin and interleukin-11, cytokines important for the survival and differentiation of endogenous neural precursor cells (Rodrigues L.P. et al., 2012).

Examples including clinical trials of stem cells are still rare. They mainly concern the mesenchymal stem cells from bone marrow. Currently, there is a limitation of the use of mesenchymal stem cells in the clinic due to a small amount of mesenchymal and progenitor cells in umbilical cord blood. Therefore, most of the studies on the therapeutic use of mononuclear UCBCs in spinal cord injury performed without isolating specific stem cell lines. Considerable efforts are focused on the development of effective methods of breeding and selection of the UCBCs as well as isolation of fraction of CD133- immature and CD34 positive hematopoietic cells from the umbilical cord blood.

There was a case of successful use of mesenchymal stem cells from umbilical cord blood to treat a patient with a fracture of the spine at the level of L1 (Ichim T.E. et al., 2010). UCSCs CD34-positive cells were injected intrathecally at 5, 8 and 14 months after injury. It was reported the recovery of muscle function, bowel, and sexual ability, without serious side effects. Recently published results of clinical trials conducted in China on 22 patients with spinal cord injury (Liu J., et al., 2013). Each patient received on $1x10^6$ injected mesenchymal stem cells from umbilical cord tissue intrathecal once a week for a month. Out of 16 patients with incomplete injuries, improvement was achieved in 13. It was noted the recovery in varying degrees of motor or sensory function, or both, as well as the recovery of bowel function and urinary bladder. In 6 patients with a complete violation of the integrity of the spinal cord no improvements were observed. However, following-up of these patients for 3 years also showed improvements. During this period, it was observed no serious complications or deterioration of achieved results.

Induced pluripotent stem cells (iPSCs) offer new prospects for regenerative medicine. Human iPSCs share many properties with human ESCs, including their stemness profile, self-renewal ability and differentiation potential (Nakamura M. et al., 2013).

Moreover, iPSCs have the advantage of being patient specific. Therefore, neural precursors derived from human iPSCs (iPSC-NPs) appear to be an ideal source for transplantation therapy in SCI. However, the efficacy of iPSC-NP transplantation in SCI treatment and the mechanisms responsible for functional improvement remain to be fully elucidated.

Despite advances in research of induced pluripotent stem cells, their use in clinical practice is still limited due to a lack of preclinical experiments. Neural precursors (NPs) derived from a clone of human iPSCs (IMR90) were used to treat a rat spinal cord lesion one week after induction of injury. Functional recovery was evaluated using Basso-Beattie-Bresnahan open field locomotor test, beam walking, rotarod and plantar tests. Lesion morphology, endogenous axonal sprouting, graft survival and iPS-NP differentiation were analyzed immunohistochemically (Romanyuk N. et al., 2014). Quantitative polymerase chain reaction (qPCR) was used to evaluate the effect of transplanted iPS-NPs on endogenous regenerative processes and to monitor their behavior after transplantation. Human iPS-NPs robustly survived in the lesion, migrated, and partially filled the lesion cavity during the entire period of observation (Romanyuk N. et al., 2014). Transplanted animals displayed significant motor improvement already from the second week after the transplantation of iPS-NPs. qPCR revealed the increased expression of human neurotrophins in 8 weeks after transplantation. Simultaneously, the white and gray matter was spared in the host tissue. The grafted cells were immunohistochemically positive for doublecortin, MAP2, III-tubulin, GFAP and CNPase in 8 weeks after transplantation. Human iPS-NPs further matured and in 17 weeks after transplantation differentiated towards interneurons, dopaminergic neurons, serotoninergic neurons and ChAT-positive motoneurons. Human iPS-NPs possess neurotrophic properties that are associated with significant early functional improvement and the sparing of spinal cord tissue. Their ability to differentiate into tissue-specific neurons leads to the long-term restoration of the lesioned tissue, making the cells a promising candidate for future cell-based therapy of SCI (Romanyuk N. et al., 2014).

Radial glial cells promote direct regeneration of axons (Nomura T. et al., 2010). On the other hand, Chang (Chang C.H. et al., 2009) states that the radial colloid is most important for improving the symptoms of SCI after radial glial cell transplantation. There has also been research work on which neurons were generated *in situ* by glial cell reprogramming with an aim to recover the spinal cord (Cheng C.H. et al., 2015). It was introduced SOX2 into damaged spinal glial cells via gene transfer and administered histidine deacetylase and valproic acid to reprogram them into neurons (Su et al. 2014).

Thus, the analysis of the literature on the use of cell therapy in spinal cord injury suggests the possibility of improving the progress of neuroregeneration. As the regenerative effects of each stem cell type varies, a treatment plan must consider both the characteristics of the type of injury as well as the characteristics of the corresponding cell types they want to apply. As stem cell therapy fails to completely dock different SCIs, with the most appropriate transplanted stem cells, their efficacy cannot be validated completely.

1.5. Magnetic stem cell delivery strategy for spinal cord injury therapy

Despite the noticed therapeutic benefits, stem cell transplantation, in general, has several serious limitations related to the low efficiency of delivery, retention and engraftment of cells (Weissman I.L., 2000; Al Kindi A. et al., 2008). To achieve a significant therapeutic benefit, minimally invasive but highly effective delivery strategies are crucial aspects for cell transplantation. It should also ensure proper retention and longevity of the cells. Interestingly, intrathecal injection (Figure 6) of stem cells has considerable advantages (higher efficacy of delivery, better retention, and survival of stem cells) over intravenous injection as a means of cell transplantation (Wu S.F. et al., 2002; Pluchino S. et al., 2003; Bakshi A. et al., 2004). Moreover, it has been demonstrated that repetitive, but not single intrathecal administration of MSCs contributes to their migration into the central lesion and aids functional recovery after SCI in rats (Cizkova D. et al., 2011, Tyler J.Y. et al., 2013). Effective cell targeting is therefore highly desirable to promote the homing of transplanted cells to the site of injury. In this regard, the use of labeling with magnetic nanomaterials represents novel effective strategy for targeting delivery, particularly in SCI (Tyler J.Y. et al., 2013).

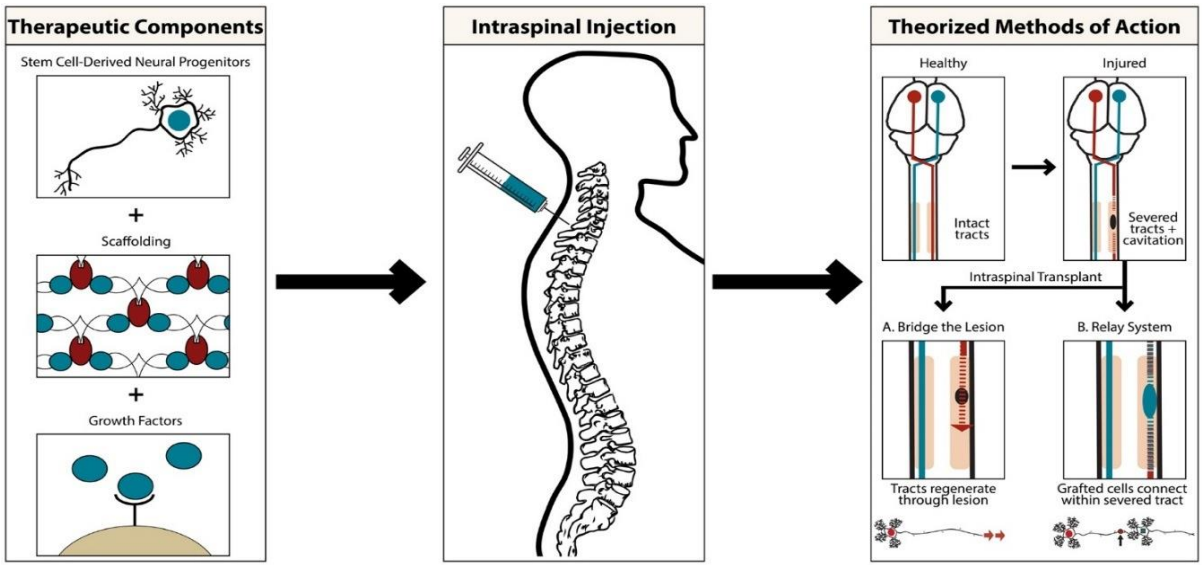

Figure 6. A combinatorial strategy for cell-based therapies in SCI. Cellular transplantation may be augmented with a combination of growth factors, scaffolds, or other biomaterials that improve cell survival, engraftment, and differentiation. Intraspinal application of these therapies leads to engraftment of transplanted cells, which may promote neural regeneration through several proposed mechanisms. Engrafted cells may provide a conduit for host axonal outgrowth across the site of injury. Alternatively, engrafted cells may act as a relay system by synapsing with neurons located cranial and caudal to the injury site (Jin M.C. et al. 2019).

Several research lines have demonstrated the efficient loading of stem cells with superparamagnetic iron oxide nanoparticles (SPIONs) and have shown that magnetically guided cell delivery is able to boost cell retention, engraftment as well as the functional benefit of the cell therapy (Landazuri N. et al., 2013; Vandergriff A.C. 2014; Cheng K. et al., 2014). Indeed, magnetic forces have already been successfully used to direct SPION-labelled cells into a vascular graft (Pislaru S.V. et al., 2006), intra-arterial stents (Polyak B. et al., 2008), the femoral artery (Riegler J. et al., 2013), bone (Panseri S. et al., 2012), cartilage (Kamei G. et al., 2013), and the retina (Yanai A. et al., 2012). However, in the case of SCI, studies on magnetically guided cell delivery have not been thoroughly performed. In fact, only two research groups have shown the therapeutic potential of the magnetic delivery of SPION-labelled cells to the SCI lesion site (Nishida K. et al., 2006; Hamasaki T. et al., 2007; Vanecek V. et al., 2012).

A common disadvantage of all previous strategies for cell delivery that utilize magnetic systems (Häfeli U.O. et al., 2006; Polyak B. et al., 2008; Zablotskii V. et al., 2010; Riegler J. et al., 2013) is their inappropriate focusing ability. Indeed, magnetic capturing of the cells takes place in the vicinity of a magnetic pole where the magnetic field gradient reaches its maximal value (Figure 7, 8). However, since a magnet cannot be placed directly into the lesion site, the focusing ability of such systems is rather limited and not convenient for efficient stem cell transplantation. Most magnet-induced cell delivery

techniques (Polyak B. et al., 2008, Riegler J. et al., 2013, Hafeli U.O. et al., 2006, Zablotskii V. et al., 2010) share the same drawback i.e., their poor focusing ability.

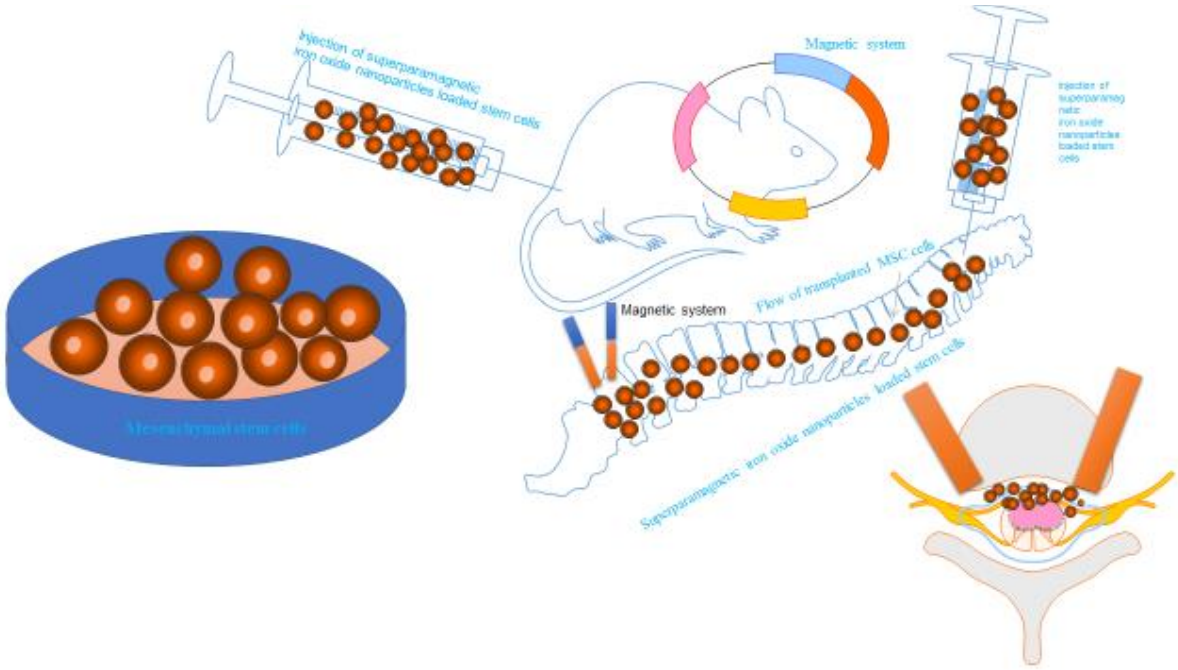

Figure 7. Schematic representation of SPION-labelled mesenchymal stem cells to the spinal cord injury lesion by magnetic field. Mesenchymal stem cells were loaded with micro-size iron particles. A group of rats with induced spinal cord injuries were injected with the loaded stem cells. A toy magnet situated near the animal's neck was used to externally guide the cells to the lesion site. The retention rates of the MSC at the site of injury increased three times and the subsequent therapy was much more effective. The magnet bearing ring was then positioned around the rat at the 10th thoracic vertebra level for two hours.

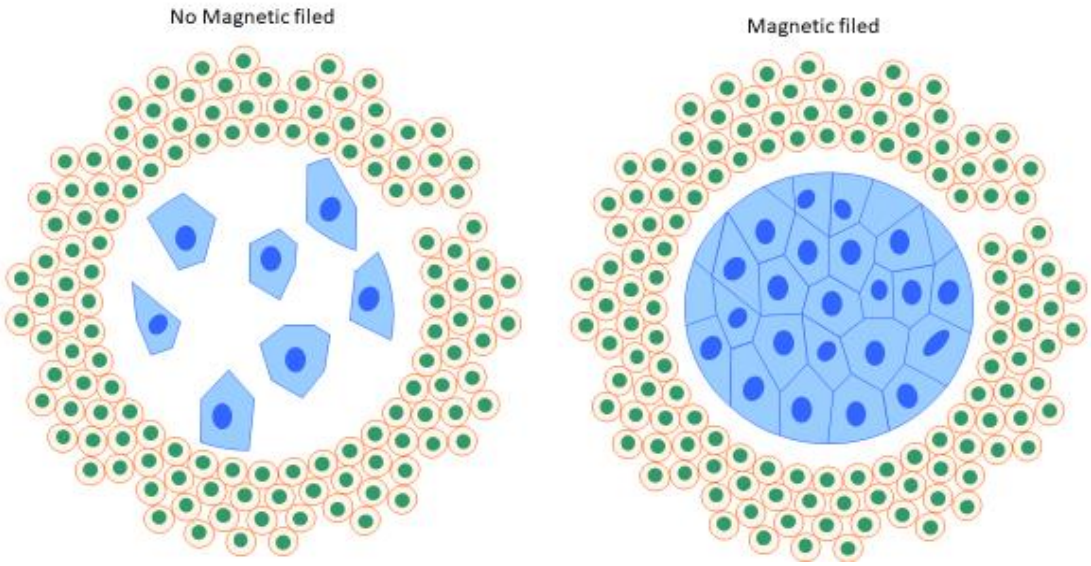

Figure 8. Influence of magnetic field on spreading of labelled cells inside hydrogel.

All's mentioned above indicates the need for a more efficient magnetic systems for stem cell delivery to the site of spinal cord injury.

1.6. Biomaterials as scaffolds for spinal cord injury repair

It is generally accepted that transplanted MSCs do not differentiate into neuronal or glial cells, but their therapeutic effects are associated with their ability to release a variety of antiapoptotic, neurotrophic, and anti-inflammatory molecules (Urdzikova L. et al., 2014; Ruzicka J. et al., 2017; Krupa P. et al., 2018; Chudickova M. et al., 2019; Petrenko Y. et al., 2020). The regenerative effects and functional recovery in SCI after intrathecal MSC transplantation, without the transplanted cells being integrated into the damaged tissue were demonstrated previously (Urdzikova L. et al., 2014; Krupa P. et al., 2018). Moreover, a comparable therapeutic effect has also been shown after the intrathecal delivery of conditioned media containing a complex of MSC-secreted products, developed as a cell-free alternative to cell therapy (Amemori T. et al., 2015; Cizkova D. et al., 2018; Chudickova M. et al., 2019). In contrast to intrathecal application, intralesional cell transplantation may provide higher cell retention and more localized and focused cell effects at the site of delivery. However, the efficacy of intralesional transplantation is often limited by poor cell survival in the unfavorable microenvironment of the injured neural tissue.

Various biomaterials of synthetic [e.g., 2-hydroxyethylmethacrylate, hydroxypropylmethacrylamid, poly L-lactic acid, poly(lactic-co-glycolic acid), poly-L-lysine, and polyethylene glycol] as well as natural origin [e.g., Hyaluronic acid (HA), alginate, chitosan, collagen, fibrin, and ECM scaffolds] have been developed to bridge the lesion and provide a stimulatory microenvironment to support the survival and efficacy of transplanted cells (Hejcl A. et al., 2010; Kubinova S. and Sykova E., 2012; Liu S. et al., 2019). In fact, scaffolds promote MSC adhesion and their survival. The effects of cell-seeded biomaterial scaffolds on improved axonal regrowth or enhanced functional outcomes after SCI than scaffolds alone have been shown in many studies (Hejcl A. et al., 2010; Kim Y.C. et al., 2016; Blasko J. et al., 2017; Peng Z. et al., 2018; Zaviskova K. et al., 2018) and reviewed in Libro R. et al. (2017) and Yousefifard M. et al. (2019).

The composition of scaffolds together with their physical properties, such as stiffness, pore size, and porosity, or three-dimensional structures should mimic the target tissue and allow appropriate scaffold integration into the site of transplantation. Additionally, the development of different types of scaffolds for 3D culture enables the

generation of *in vitro* neural-like tissue as a new approach for modeling and tackling diseases of the brain and CNS (Murphy A.R. et al., 2017).

Despite the lack of an "ideal material" to be used as a scaffold in order to promote the desired reparative processes after mammalian SCI, all candidates should possess several characteristics, as follows (Liu S. and Cao L., 2007, Tabesh H. et al., 2009):

1) Biocompatibility (that is, neither cytotoxic nor systemically toxic).

2) Immunologically inactive.

3) Controlled biodegradability or bio-resorbability.

4) Possessing inter-connecting stable pores of appropriate size to promote integration, diffusion and vascularisation.

5) Mechanically similar to the extracellular environment, thus making the scaffold suitable for implantation into the intended site and permitting its fabrication in a variety of shapes and sizes.

6) Should not induce any adverse response including additional mechanical damage to the nervous tissue.

7) Should lessen glial scar formation while facilitating cell adhesion and axonal sprouting.

Hydrogels have proved to be the most convenient material, especially due to their ability to retain high levels of water and potential to adjust their mechanical properties to imitate soft nervous tissue. The benefit of the hydrogels is their injectability, which enables *in situ* gelation in lesion cavities of irregular shape together with cell or drug encapsulation. Hydrogels for CNS repair are commonly based on ECM, such as hyaluronic acid (HA), collagen, or gelatine. HA, as a component of the ECM, is a biomaterial which is widely used in various clinical settings; it is biocompatible, biodegradable, and non-immunogenic. Native HA does not form a gel or promote cell adhesion, so various physical and chemical crosslinking methods have been developed to prepare injectable HA hydrogels. The neuroregenerative potential of an enzymatically crosslinked hydroxyphenyl derivative of HA modified with the integrin-binding peptide arginine–glycine–aspartic acid in the case of subacute spinal cord hemisection was previously demonstrated (Zaviskova K. et al., 2018). The hydrogels filled the lesion, promoting vascularization and axonal ingrowth into the lesion, and this effect was further potentiated in combination with human Wharton's jelly-derived MSCs (Zaviskova K. et al., 2018).

Other interesting materials are biological **extracellular matrix** (ECM) scaffolds prepared by means of tissue decellularization, which removes cellular components from

the tissue. These materials recapitulate the complex biochemical composition of ECM and mimic the native cell environment. The composition of ECM scaffolds can vary between tissues, but the most abundant compounds are collagen, glycosaminoglycans, fibronectin, or laminin (Costa A. et al., 2017). Generally speaking, decellularized scaffolds can be prepared as solid fibrous structures, sponges, or sheets and can also be further solubilized into the form of injectable ECM hydrogel (Costa A. et al., 2017). The advantage of ECM hydrogels is their ability to physically crosslink *in situ* at physiological pH and temperature, which allows their non-invasive injection into the lesion or cavity (Kubinova S., 2017).

For CNS repair, ECM hydrogels derived from porcine brain, spinal cord, or urinary bladder has been evaluated in *in vitro* as well as *in vivo* studies (Crapo P.M. et al., 2014; Hong J.Y. et al., 2020). Remarkably, using adult CNS tissues as a source of ECM matrix might be limited due to the presence of factors which suppress axonal growth, such as chondroitin sulfate proteoglycans and myelin-associated molecules. In this context, it has been demonstrated that decellularization in the adult optic nerve selectively removes the inhibitory compounds of the CNS tissue and preserves some axon-promoting ECM proteins, including collagen IV and laminin (Sun J.H. et al., 2020). It should therefore be emphasized that, for the development of CNS-derived ECM scaffolds, the extent of tissue decellularization must maintain an optimal balance between the effective clearance of myelin and myelin-related inhibitory factors while retaining compounds with neurotrophic properties.

Besides xenogeneic or allogeneic cadaveric tissues, ECM derived from fetal human tissue, such as the umbilical cord, represents a promising source for tissue engineering due to its human origin, easy accessibility, and absence of ethical constraints. Efficient and reproducible decellularization protocols were developed for the production of ECM-based hydrogel derived from human umbilical cord tissue and their *in vitro* biocompatibility and similarity with ECMs derived from porcine tissues such as urinary bladder, spinal cord, and brain were proved (Koci Z. et al., 2017). Moreover, the mechanical strength and bio-stability of ECM hydrogels can be further improved by crosslinking with genipin (Vyborny K. et al., 2019).

Injectable hydrogels are suitable carriers for cell or drug delivery, but during *in situ* gelation, they usually do not allow controllable microporosity, which could guide regenerating axon growth through the lesion. For this purpose, various types of solid fibrous or multichannel polymer conduits have been proposed as providing directional

support for regrowing axons together with cell or drug delivery (Liu S. et al., 2017). Such conduits are mostly implanted into the complete spinal cord transection after removal of the spinal segment. Importantly, micro/nano-structures in nerve conduits have proved to be essential in tuning a large variety of post-implantation effects (Sun X. et al., 2019).

For example, Chen X. et al. (2020b) showed the regenerative effect of BMSCs seeded into a chitosan tubular scaffold combining the two architectures of a single H-shaped central tube and several microchannels. The scaffold was implanted to bridge the 5-mm defect of a complete transverse lesion in the thoracic spinal cord of rats, and when compared with the empty scaffold, the BMSC enhanced functional improvement and the number of regenerating axons and elicited antiapoptotic effects (Chen X. et al., 2020b). Peng Z. et al. (2018) showed that rat MSCs combined with a nerve-guide collagen scaffold inhibited chronic scar formation, provided linear guidance for the nerves, and promoted M2 polarization to form an anti-inflammatory environment in a hemisected SCI rat model (Peng Z. et al., 2018). Deng W.S. et al. (2020) transplanted human WJMSCs on collagen scaffolds into complete spinal cord transection in rats and dogs. The transplantation improved motor scores, enhanced amplitude, shortened the latency of motor evoked potential, and decreased the lesion area, which was further potentiated when the scaffold was used in combination with stem cells (Deng W.S. et al., 2020).

SIKVAV-modified superporous poly (2-hydroxyethyl methacrylate) hydrogel with oriented pores was previously tested (Kubinova S. et al., 2015). The hydrogels, either empty or seeded with rat MSCs, were implanted in the spinal cord transection. However, MSCs seeded in the scaffold did not enhance tissue infiltration into the pores, and only rare axons crossing the hydrogel bridge were observed after 6 months, which suggests that this type of scaffold did not provide an optimal environment for neural tissue repair (Hejcl A. et al., 2018).

To support the effects of MSCs, combined strategies have been proposed to further stimulate axonal growth and tissue regeneration. For example, the effect of rat BM-MSCs in a multichannel polymer poly (lactic-co-glycolic acid) scaffold was enhanced by their co-transplantation with Schwann cells, which promoted MSC survival and differentiation into neuron-like cells and resulted in the regeneration of axons and functional recovery after complete spinal cord transection (Yang E.Z. et al., 2017).

Despite the number of preclinical studies using various scaffolds for SCI repair, only a few of them are currently approved for clinical trials. The safety and benefit of implantation of poly(lactic-co-glycolic acid)-b-poly(L-lysine) scaffold (neuro-spinal

scaffold) has been evaluated in patients with thoracic AISA A spinal cord injury at a level of injury of T2–T12 (NCT02138110). No adverse effects related to acute scaffold implantation were reported in the 6-month study (Layer R.T. et al., 2017).

In another clinical study, a collagen scaffold with linearly aligned pores and functionalized with neuroactive factors (NeuroRegen scaffold) was loaded with autologous BM mononuclear cells and transplanted into the surgically cleaned lesion in seven patients with acute complete SCI. No adverse symptoms were present in the 3-year follow-up period. In some patients, partial sensory and autonomic nervous functional improvements, but no motor function recovery, were observed (Chen W. et al., 2020a). In the following study, a NeuroRegen scaffold was loaded with human WJMSCs and implanted into the surgically cleaned lesion in eight patients with chronic complete SCI. No adverse events were reported during 1 year of follow-up. In some patients, increase of sensation level and motor evoked potential-responsive area, enhanced finger activity and trunk stability, defecation sensation, and autonomic neural function recovery were found (Zhao Y. et al., 2017).

Deng W.S. et al. (2020) published the results of a phase I clinical trial on 40 patients with acute complete cervical injuries. The group of patients (n = 20) obtained collagen scaffolds seeded with MSCs derived from umbilical cord tissue. No serious complications were reported during the 12-month follow-up. In the treatment group, an improvement in neurological functions was observed over the follow-up period, while no neurological functions were improved in the control group of patients (Deng W.S. et al., 2020).

An overview of recent advances in the application of matrix materials, alone or in combination with stem cells/growth factors, to treat SCI is presented in Table 5 (Kubinova S. and Sykova E., 2012).

Encouraging first clinical results indicate the safety and feasibility of MSC-seeded scaffold-based therapy in SCI repair; however, the observed weak functional recovery suggests the need to develop more advanced combinatorial approaches which would further target the inhibitory environment of the adult CNS tissue as well as the limited regenerative ability of the long-track axons.

Table 3. Completed clinical trials on stem cell therapy in acute SCI (Jin M.C. et al., 2019).

ClinicalTrials.gov Identifier	Title	Phase (s)	No. Enrolled	Completion Date	Primary end Point	Secondary end Point	Interventi on	Injection Site	Status	Results Pub	Findings
	Autologous Bone Marrow Transplantation in Patients With Subacute and Chronic Spinal Cord Injury	I/II	20	2006	Safety	NA	Autologou s BM-MSCs	Intravenous , intra-arterial	Completed	Sykova E. et al., 2006	NA
NCT02482194	Autologous mesenchymal stem cells transplantation for spinal cord injury-a phase I clinical study	I	9	Mar 2016	Safety	NA	Autologou s BM-MSCs	Intrathecal	Completed	Satti H.S. et al., 2016	Intrathecal administrati on of BM-MSCs is safe w/ no adverse events
NCT01186679	Safety and efficacy of autologous bone marrow stem cells in treating spinal cord injury	I/II	12	Aug 2010	Safety/ASI A score	NA	Autologou s BM-MSCs	Intrathecal	Completed	NA	NA
NCT02027246	Safety and efficacy of stem cell therapy in spinal cord injury	I	166	Feb 2013	Safety	NA	Autologou s BM-MSCs	Intrathecal	Completed	NA	NA
NCT01769872	Safety and effect of adipose tissue derived mesenchymal stem cell implantation in patients with spinal cord injury	I/II	15	Jan 2016	ASIA score	MRI; MEP/SSEPs; ADL; SF-36; ODI; safety	Autologou s AD-MSCs	Intravenous ; intrathecal	Completed	NA	NA

NCT01873547	Different efficacy between rehabilitation therapy and stem cells transplantation in patients with SCI in China	III	300	Dec 2015	ASIA score	McGill Pain Questionnaire; Barthel Index; SSEPs/MEPs	U-MSCs	Intrathecal	Completed	NA	NA
NCT01274975	Autologous adipose derived MSCs transplantation in patient with spinal cord injury	I	8	Feb 2010	Safety	NA	Autologous AD-MSCs	Intravenous	Completed	Ra J.C. et al., 2011	Intravenous administration of AD-MSCs is safe w/ no adverse events
NCT01624779	Intrathecal transplantation of autologous adipose tissue derived MSC in the patients with spinal cord injury	I	15	May 2014	MRI changes	NA	Autologous AD-MSCs	Intrathecal	Completed	NA	NA
NCT01328860	Autologous stem cells for spinal cord injury (SCI) in children	I	10	Jun 2016	ASIA score	Neuropathic pain	Autologous BM-MSCs	Intravenous	Terminated	NA	NA
NCT01162915	Transfer of bone marrow derived stem cells for the treatment of spinal cord injury	I	10	May 2014	Safety	NA	Autologous BM-MSCs	Intrathecal	Suspended	NA	NA
NCT02163876	Study of human central nervous system (CNS) stem cell transplantation in cervical spinal	II	31	May 2016	ISNC-SCI upper-extremity scores	Safety	Human CNS stem cells	Intramedullary	Terminated	NA	NA

	cord injury										
NCT02237547	Safety and feasibility study of cell therapy in treatment of spinal cord injury	I/II	0	Oct 2019	Safety	ASIA score; Frankel grade	Autologous BM-MSCs; allogeneic AD-MSCs	Intrathecal; intravenous	Withdrawn	NA	NA
NCT01725880	Long-term follow-up of transplanted human central nervous system stem cells (HuCNS-SC) in spinal cord trauma subjects	I/II	12	May 2016	ASIA score	NA	Human CNS stem cells	Intramedullary	Terminated	NA	NA
NCT01393977	Difference between rehabilitation therapy and stem cells transplantation in patients with spinal cord injury in China	II	60	May 2012	EMG; ENP test	NA	U-MSCs	Intrathecal	Completed	Cheng H. et al., 2014	Patients receiving U-MSCs demonstrate improved urinary control, muscle tension, motion, & self-care ability
NCT01694927	Autologous mesenchymal stem cells in spinal cord injury (SCI) patients (MSC-SCI)	II	30	Jun 2014	Safety	Muscle, sphincter; spastic control	Autologous MSCs	Intralesional	Unknown	NA	NA
NCT01730183	To study the safety and efficacy of autologous bone	I/II	15	Nov 2014	Safety	ASIA score	Autologous BM-MSCs	Intrathecal	Unknown	NA	NA

	marrow stem cells in patients with spinal cord injury (ABSCI)										
NCT01833975	Study the safety and efficacy of bone marrow derived autologous cells for the treatment of spinal cord injury (SCI)	I/II	50	Sept 2016	Frankel grade	Pain sensation; ASIA score	Autologous BM-MSCs	Intrathecal	Unknown	NA	NA
NCT01446640	Mesenchymal stem cells transplantation to patients with spinal cord injury (MSC)	I/II	20	Jun 2014	Safety	EMG; ENP test; ASIA & Frankel grade	Autologous BM-MSCs	Intravenous; intrathecal	Unknown	NA	NA
NCT02034669	Transplantation of autologous adipose derived stem cells (ADSCs) in spinal cord injury treatment	II	48	Mar 2015	Safety	MRI; urinary & bowel function; EMG; ASIA score	Autologous AD-MSCs	Intradural; intrathecal; intravenous	Unknown	NA	NA

ADL = activities of daily living; EMG = electromyography; ENP = electroneurophysiological; ISNC-SCI = International Standards for Neurological Classification of Spinal Cord Injury; NA = not applicable; ODI = Oswestry Disability Index; Pub = published; SSEP = somatosensory evoked potential.

Despite the scarcity of published results outlining findings in cell-based SCI therapy trials, early trials suggest a lack of serious adverse effects associated with the introduction of MSC-derived therapies. The majority of completed studies evaluated MSC-derived cell transplantation, necessitating additional inquiry into iPSC-centered methods and combinatorial approaches. (Results were queried from the NIH clinical trial repository [clinicaltrials.gov] using the key terms "spinal cord injuries" and "stem cell." Filtering was done to only include trials addressing acute or subacute SCI. Completed, suspended, and terminated trials are included the table. Unknown trials with a past expected end date are also included.) Soucee: (Jin M.C. et al., 2019).

Table 4. Currently active/recruiting trials exploring cell therapy in acute SCI (Jin M.C. et al., 2019).

ClinicalTrials.gov Identifier	Title	Phase(s)	No. Enrolled	Completion Date	Primary End Point	Secondary End Point	Intervention	Injection Site	Status
NCT02326662	Neural stem cell transplantation in traumatic spinal cord injury	I/II	30	Dec 2018	Feasibility/safety	324-point ASIA; MRI	Autologous NSCs + 3D matrix	Intraspinal; intrathecal	Active, not recruiting
NCT02481440	Umbilical cord mesenchymal stem cells transplantation to patients with spinal cord injury	I/II	44	Dec 2018	ASIA score; IANR-SCIRFS score	Adverse events; EMG/ENP test; MRI	Allogeneic UC-MSCs	Intrathecal	Recruiting
NCT03521336	Intrathecal transplantation of UC-MSC in patients with sub-acute spinal cord injury	II	130	Dec 2022	ASIA score	IANR-SCIRFS score; EMG; residual urine	Allogeneic UC-MSCs	Intrathecal	Recruiting
NCT02981576	Safety and effectiveness of BM-MSC vs AT-MSC in the treatment of SCI patients	I/II	14	Jan 2019	ASIA score; MRI	Safety & effectiveness	Autologous BM-MSC; autologous AD-MSCs	Intrathecal	Active, not recruiting
NCT02009124	Stem cell therapy in spinal cord injury	II	500	Dec 2018	Change in clinical symptoms	Functional Independence Measure score	Autologous BM-MSCs	Intrathecal	Recruiting
NCT03225625	Stem cell spinal cord injury exoskeleton and virtual reality treatment study	NA	40	Jul 2022	ASIA score	ANS function; general well-being	Autologous BM-MSCs	Paraspinal; intravenous; intranasal	Recruiting
NCT02917291	Safety and preliminary efficacy of FAB117-HC in patients with acute	I/II	46	Jan 2020	Safety	ISNC-SCI; SCIM III; SSEPs;	Autologous AD-MSCs	Intramedullary	Recruiting

	traumatic spinal cord injury					MEPs			
NCT02302157	Dose escalation study of AST-OPC1 in spinal cord injury	I/II	35	Dec 2018	Safety	ISNC-SCI	ESC-derived OPCs	Unknown	Active, not recruiting

ANS = autonomic nervous system; AT = adipose tissue; IANR-SCIRFS = International Association of Neural Restoration Spinal Cord Injury Functional Rating Scale; NSC = neural stem cell; SCIM III = Spinal Cord Independence Measure III; UC = umbilical cord.

Currently active clinical trials are primarily early phase and are aimed at expanding understanding of the safety profile of stem cell therapies in SCI. Only two studies (NCT03521336 and NCT02009124) plan to enroll more than 50 subjects, highlighting a need for large, controlled clinical trials. (Trials were identified from the NIH repository of clinical trials [clinicaltrials.gov]. Results were queried using the key terms "spinal cord injuries" and "stem cell." Filtering was done to only include trials addressing acute or subacute SCI. Only active or recruiting trials are included.), Sources (Jin M.C. et al., 2019).

Table 5. Stem cell-seeded scaffolds for SCI treatment (adopted from (Kubinova and Sykova, 2012)

Cell type	**Scaffold**	**Degradability**	**Additional compounds**	**Lesion type/behavioural study**	**Type of transplantation/ analysis**	**Described effect**	**Citation**
SCs	PAN/PVC guidance channels	No	-	Transection/x	Immediate/ weeks 4	Improved axonal myelination and of propriospinal and sensory axons. regeneration	(Xu et al., 1997 Xu et al., 1995b)
SCs	PAN/PVC guidance channels	No	BDNF, NT-3	Transection/x	Immediate/6 weeks	Improved regeneration of long descending axons.	(Xu et al., 1995a)
SCs	PAN/PVC guidance channels	No	Mnisolone ethylpred	Transection/x	Immediate/ weeks 6	Improved axonal myelination and axonal extension of long distant neurons.	(Chen et al., 1996)
SCs	PAN/PVC guidance channels	No	-	Hemisection/ x	Immediate/ weeks 2, 4	Axonal regeneration and their re-entry into distal host tissue.	(Hsu and Xu, Xu et al., 1999, 2005)
SCs	PAN/PVC guidance channel	No	BDNF, NT-3 (intraspinal infusion)	Hemisection/ x	Immediate/4 weeks	Axons crossed the lesion and penetrated into the distal host spinal cord	(Bamber et al., 2001)
SCs	PAN/PVC guidance channel	No	GDNF	Hemisection/ x	Immediate/ weeks 4	Synergistic effect of combined therapy on axonal regeneration and myelination.	(Iannotti et al., 2003)
SCs	PAN/PVC guidance channel	No	ChaseABC	Hemisection/ x	Immediate/ weeks 4	Improved axonal growth across the graft-host interface.	(Chau et al., 2004)

SCs	poly-(beta hydroxybutyrate) tubular conduit	Yes	-	Hemisection/ x	Immediate/4 weeks	Axonal regeneration of long spinal tracks.	(Novikova et al., 2008)
SCs	PLGA multichannel scaffold	Yes	-	Transection/x	Immediate/1 or 2 months	Facilitation of axonal regeneration.	(Moore et al., 2006, Chen et al., 2009a)
SCs	PLGA multichannel scaffold	Yes	-	Transection/x	Immediate /1,2 and 3 months	Scaffolds with 450um diameter channels promoted greater axonal regeneration than 660 um diameter channels.	(Krych et al., 2009)
SCs	PLGA, PCLF, OPF & OPF+ multichannel scaffold	Yes	-	Transection/-	Immediate / weeks 4	Comparison of polymer scaffolds with different of the regenerative capacity stiffness.	(Chen et al., 2011)
SCs	PLA tube	Yes	-	Transection/x	Immediate /1, 2 and 4 months	Collapse of the tube reversed the regenerative effect.	(Oudega et al., 2001)
SCs and SCs producin g BDNF and NT-3	Freeze-dried PLA macroporous tubular scaffold	Yes	-	Transection/-	Immediate /1, 2 and 6 weeks	Limited axonal ingrowth into the scaffold. Low cell survival. No significant differences in BBB score between cell groups.	(Hurtado et al., 2006)
SCs or NSCs	PLGA multi channel scaffold	Yes	-	Transection/-	Immediate/ weeks 4	No significant differences in BBB score group. Greater axonal regeneration in the SC-treated.	(Olson et al., 2009)
SCs and NSC	PLGA	Yes	-	Hemisection/ +	Immediate/ and 6 months 1, 2, 3	Co-transplantation promoted functional recovery.	(Chen et al., 2010)
SCs or NPC	SA peptide nanofiber	Yes	-	Hemisection/ x	Immediate/ weeks 6	Greater axonal regeneration in the SC Survival of transplanted cells. -treated group.	(Guo et al., 2007)
Periphera l nerve graft	Chitosan guidance channels	Yes	-	Chronic clip SCI/-	Immediate/ weeks 14	No functional improvement. Axonal regeneration and myelination.	(Nomura et al., 2008a)
MSC	PHPMA-RGD macroporous hydrogel	No	-	Chronic compression lesion/+	Delayed/6 months	Prevention of tissue atrophy, axonal regeneration and significant functional improvement with combined treatment.	(Hejcl et al., 2010)
MSC	PHEMA hydrogel	No	-	Hemisection/ x	Immediate/6 weeks	Axonal ingrowth into the scaffold. In vivo MRI visualization of superparamagnetic iron-oxide	(Sykova and Jendelova, 2005)

						nanoparticles-labelled MSC.	
MSC	Serotonin modified PHEMA	No	-	Hemisection/ x	Immediate/4 weeks	Transplanted cells survived and migrated out of the scaffold into the spinal cord tissue.	(Kozubenko et al., 2010)
MSC	PLGA/small intestine mucosa	Yes	BDNF	Transection/+	Immediate/4 and 8 weeks	Axonal regeneration and significant improvement with combined treatment. functional	(Kang et al., 2011)
MSC	Gelatine sponge in PLGA tube	Yes	-	Transection/x	Immediate/1 8 weeks and	Reduced inflammation, promoted angiogenesis and reduced cavity formation	(Zeng et al.)
MSC	Fibrin gel	Yes	-	Hemisection/ +	Immediate/4 weeks	Significant functionnal improvement.	(Itosaka et al., 2009)
MSC	PLGA	Yes	-	Transection/x	Immediate/10 weeks	Development of complete transection model.	(Min et al., 2011)
NSC /NSC overexpr essing NT-3	PCL	Yes	ChaseABC	Hemisection/ +	Immediate/9 weeks	Enhanced axonal regeneration and significant functional improvement with combined treatment.	(Hwang et al.)
NSC	PLGA with complex guidance architecture	Yes	-	Hemisection/ +	Immediate/2 and 4, 12 months	Enhanced axonal regeneration and significant long term functional improvement.	(Teng et al., 2002)
NSC	PLGA with complex guidance architecture	Yes	Peroxynitrit e scavengers	Hemisection/ x	Immediate/24 hours	Anti-apoptotic effect of free radical scavengers on grafted NSCs.	(Yu et al., 2009)
NSC	Chitosan guidance channels	Yes	-	Transection/-	Immediate/14 weeks	Survival of transplanted cells and axonal regeneration. No functional improvement.	(Nomura et al., 2008b)
mESC NP	Fibrin gel	Yes	PDGF NT-3,	Hemisection/ x	Delayed/2 weeks	Enhanced survival and neural neural progenitor cells with combined differentiation of treatment.	(Johnson et al., 2010)
hESC NP	Collagen	Yes	-	Hemisection/ +	Delayed/5 weeks	Neural and glial functional improvement. *in vivo* differentiation,	(Hatami et al., 2009)
Astrocyt es	Collagen gel	Yes	-	Hemisection/ +	Immediate/4 weeks	Increased axonal ingrowth. Mild functional improvement.	(Joosten et al., 2004)

2. AIMS AND HYPOTHESES

The major aim of this work was improvement the results of treatment of traumatic spinal cord injury on the basis of experimental study of neuroregenerative properties of implanted biomaterials. Hydrogels based on natural extracellular matrixes, synthetic hydrogel with controlled structure and modifications of hyaluronic acid were studied to find the best substrate for implantation and support of stem cells for SCI treatment.

The major goals are summarized below:

1. Design of a magnetic system for stem cells delivery, evaluate its effectiveness on laboratory animals and use it to accumulate mesenchymal stem cells labelled with superparamagnetic iron oxide nanoparticles at a specific site of a SCI lesion.

2. Evaluation of filling the SCI lesion cavity, vessel and axonal ingrowth into CNS-derived SC-ECM hydrogel and non-CNS-derived UB-ECM hydrogel materials, in the model of SCI *in vivo*.

3. Study of the time-dependent dynamics of tissue ingrowth inside the scaffold of SIKVAV (Ser-Ile-Lys-Val-Ala-Val)-modified highly superporous poly (2-hydroxyethyl methacrylate) (HEMA) hydrogels with oriented pores.

4. Evaluation of axonal and blood vessels ingrowth in hydrogels based on modified hyaluronic acid HA-PH-RGD in the presence and absence of stem cells and fibrinogen in acute and subacute model of SCI in rats.

Hypothesis: Magnetic field allows to target and accumulate SPION-labelled stem cells specifically at the spinal cord lesion site due to focusing field in this point and superparamagnetic properties of nanoparticles. CNS-derived SC-ECM hydrogel is more compatible with spinal cord tissue and efficiently promote of neuroregeneration processes. Oriented porous structure of hydrogel better supports the neurofilaments ingrowth. Modification of hyaluronic acid by adding RGD peptide improves neurorenerative potential of scaffold hydrogels based on HA. Addition of fibrinogen enhances proliferation of stem cells.

3. MATERIALS AND METHODS

3.1. Hydrogels preparation

3.1.1. Preparation of porcine urinary bladder and spinal cord extracellular matrix hydrogels

The preparation of the ECM hydrogels from porcine spinal cord and porcine urinary bladder was based on a previously described procedure (Crapo P.M. et al., 2012; Medberry C.J. et al., 2013; Wolf M.T. et al., 2012). The urinary bladders and spinal cords of sows were obtained from animals (~120 kg) at a local abattoir and were frozen (>16 h at −80 °C). Until ECM preparation tissues were completely thawed and separated from all other tissue. Dura mater was removed, tissues were longitudinally quartered and cut into lengths (<3 cm). The decellularization process consisted of a series of agitated baths: water (type I reagent water per ASTM D1193; 16 h at 4 °C; 60 rpm), 0.02% trypsin/0.05% EDTA (60 min at 37 °C) (Invitrogen Corp., Carlsbad, CA, USA), 3.0% Triton X-100 (60 min) (Sigma-Aldrich Corp., St. Louis, MO, USA), 1.0 M sucrose (15 min), water (15 min), 4.0% deoxycholate (60 min) (Sigma), 0.1% peracetic acid in 4.0% ethanol (120 min), PBS (15 min), water (15 min), and PBS (15 min). Agitation speed was 200 rpm. Decellularized spinal cord and bladders were lyophilized and stored dry until use.

ECM samples were solubilized with 1.0 mg/ml pepsin in 0.01 N HCl (Sigma-Aldrich, Steinheim, Germany) at a concentration of 10 mg ECM/mL and stirred at room temperature for 48 h to form a pre-gel solution (pH ~ 2). The pepsin-HCl ECM solution was neutralized to pH 7.4 with 0.1 N NaOH, isotonically balanced with 10x PBS, and diluted with 1x PBS to the concentration 8 mg/ml. To form the hydrogel, the neutralized pre-gel was placed in 37°C for 45 min. The composition and biomechanical properties of the ECM hydrogels have been described in detail in (Crapo P.M. et al., 2012; Medberry C.J. et al., 2013; Wolf M.T. et al., 2012).

3.1.2. Preparation of poly(2-hydroxyethyl methacrylate-*co*-2-aminoethylmethacrylate) hydrogel with oriented porosity

Initiator, 2,2′-azobisisobutyronitrile (AIBN; Fluka, Buchs, Switzerland), was recrystallized from ethanol. The monomers, 2-hydroxyethyl methacrylate (HEMA; WichterleVacík, Prague, Czech Republic) and ethylene dimethacrylate (EDMA; Ugilor S.A., France), were purified by vacuum distillation. Ammonium oxalate and 1,4-dioxane were obtained from Lach-Ner (Neratovice, Czech Republic). 2-Aminoethyl methacrylate

hydrochloride (AEMA), ɤ-thiobutyrolactone, 2,2′-dithiodipyridine, imidazole and 1,1,1,3,3,3-hexafluoro-2-propanol were from Sigma Aldrich (St. Louis, MO, USA) and used as received. Ultrapure Q-water ultrafiltered on a Milli-Q Gradient A10 System (Millipore, Molsheim, France) was used for all experiments. HS-CGGASIKVAVS-OH peptide was synthetized according to a published procedure (Kubinova S. at al, 2010).

Preparation of the poly(2-hydroxyethyl methacrylate-*co*-2-aminoethylmethacrylate) (P (HEMA-AEMA)) hydrogel is schematically shown in Fig. 9. Briefly, freshly crystalized 30–90 μm thick and 0.3–10 mm long ammonium oxalate needles of high aspect ratio were used as a porogen for the preparation of PHEMA-based scaffolds. The ammonium oxalate crystals were parallel oriented by shaking, which was followed by their slow sedimentation in a removable channel (12 mm in diameter) embedded in a narrow vessel on an orbital shaker (Fig. 9a). To maintain the crystal orientation, they were carefully transferred into the 5-ml polyethylene injection syringe with an inserted stainless sieve (32 μm), quickly washed with ethanol and dried in the air flow. The content of the crystals in the syringe was increased by the double filling of hot (90 °C) saturated oxalate solution, subsequent cooling and removing of redundant solution under vacuum (Fig. 9d). The ammonium oxalate in the syringe was then washed with ethanol and dried in an air flow and loaded with a polymerization mixture consisting of monomers (2.4 g HEMA, 0.025 g EDMA, 0.025 g AEMA), AIBN initiator (10 mg) and solvent (1,4-dioxane; 1.25 ml). The bottom of the syringe was then closed by the pressure cap and the mixture centrifuged (2000 rpm) to remove air bubbles and to homogenize the mixture. Finally, the syringe was completed with a rubber plunger and the mixture polymerized at 60 °C for 16 h. After the completion of the polymerization, the syringe was cut, and the hydrogel removed (Fig. 9e). The resulting P(HEMA-AEMA) cylinder was immersed in 25% NaCl aqueous solution for 24 h to replace 1,4-dioxan and to protect the hydrogel from fast inhomogeneous swelling accompanied with hydrogel cracking. The cylinder was then transversely cut with a razor blade into discs 12 mm in diameter and 3 mm thick. Each disc was repeatedly washed with Q-water at room temperature to remove the ammonium oxalate.

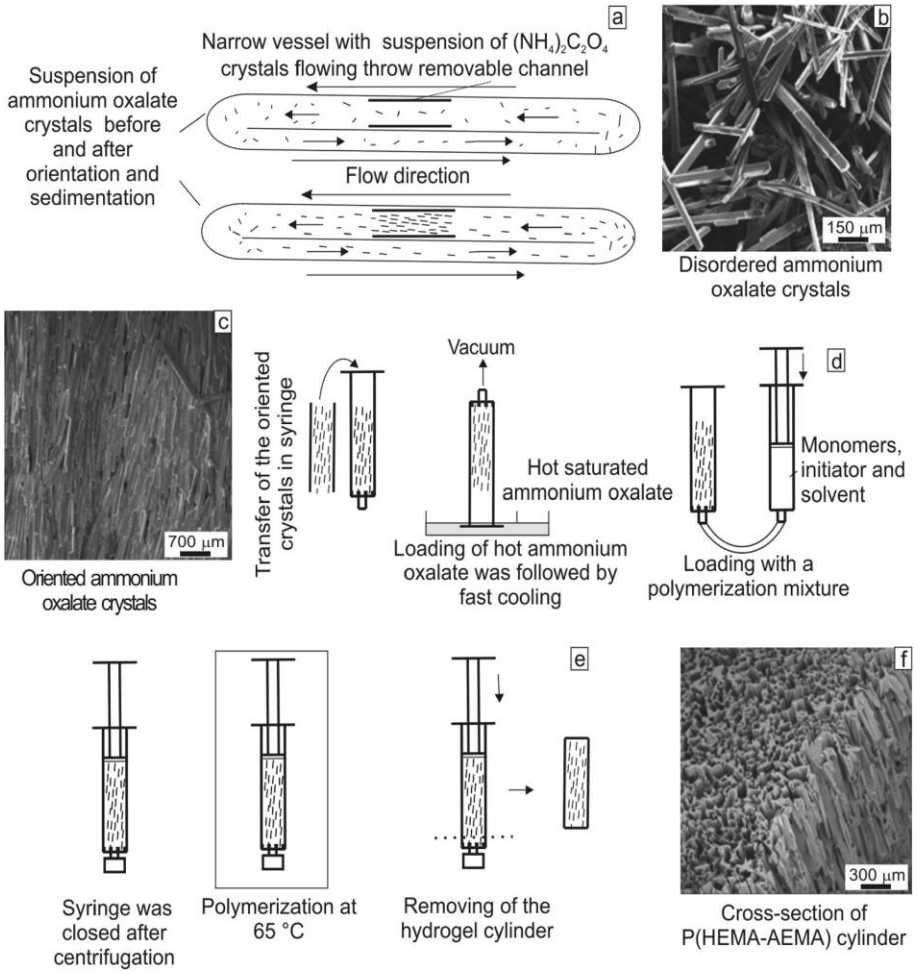

Figure 9. Scheme of preparation of P(HEMA-AEMA) hydrogel. (a) Orientation of ammonium oxalate needles. SEM micrographs of (b) disorder and (c) oriented crystals. (d) Transfer of crystals and polymerization mixture to the syringe. (e) Preparation of P(HEMA-AEMA) cylinder. (f) SEM micrograph of P(HEMA-AEMA) hydrogel with oriented porosity.

3.1.2.1. Immobilization of HS-CGGASIKVAVS-OH on the P(HEMA-AEMA) discs

P(HEMA-AEMA) discs were immersed in 10 ml of aqueous 0.15 M imidazole solution and 2 ml of ethanol was added to improve the penetration of reagents in the hydrogels. 0.1 ml of ɤ-thiobutyrolactone was added under Ar and the mixture was gently shaken for 70 min. Discs were washed five times with Q-water and then transferred into 10 ml of 0.1 M phosphate buffer (pH 8) containing 3 ml of ethanol. A solution of 20 mg of 2,2′-dithiodipyridine in ethanol (2 ml) was added under Ar and the discs were incubated for 1 h. The discs were again repeatedly washed with the above-described mixture of phosphate buffer and ethanol (10:3 v/v) under Ar. Finally, a solution of HS-CGGASIKVAVS-OH (2.5 mg) in 1,1,1,3,3,3-hexafluoro-2-propanol (0.25 ml) and phosphate buffer (pH 8; 6 ml) was added to the activated P(HEMA-AEMA) discs that were gently shaken for 60 min under Ar. The resulting HS-CGGASIKVAVS-modified

P(HEMA-AEMA) discs were washed five times with Q-water, sterilized in 70% ethanol for 16 h and transferred in sterile 100-ml bottles.

3.1.2.2. Characterization of P(HEMA-AEMA) discs

P(HEMA-AEMA) discs were analyzed by a JSM 6400 scanning electron microscope (SEM; Jeol; Tokyo, Japan). The samples were sputter-coated with 4 nm Pt before imaging. The immobilization HS-CGGASIKVAVS-OH was indirectly determined by the observation of UV spectra of 2-thiopyridine, measured with a Lambda 20 spectrometer (Perkin-Elmer; Norwalk, CT, USA). Pascal 140 and 440 mercury porosimeter (ThermoFinigan; Rodano, Italy) was used for measuring the average pore size of the dry hydrogels in two pressure intervals, 0–400 kPa and 1–400 MPa (Salek P, 2011). A specific surface area of the dried hydrogels was measured by nitrogen adsorption, using a Gemini VII 2390 Analyzer (Micromeritics; Norcross, USA) at 77 K.

3.1.3. Hyaluronan RGD modification

A solid phase synthesis via Fmoc-SPPS protocol was administered to develop the HPA-K-AHA-GRGD oligopeptide sequence (Amblard M., 2006). Addition and attachment of lysine, 6-aminohexanoic acid (Ahx) and glycine was done to modify the N-termini of the RGD adhesive peptide, for a short while. The α-amino group of lysine was also acylated by 3-(4-hydroxyphenyl) propionic acid (HPA). Subsequently, the purification and characterization of the peptide sequence (HPA-K-Ahx-GRGD) was done using ^{1}H NMR and Mass Spectroscopy.

Reductive amination of the RGD sequence with hyaluronan polyaldehyde (HA-CHO; DS = 10 %; Mw = 400 kDa; purchased from Contipro a. s.) led to the conjugation of these two components. They were then dissolved in 100 ml of demineralized water.

To the reaction mixture 0.25 mmol of HPA-K-Ahx-GRGD was introduced. The resulting mixture was subjected to an hour long mixing and stirring at room temperature. Finally, a solution of picoline-borane complex (PIC-BOR; 0.625 mmol) in 10 ml of 50% propan-2-ol was added to the mixture. Another 12 hours of stirring at room temperature, followed by precipitation by propan-2-ol, yielded the final mixture. The degree of substitution of HPA-K-Ahx-GRGD of such modified HA-PH-RGD derivative was 2.5%.

3.1.3.1. Chemical characterization of HA-PHA-RGD derivative

A Bruker Advance III 500 MHz instrument operating at a proton frequency of 500.25 MHz and elaborated by Bruker 2.1 Topspin software was employed for performing the ^{1}H NMR and HSQC spectroscopy. A mixture of D2O and NaOD (0.75 ml) was used as the medium for dissolving the samples before moving them into 5 mm NMR quartz tubes.

^{1}H NMR was also used to determinate the degrees of substitution (DS) of the prepared HA-PHA-RGD derivative. The DS was calculated from the ratio of the signal intensity of aromatic protons of the 3-(4-hydroxyphenyl) propionic acid (HPA; doublets 6.47 and 6.89 ppm) with respect to the signal of hydrogens of the N-acetyl group (singlet 2.01 ppm).

The RGD sequence isolation was done using an LCMS-2020 Single Quadrupole Liquid Chromatograph Mass Spectrometer (LC/MS) with the column C18 (250 × 10.00 mm, Jupiter 4u Proteo 90A). To purify the peptide, a gradient elution was done (phase A – 0.1 % formic acid; phase B – acetonitrile). The gradient was set as follows: 0 – 8 min 30 % B, 8 – 15 min 30– 50 min % B, 15-16 min 50 – 95 % B, 16 – 20 min 95 % B, 20 – 22 min 95 – 30 % B, 22 – 32 min 30 % B. Size exclusion chromatography (SEC) combined with a multi-angle laser light scattering (MALLS) detector was used to determine the molecular weight of the HA-PHA- RGD. A refractive index increment (dn/dC) of 0.155 mL g^{-1} was used to calculate the molecular weight and polydispersity (Mw/Mn).

3.1.3.2. HA-PH-RGD hydrogel preparation and crosslinking

20 mg/ml of the HA-PH-RGD was integrated into 0.9 % NaCl. The solution was stirred for nearly 6 hours at room temperature to attain homogeneity in the solution. The introduction of 0.04 U/ml HPR (Sigma) and 0.165 mM H_2O_2 (Merck, Germany) to the HA-PH-RGD solution resulted in kicking off the crosslinking of HA-PH-RGD solution and hydrogel formation. Gel forming and maturing was aided by cylindrical teflon moulds of 0.4 ml volume each.

3.1.3.3. HA-PH-RGD hydrogel characterization

TA instruments AR-G2 rheometer and Rheology Advantage Data Analysis software were used for the rheological measurements. The device settings were as follows: parallel plate (40 mm), gap 400 μm, dose volume 500 μl and temperature 37°C. For evaluation of the viscoelastic properties of material, i.e., storage modulus G', loss modulus G" and shear loss angle δ (tan δ = G" / G'), strain sweep mode was used (frequency 1 Hz and

displacement from 0.001 to 2 rad). To prevent slippage of the samples, a crosshatched geometry was used. The gelation period was evaluated from the intersection of the G' and G" moduli using time sweep step mode (frequency 1 Hz and displacement 0.001 rad).

Using Teflon moulds, the hydrogels used for the stability study were made. The samples had a volume of 0.4 ml. They were kept in phosphate-buffered saline (PBS) for 7, 14 and 21 days. The swollen hydrogel discs were then lightly blotted dry and measured on a rheometer in strain sweep mode. The increasing deformation – displacement set from 0.001 to 2 rad was performed at 1 Hz, to achieve elastic modulus of the material.

Here too, a crosshatched geometry to prevent slippage of the samples was used. However, it was not possible to evaluate the swelling ratio of the samples. Owing to the swollen hydrogel consistency, it was not possible to blot up the swollen samples completely and equivalently, which would have affected the obtained values. Such a condition would cast deleterious effects on the sample structure. Scanning electron microscope (SEM) was used to show the hydrogel structure.

3.2. Stem cell cultures

3.2.1. GFP-positive rat mesenchymal stem cells preparation

The transgenic Sprague–Dawley rats [SD-Tg(CAG-EGFP)CZ-004Osb] were kindly provided by Dr. Masaru Okabe (Osaka University, Japan) (Okabe M, 1997), bred at the laboratory of Dr. Martin Marsala (University of California, San Diego, CA), then subsequently sent to our Institute, and bred in our animal facility. The preparation of GFP-positive MSCs and labelling with poly-*L*-lysine-coated SPION was done in accordance to published methods (Vanecek V. et al., 2012; Babic M. et al., 2008). MSCs were obtained from 4-week-old green fluorescent protein transgenic Sprague-Dowley rats, TgN (acro/act-EGFP) 4Osb. The animals were deeply anesthetized, the femurs and tibias were dissected, and the bone marrow was plated on Petri dishes in medium containing DMEM (PAA Laboratories GmbH, Pasching, Austria), 10% FBS (PAA Laboratories GmbH, Pasching, Austria), and Primocin^{TM} (100 μg mL^{-1}) (Lonza Cologne AG, Koln, Germany). Cells were allowed to adhere; non-adherent cells were removed after 48 days by replacing the medium. Adherent cells were cultivated at 37 °C in a humidified atmosphere containing 5 % CO_2, and the medium was changed twice a week. After reaching near-confluency, the cells were harvested by a trypsin/EDTA solution. MSCs from passage 3 were used for *in vitro* and *in vivo* experiments.

3.2.2. GFP-positive rat MSCs labelling with SPIONs

Poly-*L*-lysine-coated (PLL) SPIO nanoparticles were used in this study for cell labelling. The nanoparticles were prepared and characterized as described (Babic M. et al., 2008). The diameter of the dry-state particles measured by TEM was 6.2 nm. The hydrodynamic diameter of the used particles, measured by dynamic light scattering, was D_h = 141 ± 10 nm, PDI = 0.52 ± 0.1, zeta potential was ζ = 47 ± 4 mV. The saturation magnetization of neat particles M_s ~ 70 $A \cdot m^2 \cdot kg^{-1}$ was obtained by measuring the magnetization curves with SQUID magnetometer. Because the weight of the coating agent is 1 % of the weight of iron oxide, the reduction of M_s by coating can be omitted. The coating of maghemite nanoparticles surface of with PLL was investigated using a Thermo Nicolet Nexus 870 FTIR spectrometer (Madison, WI, USA) in an H_2O-purged environment with DTGS (deuterated triglycine sulfate) detector. The Golden Gate single-reflection ATR system (Specac Ltd., Orpington, Great Britain) was applied to measure the ATR spectra of powdered samples over a wavenumber range 400–4000 cm^{-1}. Typical parameters were as follows: 256 sample scans, resolution 4 cm^{-1}, Happ-Genzel apodization, KBr beam splitter. The samples for measurements were prepared by freeze-drying of PLL-coated nanoparticles purified by multiple centrifugations and redispersion in ultrapure water (four times at 14 000 rpm for 1 h). Cultures of MSCs were incubated with SPION (50 μL per 10 mL of culture medium, i.e., 15.4 μg of iron per 1 mL media) 72 hours prior to the experiments. After this, the nanoparticles were washed out and the labelled cells were implanted into the animals.

3.2.3. Seeding GFP-positive rat MSCs on HEMA hydrogel

The GFP-positive MSCs from rat bone marrow were plated in DMEM/10% fetal bovine serum with primocin (2 ml/ml). After 24 h, the non-adherent cells were removed by replacing the medium. When cells reached 75%–90% confluence, they were detached by trypsin/EDTA treatment and transferred into 75-cm^2 cell culture flasks. On the day of the hydrogel seeding, the cultures were trypsinized with a 0.25% trypsin/ethylenediaminetetraacetic acid (EDTA) solution. Two million cells per milliliter were then placed in a test tube along with a 2 × 2 × 2 mm cube of hydrogel and put on a shaker (500 rpm) for 15 min to seed the 3D scaffold. We performed no quantitative analysis regarding the actual number of seeded cells. However, in the study (Hejcl A. et. al, 2013) was shown that the HEMA hydrogel provides good affinity to MSCs. The hydrogels were implanted within 3 h after seeding.

3.2.4. Human Wharton's jelly mesenchymal stem cells culture preparation

Fresh human umbilical cord samples were collected from healthy full-term neonates after spontaneous delivery with the informed consent of the donors using the guidelines approved by the Institutional Ethics Committee at University Hospitals in Pilsen and Prague, Czech Republic. About 10-15 cm per umbilical cord were aseptically transported into sterile PBS (IKEM, Prague, Czech Republic) with antibiotic-antimycotic solution (Sigma) at 4°C. After removal of blood vessels, the remaining tissue was chopped into small pieces (1-2 mm^3) and transferred to 10 cm Nunc culture dishes (Schoeller, Prague, Czech Republic) containing the complete medium alpha-MEM (EastPort, Prague, Czech Republic) supplemented with 5% platelet lysate (IKEM) and gentamicine 10 μg/ml (Sandoz, Prague, Czech Republic), and cultivated at 37°C and 5% CO_2 in a humidified atmosphere. On day 10, the explants were removed from the culture dishes and remaining adherent cells were cultured for 3 weeks or until 90% confluence and passaged using 0.05% Trypsin/EDTA (Life Technologies, USA). The cells were then seeded into culture flasks (Nunc) at a density of 5 x 10^3 cells/cm^2. The medium was changed two times a week. Cells of the 3rd passage were identified by flow cytometry (FACSAria^{TM}, Becton Dickinson, San Jose, California) to confirm their purity. Adipogenic, osteogenic and chondrogenic differentiation was employed to characterize the MSC phenotype. The following antibodies against human antigens were used: CD34, CD45, CD105, (Exbio, Vestec, Czech Republic); CD29, CD73, CD90, CD271, CD31, HLA- ABC and CD235a (BD Pharmingen, San Jose, California, USA); CD133 (Miltenyi Biotec, Bergisch Gladbach, Germany). Data analysis was performed using BD FASCDiVa software.

3.2.5. Seeding hWJ-MSCs on porcine SC- and UB-ECM hydrogels

In 3D culture, cells were seeded onto the hydrogels by adding concentrated cell suspension in PBS to neutralized liquid pre-gel solution for a final cell concentration of 2.5 × 10^6 cells/ml. Cells were thoroughly mixed in the pre-gel and 200 μl of the suspension was transferred inside the seeding rings with a diameter 0.8 cm (Scaffdex, Tampere, Finland) placed in the 24-well plates, and transferred to 37°C for 45 minutes, to form a hydrogel around the cells. Following this, the seeding rings were removed, 1 ml of media was added, and the hydrogel discs were imaged after 4 h, 24 h, 4 and 7 days in culture to quantify gel contraction. The cell-seeded hydrogels used for *in vivo* experiments were placed into PBS and incubated at 37°C and 5% CO_2 in a humidified atmosphere for ~ 4 h prior to their implantation into the hemisection cavity.

3.2.6. Seeding hWJ-MSCs on HA-PH-RGD hydrogel

hWJ-MSCs were mixed with HA-PH-RGD/F hydrogel to form 3D culture (20 µl, 8 x 10^4 cells) in 1 ml of medium in a 24-well plate. To further promote cell proliferation, the initial HA-PH or HA-PH-RGD solutions alone or mixed with fibrinogen (1 mg/ml, Sigma) in 0.9 % NaCl were formed into hydrogel film to cover the 24-well culture plate. 1.5 x 10^5 of hWJ-MSCs were used to seed each culture well. 3, 7 or 12 days after cultivation, CellTiter-Glo reagent was used to analyse the cell proliferation.

3.2.7. *In vitro* hWJ-MSCs growth and viability

In vitro cell growth on the surface of hydrogels was characterized using hWJ-MSCs cultures. Cell viability was determined after 1, 3, 7 and 14 days in culture using WST-1 reagent (Roche, Mannheim, Germany). Cells were cultured in 96-well plates (5,000 cells/per well) coated with both, UB-ECM, and SC-ECM hydrogels (90 µl/well) prior to cell seeding.

At time intervals of 3 hours, 1 day and 3 days of culture, the proliferation of hWJ-MSCs in the presence of HA-PH-RGD hydrogel, combined with fibrinogen (HA-PH-RGD/F) was further determined via a WST-1 reagent (Roche, Germany). The same volume of hydrogel without cells served as a background.

At the measured time points, 10 µl of WST-1 reagent was added to each well with 100 µl culture media and the plates were incubated for 2 hours at 37°C. The absorbance was measured using a Tecan-Spectra ELISA plate reader (Tecan Trading, Mannedorf, Switzerland) at 450 nm. Each type of hydrogel was seeded in triplicate; 14 independent experiments in three hydrogel batches were performed for each hydrogel type. Cell viability on the culture without hydrogels was used as a control.

3.2.8. Rat dorsal root ganglia explant culture preparation

Wistar rats (Velaz, Unetice, Czech Republic), aged 3-5 days, were used for dorsal root ganglia (DRG) extraction. Rats' spinal cords were dissected and DRGs from low thoracic and lumbar parts were isolated, placed in cold Hank's Balanced Salt Solution without Ca^{2+}/Mg^{2+} (Invitrogen, Waltham, USA), and cleaned of peripheral nerve processes. DRG explants were then placed on SC-ECM (n = 5) or UB-ECM (n = 4) hydrogels in 24-well plates and cultured in Neurobasal medium (Invitrogen) supplemented with 2% B27 (Life Technologies), 2mM L-glutamine (Invitrogen), 0.5% NGF (50 ng/ml, PeproTech, Prague, Czech Republic), uridine (17.5 µg/ml, Sigma) and primocine

(PeproTech, Prague, Czech Republic) in humidified atmosphere at 37°C and 5% CO_2. The medium was changed every 3 days. After 7 days of culture, DRGs were fixed with 4% paraformaldehyde in PBS for 10 min and subjected to immunocytochemical staining for neurofilaments (NF160, 1:200), (Abcam, Cambridge, United Kingdom) and cell nuclei (DAPI, 1:1000). Imaging was performed using a Leica fluorescent microscope (Leica DMI 6000B) and TissueGnostic software (TissueGnostics GmbH, Vienna, Austria). The neurite extension area and the longest neurite length were determined using ImageJ software with the NeuriteJ plug-in, as described by (Torres-Espin A. et al., 2014).

3.3. Animal experiments

3.3.1. Animal handling and surgery

All experiments with animals were performed in accordance with the European Communities Council Directive of 22nd of September 2010 (2010/63/EU) regarding the use of animals in research and was approved by the Ethics Committee of the Institute of Experimental Medicine, Academy of Sciences of the Czech Republic.

3.3.2. Balloon-induced compression lesion model

As a model of acute spinal cord injury, we used a protocol of a balloon compression lesion (Figure 10) that was described by the Department of Neurobiology, University of Kosice and developed in our laboratory (Vanicky I. et al., 2001; Urdzikova L. et al., 2006).

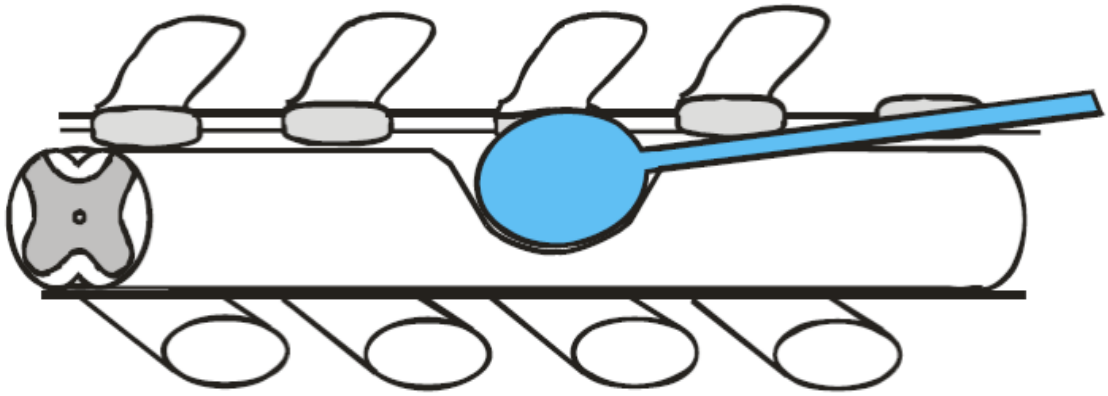

Figure 10. Balloon-induced compression lesion (Vanicky I. et al., 2001)

A balloon compression lesion was performed in a total of 15 male Wistar rats (280-400 g). All animals received initial anesthesia. Rats were placed into a plastic box with an

approximate diameter of 16.5 cm and a height of 13 cm and closed by a cover to maintain the gas concentration. Then a mask connected to an Isoflurane Vapor 19.3 apparatus (Drägerverk AG Lübeck, Germany) was introduced into the box, and isoflorane (Forane®, Abbott Laboratories, Queenborough, Great Britain) at a concentration of 5% vapor inhalation in air was administered at a flow of 300 ml/min for 5-7 minutes. All animals were shaved on the back from *C7* to *Th1*. Under sterile conditions the skin was cut in the midline from *Th7-Th12*. The soft tissue was removed, as well as the spinous processes of vertebrae *Th8-Th11*. A catheter was filled with saline and connected to a Hamilton syringe. The catheter was inserted into the epidural space and advanced cranially for 1 cm, so that the centre of the balloon rested at the *Th8-Th9* level of the spinal cord. The balloon was rapidly inflated with 15 μL of saline for 5 min. The catheter was then deflated and removed.

3.3.3. SPION-labelled GFP-MSCs transplantation

One week after the induction of the lesion, 5 x 10^5 cells in 50 μL of phosphate-buffered saline were injected intrathecally at the *L5-L6* level, at 10 cm from the lesion site (Figure 11). Subsequently the external magnetic system was placed around the rat, under the top of the vertebral column at *Th8–Th9* above the lesion site, for 2 h to improve cell retention and attachment (Figure 12). It consists of a pair of cylindrical NdFeB magnets (1 cm diameter and 5 cm height, out-of-plane remanent magnetization values 1.2 T) fitted some distance apart from one another on an annular holder (Figure 11 and 12). The obliquely tilted magnets are such that their alike poles face each other. This arrangement creates a focusing zone or trapping area in the magnetic system where the horizontal and vertical magnetic force components (X and Z components) are nearly zero.

Cell quantification was performed 24 hours after cell transplantation in longitudinal sections.

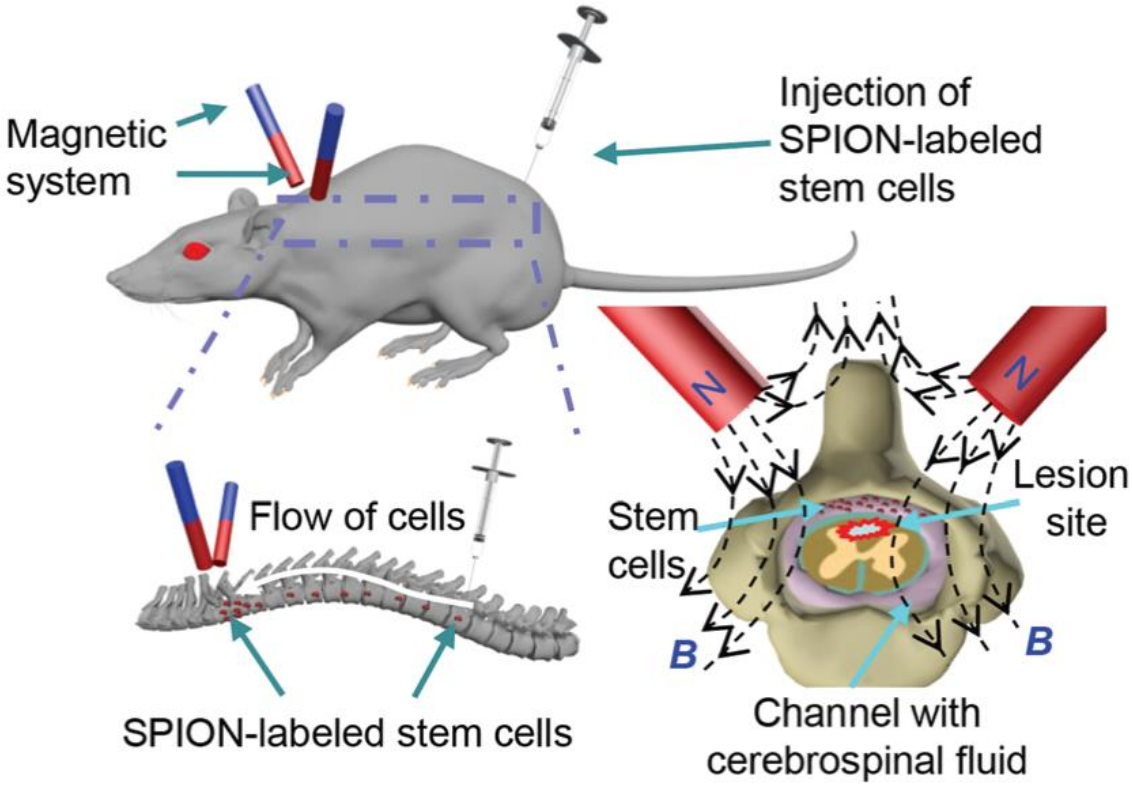

Figure 11. Schematic representation of the magnetic targeting strategy.

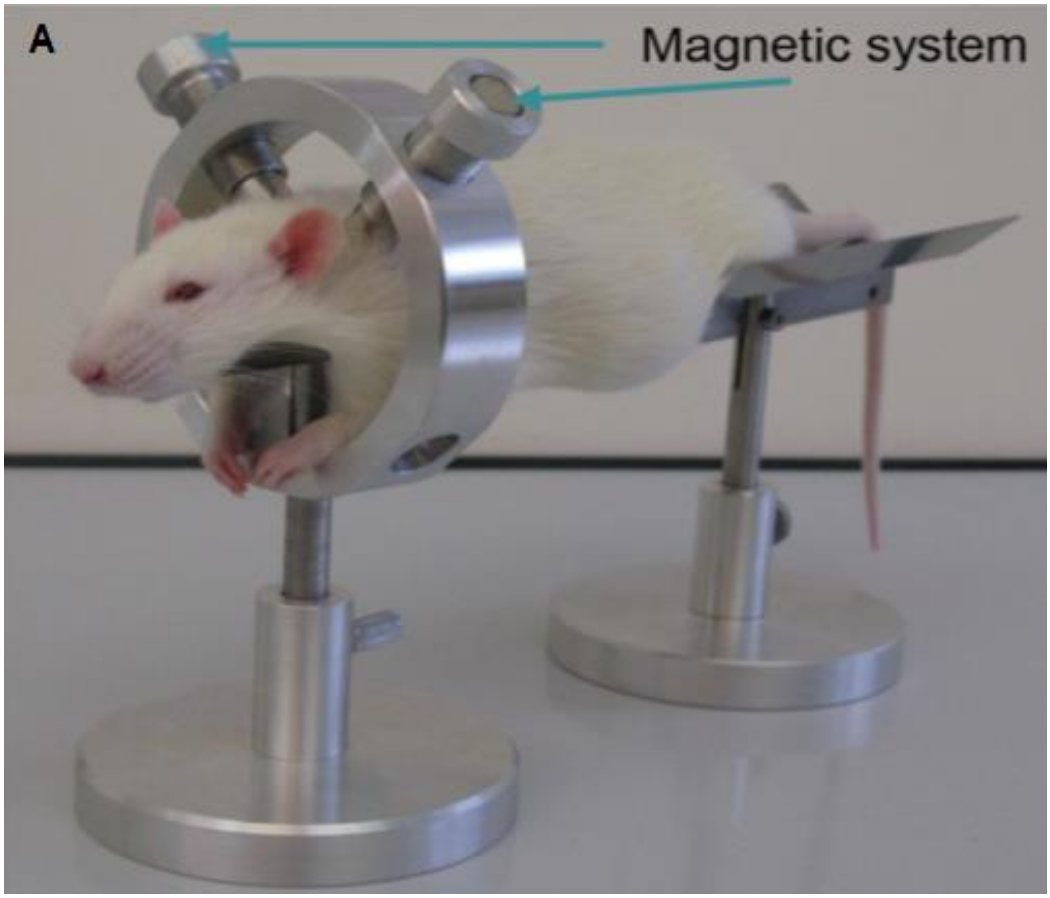

Figure 12. In vivo application of the non-invasive magnetic system for MSC targeting into SCI of a rat.

3.3.4. Spinal cord transection

Forty-six male rats (Wistar, Anlab, Czech Republic) with a weight of 300–350 g, underwent transection at the Th8 level. The animals were intraperitoneally injected with pentobarbital for anesthesia (0.06 g/1 kg i.p.); one dose of ATB (gentamicin 8 mg/1 kg i.m.), atropine (0.08 mg/1 kg s.c.), and mesocain to enhance local anesthesia (1 mg/1 kg s.c. + i.m.) was administered preoperatively. In addition, the rats received cyclosporine (Novartis; 10 mg/kg i.p.) before surgery and then daily until sacrifice. A linear skin incision was performed above the spinous processes of Th7-9; the paravertebral muscles were detached from the laminae Th7-9, and a Th8 laminectomy was performed. The dura was incised longitudinally in the midline and about a 2 mm segment of spinal cord was dissected, creating a cavity resulting in complete spinal cord transection. The size and the character of the lesion were identical to our earlier study (Hejcl A. at al., 2008).

3.3.5. HEMA hydrogel application into the SCI lesion

One week after the transection, we reopened the scar tissue from the skin to the spinal cord. We extracted the suture from the dura and removed the debris from the lesion. The hydrogels were properly trimmed to adjust to the size and shape of the cavity. The hydrogel was taken from the EDTA solution and implanted wet in such a way as to ensure that it would firmly adhere to the edges of the transection cavity without causing any undue pressure onto the surrounding spinal cord tissue. Such approach ensures no further swelling of the hydrogel within the cavity. The muscles and skin were sutured again, and the animals were housed two in a cage with food and water ad libitum. The number of animals in each group regarding therapy (hydrogel with or without MSCs) and timing are summarized in Table 6.

Table 6. Numbers of experimental animals

Days after hydrogel implantation	2	7	14	28	49	168
SIKVAV-HEMA	3	3	3	4	3	0
SIKVAV-HEMA with MSCs	3	4	5	6	3	3
Total	6	7	8	10	6	3

3.3.6. Spinal cord hemisection

Male Wistar rats (250 - 300 g, Velaz, Czech Republic) were subjected to a surgical procedure to create a hemisection on their right side at the level of the 8th thoracic vertebra (Th8). For a short time, the rats were given a pentobarbital anaesthesia (60 mg/kg). The animals received local injections of mesocain (0.3 mL s.c. at the surgery site) in addition to general anesthesia, as well as gentamicin (0.05 mL i.m., Sandos) and atropine (0.2 mL, atropine solution 1:5) (both from BB Pharma, Prague, Czech Republic) injections. First a micro-section of the skin was made at the level of Th8 spinal processes using a scalpel. Then the laminectomy at Th8 was performed using rongeur and the dura was incised with capsulotomy scissors. A dissection of the right half of one 2 mm long spinal cord segment of the volume ~ 6 mm^3 was made using delicate tissue scissors to generate a hemisection cavity. Then the dissected segment was removed using a small piece of cellulose and fine forceps. Instruments were purchased from (Medicon®, Tuttlingen, Germany).

The dura mater was sutured with 10/0 monofil unresorbable thread (B Braun, Aesculap, Melsungen, Germany). The muscles and skin were sutured with 4/0 monofil unresorbable thread (4/0 Chirmax, Prague, Czech Republic), and the animals were housed two rats in a cage with food and water ad libitum.

3.3.7. UB- and SC-ECM hydrogel application into the SCI lesion

The neutralized and isotonically balanced liquid pre-gel solution of SC-ECM and UB-ECM hydrogels (8 mg/ml), were acutely injected into the spinal cord defect after hemisection in a single injection using an Omnican®Insulin syringe for U-100 Insulin (Melsungen, Germany) and allowed to gelate *in situ*, followed by histological evaluation after 2, 4 and 8 weeks after implantation (n = 5 per group, per time point). In the control SCI group (n = 4) the hemisection defect was filled with saline. In the animal group treated with SC-ECM hydrogel seeded with hWJ-MSCs (n = 4), the hydrogels were implanted into the hemisection cavity. This animal group received a daily injection of the immunosupressants cyclosporin A (10 mg/kg, intraperitoneally) (Sandimmun; Novartis), azathioprine (2 mg/kg, perorally) (Imuran, Aspen Europe GmbH, Bad Oldesloe, Germany) and methylprednisolon (2 mg/kg, intramuscularly) (Solu-Medrol, Pfizer, Puurs, Belgium) to prevent the rejection of the transplanted cells. From the 56 animals that underwent the hemisection, 4 animals died during the operation and 2 animals died 2-4 weeks after operation.

3.3.8. HA-PH-RGD hydrogel application into the SCI lesion

In certain animals with acute application of hydrogel (n = 3, in each time point and group), just after the formation of the hemisection cavity, it was immediately filled with hydrogel. There were two techniques used for doing this. Either 20 mg/ml of HA-PH-RGD solution was mixed with crosslinking components to form a gel in the teflon mould before adjusting the hydrogel volume and implanting it into the lesion to fill the hemisection cavity, or about 5 µl of HA-PH-RGD hydrogel solution mixed with crosslinking agents could be injected by Omnican Insulin syringe for U-100 Insulin (B.Braun, Germany) into the lesion cavity, where the complete *in situ* gelation occurred. The control lesion was filled with saline.

In those animals that had a subacute lesion, the hemisection cavity was made a week prior hydrogel injection. The liquid pre-gel solution of HA-PH-RGD hydrogel (n = 6), HA-PH-RGD/F (n=6) and HA-PH-RGD/F combined with hWJ-MSCs (3 million/0.5 ml, ~ 3 x 10^4 transplanted cells in 5 µl of the hydrogel) (n = 7), was mixed with crosslinking agents and spontaneously injected into the hemisection cavity by Omnican Insulin syringe for U-100 Insulin (B.Braun, Germany), for *in situ* gel formation. The hemisection defect was filled with saline in the control SCI group (n=8).

An injection of immunosuppressant cyclosporin A (10 mg/kg, i.p.) (Sandimmune; Novartis, Switzerland), azathioprine (2 mg/kg p.o.) (Imuran; Aspen Europe GmbH, Germany) and methylprednisolone (2 mg/kg, i.m.) (Solu-Medrol; Pfizer Manufacturing, Belgium) was administered daily after 5 days of induction of the hemisection in all animal groups having a subacute hydrogel injection as well as the control groups. These substances were injected with the aim of avoiding rejection of the transplanted cells. All the rats were then put into cages with two rats per cage with food and water *ad libitum*.

3.3.9. Analysis of locomotor functions

Hind limb motor function between the first- and fourth-weeks post-SCI was recorded for the sham operated control group, SC-ECM alone and SC-ECM combined with hWJ-MSCs using the Basso–Beattie–Bresnahan (BBB) open field locomotor test (Basso D.M. at al., 1995).

Quantitative evaluation of locomotor functions was done using MotoRater 303030 and TSE Motion 8.5.11 software (TSE-systems, Germany).

3.4. Tissue processing and histology

3.4.1. Spinal cord lesion processing and histology

In corresponding time after induction of spinal cord lesion, the animals were deeply anesthetized with an intraperitoneal injection of overdose pentobarbital (pentobarbital 150 mg kg^{-1}; Sigma, St Louis, MO) and perfused with phosphate buffer (PBS) followed by 4 % paraformaldehyde in 0.1 M PBS. The spinal cord was left in the bone overnight, then removed and postfixed in the same fixative for at least 1 week.

A 3 cm long segment of the spinal cord containing the lesioned site was dissected out and transferred to 10% and 30% sucrose. After freezing, the spinal cords were cryosectioned into 40 μm thick longitudinal sections.

3.4.2. SPION-labelled GFP+ MSCs visualization and quantification in rat spinal cord lesion

Cell quantification was performed in longitudinal sections (20 μm) using a fluorescent microscope (Carl Zeiss, Rochester, NY). GFP-positive MSCs were counted in 360 μm thick upper segments of an area 36 mm^2 (18 × 2 mm), with the epicenter of the lesion in the center of the segment. Image quantifications were performed using ImageJ software (NIH). Cell number was calculated by normalizing corrected total cell fluorescence (CTCF) of the full area of interest to average fluorescence of a single cell. The net average CTCF intensity of a pixel in the region of interest was calculated for each image utilizing a previously described method (Gavet O. and Pines J., 2010). The region placed in an area without fluorescent objects was used for background subtraction. CTCF was determined as the sum of pixel intensity for a single image with the subtracted average signal per pixel for a region selected as the background. Averages of normalized intensity values of at least 10 morphologically identical cells were calculated to determine the mean fluorescence of a single cell.

To visualize the SPION labelling in cell culture, cells were fixed in paraformaldehyde and phosphate buffer (PBS) for 15 min, washed with 0.1M PBS and then stained for iron using potassium ferrocyanide (Lachema, Brno, Czech Republic) to produce ferric ferrocyanide (Prussian blue) according to a standard staining protocol.

3.4.3. Immunohistochemical staining

Hematoxylin-eosin (H&E) and Masson´s trichrome staining was performed using the standard protocol and the slides were specifically evaluated using an Axio Observer D1 microscope (Carl Zeiss Microimaging GmbH).

For immunohistological analysis, the following antibodies were used: against neurofilament 160 kDa (NF 160, 1:200), endothelial cells of blood vessels (RECA-1, 1:500), glial fibrillary acidic protein, (GFAP, conjugated with Cy3, 1:800; all from Sigma); growth associated protein 43 (GAP43, 1:100), astrocytes (Cy3-conjugated mouse Glial Fibrillary Acidic Protein, GFAP, 1:200), all from Sigma; oligodendrocytes (1:200; CE-1, Merck-Millipore, Germany); Schwann cells p75 (1:200), serotonin-positive axons (R-SERO, 1:100), oligodendrocytes (OSP, 1:1000), macrophages (ED1, 1:100 Serotec, Oxford, UK), M1 macrophages (CD86, Cy5-conjugated donkey anti-rabbit IgG-PerCp-Cy5,5, 1:2500), human mitochondria (MTCO2, 1:250; all from Abcam, UK), and M2 macrophages (CD206, 1:250; all from Santa Cruz), axonal growth cone (GAP43, 1:100), all from Santa Cruz, Heidelberg, Germany.

The following secondary antibodies were used: Alexa Fluor® 488-conjugated goat anti-mouse IgG (1:200), donkey anti-mouse IgG AlexaFluor® 488, goat anti-mouse IgG Alexa Fluor® 488 (1:400; Life Technologies, USA); Alexa Fluor® 594-conjugated goat anti-mouse IgG (1:200), donkey anti-goat IgG AlexaFluor® 594, goat anti-mouse IgG Alexa Fluor® 594 (1:400; Life Technologies, USA); Alexa Fluor® 488-conjugated donkey anti-goat IgG (1:700); Alexa Fluor 594 goat anti–rabbit IgG (1:200; Invitrogen); Cy3-conjugated anti-mouse IgM (1:100; Invitrogen) and goat anti-mouse IgM-Cy3 (1:200; Merck-Millipore, Germany).

On the basis of the secondary antibody host organism, blocking goat or donkey serum (1:10; G9023 or D9663, Sigma) was utilized to prevent non-specific immunohistological staining. Triton X-100 (0.1% in 0.1M PBS; Sigma) was used for the permeabilization of cell membranes.

The morphology of the cells on the hydrogels was examined by immunofluorescent staining for actin filaments. After fixation in paraformaldehyde in PBS for 15 min, the cells were washed with 0.1M PBS and stained with Alexa-Fluor 568 phalloidin (1:300).

The nuclei were visualized by using 4',6-diamidino-2-phenylindole (DAPI) fluorescent dye (1:1000; Invitrogen, UK).

Fluorescent micrographs were taken using an AxioCam HRc Axioskop 2 Plus fluorescent microscope (Zeiss, Jena, Germany), a laser scanning confocal microscope LSM

510 DUO laser scanning confocal microscope (Zeiss, Germany) and fluorescence microscope Observer D1 with AxioVision 4.8.2 software (Zeiss, Germany), LEICA DMI6000B (Leica, Germany) with TissueFAXS software (TissueGnostics GmbH, Austria).

3.4.4. HEMA hydrogel retrograde staining

Six months after SCI, under isoflurane anesthesia, a laminectomy of the lumbar vertebra 12 and 13 was performed and 2 µl of 2% hydroxystilbamidine (Fluorogold, Invitrogen, Carlsbad, CA) were stereotactically injected by a Nano-Injector (Stoelting Co., Wood Dale, IL) into the dorsal columns of 5 animals treated with HEMA hydrogel and MSCs. Two days later, the animals were perfused transcardially with phosphate-buffered saline (PBS) followed by 4% paraformaldehyde.

Sections were first incubated with anti-fluorogold antibody (1:10,000; Chemicon International, Temecula, CA) then with biotinylated goat anti-rabbit secondary antibody (1:1000; Vector Labs, Burlingame, CA). They were processed using Vectastain ABC reagent (Vector Labs) and developed with diaminobenzidine (Vector Labs).

3.4.5. Axonal and blood vessel ingrowth analysis

For axonal and vessel ingrowth analysis, multiple images across the entire lesion (cranial side, central and caudal side from three longitudinal sections for each animal) were taken using a 20x objective. Five images from each sample were selected and the total area of the axons (NF160 staining) and blood vessels (RECA staining) within the lesion area was outlined using ImageJ software (National Institutes of Health, Bethesda, MD, USA) and divided by the area of the lesion to determine the percentage of the lesion that was occupied by new axons or vasculature. Quantification analysis expressed the percentage of NF160 or RECA positive area from a total lesion area.

For each spinal cord, 4 to 5 slices were used for the quantification of axons. The hydrogels were divided into 3 parts: the cranial end, the central part and the caudal end. We calculated the number and the length of axons in each part of the scaffold, using the program Tissue Quest Analysis Software (Tissue Gnostics GmbH, Vienna, Austria). We then combined the data from the peripheral parts of the hydrogels (cranial and caudal ends) and evaluated them together. The central part was quantified and analyzed separately.

Blood vessels were evaluated via a semi-quantitative method using 4 slices for each spinal cord, as described in previous paper (Hejcl A. at al., 2013). We analyzed the number

of green objects, regardless of the size of each object (number of areas), the total number of the green objects (sum of areas), and the intensity of the green color on each slice (densitometry) using Axio Vision 4.8 software (Carl Zeiss Microimaging GmbH, Jena, Germany). However, when the shape of the object was obviously not a blood vessel, it was manually excluded in order to avoid counting artifacts. By multiplying the "sum of areas" and the "densitometry" parameters, we obtained a semi-quantitative parameter, directly related to the number of blood vessels in the hydrogel *in vivo*.

Since glial scarring also had to be analysed, three mosaic images of GFAP staining for each animal was taken using a 20x objective. Integrated density and mean grey value of three areas around the lesion (cranial side, central and caudal side) and background (uninjured part of spinal cord) were measured by ImageJ software. The results obtained were presented as the corrected total cell fluorescence (CTCF), while CTCF = Integrated Density – (Area x Mean grey value of background) (McCloy RA, 2014).

3.5. Gene expression analysis

The specific gene expression (Table 7) was studied using quantitative real-time polymerase chain reaction (qRT-PCR).

RNA was isolated from paraformaldehyde-fixed frozen tissue sections using the High Pure RNA Paraffin Kit (Roche, Penzberg, Germany), following the manufacturer's recommendations. RNA amounts were quantified using a spectrophotometer (NanoPhotometer™ P-Class, Munchen, Germany). The isolated RNA was reverse transcribed into cDNA using Transcriptor Universal cDNA Master (Roche, Germany) and a thermal cycler (T100™ Thermal Cycler, Bio-Rad, Hercules, CA, USA). The qPCR reactions were performed using cDNA solution, FastStart Universal Probe Master (Roche, Germany) and TagMan® Gene Expression Assays (Life Technologies, Carlsbad, CA, USA), (Table 7). The qPCR was carried out in the final volume of 10 µL containing 25 ng of extracted RNA. Amplification was performed on the real-time PCR cycler (StepOnePlus™, Life Technologies). All amplifications were run under the same cycling conditions: 2 min at 50°C, 10 min. at 95°C, followed by 40 cycles of 15 s at 95°C and 1 min at 60°C. All samples were run in duplicate and a negative control was included in each array. Relative quantification of gene expression was determined using the ΔΔCt method. Results were analyzed with StepOnePlus® software. The gene expression level was normalized on Gapdh as a reference gene; control samples from unlesioned spinal cord tissue were used as a calibrator.

Table 7. TagMan Gene Expression Assays

Glyceraldehyde 3-phosphate dehydrogenase/GAPDH	Rn01775763_g1
Basic fibroblast growth factor/Fgf2	Rn00570809_m1
Growth associated protein 43/Gap43	Rn01474579_m1
Glial fibrillary acidic protein/Gfap	Rn00566603_m1
Vascular endothelial growth factor A/Vegfa	Rn01511601_m1
Neurotrophin 3/Sort1	Rn01521847_m1
Irf5	Rn01500522_m1
CD86	Rn00571654_m1
Inducible nitric oxide synthase 2/Nos2	Rn00561646_m1
Macrophage mannose receptor 1/Mrc1	Rn01487342_m1
CD163	Rn01492519_m1
Arginase 1/Arg1	Rn00566603_m1
Caspase 3/Casp3	Rn00563902_m1
Macrophage inflammatory protein 1a/Ccl3	Rn01464736_g1
Chemokine (C-C motif) ligand 5/RANTES/Ccl5	Rn00579590_m1
Prostaglandin-endoperoxide synthase 2/Ptgs2	Rn01483828_m1
Interleukin 2/Il2	Rn00587673_m1
Interleukin 6/Il6	Rn01410330_m1
Interleukin 612b/Il12b	Rn00575112_m1

3.6. Mathematical modeling

The magnetic field and force distributions were calculated with the help of explicit analytical expressions for magnetic field induction generated by a cylindrical permanent magnet magnetized along its symmetry axis. For homogeneously magnetized cylinder of the radius and length L, the axial (B_z) and radial (B_p) components of the magnetic field induction can be calculated as (Blinder S.M., 2011):

$$B_z = -\frac{\mu_0}{4\pi} M \int_0^{2\pi}\int_0^{a}\left(\frac{R(L/2-z)}{(R^2+(L/2-z)^2+\rho^2-2R\rho\cos\Phi)^{3/2}}+\frac{R(L/2+z)}{(R^2+(L/2+z)^2+\rho^2-2R\rho\cos\Phi)^{3/2}}\right)dRd\Phi \quad (1)$$

and

$$B_\rho = -\frac{\mu_0}{4\pi} M \int_0^{2\pi}\int_0^{a}\left(-\frac{R(2\rho-2R\cos\Phi)}{2(R^2+(L/2-z)^2+\rho^2-2R\rho\cos\Phi)^{3/2}}+\frac{R(2\rho-2R\cos\Phi)}{2(R^2+(L/2+z)^2+\rho^2-2R\rho\cos\Phi)^{3/2}}\right)dRd\Phi \quad (2)$$

3.7. Statistical evaluations

The statistical significance of differences in cell counts in the spinal cord lesions between the groups was determined by using ANOVA Fisher's LSD and Newman-Keuls tests.

A two-way ANOVA was used to determine the statistical significance of variations in histological analysis between the groups with acute HA hydrogel application at two time points.

A one-way ANOVA with Holm-Sidak method for all pairwise multiple comparison was used for the comparison of histological analysis and gene expression between the groups with subacute injection of HA hydrogels in 2 months (SigmaPlot V13; Systat Software Inc., USA).

The one-way ANOVA was also used for the comparison of gene expression between groups with SC-ECM hydrogel in 4-week intervals and cell proliferation (Sigmastat 3.1, Sistat Software Inc., San Jose, CA, USA).

The mean values are reported as mean ± SEM to plot all the data in graphs. Intergroup differences were analyzed using ANOVA and Student's two-sample t-test (probability values <0.05 and <0.01 were considered statistically significant).

4. RESULTS AND DISCUSSIONS

4.1. ANEFFECTIVE STRATEGY OF MAGNETIC STEM CELL DELIVERY FOR SPINAL CORD INJURY THERAPY

4.1.1. Design of magnetic system with trapping area

To enhance the efficacy of stem cell delivery in a rat model of SCI, we proposed a new magnetic system consisting of two cylindrical NdFeB magnets (1 cm diameter and 5 cm height, out-of-plane remanent magnetization values 1.2 T) placed on a ring-shaped holder with the alike poles facing each other (Figure 12). A specific feature of the proposed magnetic system is the existence of a focusing zone – trapping area – where both the horizontal and vertical magnetic force components (X- and Z-components) are almost zero (Figure 14). This focusing zone is located just between the two maxima of the planar components (parallel to the X–Z-axis) of the magnetic gradient force (Figure 14). Thus, the magnetically labelled cells must be focused namely in this trapping area. Figure 14 shows the magnetic force distributions in the X–Z-plane between two magnets with opposing magnetization that were calculated analytically using the explicit expressions for the magnetic stray fields produced by a uniformly magnetized magnet (Zablotskii V. at al., 2010). The area outlined by the ellipse represents the focusing zone for the given configuration of the magnetic poles and their geometry.

4.1.2. Evaluation of SPION-labelled MSCs distribution under magnetic field

For MSCs labelling the poly-L-lysine-coated SPIONs were chosen as non-toxic and non-inducing pathophysiological effect nanoparticles as described in previously performed biocompatibility screening (Novotna B. at al., 2012, Lunov O. at al., 2010, Lunov O. at al., 2010b). Some of the physicochemical properties of SPIO nanoparticles are presented in Figure 15.

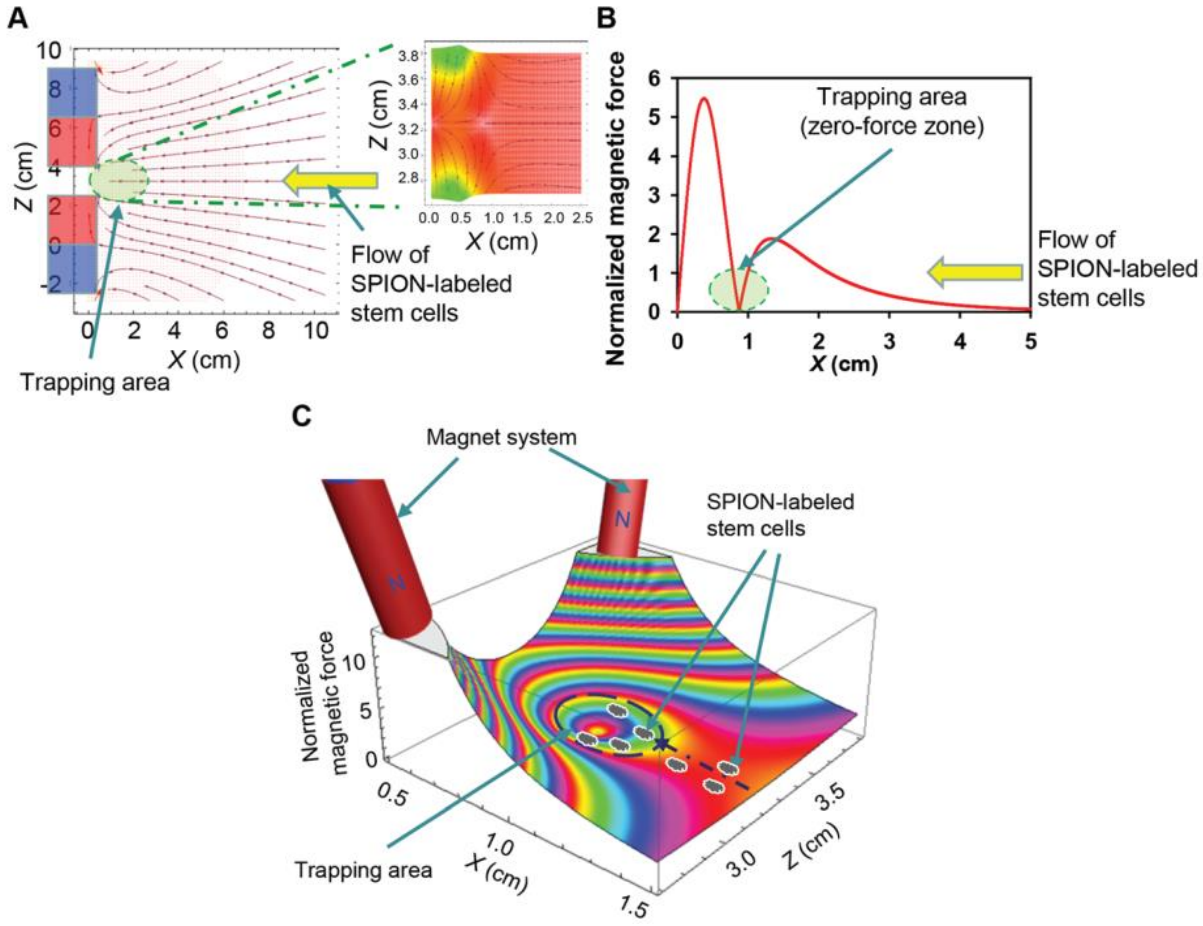

Figure 14. Spatial distribution of the magnetic gradient forces between the magnets of the designed magnetic system. (A) Calculated vector field plot of the magnetic gradient force (X–Z-plane – the vertical cross-section of the spinal cord). The insert represents an enlarged region of the trapping area (zero-force zone). The arrows show the directions of the magnetic gradient forces (f_m α ∇B^2) applied to a cell (where B is the magnetic induction). (B) Modulus of magnetic gradient force, $\left|(\vec{B}\vec{\nabla})\vec{B}\right|$, normalized to $(\mu_0 M_r)^2 r^{-1}$, as a function of the X-coordinate which is along the cerebrospinal channel (M_r represents the remnant magnetization and $\mu_0 M_r$ = 1.2 T for the used magnets, magnet radius r = 0.5 cm). In (A) and (B) the focusing area is shown by the green ellipses. (C) 3D plot of the normalized magnetic gradient force (X–Z-plane).

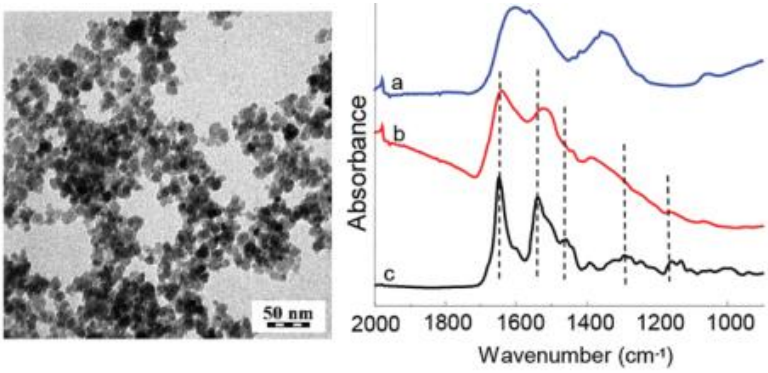

Core diameter (nm)	PDI	Hydrodynamic diameter (nm)	Zeta-potential (mV)	Saturation magnetization ($A \cdot m^2 \cdot kg^{-1}$)
6.2	0.52 ± 0.1	141 ± 10	+ 47 ± 4	70

Figure 15. Physicochemical properties of SPIONs.

First, we tested whether the MSCs labelled with SPIONs can be efficiently attracted by a magnet *in vitro* (Figure 16A). As shown in Figure 16A, SPION-labelled cells are effectively concentrated in the magnetic field focusing area.

Then, the distribution of SPION-labelled MSCs under magnetic field was evaluated *in vivo*. Rats with balloon compression induced SCI were divided into three groups: SPION-labelled MSCs exposed to MF, non-labelled MSCs exposed to MF and SPION-labelled MSCs without exposure to MF. One week after the induction of the lesion, 5×10^5 cells were injected intrathecally at the L5–L6 level and at a distance of 10 cm from the lesion site (Figure 11). Subsequently, the above-described external magnetic system was placed around the rat (Figure 12), under the top of the vertebral column above the lesion site at Th10, for two hours to provide cells retention and attachment.

According to results presented in Figure 16B, 17B and C, we can observe dramatic increase of SPION-labelled stem cells retention at the lesion site in the group of animals injected with SPION-labelled MSCs and exposed to MF. On the other hand, in animal groups injected by cells without SPIONs or cells loaded with SPIONs but without magnets exhibited, practically homogenous distribution through the spinal cord channel was observed (Figure 16B). The number of SPION-labelled cells in the center of the lesion under MF exposition was significantly higher compared to the other groups (Figure 16). It is worth noting that the cell distribution in the vicinity of the lesion site (Figure 16B) was quantitatively consistent with the calculated magnetic gradient force distribution (Figure 14B and C): SPION-labelled cells accumulated maximally in the trapping area of the magnetic system (Figure 16B and 17A).

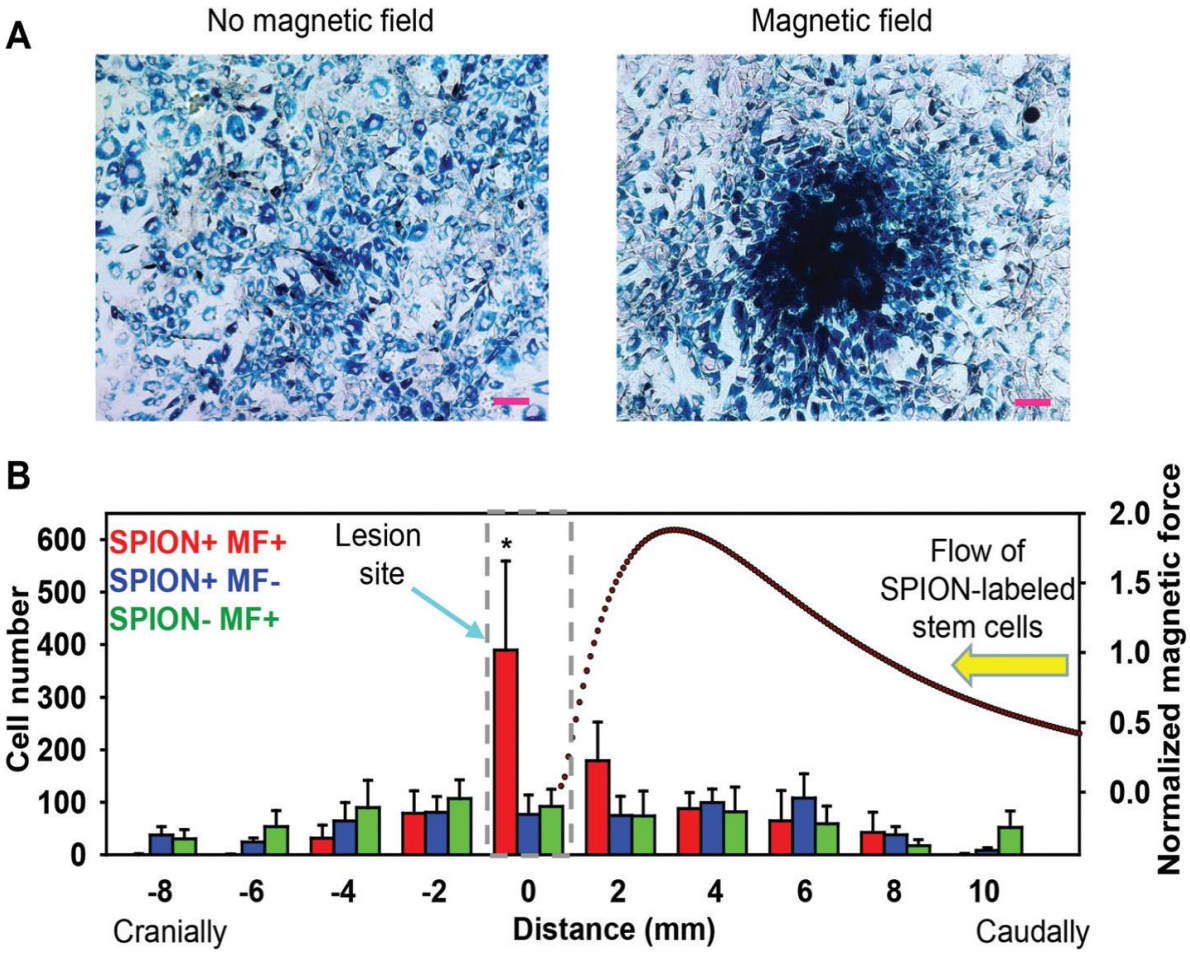

Figure 16. Distributions of SPION-labelled cells and non-labelled cells with and without the magnetic field. (A) Attraction of SPION-labelled cells to a cylindrical magnet in vitro. MSCs were labelled with SPIONs at a concentration of 15.4 µg mL^{-1} and exposed to an external magnetic field for 48 h. Cells were stained for intracellular iron using Prussian blue. Scale bar: 100 µm. (B) Numbers of the captured SPION-labelled cells and non-labelled cells in the rat model as a function of the distance from the lesion site of the SCI. After lesion induction, SPION-labelled MSCs were injected intrathecally at the L5–L6 level, at a distance of 10 cm from the lesion site. Thereafter, animals were subjected to the magnetic system exposure for 2 h in longitudinal spinal cord segments. The dotted curves represent the respective magnetic gradient force distribution taken from Figure 14B. Data are expressed as mean ± SEM, *P < 0.05.

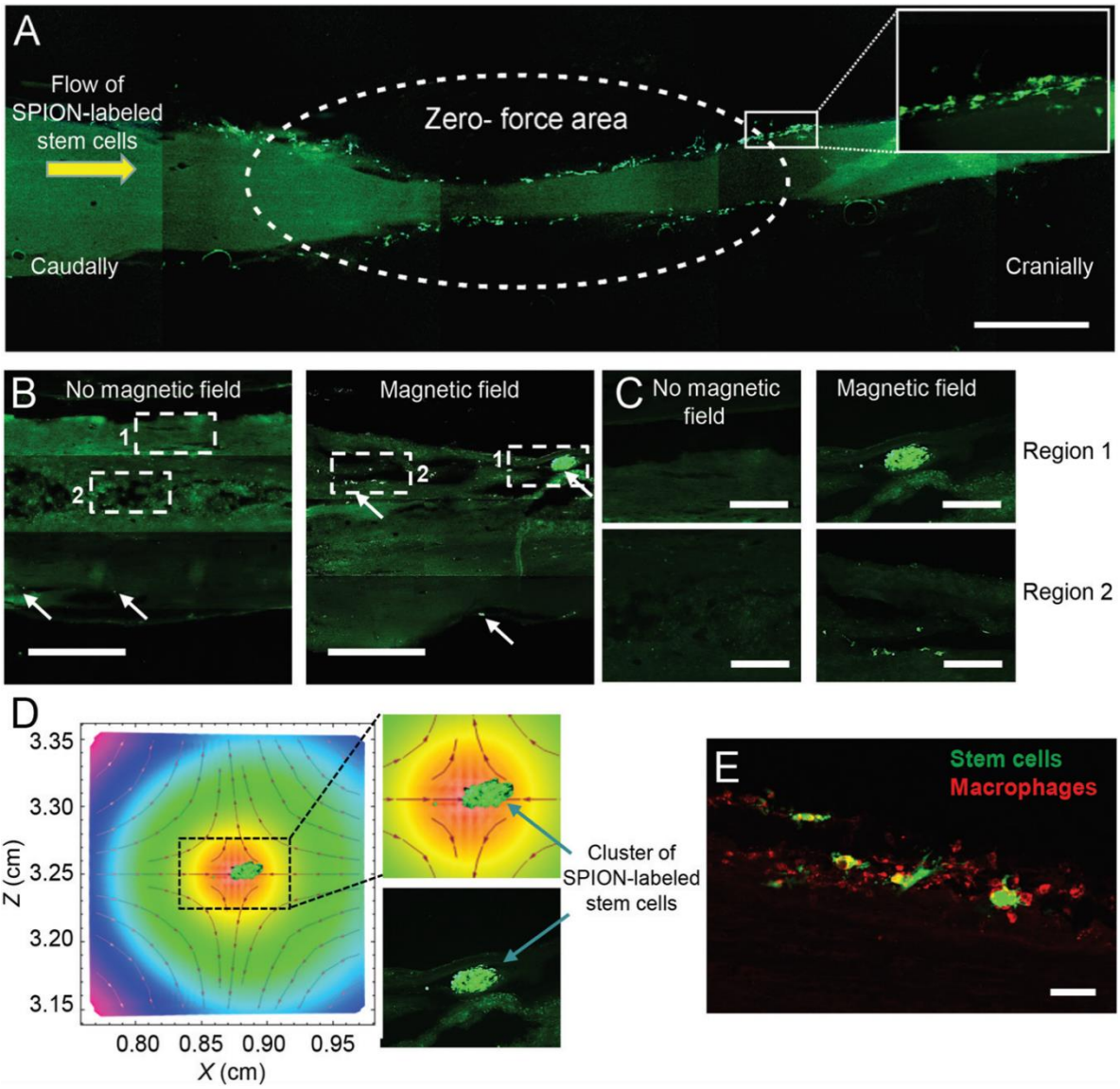

Figure 17. Longitudinal spinal cord sections of the targeted SPIONs-labelled MSCs.

(A) Spinal cord sections of SPION-labelled MSCs captured in the trapping area of the magnetic system. Scale bar – 1 mm.

(B) Longitudinal sections of the lesion site showing MSC distribution within the lesion with or without exposure to the magnetic field. The arrows show clusters of delivered SPION-labelled MSCs on the surface of the spinal cord (region 1) and SPION labelled MSCs that migrated in the deeper area of the lesion (region 2). Scale bar – 500 µm.

(C) Higher magnification of regions 1 and 2 of (B). Upon application of the magnetic field system, one can clearly see clusters of delivered SPION-labelled MSCs on the surface of the spinal cord (region 1) and intothe deeper area of the lesion (region 2). Scale bar – 100 µm.

(D) Overlay vector field of the calculated magnetic gradient force (X–Z-plane) with a cluster of accumulated cells. The binary image was generated from the respective fluorescent picture using ImageJ software (NIH). A representative enlarged region of the magnetic gradient force distribution (Figure 15A) was calculated in accordance with the magnetic system positioning. The insert shows a zoomed in section of the indicated region.

(E) Immunofluorescence staining of MSCs and macrophage infiltration in the lesion site. Macrophages were stained for the CD68 marker. Scale bar – 50 µm.

Furthermore, very few cells were detected in the cranial direction from the magnetic gradient force (Figure 16B and 17A), which verifies the capture of the SPION-labelled

cells within the MF. In contrast, non-labelled cells used with MF and SPION-labelled cells without MF revealed a homogeneous distribution without any apparent effect of the MF on cell accumulation at the SCI lesion site (Figure 16B). Interestingly, stem cell infiltration into the tissue was achieved by the application of MF for only 2 h (Figure 17B and C).

The ratio (E) between the number of cells captured at the lesion site and the total number of cells in the operating range of the spinal cord may serve as a convenient measure of the efficiency of cell delivery. From Figure 16B, the ratio E was calculated for the three animal groups studied: E = 45% for the SPION-labelled MSCs exposed to MF; E = 14% for the nonlabelled MSCs exposed to MF and E = 13% for the SPION-labelled MSCs without exposure to MF.

Finally, as revealed by superimposing the immunofluorescence images with the calculated normalized magnetic force distribution, the designed magnetic system targeted SPION-labelled cells to the trapping area (Figure 17D). However, after stem cell delivery to the lesion site, an adverse reaction occurred. Microglia/macrophages attacked the SPION-labelled stem cells (Figure 17E).

4.1.3. Discussion

The delivery technique of stem cells is a major factor determining the success of the transplantation. Targeted cell delivery is a promising method of enhancing the efficacy of treatment in SCI. Hence, using magnetic nanomaterials to guide and track the cell migration has much potential for expanding the scope of this therapy. Retention of cells at the lesion site, engraftment efficacy and functional recovery are all significantly enhanced when stem cell delivery is magnetically guided using superparamagnetic iron oxide nanoparticles (SPION) loaded stem cells, as some previous studies suggest (Landazuri N. et al., 2013; Vandergrif A.C. et al., 2014; Cheng K. et al., 2014). Such delivery procedures were successfully applied for vascular graft (Pislaru S.V. et al., 2006), intra-arterial stents (Polyak B. et al., 2008), the femoral artery (Riegler J. et al., 2013), bone (Panseri S. et al., 2012), cartilage (Kamei G. et al., 2013) and the retina (Yanai A. et al., 2012) as target sites. However, there have been only few research projects that demonstrate the use of such procedures for SCI treatment (Nishida K. et al., 2006; Vanecek V. et al., 2012; Hamasaki T. et al., 2007). Therefore, extensive work in this field for application to SCI is yet to be done.

Most magnet-induced cell delivery techniques (Polyak B. et al., 2008; Riegler J. et al., 2013; Häfeli U.O. et al., 2006; Zablotskii V. et al., 2010) share the same drawback, i.e.,

their poor focusing ability. A loaded stem cell can be captured only when it is close to a magnetic pole and within the area of maximum magnetic field strength. Therefore, placing a magnet at the lesion site is not doable, the focusing ability of the magnet is compromised. In this study we exploit magnetic system with a new design which allows us to focus the magnetic field at the spinal cord lesion site.

To enhance the efficacy of stem cell delivery in the rat model of SCI we proposed a new magnetic system (Figure 12, 14) with a specific feature – the existence of a focusing zone – trapping area, where the magnetically labelled cells have to be focused. The existence of the trapping area (with zero magnetic forces) is determined by two reasons: (i) the maximums of the planar and vertical components of the magnetic field (MF) gradient must reach close to the magnets' edges; (ii) in the mirror symmetry plane of the system, the planar and vertical components of the MF gradients have opposite directions and compensate for each other. MSCs labelled by the poly-L-lysine-coated SPIONs with proved biocompatibility (Novotna B. at al., 2012, Lunov O. at al., 2010, Lunov O. at al., 2010b) were efficiently attracted by a magnet and concentrated in the magnetic field focusing area *in vitro* as well as *in vivo* after injection intrathecally at the L5–L6 level, SPION-labelled cells concentrated at the lesion site. As in animal groups injected by cells without SPIONs or cells loaded with SPIONs but without magnets exhibited, practically homogenous distribution through the spinal cord channel was observed. The lesion itself, which releases various chemoattractants, is unable to retain the transplanted cells and therefore cannot enhance their homing to the damaged tissue area. It is worth noting that the cell distribution in the vicinity of the lesion site was quantitatively consistent with the calculated magnetic gradient force distribution. Thus, SPION-labelled cells accumulated maximally in the trapping area.

The efficacy of stem cell transplantation to the lesion site is low and variable (Neuhuber B. at al., 2005) with typical delivery time to SCI varying from 12 to 24 h (Vanecek V. at al., 2012, Fan L. at al., 2008, Donega V. at al., 2014), while in our experiment the application of MF for only 2 h resulted in stem cell infiltration into the tissue. Aside from this, the use of the magnetic system resulted in a significant increase in SPION-labelled cell accumulation directly at the lesion site in comparison to no MF application.

The efficiency of stem cells delivery shows the ratio (E) between the number of cells captured in the lesion site and the total number of cells in the operating range of the spinal cord, which contains 45% for the SPION-labelled MSCs exposed to MF in

comparison with 13-14% for control groups. Thus, there is an obvious advantage of the proposed magnetic delivery strategy resulting in a 3-fold increase of the ratio E. Furthermore, the migration of stem cells from the cerebrospinal fluid into the tissue has been associated with a better prognosis of SCI treatment (Sykova E. and Jendelova P., 2007).

However, after stem cell delivery to the lesion site, microglia/macrophages attacked the SPION-labelled stem cells. Thus, the long-term effects of transplanted SPION-labelled stem cells should be investigated in more details in future studies.

Therefore, the application of our magnetic system demonstrates the potential benefits of fast and efficient stem cells delivery into SCI lesion. The proposed strategy can be used for stem cells-based treatments of not only traumatic SCIs, but also for non-traumatic SCI or neurodegenerative diseases (Sykova E. at al., 2006, Forostyak S. at al., 2013). The fate and regenerative capacity of magnetically labelled MSCs after their forced accumulation near the lesion would be a challenging direction for further study. The efficacy of such magnetic targeting strategy and the possibilities of reaching therapeutic concentrations should be assessed together with physiological and biological factors that decrease the number of captured living cells at the lesion site.

4.2. INJECTABLE EXTRACELLULAR MATRIX HYDROGELS FOR SPINAL CORD INJURY REPAIR

4.2.1. Porcine spinal cord and urinary bladder extracellular matrix hydrogels

4.2.1.1. Biocompatibility and bioadhesive properties of SC-ECM and UB-ECM hydrogels for hWJ-MSCs

Solubilized ECM matrixes self-assemble from pre-gel form into the hydrogel at physiological pH and 37^{o}C temperature (Medberry C.J. et al., 2013). The biocompatibility and bioadhesive properties of both ECM hydrogels were confirmed by the assessment of *in vitro* growth of hWJ-MSCs in 2D and 3D cell cultures based on these hydrogels (Figure 18). hWJ-MSCs purity was evaluated by flow cytometry. CD markers were found positive for CD29, CD105, CD90, CD73, HLA-ABC and negative for CD31, CD34, CD45, CD133, CD235a and CD271.

After seeding on the ECM hydrogels, the cells spread and proliferated on both hydrogel types (Figure 18). WST-1 assay was conducted after 1, 3, 7 and 14 days of the culture to detect the cell proliferation. Both ECM hydrogels showed comparable ability to support *in vitro* stem cells proliferation, which did not significantly differ from the control cell culture seeded on standard plastic tissues (TCP). Cell viability increased until day 7, then, after reaching the confluency of the culture, decreased on both hydrogel types as well as on TCP (Figure 18G).

When seeded in 3D culture (0.5 million cells per 0.2 mL), hWJ-MSC extended their lamellipodia within the hydrogels and formed a 3D network as shown in Figure 18 C-F. Rapid hydrogel contraction was observed as early as 4 hand progressed during the culture to at least 10 % of the initial area after 7 days (Figure 19).

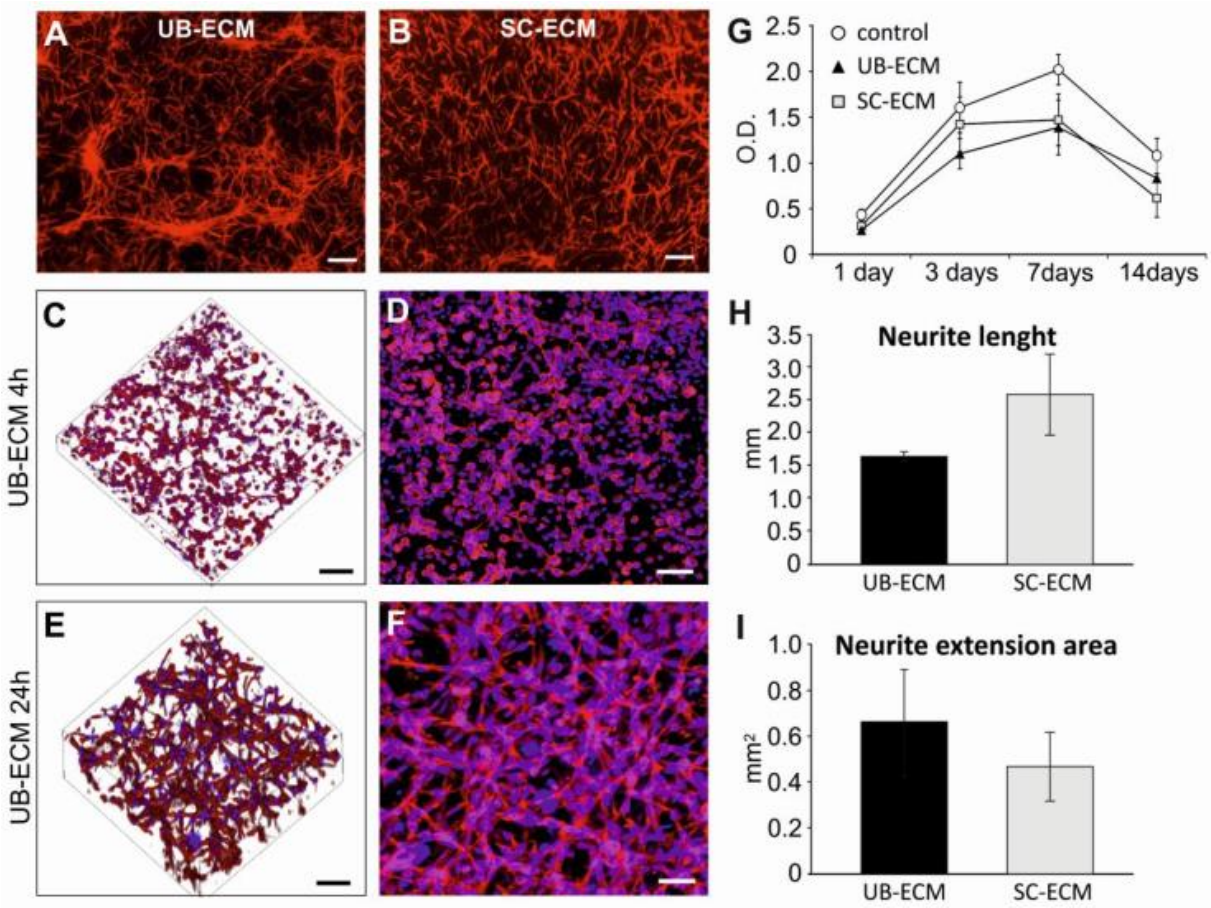

Figure 18. In vitro cell growth on ECM hydrogels. 2D cell culture on (A) UB-ECM and (B) SC-ECM hydrogels at 3 days. (C-F) 3D cell culture in UB-ECM at (C, D) 4 h and (E, F) 24 h. Cells were stained for (A -F) phalloidin and (C-F) cell nuclei (DAPI). (G) Proliferation of hWJ-MSC on ECM hydrogels using WST-1 assay. (H) Quantification of the highest neurite length and (I) neurite extension area of DRG explants on ECM hydrogels using Neurite-J plugin for Image J software. Scale bar: (A, B) 100 µm, (C-F) 50 µm.

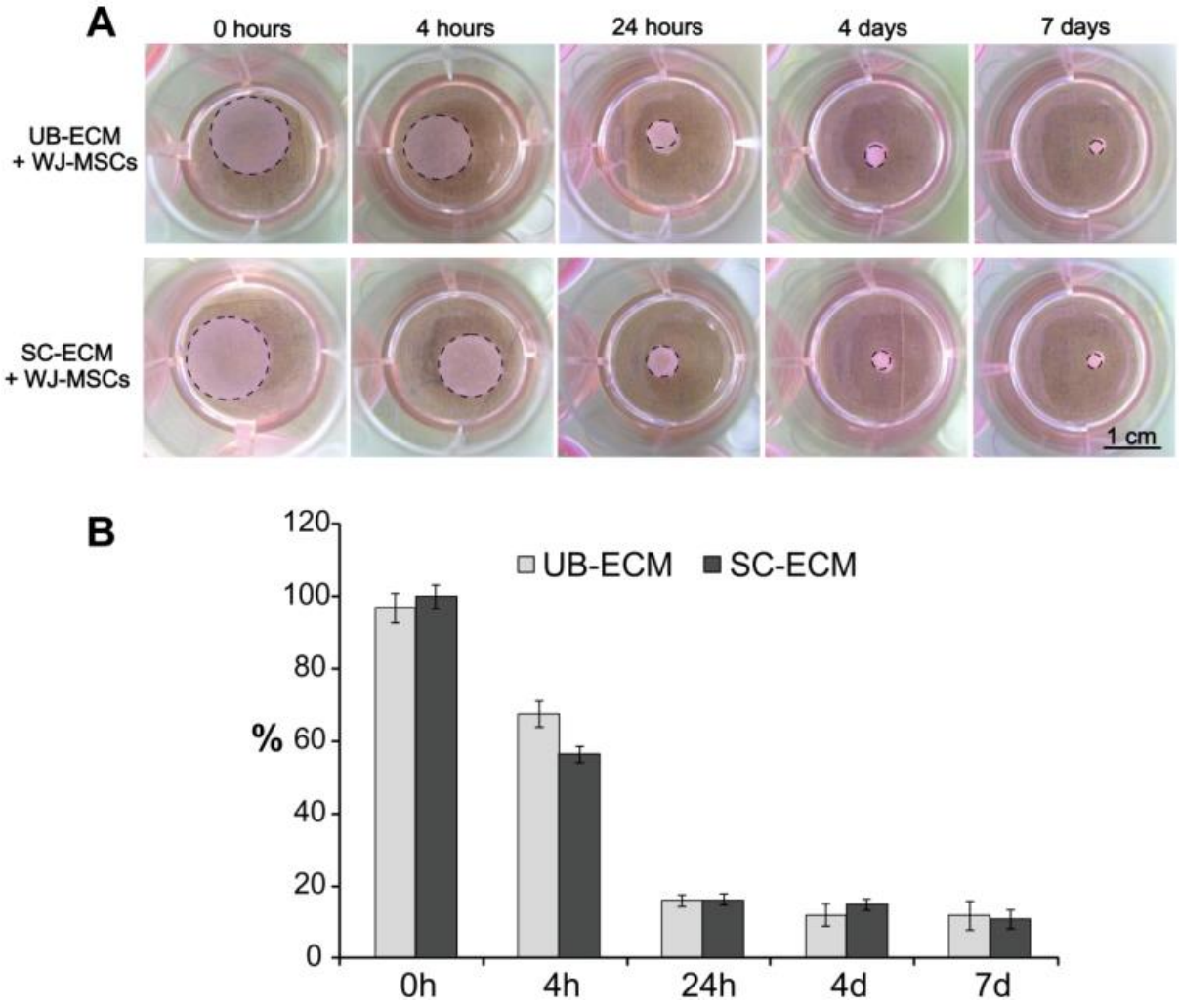

Figure 19. (A) Free floating hydrogel discs combined with WJ-MSC after 4 h, 24 h, 4 days and 7 days of the culture. (B) The area of the hydrogel discs in time in relation to the unseeded control hydrogels.

4.2.1.2. Neurotrophic properties of SC-ECM and UB-ECM hydrogels

Dorsal root ganglion (DRG) explant cultures were used to compare the neurotrophic properties of the CNS- and non-CNS derived ECM hydrogels. After cultivation for 7 days, neurites densely extended from the DRG bodies (Figure 20). No significant differences were found between UB-ECM and SC-ECM in both examined parameters, total neurite extension area and longest neurite length (Figure 18 H, I).

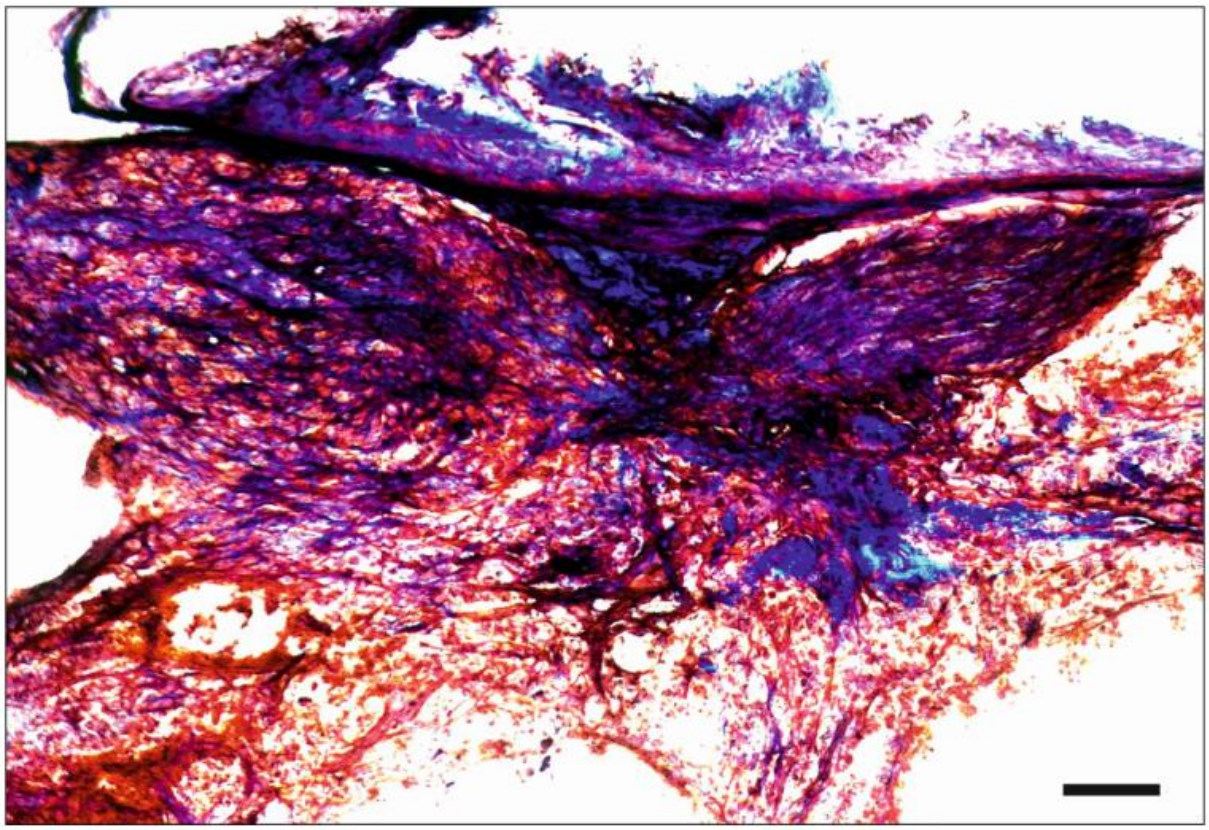

Figure 20. Representative confocal images of neurite outgrowth from DRG explants on (A) UB-ECM and (B) SC-ECM (staining for NF160 and DAPI). Scale bar: 100µm.

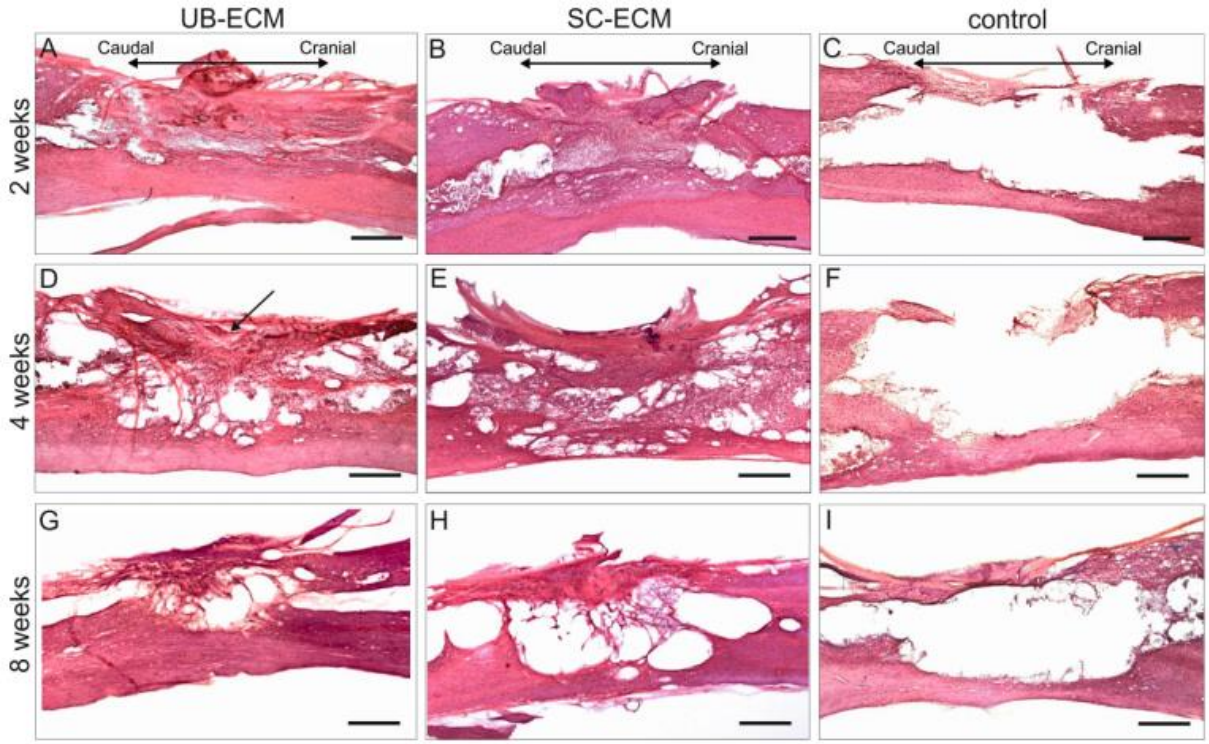

Figure 21. Representative hematoxylin-eosin staining of the spinal cord lesion (A-C) 2, (D-F) 4 and (F-I) 8 weeks after injection of (A, D, G) UB-ECM hydrogels; (B, E, H) SC-ECM hydrogels. (C, F, I) represent a sham-operated control lesion. The arrow (D) shows the nondegraded part of the hydrogel. Scale bar: 500 µm.

4.2.1.3. Histological evaluation of injected UB-ECM and SC-ECM hydrogels

Both UB-ECM and SC-ECM hydrogels were injected into the cavity of the spinal cord hemisection and examined at 2, 4 and 8 weeks. The tissue response to the scaffolds was histologically evaluated by analyzing axonal ingrowth, vascularization and infiltration of macrophages/microglia, astrocytes and oligodendrocytes within the injury site. At 2 weeks after injection, haematoxylin-eosin (H&E) staining of longitudinal spinal cord sections demonstrated that both hydrogel types were biocompatible with the surrounding host tissue and entirely filled the lesion cavity (Figure 21 A, B). The hydrogels were mostly degraded but still remained detectable in the lesion area (Figure 22) and were densely populated by the host cells. By 4 weeks post injection, small areas of the original hydrogel were still present (Figure 21 D), while the newly formed tissue interconnected with the host tissue, bridging the lesion center. Macrophages massively infiltrated the periphery of the lesion where several small cysts developed due to rapid degradation of the graft. A similar tissue response was found at 8 weeks, when the hydrogels had fully degraded, followed by further progression of cyst formation. In contrast to the tissue remodeling process observed in the lesion after hydrogel injection, large pseudocysts formed in the control sham-treated lesion (Figure 21 C, F, I).

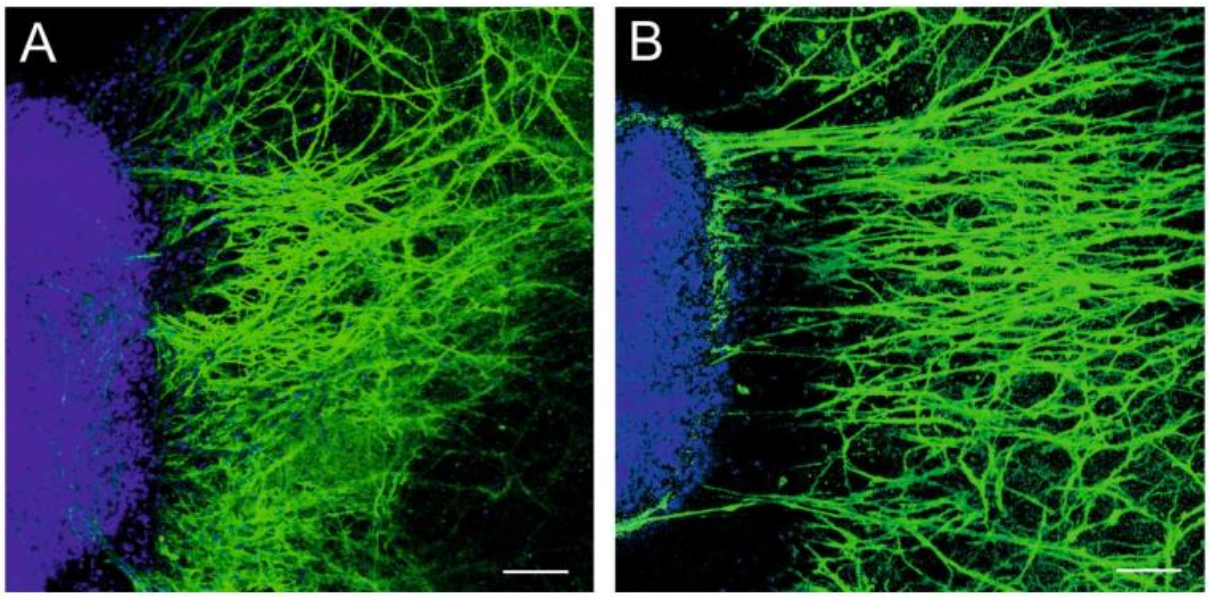

Figure 22. Trichrome staining of longitudinal sections of the spinal cord lesion at 2 weeks after injection of SC-ECM hydrogels. Non degraded parts of the hydrogel are stained blue. Scale bar: 200μm.

To evaluate axonal ingrowth into the hydrogels, a neurofilament marker (NF160) was used (Figure 23). Robust ingrowth of NF-positive fibers into the hydrogel-treated lesion was observed from both the rostral and caudal stumps of the lesion, while dense

infiltration of NF was also found in the center of the lesion (Figure 23). Quantification analysis expressed the relative value of NF160 immunopositive area as a percentage of the lesion area. The ingrowth of NF was maximal at 2 weeks in both hydrogel groups and did not further increase at later time points (Figure 24). No differences in the NF area were found between SC-ECM and UB-ECM hydrogels at all time points (Figure 24). Despite the isotropic structure of the ECM hydrogels, the ingrowing axons linearly bridged the SCI lesion while forming multiple bundles organized in a longitudinal direction along the spinal cord (Figure 23 B). Newly sprouted axonal fibers were also detected using GAP 43 staining (Figure 25 G). Astrocytes, evaluated by immunofluorescent staining for GFAP, did not migrate inside the lesion and thus served as a clear demarcation of the lesion area (Figure 23 C, F). Only a few astrocytic processes grew into the graft from the lesion border (Figure 23 F). In terms of neo-vascularization, a number of blood vessels (RECA staining) grew into the hydrogel treated lesions and formed a dense network (Figure 26 A-D). The area of blood vessels gradually increased with time, but no differences in blood vessel density were found between the UB-ECM and SC-ECM hydrogels at any time point (Figure 27). The host tissue remodeling response was characterized by robust infiltration of CD68+ cells throughout the entire lesion area (Figure 25 A, B), which populated the hydrogels at all time points and remained in the lesion site after the hydrogel had degraded. As is apparent from the staining of M1 and M2 macrophages in Figure 25 E, macrophages at the interface of the ECM hydrogel and the host tissue were predominantly of the M1 phenotype (CD86 staining), while M2 phenotype macrophages (CD206 staining) were mostly present within the hydrogel area. Infiltration of serotonin-positive axons (Figure 25 C, D) was observed from the rostral part of the hydrogels, but these axons did not spread across the lesion. Infiltration of oligodendrocytes (OSP staining, Figure 25 F) within the lesion site indicated that myelination occurred in some of the regenerated axons. Numerous endogenous Schwann cells that had migrated from the nerve roots were detected within the lesion site as well as in the surrounding tissue (Figure 25 H).

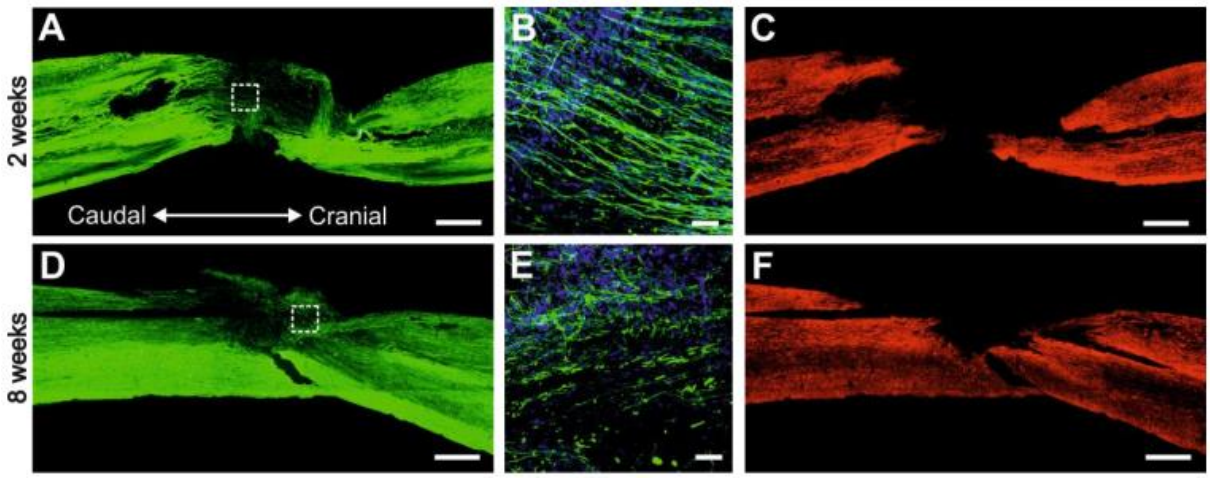

Figure 23. Representative images of the spinal cord lesion (A-C) 2 and (D-F) 8 weeks after injection of SC-ECM hydrogels. Immunofluorescent staining for (A, B, D, E) neurofilaments (NF160), (C, F) astrocytes (GFAP) and (B, E) cell nuclei (DAPI, blue). Squares (A, D) are also shown under the higher magnification insets (B and E).

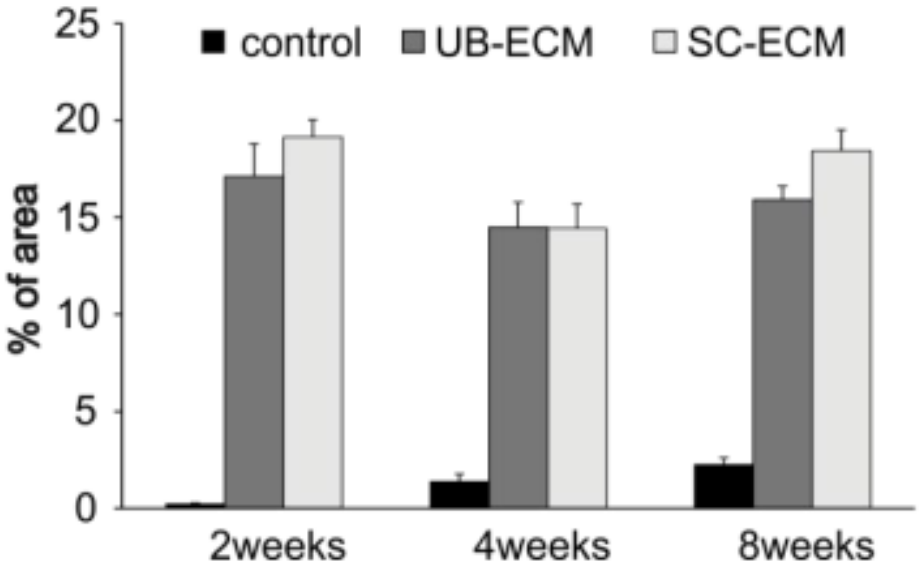

Figure 24. The effect of ECM hydrogels on the ingrowth of NF. Significantly higher NF ingrowth was found in both ECM hydrogel groups when compared to the control lesion at all time points. Scale bar: (A, C, D, F) 500 μm; (B, E) 50 μm.

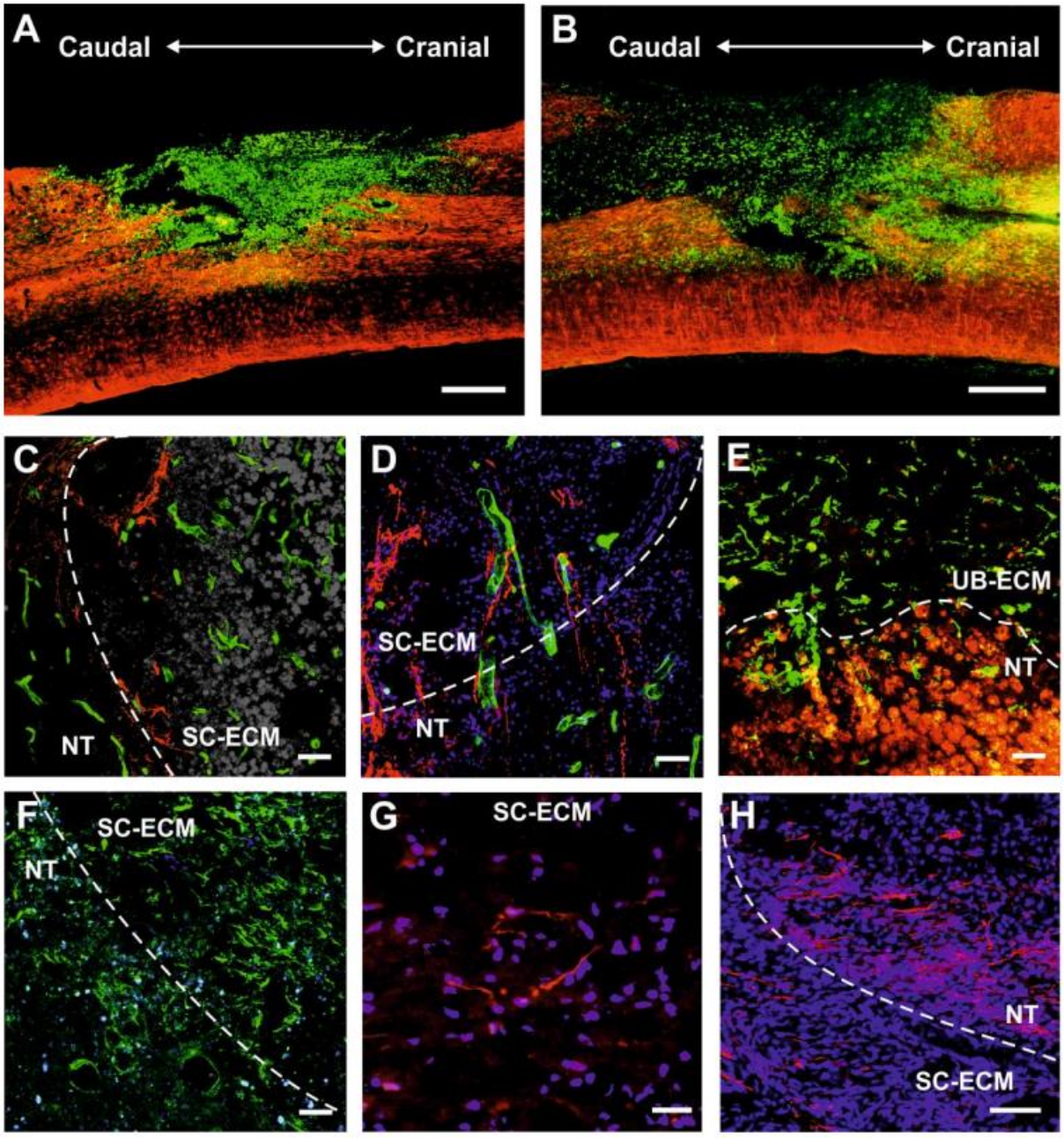

Figure 25. Representative immunofluorescent staining for (A, B) macrophages (ED1, green) and astrocytes (GFAP, red) in (A) UB-ECM at 2 weeks and (B) SC-ECM seeded with hWJMSCs at 4 weeks. Confocal micrographs of staining for (C) serotonin-positive axons (5- HT, red) and blood vessels (RECA, green) in SC-ECM at 4 weeks; (D) serotonin-positive axons (5-HT, red), blood vessels (RECA, green) and cell nuclei (DAPI, blue) in SC-ECM seeded with WJ-MSCs at 4 weeks; (E) M1 macrophages (CD86, red) and M2 macrophages (CD206, green) in UB-ECM hydrogel at 2 weeks; (F) oligodendrocytes (OSP, green) and cell nuclei (DAPI, blue) in SC-ECM at 4 weeks; (G) neuronal growth cones (GAP 43, red) and cell nuclei (DAPI, blue) in SC-ECM at 4 weeks; (H) Schwann cells (p75, red) and cell nuclei (DAPI, blue) in SC-ECM at 4 weeks. The dotted line in (C, D, E, F, H) describes the border between the ECM hydrogel and the neural tissue (NT). Scale bar: (A, B) 500 µm; (C, H) 100 µm; (D, E, F) 50 µm; (G) 25 µm.

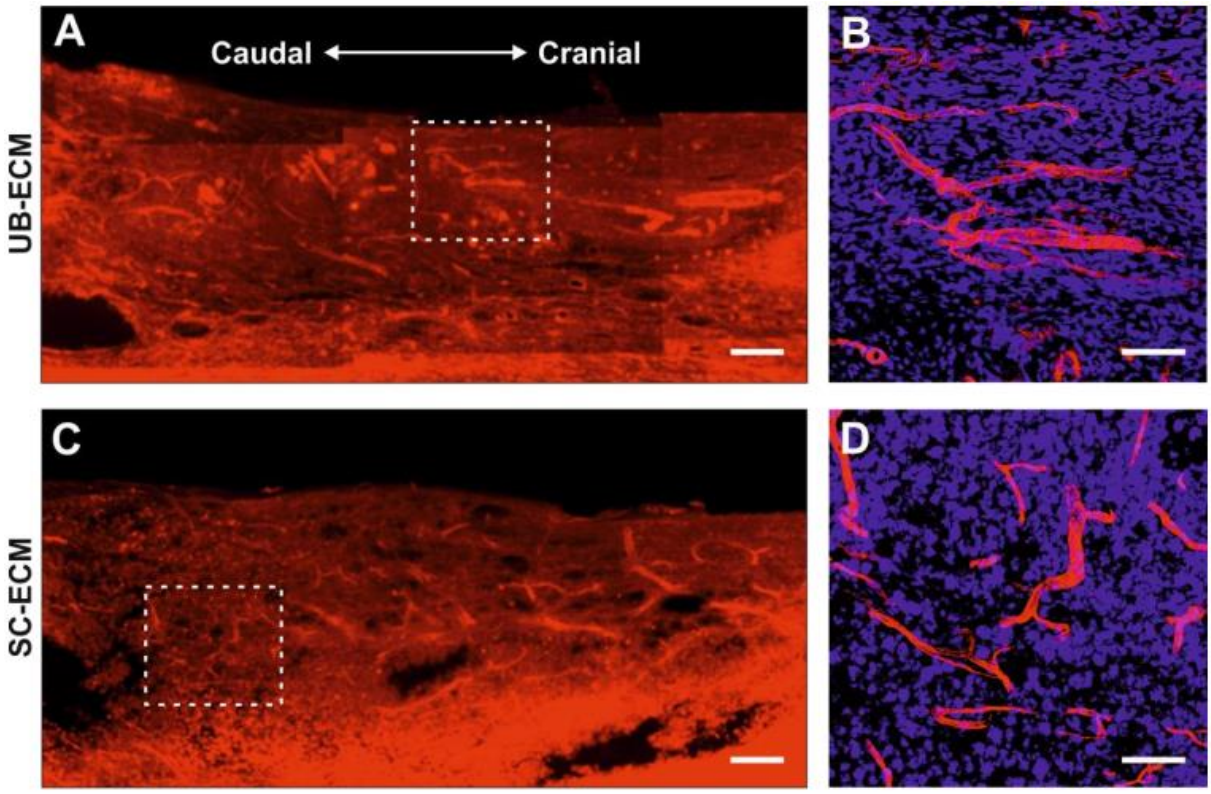

Figure 26. Representative images of the spinal cord lesion at 2 weeks after injection of (A, B) UBM-ECM and (C, D) SC-ECM hydrogels. (A – D) Immunofluorescent staining for blood vessels (RECA) and (B, D) cell nuclei (DAPI). Squares (A, C) are also shown under the higher magnification insets (B and D).

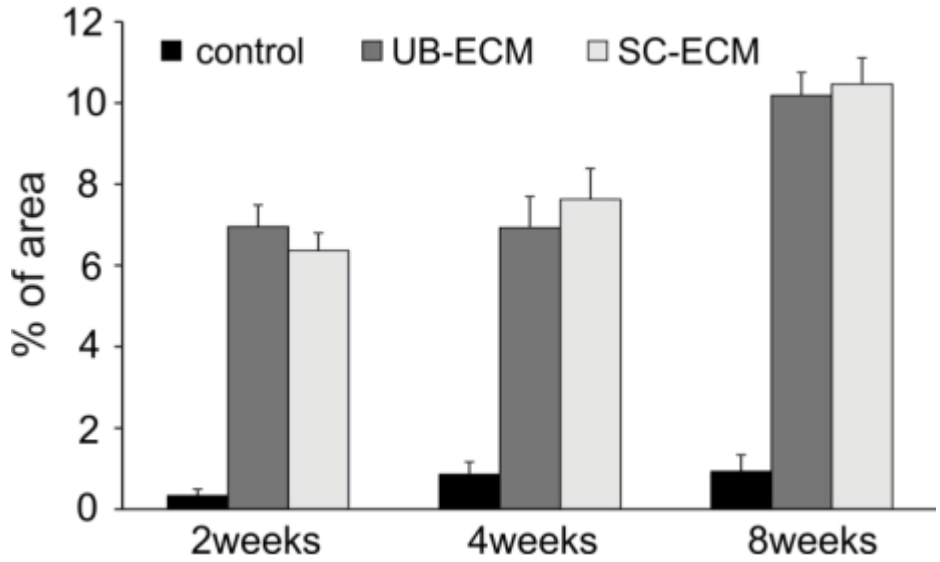

Figure 27. The effect of ECM hydrogels on vascularization. Significantly higher ingrowth of blood vessels was found in both ECM hydrogel groups when compared to the control lesion at all time points. Scale bar: (A, C) 500 µm; (B, D) 50 µm.

4.2.1.4. Histological evaluation of implanted UB-ECM and SC-ECM hydrogels combined with hWJ-MSCs

To evaluate the potential of ECM hydrogels as a cell vehicle, the SC-ECM hydrogels were mixed with hWJ-MSCs (0.5 million cells per 0.2 mL) and the mixtures containing ~15,000 cells were acutely implanted into the hemisection cavity. Four weeks after surgery, the grafts were densely infiltrated by endogenous tissues while cysts had developed at the graft-tissue interface (Figure 28). Only very few surviving cells, positive for human mitochondria MTCO2 marker, were detected in the lesion (Figure 28 B). Transplanted cells did not further promote the ingrowth of NF-positive fibers or blood vessels. However, an increase in NF positive fibers was found in the groups of animals which received immunosuppression (Figure 28 F, G). As in the empty ECM hydrogels, M2 phenotype macrophages were mostly present within the hydrogel area (Figure 28 E).

4.2.1.5. Gene expression induced by UB-ECM and SC-ECM hydrogels

Changes in the mRNA expression of genes related to inflammation (Ptgs2, Ccl3, Ccl5, Il2, Il6, Il12b), M1 macrophages (Irf5, CD86, Nos2), M2 macrophages (Mrc1, CD163, Arg1), growth factors (NT-3, Fgf2), axonal sprouting (Gap43), astrogliosis (Gfap), angiogenesis (Vegfa) and apoptosis (Casp3) were determined at 2, 4 and 8 weeks after hydrogel injection and compared to the control SCI lesion (Figure 29, Table 8). The most profound host tissue response to the ECM hydrogels was observed 2 weeks after the injection, when a significant downregulation was found in the expression of Fgf2, CD163, Irf5, Ccl5 and Gap43 in both hydrogel groups and of Gfap in the UB-ECM hydrogel group only compared to the control SCI lesion. At 4 weeks, no significant changes were detected between both hydrogel groups and the control group, except for a significant upregulation of Arg1 in the UB-ECM hydrogel group compared to SC-ECM (Table 8). A potential tissue specific effect of SC-ECM was observed at week 8, when a significant upregulation of mRNA expression was detected for NT-3, Fgf2, Irf5 and Casp3. Expression of pro-inflammatory cytokines IL-2, IL-6, Il12b and Nos2 was undetectable in all groups.

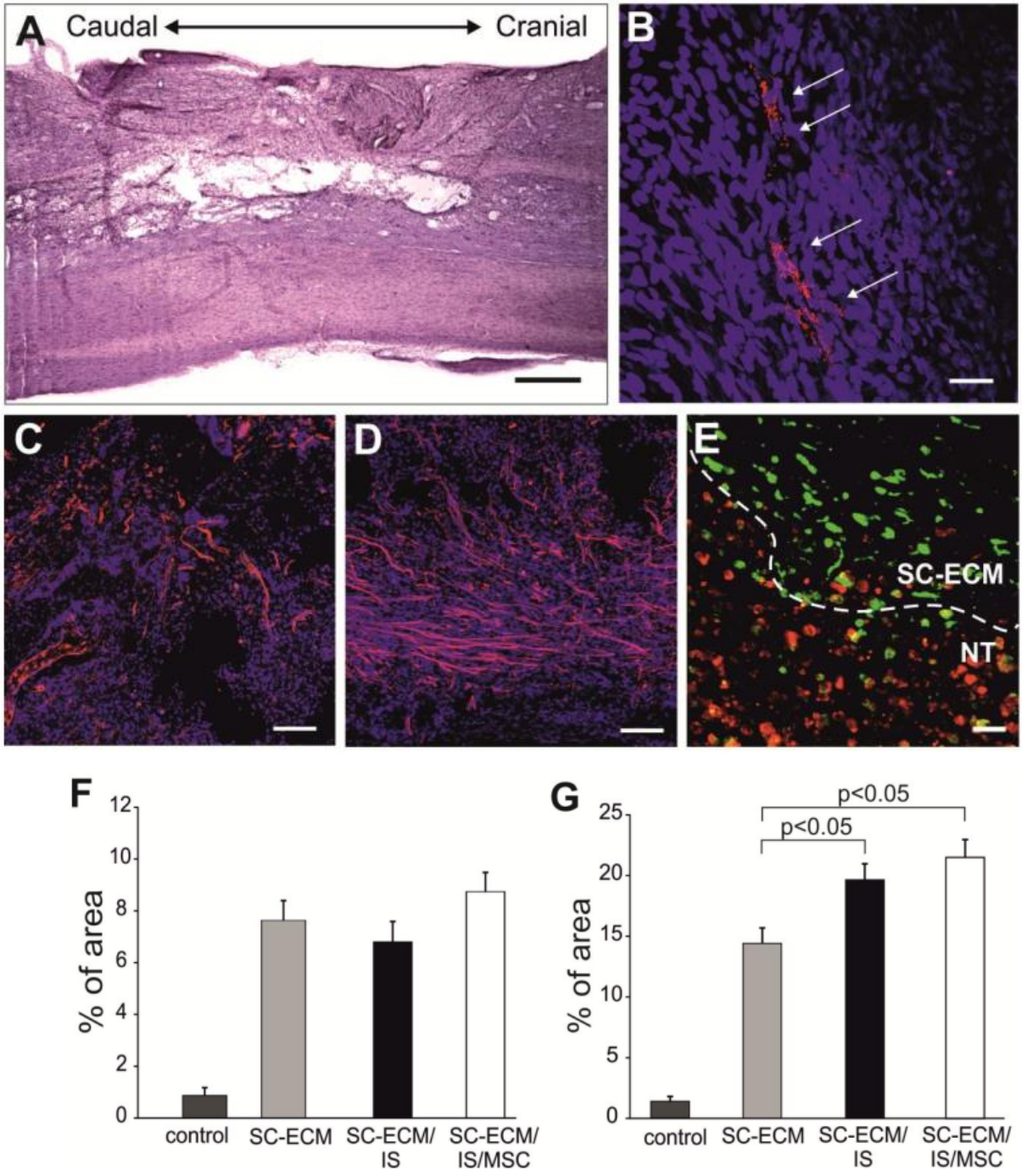

Figure 28. Representative images of the spinal cord lesion after implantation of SC-ECM seeded with hWJ-MSCs at 4 weeks. (A) Hematoxylin-eosin staining. Confocal micrographs of the staining for (B) human mitochondria (MTCO2); (C) blood vessels (RECA); (D) neurofilaments (NF160) and (B - D) cell nuclei (DAPI, blue); (E) M1 macrophages (CD86, red) and M2 macrophages (CD206, green). The dotted line in (E) describes the border between the ECM hydrogel and the neural tissue (NT). The effect of the SC-ECM hydrogels seeded with hWJMSCs on the ingrowth of (F) blood vessels and (G) neurofilaments. (IS) - animal groups that received immunosuppression. Scale bar: (A) 500µm, (B, E) 50µm, (C, D) 100µm.

The effect of hWJ-MSCs combined with the SC-ECM hydrogels was determined 4 weeks after the scaffold implantation in animals receiving immunosuppression to prevent rejection of xenogeneic cells. Interestingly, the immunosuppression significantly decreased

the mRNA expression of Gfap in both empty and cell seeded hydrogels, and of Fgf2, Casp3, Ccl3 and CD86 in empty hydrogels when compared to the control lesion (Figure 29). Moreover, a significant increase in the expression of Vegfa and Gap43 was also found in cell-seeded hydrogels when compared to the empty hydrogels.

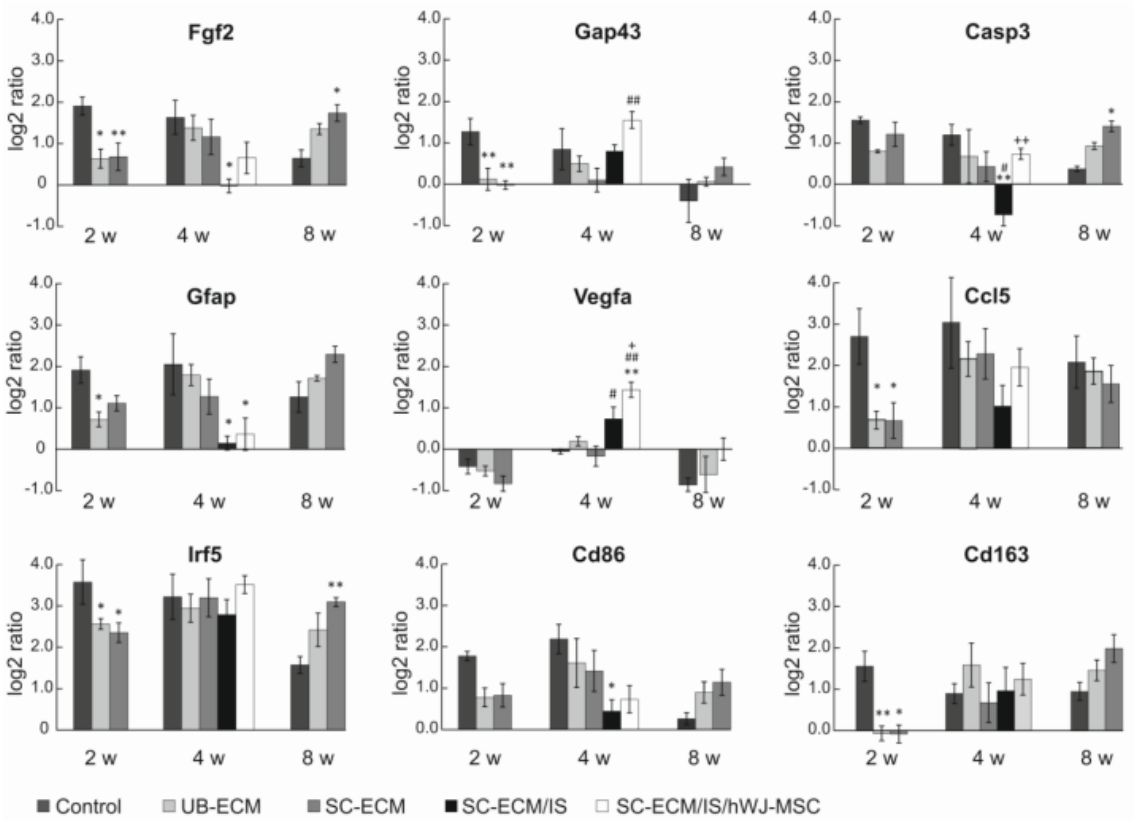

Figure 29. Analysis of mRNA gene expression of several genes involved in inflammatory and reparative processes following SCI treated with ECM hydrogels. The graphs show the log2 fold changes in gene expression over intact spinal cord tissue. (IS) - animal groups that received immunosuppression. * $p < 0.05$, ** $p < 0.01$ ΔCt values of ECM hydrogel vs control lesion # $p < 0.05$, ## $p < 0.01$ ΔCt values of SC-ECM hydrogel with IS vs SC-ECM + $p < 0.05$, ++ $p < 0.01$ ΔCt values of SC-ECM hydrogel with IS and hWJ-MSCs vs empty SC-ECM with IS.

Table 8. Expression of selected genes in the spinal cord lesions treated with UB-ECM and SC-ECM hydrogels

	Control	UB-ECM	SC-ECM	SC-ECM/IS	SC-ECM/IS + hWJ-MSCs
Sort1					
2 weeks	0.66 ± 0.36	-0.56 ±0.21**	-0.02 ±0.33		
4 weeks	0.83 ± 0.20	0.47 ±0.21	0.004 ±0.39	-0.56 ±0.12 *	0.22 ±0.28
8 weeks	-0.30 ± 0.07	0.35 ±0.21	0.81 ±0.08 *		
Arg1					
2 weeks	0.62 ±0.17	-1.17 ±0.41	-1.07 ±0.35		
4 weeks	0.18 ±0.41	1.88 ±0.43 #	-0.06 ±0.81	0.80 ±0.72	1.56 ±0.57
8 weeks	-0.18 ±0.30	1.04 ±0.41	0.21 ±0.22		
Cel3					
2 weeks	5.01 ±0.08	4.96 ±0.53	5.14 ±0.57		
4 weeks	5.69 ±0.62	5.90 ±0.76	5.26 ±0.60	2.89 ±0.22 *#	4.05 ±0.79
8 weeks	3.14 ±0.56	4.16 ±0.89	4.09 ±0.99		
Ptgs2					
2 weeks	2.22 ±0.58	1.48 ±0.14	1.60 ±0.52		
4 weeks	2.35 ±0.83	1.51 ±0.13	1.79 ±0.46	0.91 ±0.33	2.31 ±0.31
8 weeks	1.14 ±0.59	1.64 ±0.15	2.40 ±0.37		
Mrc1					
2 weeks	3.63 ±0.48	2.67 ±0.26	2.50 ±0.34		
4 weeks	3.16 ±0.36	3.19 ±0.64	2.63 ±0.40	0.77 ±0.23	1.44 ±0.12
8 weeks	2.01 ±0.31	2.57 ±0.10	2.59 ±0.07		

Log2ratio of ΔΔCt ± S.E.M.
* $p < 0.05$, ** $p < 0.01$ ΔCt values of ECM hydrogel vs control lesion
# $p < 0.05$ ΔCt values of SC-ECM hydrogel with IS vs SC-ECM
Il2, Il6, Il12b and Nos2 were undetectable in all groups

4.2.1.6. Evaluation of hind limb motor functions

Hind limb motor function was recorded between the first and fourth week post-SCI for the sham-operated control group (animals were treated with SC-ECM alone and SC-ECM combined with hWJ-MSCs, n = 5) using the Basso–Beattie–Bresnahan (BBB) open field locomotor test. The animals were tested by two blind observers once a week starting 7 days after surgery. No significant differences in average hindlimb locomotor score were observed between the tested groups (Figure 30).

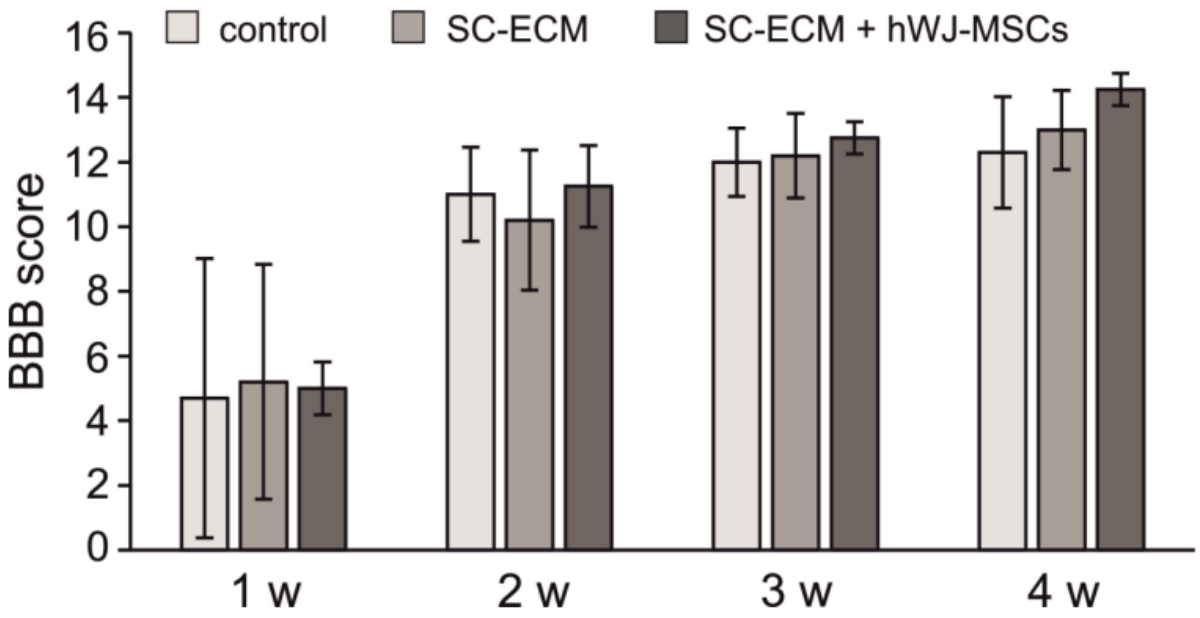

Figure 30. The Basso, Beattie, and Bresnahan (BBB) average hindlimb locomotor scale in sham-operated animals and animals treated with SC-ECM alone or combined with hWJ-MSCs (mean ± S.D., n = 5 per group).

4.2.1.7. Discussion

Tissue engineered scaffolds play an important role in providing supportive substrates that contribute to the replacement of lost tissue and reestablishment of damaged connections after injury (Kubinova S. and Sykova E., 2012, Assuncao-Silva R.C. at al., 2015, Macaya D. and Spector M., 2012, Siebert J.R. at al., 2015). Biological scaffolds composed of native extracellular matrix (ECM) represent structures very similar to those of uninjured host tissue with advantages such as a natural three-dimensional structure, biological activity promoting cell adhesion and proliferation, and biodegradability (Crapo P.M. at al., 2012).

Currently, ECM scaffolds are being widely used for various tissue reconstructions, including heart valves, blood vessels, skin, bone, cartilage, trachea, lung or peripheral nerves. In contrast, there are only a few studies addressing biological scaffolds for the repair of SCI based

on acellular muscle scaffold (Zhang X.Y. at al., 2011), acellular sciatic nerve (Li C. at al., 2012) or acellular spinal cord scaffolds (Liu J. at al., 2012).

Tissue specific injectable ECM hydrogels prepared by decellularization of porcine brain, spinal cord (SC-ECM) and porcine urinary bladder (UB-ECM) have been recently described in terms of their composition, biomechanical properties and neurotrophic properties (Medberry C.J. at al., 2013, DeQuach J.A. at al., 2011). These materials have proven to be beneficial for providing a supportive environment for *in vitro* neural cell growth. However, experimentally, it is unknown whether these materials can be successfully used for SCI repair, either alone or in combination with various types of cells. To evaluate the potential neuroregenerative properties of CNS and non-CNS derived materials *in vivo*, we examined the effects of ECM hydrogels based on SC-ECM and UB-ECM in an acute model of SCI.

The ECM matrices were derived from porcine spinal cord and urinary bladder and processed into an injectable hydrogel form as was described in (Medberry C.J. at al., 2013, Wolf M.T. at al., 2012). Due to different tissue sources, these two hydrogels were prepared using different decellularization methods and they were differed in their composition as well as in their physicochemical and biological properties (Medberry C.J. at al., 2013, Wolf M.T. at al., 2012). Despite the lack of native three-dimensional ultrastructure intrinsic to the source tissue, ECM hydrogels retain their biological activity and possess mechanical properties similar to that of soft neural tissue, with the advantage of injectability and *in situ* polymerization, which offers minimally invasive delivery techniques and facilitates the possibility of clinical translation.

When injected into the SCI, both hydrogel types were well integrated into the surrounding tissue and supported massive cell infiltration and neovascularization. A potentially important factor for tissue regeneration is the tissue source for the ECM hydrogel. However, both studied materials proved to be advantageous for providing a supportive environment and revealed similar neurotrophic properties *in vitro* in DRG explant culture as well as *in vivo* with regards to the ingrowth of neurofilaments and neovascularization. These findings are consistent with those of a previous study which showed no advantage of CNS-derived ECM materials versus non-CNS derived ECM materials with respect to effects upon neural stem/progenitor cells (Crapo P.M. at al., 2014).

When applied immediately to the SCI, the neuroregenerative potential of ECM hydrogels might be burdened by the hostility of the acute SCI lesion due to the acute inflammatory response, which may in return significantly influence the speed of hydrogel degradation and thus the nature of tissue replacement.

Macrophages were predominantly infiltrating cells within the grafts that participated in ECM degradation. As shown previously, degradation of ECM scaffolds is essential for the constructive tissue remodeling process in which a degradable biomaterial serves as a temporary inductive niche which is gradually replaced by anatomically appropriate and functional tissue as opposed to scar tissue (Badylak S.F. at al., 2009, Tottey S. at al., 2011, Valentin J.E. at al., 2009). Moreover, degradation of ECM scaffolds stimulates the release of matricryptic molecules which possess a variety of bioactive properties such as antimicrobial activity, angiogenic effects as well as recruitment of endogenous stem and progenitor cells (Valentin J.E. at al., 2009). In our study, however, despite the filling of the ECM hydrogels in the lesion cavity with endogenous cells 2 weeks after their injection, further progression in matrix degradation at later time points was not followed by full neural tissue replacement, but rather resulted in the formation of a dense network of tissue containing axons, blood vessels and other neural tissue elements interrupted by a number of small cysts.

ECM degradation *in vivo* was associated with a significant decrease in the expression of markers of pro-inflammatory/M1 macrophages (Irf5) and regulatory/M2 macrophages (CD163), inflammation (Ccl5/RANTES), as well as genes responsible for growth factor Fgf2, astrogliosis (Gfap) and neuronal growth cones (Gap43). Expression of other markers related to immune response, such as CD86, Mrc1 and Ptgs2, also decreased, but these changes were not found to be significant. Interestingly, these effects were detected during the early phase after injury but decreased or even reversed at later time points, suggesting that ECM hydrogel degradation played a significant role in the transient modulation of the innate immune and tissue repair response.

Notably, immunosuppression significantly promoted axonal ingrowth, decreased expression of Gfap, Fgf2, Casp3, Ccl3 and CD86, and increased expression of Vegfa, confirming the neurotrophic effect of immunosuppressive agents (Sosa I. at al., 2005).

Previous reports have shown increased numbers of M2 macrophages and a more positive polarization towards the M2 phenotype associated with ECM *in vivo* degradation and promotion of constructive tissue remodeling (Badylak S.F. and Gilbert T.W., 2008, Brown B.N. at al., 2012). Recent studies have desribed the M2 polarizing effects of ECM derived from several tissues (Sicari B.M. at al., 2014, Slivka P.F. at al., 2014). In the present study, the expression of genes related to both M1 and M2 macrophages decreased at 2 weeks, which reflects that both inflammatory as well as anti-inflammatory responses were inhibited after ECM hydrogel treatment. Nevertheless, according to positive staining of CD206, ECM hydrogel treatment led to spatial differences in macrophage distribution within the lesion, where M2 macrophages were

mostly accumulated within the hydrogel, while M1 macrophages concentrated in the surrounding tissue.

The ability of ECM hydrogels to promote *in vitro* cell growth and proliferation was examined using human hWJ-MSCs. hWJ-MSCs currently represent a promising cell type in regenerative medicine and are already being evaluated in various clinical trials including SCI (Cheng H. at al., 2014). *in vitro* 2D cell culture demonstrated that both types of ECM hydrogels promoted adhesion and proliferation of hWJ-MSCs. However, when seeded in 3D culture, hWJ-MSCs triggered rapid gel contraction. This well-known phenomenon is characteristic of collagen gels seeded with fibroblasts, which generate tension on the matrix during both extension and retraction of pseudopodia (Brown R.A., 2013). A similar effect has also been described for ECM hydrogels derived from porcine dermis as well as urinary bladder seeded with fibroblasts (Wolf M.T. at al., 2012). Using ECM as a cell vehicle *in vivo* to fill the lesion cavity may result in inhomogeneous scaffold distribution within the lesion due to rapid gel contraction. Moreover, when injected into the lesion, the ECM hydrogels may further contract over time as they are populated with various endogenous cells such as fibroblasts or epithelial cells. Of note, a similar collagen concentration (~700 μg collagen/mg dry weight) as well as gel contraction rate were found for both SC-ECM and UB-ECM, while the sulfated glycosaminoglycan concentration was higher in UB-ECM (~ 4 μg/mg dry weight) than in SC-ECM (~ 1 μg/mg dry weight) (Medberry C.J. at al., 2013).

Implantation of ECM hydrogels with seeded stem cells may partly prevent the massive scaffold contraction within the lesion cavity. However, the inflammatory milieu of the acute lesion together with massive infiltration of macrophages did not support cell survival. Furthermore, only few cells were detected within the lesion in 4 weeks after the implantation. On the other hand, due to the limited volume of the implanted scaffold, the total number of implanted cells within the hydrogel was relatively small (~15,000). By increasing the number of implanted cells, a higher *in vivo* cell survival rate could be achieved, however, the increased degree of gel contraction may result in enhanced formation of dense cell bulks within the lesion cavity.

Chemical crosslinking of the ECM hydrogel may attenuate injected scaffold degradation and offer longer persistence within the lesion, thus providing more time to complete tissue remodeling. However, recent studies suggest that degradation of the ECM scaffold is an essential component of a rapid constructive remodeling response. Moreover, crosslinking of the ECM may reduce or eliminate the rate of cellular infiltration into the implant or even cause a foreign body reaction (Badylak S.F. and Gilbert T.W., 2008). Alternatively, hydrogels composed of

concentrations higher than 8 mg/mL, as used in the present study, may slow the degradation process.

Remarkably, acute lateral hemisection, which we used to evaluate the feasibility of ECM hydrogels in CNS repair, is the least invasive and devastating SCI model. On the other hand, hemisection is a case of partial lesions with a high rate of spontaneous recovery and a high risk of inconsistencies in injuries from one animal to another, which might lead to misinterpretation of behavioral evaluation (Cloud B.A. at al., 2012, Fouad K. at al., 2013). Therefore, the next step in the evaluation of the neurogenerative properties of ECM hydrogels *in vivo* is the intention to use a subacute or chronic compression SCI model together with systematic functional analysis.

4.2.2. DYNAMICS OF TISSUE INGROWTH INTO SIKVAV-MODIFIED HIGHLY SUPERPOROUS PHEMA SCAFFOLDS WITH ORIENTED PORES AFTER BRIDGING A SPINAL CORD TRANSECTION

4.2.2.1. P(HEMA-AEMA) hydrogel scaffold production and characterization

2-hydroxyethyl methacrylate (HEMA), ethylene dimethacrylate (EDMA) and aminoethylmethacrylate (AEMA) were used for the radical polymerization process to prepare non-degradable poly(2-hydroxyethylmethacrylate) (PHEMA) scaffolds. Porogen-ammonium oxalate in small polyethylene syringes modified according to a previoulsy described procedure was also used (Kubinova S. et al., 2015). The hydrogel cylinders thus formed were then cut into discs. Polymerization in syringes confers the additional advantage for minimizing the contact of the hydrogel surface with the polymerization mold, which should induce inhomogeneity of the hydrogel at the interface. EDMA was used at a low concentration of 1 wt.% to ensure desirable mechanical properties of the hydrogel. Copolymerization of the monomers with 1 wt.% AEMA was done to introduce reactive amino groups.

The hydrogel must have a system of recurring pores to assist the ingrowth of axons when it is implanted into the lesion site. To achieve such pores, the $(NH_4)_2C_2O_4$ crystals must be oriented by gentle shaking on an orbital shaker. Figure 9B, C (Materials and methods) shows the $(NH_4)_2C_2O_4$ crystals before and after the orientation. These $(NH_4)_2C_2O_4$ crystals have a needle-like shape which promotes inter-pore connectivity while enabling greater filling owing to its ordered crystal structure. This proves advantages over other conventional porogenssuch as cubic NaCl (Horák D. et al., 2008) or sucrose (Horák D. et al., 2004). On double loading the saturated $(NH_4)_2C_2O_4$ solution, the crystal content in the syringe got raised because the crystals/cylinder volume ratio increased from 0.52 to 0.75.

In a scanning electron microscope (SEM) micrograph of a cross-section of the P(HEMA-AEMA) hydrogel, it was noted that the crystal orientation during loading continued to be the same as before and once the polymerization was complete, a hydrogel with continuous pore channels was made (Figure 9E). The pore size according to SEM was identical to that of the original crystals, i.e., ~60 μm in diameter and a few mm in length. On conducting mercury porosimetry, a 70 μm pore size in the dry hydrogels was confirmed. BET isotherm was used to analyze the large specific surface area of the P(HEMA-AEMA) hydrogel (82 m^2/g) and this also led to the detection of macropores (<1 μm) in the polymer. These macropores may contribute to the nourishment of the cells.

HS-CGGASIKVAVS-OH peptide was used to coat the P(HEMA-AEMA) hydrogel to assist cell adhesion. By measuring the UV spectra of the solutions before and after the reaction, the immobilization of the hydrogel on the polymer surface was confirmed. The characteristic adsorption bands of 2-thiopyrine in the spectrum at 272 and 337 nm can be seen in Figure 31A. These indicate that 2-thiopyrine is released from the activated P(HEMA-AEMA) discs in the supernatant after the reaction with peptide. On seeding with MSCs, the stem cells adhered and spread almost parallel to the oriented pores of the hydrogels (Figure 31B).

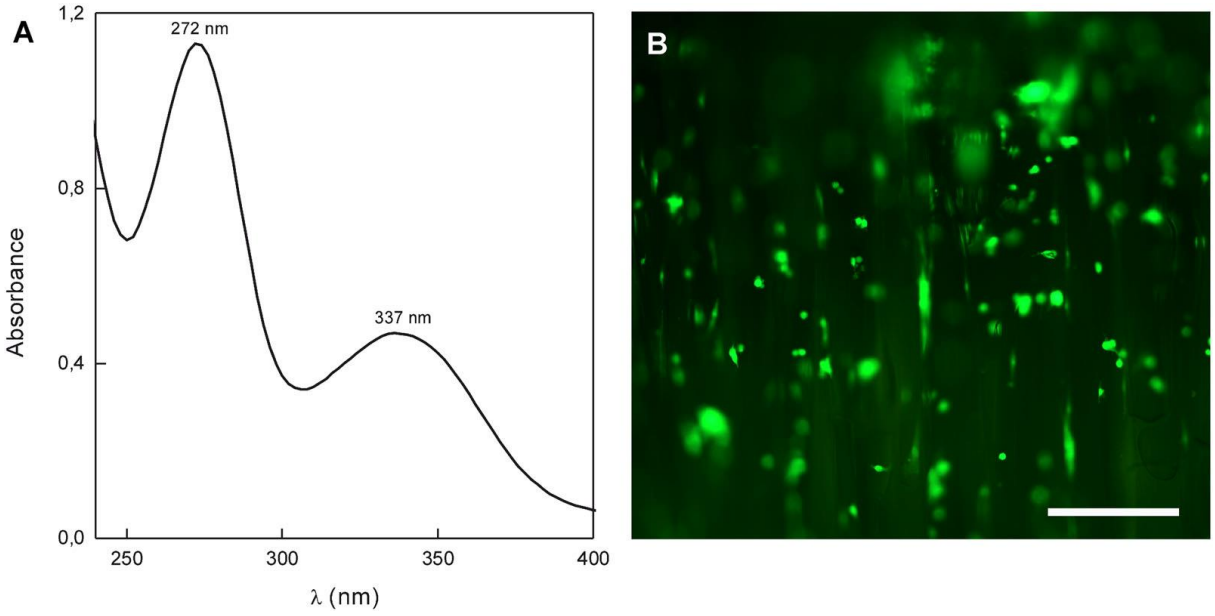

Figure 31. (A) UV-spectrum of 2-thiopyridine released after immobilization of Ac-CGGASIKVAVS-OH on activated P(HEMA-AEMA) hydrogel. (B) MSCs attached to the hydrogel, many of them oriented along the pores of the scaffold.

4.2.2.2. Bridging the post-traumatic cavity with P(HEMA-AEMA) hydrogel

In the course of implantation and adjustments made to the hydrogel, the soft and pliable scaffold adjusted to the shape and size of the post-transection cavity. The transection cavity was

satisfactorily bridged by the hydrogel. Negligible pseudocystic cavities were observed at that time or even after a time period, and the hydrogel showed good adherence to the spinal cord. Through the course of the implantation and for a long time afterwards as well, no foreign body reactions were noted in or around the hydrogels.

4.2.2.3. Connective tissue infiltration in P(HEMA-AEMA) hydrogel scaffold

Figure 32A demonstrates that blood vessels dominantly infiltrated the hydrogels two days post the implantation. Although connective tissue elements were not present, a few myofibrils growing in the border zones of both groups of animals treated with hydrogels (with or without MSC) were seen. Connective tissue elements also appeared in the complete volume of the hydrogels one week after the hydrogel implantation was done.

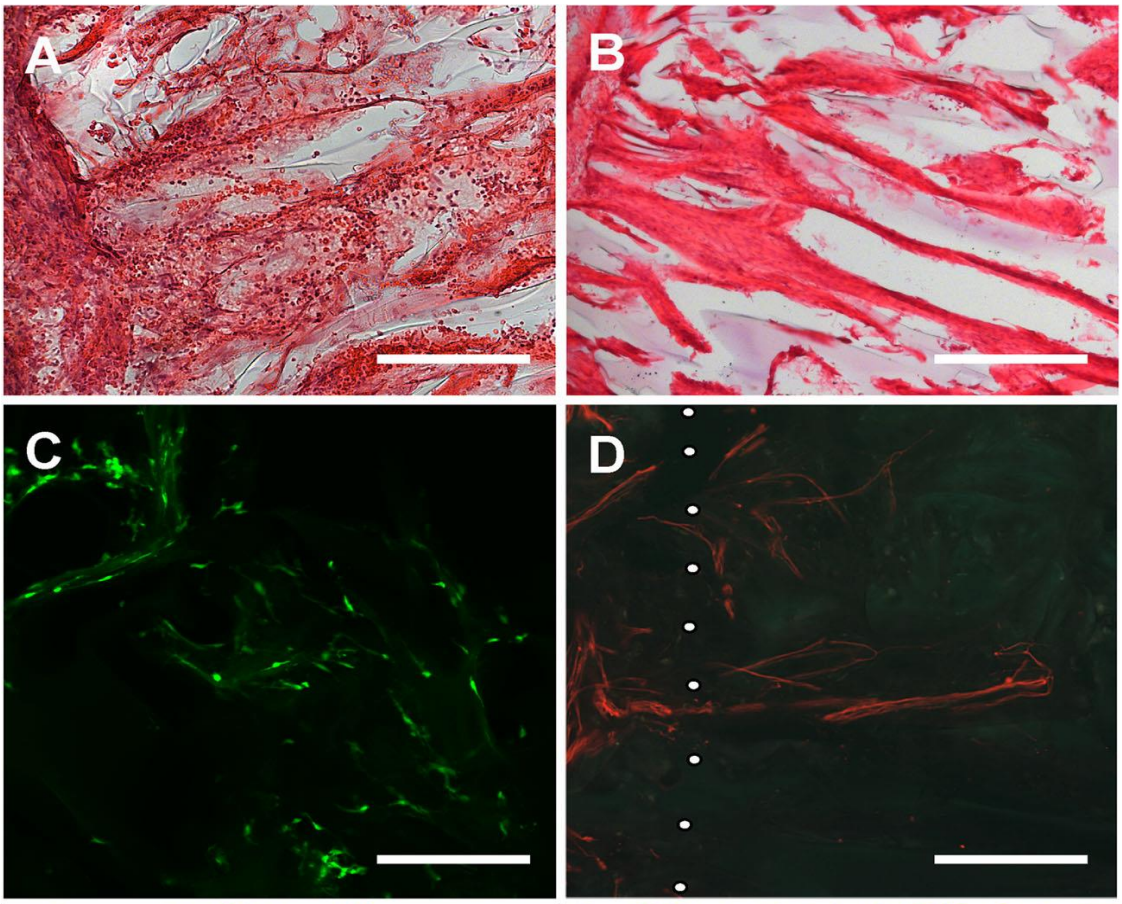

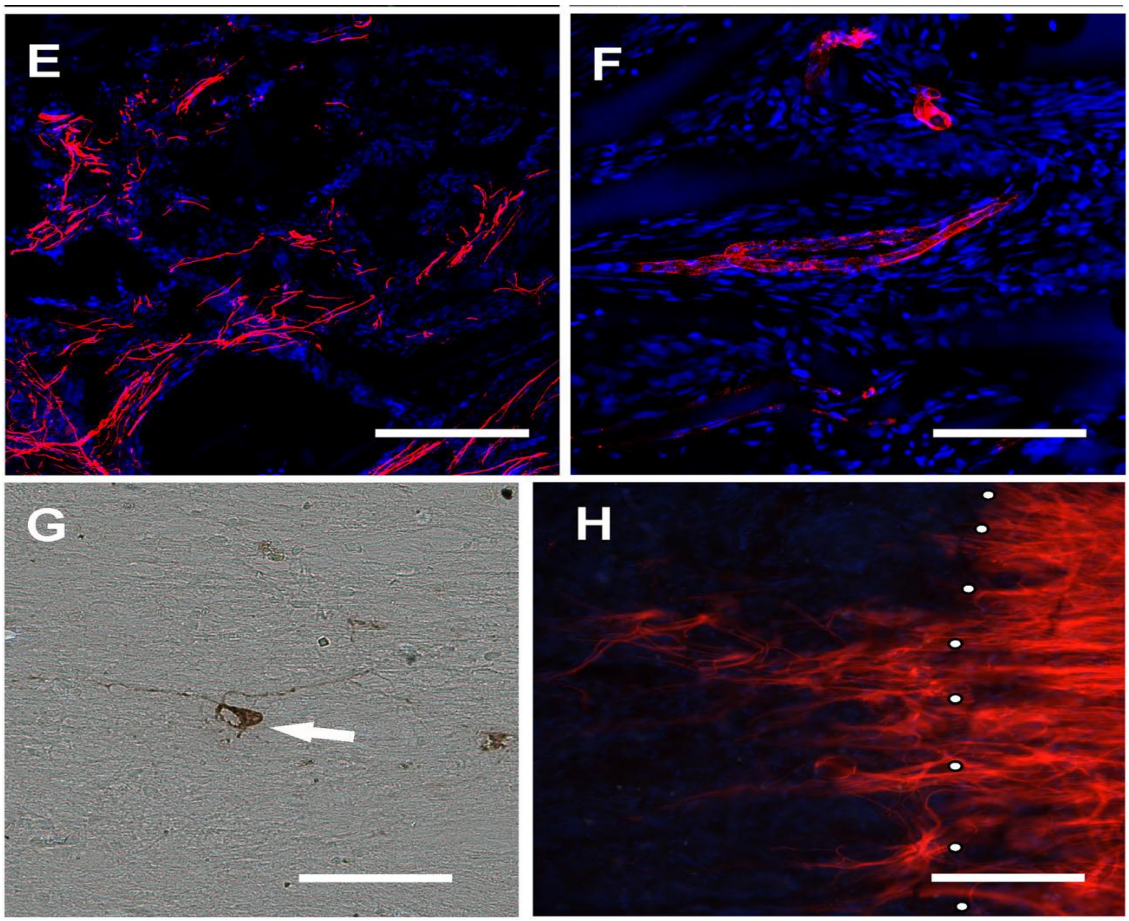

Figure 32. SIKVAV-HEMA scaffolds bridging the posttraumatic cavity after spinal cord transection. (A) Left border region of the HEMA hydrogel 2 days after implantation in SCI. The pores are filled with blood elements without any connective tissue (HE staining, scale bar = 100 µm). (B) One week after implantation of the HEMA scaffold the pores are completely filled with connective tissue (HE staining, scale bar = 100 µm). (C) GFPpositive MSCs 6 months after implantation of the HEMA scaffold seeded with MSCs (GFP staining, scale bar = 50 µm). (D) Neural sprouts invading pores of the bordering zone of the HEMA scaffold 2 weeks after implantation (NF160-g594 immunostaining, scale bar = 100 µm). (E) Axons in the central part of the HEMA scaffold seeded with MSCs 7 weeks after implantation are directed through the pores predominantly in the cranio-caudal or caudocranial direction (NF160-g594 immunostaining, scale bar = 100 µm). (F) Blood vessels infiltrating the pores of the HEMA scaffold (RECA-g594 immunostaining, scale bar = 100 µm). (G) Rare neurons were found to be fluorogold-positive in the spinal cord cranial from the tissue-scaffold border (white arrow, fluorogold staining, scale bar = 25 µm). (H) Astrocytes invading the peripheral part of the HEMA-scaffold 6 months after implantation (GFAP-Cy3, scale bar = 100 µm).

These elements infiltrated both the periphery as well as the central part (Figure 32B). MSCs were present in the pores of the hydrogel throughout the whole period, up to 6 months after SCI (Figure 32C). The amount of connective tissue in both types of hydrogels (with and without MSCs) remained the same. From week 1 to week 7 of the implantation, no changes in the amount of connective tissue in the peripheral and central parts of the hydrogels were noted (Figure 33).

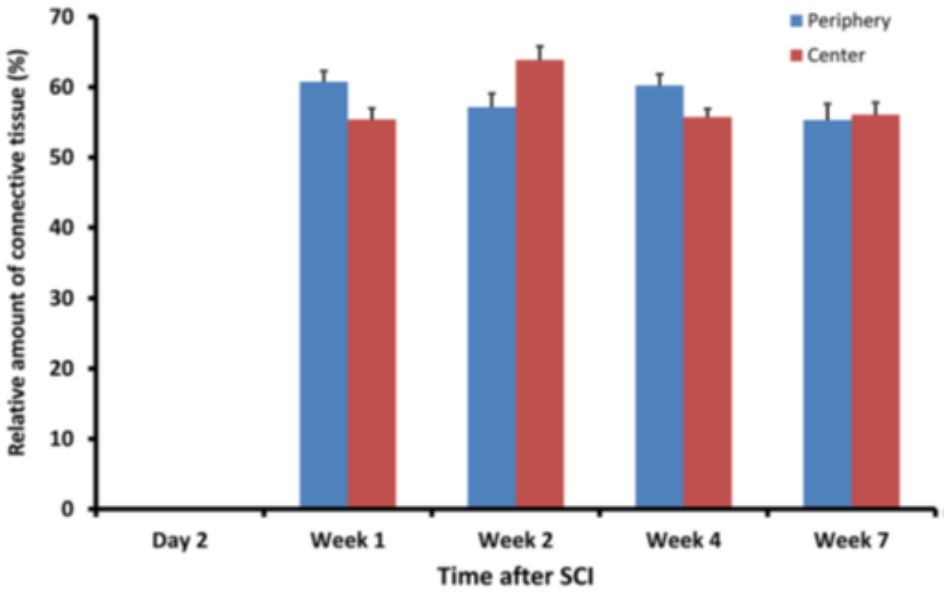

Figure 33. Dynamics of connective tissue infiltration in the SIKVAV-HEMA scaffolds.

4.2.2.4. Dynamics of axonal infiltration in P(HEMA-AEMA) hydrogel

The periphery as well as the central part of the hydrogel lacked axons when examined two days after hydrogel implantation. However, a week after the implantation, there were a few axons present specifically in the peripheral parts of the scaffold (mean total length = 71 ± 83 μm) (Figure 32D). Examination half a month post infiltration revealed a notable increase in the number of axons in the peripheral parts of the scaffold (mean total length = 188 ± 76 μm). The neural sprouts grew into the central parts of the scaffold (mean total length = 96 ± 57 μm). The neural sprouts kept infiltrating the peripheral part of the scaffold even at a time period of one month post implantation (mean total length = 344 ± 160 μm).

The central part of the scaffold was also occupied by axons with a mean total axon length of 134 ± 80 μm. The number of axons infiltrating the hydrogel gradually plateaued seven weeks after the implantation, compared to 4 weeks after the implantation (mean total length = 327 ± 153 μm), while in the central part the number of axons was 171 ± 124 μm (Figure 34). The axons continued to occupy the hydrogel pores, but the process was significantly slower.

The oriented pores of the hydrogel helped to guide axonal ingrowth in either the cranio-caudal or the caudo-cranial direction. The axons occupied nearly 2-4% of the complete scaffold volume in the peripheral regions and nearly 1.5–2% in the central part (Figure 32E). As part of our research, we evaluated hydrogels seeded with MSCs and those without MSCs separately. No statistically notable difference was seen between the two groups at any point in time. This was maintained in both the central as well as the peripheral parts of the hydrogel scaffold.

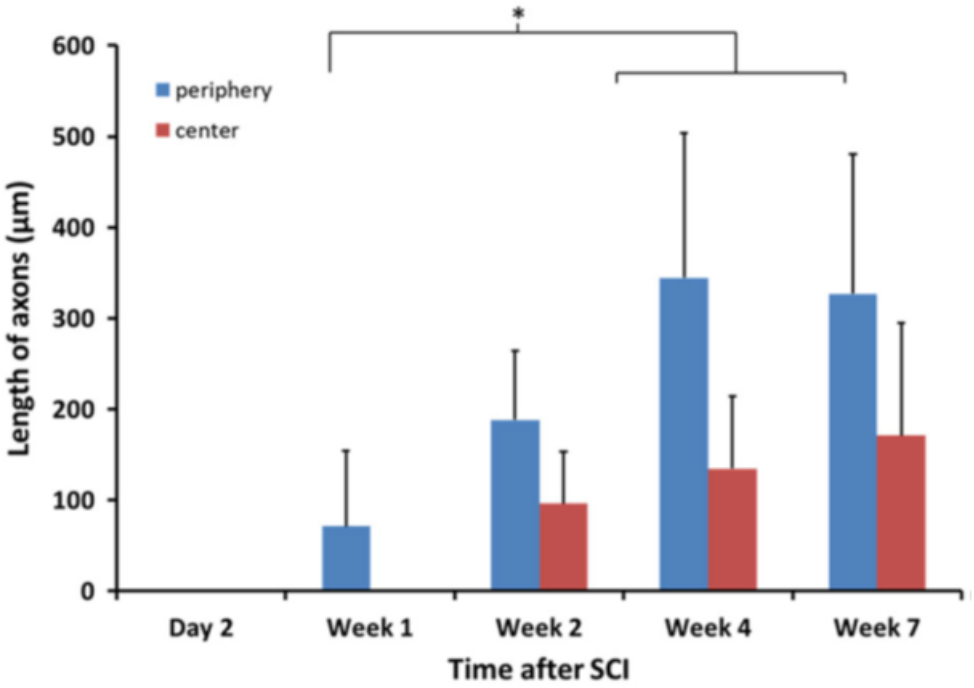

Figure 34. Dynamics of axonal ingrowth in the SIKVAV-HEMA scaffold. A statistically significant increase in the number of axons is apparent between Day 7 and Weeks 4 and 7 after hydrogel implantation (*p <0.05). There is a gradual increase in the number of axons infiltrating the scaffold.

4.2.2.5. Dynamics of blood vessels ingrowth into P(HEMA-AEMA) hydrogel

Although the scaffold did not carry any blood vessels two days after the implantation, both the peripheral and the central regions of the hydrogel were occupied by blood cells. Only one week after the implantation the first blood vessels started infiltrating the peripheral parts of the hydrogel (Figure 32F). It is notable that the number of blood vessels did not increase between day 7 and days 14, 28 or 49 and it became rather static by day 49 after SCI (Figure 35).

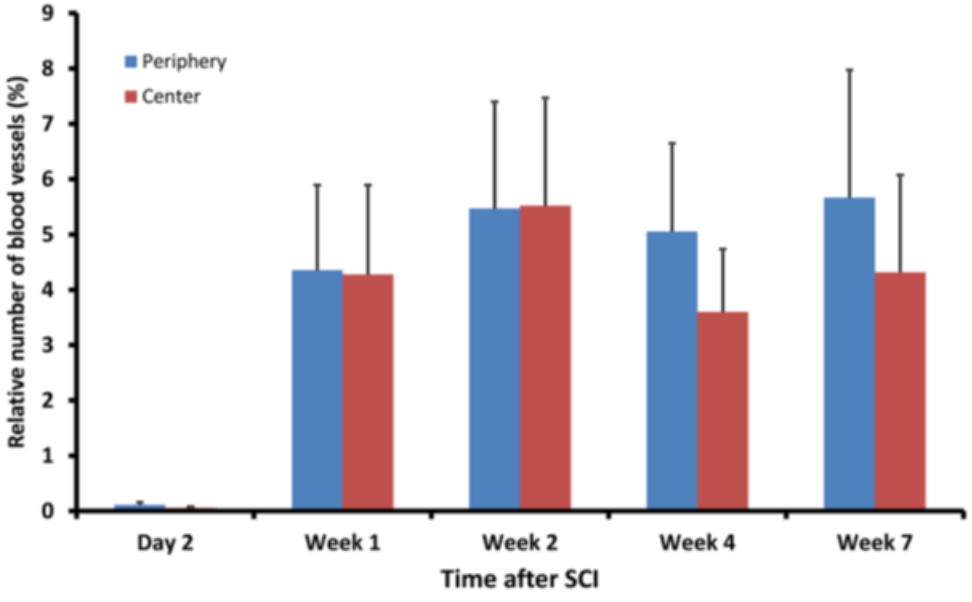

Figure 35. Blood vessel ingrowth in the SIKVAV-HEMA scaffolds.

The number of blood vessels observed remained more or less statistically static during that period of time. The extent of growth of blood vessels into the peripheral and central parts of the hydrogel was similar (Figure 34). Hydrogels seeded with MSCs displayed nearly identical dynamics to those hydrogels that lacked MSCs.

4.2.2.6. Long-term effects of implanted MSCs-seeded P(HEMA-AEMA) scaffold hydrogels

Three rats that had been treated with MSCs-seeded hydrogels were sacrificed half a year post SCI. During this six-month period, only some axons infiltrated the hydrogel and most of them remained concentrated at the tissue-hydrogel border. Very few positively-stained fluorogold neuron that projected into the cranial region of the spinal cord were observed (Figure 32G). Figure 32H shows that relative to previous stages, a significantly greater number of astrocytes grew into the hydrogel scaffold without entering the central region of the hydrogel.

4.2.2.7. Discussion

A full-blown case of SCI has the potential to severely damage spinal cord tracts and lead to the formation of pseudocystic cavity, glial and mesenchymal scar (Fitch M.T. et al., 1999). Several experiments for evaluating the efficacy of biomaterials in spinal cord injury treatment have been conducted for several types of hydrogel scaffolds, where progressive ingrowth of axons that continued only for the first few weeks was shown (Hejcl A. et al., 2010; Hejcl A. et al., 2013; Kubinova S. et al., 2015; Hejcl A. et al., 2009; Hejcl A. et al., 2008; Hejcl A., Lesny P. et al., 2008; Ruzicka J. et al., 2013). Only few studies throw light on the time-related dynamics of tissue infiltration of these scaffolds. Therefore, we estimated the ingrowth of connective tissue, axons and blood vessels inside the implanted scaffold hydrogel with or without seeded stem cells in 2, 7, 14, 28, 49 days and 6 months post the SCI. SIKVAV (Ser-Ile-Lys-Val-Ala-Val)-modified highly superporous poly(2-hydroxyethyl methacrylate) hydrogel with oriented pores was chosen for this purpose because it possesses a moderate modulus of elasticity which has been shown to promote good bridging, tissue infiltration and abundant axonal ingrowth (Kubinova S. et al., 2010). Other significant findings include the observation that the oriented pores of the hydrogel directed axonal growth in the cranio-caudal and caudo-cranial direction. Such aligned ingrowth enabled easier evaluation of the amount and the length of axons into the scaffold.

Spinal cord transections in the eighth thoracic vertebra (Th8) of animal models were implanted with mesenchymal cells seeded or plain hydrogels. By seeding one set of hydrogels with MSCs, we assessed the possible benefits that these cells may provide for the ingrowth of axons or blood vessels over time.

The spinal cord transection cavities into which we implanted the hydrogels were made to resemble the worst and most severe kind of clinical SCI, wherein the tissue is completely mechanically damaged and physically torn. Since there is no risk of compromising residual function in patients with the most severe spinal cord injuries (ASIA A), such patients are given the highest priority for inclusion in clinical trials where the spinal cord lesion would be reconstructed utilizing non-injectable scaffolds (Amr S.M. et al., 2014).

It would be possible to conduct such procedure only in some time post injury, because it takes some time to indicate and include suitable patients into the study group. Due to these factors, we carried out the implantation a week after the injury took place. As mentioned before, such a delay may actually be beneficial rather than detrimental, because it will improve adhesion to the edges of the spinal cord and also attenuate the damage caused by the implantation and reduce the rate of occurrence of post-traumatic cavities (Hejcl A. et al., 2008).

Observations revealed that the SIKVAV-HEMA-based hydrogel scaffold environment supported the ingrowth of connective tissue, blood vessels and axons. Axonal infiltration into the scaffold was a slow and gradual process compared to the much faster connective tissue ingrowth. For a certain period of time, the hydrogel scaffold invited new axonal ingrowth. There is a wide range of factors to consider that lead to this kind of time-limited infiltration of the hydrogel scaffolds. One reason could be the spatial limitation in the hydrogel pores due to connective tissue infiltration. Our studies have shown that the progressive infiltration of the connective tissue into the hydrogel pores continues only for the first week, after which it plateaus for the next 2 months. In contrast, the axons continue to grow into the hydrogel pores even at the time of one month after the implantation. Hence, we cannot term space limitation as a major influencing reason.

Deficiency of nutrients and growth factors can, however, be another plausible cause. Some of our hydrogels were seeded with MSCs. These MSCs were thought to enhance the repair of the lesion and provide protection against the onset of neuronal apoptosis by releasing growth factors such as BDNF (brain-derived neurotrophic factor), VEGF (vascular endothelial growth factor), NGF (nerve growth factor) or GDNF (glial-derived neurotrophic factor) (Li N. et al., 2010). Furthermore, MSCs promote CNS plasticity (Hao P. et al., 2014). Despite these properties of

MSCs, our study revealed no difference in the quantity or growth dynamics of axons in hydrogels seeded with MSCs in comparison to those that did not contain MSCs.

Certain other research groups have also obtained the same results (Gunther M.I. et al., 2015). Our study demonstrated the abundance of MSCs in the scaffold even six months after SCI. However, the number of cells does not directly correlate with the degree of metabolic activity (Oliveira E. et al., 2017). Our research, alongside several others, has confirmed the greater importance of tissue preservation and neuroprotective nature of MSCs over their negligible influence on increased ingrowth of neural sprouts within the scaffold (Hejcl A., Sedy J. et al., 2010; Qu J., Zhang H., 2017; Papa S. et al., 2018).

By using genetically engineered MSCs that overexpress some of the growth factors like BDNF and VEGF instead of simple MSCs, it may be possible to stimulate axonal ingrowth and improve tissue repair (Stewart A.N. et al., 2017). Inclusion of some other supportive cells, such as Schwann cells, may also improve neuroregenerative effects alongside the MSCs (Yang E.Z. et al., 2017). Thus, it is safe to assume that modified MSCs may promote their positive effect on neuronal repair after SCI. A major determinant of this is the microenvironmental milieu of the scaffold.

The physical and chemical properties of the scaffold dictate its inner architecture and structure, which is a vital part of the microenvironmental milieu. In one of the previous studies, it was found that the web-like architecture of the hydrogel together with the HPMA-based backbone promotes the ingrowth of new axons, despite promoting the adhesion of fewer MSCs compared to HEMA-based hydrogels (Hejcl A. et al., 2013). The results of these studies have yielded points to the fact that the effect of MSCs seeded on hydrogels is less important than the inner milieu of the hydrogel, influenced by the chemical backbone and the architecture of the scaffold.

In our study we used the SIKVAV sequence attached to the hydrogels. This sequence is a synthetic peptide from the active regions of the chain A of basement membrane laminin which promotes cell adhesion and neural outgrowth by binding transmembrane integrin receptors (Tashiro K. et al., 1989). Earlier experiments have also established the benefits of the SIKVAV sequence on axonal regeneration and functional outcome (Tysseling-Mattiace V.M. et al., 2008; Tysseling V.M. et al., 2010). In a previous study, PHEMA-based scaffolds modified with the SIKVAV sequence were shown to promote *in vitro* cell adhesion and axonal regeneration (Kubinova S. et al., 2010). Despite all this, using the SIKVAV sequence is still not a solution to the problem of how to achieve long-term survival and promotion of axons in hydrogel scaffolds.

Genetical manipulation of injured neurons is one of the possible methods to regenerate axons. Axonal growth cones need an adhesion complex that signals and links to the cytoskeleton to be able to migrate. As integrins are the main extracellular matrix (ECM) receptors, they can be used as one of the target adhesion molecules because axons during regeneration in the CNS, and particularly in the scar tissue, must penetrate the extracellular matrix. Integrins, particularly α9β1, are expressed in the CNS and PNS during embryogenesis, then downregulated and not expressed after injury (Andrews M.R. et al., 2009).

By transducing sensory neurons with tenascin-binding integrin and integrin activator, Fawcett's group was able to obtain very extensive long-distance sensory axon regeneration in the spinal cord (Cheah M. et al., 2016). The hydrogels designed by our group can have different peptide sequences bound to the surface. Although due to the missing integrin subunits, the axons are totally unable to use these signals. Thus, modifying the axons for expressing a growth-promoting receptor to match such signaling sequence can make the use biomimetic materials more promising.

It is also possible to create a continuous milieu of trophic factors, such as the combination of olfactory ensheathing cells (OEC) together with olfactory nerve fibroblasts injected into the hydrogel scaffold and with injections into both the rostral and caudal ends of the adhering spinal cord (Deumens R. et al., 2006). This approach helps to promote axons rostral to the lesion but not across the lesion (Deumens R. et al., 2006). In another study, a scaffold with guiding mini-channels seeded with GDNF-overexpressing Schwann cells resulted in the growth of propriospinal axons across the bridge, their regeneration, formation of synapses and partial functional recovery (Deng L.X. et al., 2013).

Oxygen and nutrition concentrations for axonal regeneration at the lesion site may increase due to neovascularisation. Promoting the ingrowth of vasculature may lead to improved axonal regrowth and functional recovery (Iida T. et al., 2006; Glaser J. et al. 2006). Considering these probabilities, it will not be wrong to say that manipulating the endogenous response towards promoting vascular repair may actually bear fruit in genetic engineering.

The results from our study showed that blood vessels started growing into the peripheral and central parts of the hydrogel scaffold several days after the lesion formed. After the first week, however, there was no further increase in the amount and rate of infiltration. Hydrogels seeded with MSCs did not show any increased ingrowth of new blood vessels into the hydrogel scaffold, although many studies have shown that MSCs induce angiogenesis in injured tissues (Gao X.R. et al., 2017), which was promoted by the paracrine secretion of vascular endothelial growth factor (VEGF) (Hou Y. et al., 2014). As was demonstrated earlier, new blood vessels

often grow into the pores of the scaffold in close proximity to MSCs seeded into the hydrogel (Hejcl A., Sedy J. et al., 2010).

Several approaches to promote angiogenesis have been shown to be successful (Hejcl A. et al., 2013; Wang C. et al., 2014). For example, RGD peptide sequence promotes vascular growth into the hydrogel scaffolds when implanted into a spinal cord lesion (Hejcl A. et al., 2013).

Since the exogenous growth factors degrade very quickly, they need to be introduced into the injury site at supraphysiological level. On the other hand, the tissue response to injury entails increasing VEGF levels and the implantation of biomaterials activates the secretion of several cytokines (Golebiewska E.M., 2015, Ullm S., 2014). Feng with coauthors therefore propose taking advantage of such endogenous processes (Feng Y. at al., 2017). They used engineered injectable hydrogels to activate macrophages for releasing pro-angiogenic cytokines and endogenous angiogenesis promoting growth factors inside the hydrogel. Therefore, the pro-angiogenic effects of growth factors have shown greater effects than simple presence of MSCs.

4.2.3. INJECTABLE HYDROXYPHENYL DERIVATIVE OF HYALURONIC ACID HYDROGEL MODIFIED WITH RGD AS A SCAFFOLD FOR SPINAL CORD INJURY REPAIR

4.2.3.1. Characterization of HA-PH-RGD hydrogel

A new peptide sequence HPA-K-AHA-GRGD (PH-RGD) was designed to provide a polymer backbone for attaching both the PH moiety and the RGD cell-adhesive motive in one synthetic step. Reductive amination was performed to conjugate this sequence with hyaluronan polyaldehyde. The degree of substitution of the prepared conjugate was determined by ^{1}H NMR as 2.5 %, and thus the achieved concentration of the RGD sequence was 1 μmol/ml of a hydrogel containing 20 mg/ml HA-PH-RGD derivative (NMR spectra, not shown).

HRP and H_2O_2 were used to crosslink the HA-PH-RGD derivative, with the gelation rate being monitored by rheological measurement. The dosage of the crosslinking agents (HRP, H_2O_2) was optimized to 0.04 U/ml HRP and 0.165 mM H_2O_2, to obtain a compressive modulus similar to the native neural tissue and a gelation time of 61 ± 4 sec (n = 3), which is appropriate to achieve safe application of the viscous pre-gel solution to the site of the defect using a syringe (Figure 36C). Figure 36D demonstrates the effect of hydrogel swelling on mechanical strength. The G' modulus of the samples decreased alongwith the strength of the material.

4.2.3.2. hWJ-MSCs proliferation *in vitro* on HA-PH and HA-PH-RGD hydrogels

The toxicity of the crosslinking agents (HRP and H_2O_2) to hWJ-MSC culture was analyzed. No cytotoxic effects were seen at the concentrations used for the hydrogel gelation (not shown). Figure 37A demonstrates the proliferation of hWJ-MSCs seeded on HA-PH and HA-PH-RGD hydrogels, combined with fibrinogen (F). The unmodified HA-PH hydrogel showed the lowest stem cell proliferation, while the modified HA-PH-RGD provided increased cell proliferation (Figure 37A).

When the HA-PH and HA-PH-RGD hydrogels were integrated with fibrinogen, an outstanding surge in cell proliferation rate was achieved (Figure 37A). Thus, for cell encapsulation, fibrinogen (1 mg/ml) was added into the HA-PH-RGD hydrogel. Cell proliferation analysis with WST-1 reagent was carried out at time periods of 3 hours, 1 and 3 days to confirm the ability of HA-PH-RGD/F to support cell proliferation in 3D culture (Figure 37B). Although enhanced cell proliferation was noted, the hWJ-MSC morphology after 1 day in 3D culture was found similar in HA-PH-RGD and HA-PH-RGD/F (Figure 37C, D).

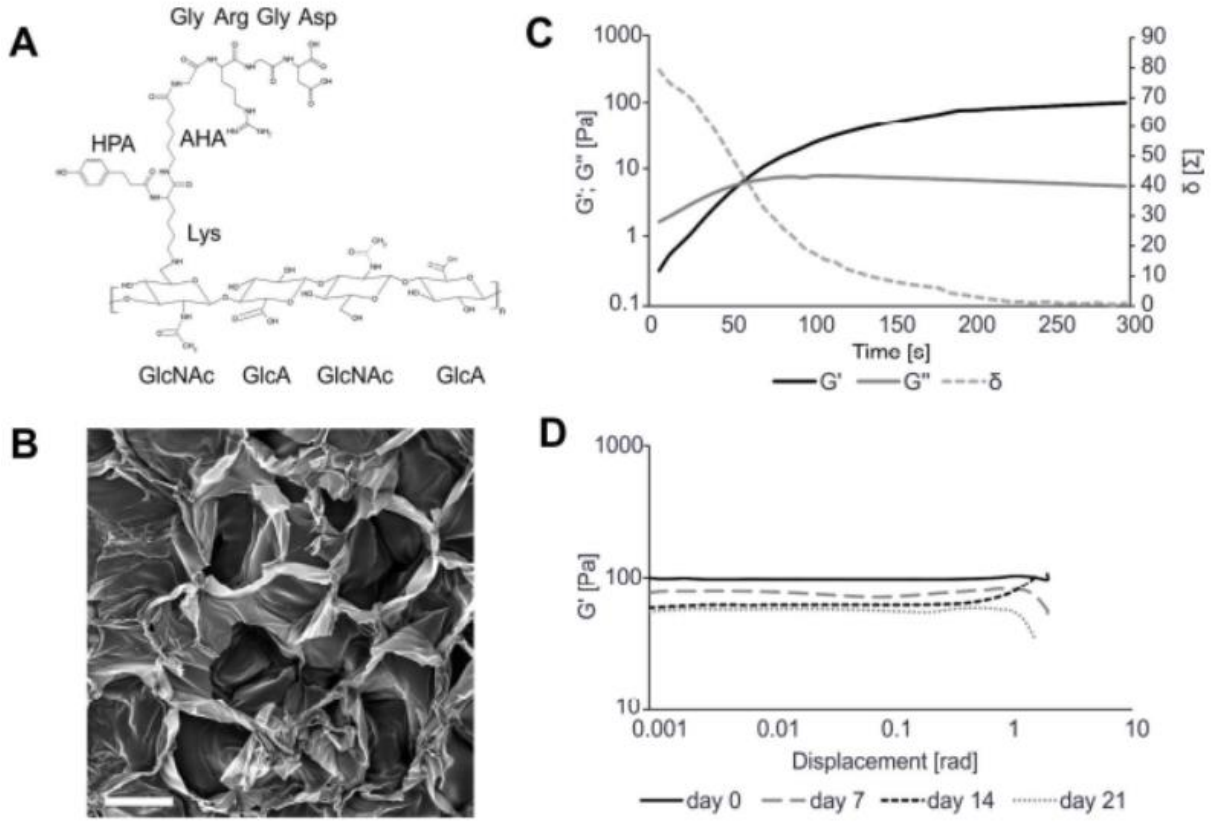

Figure 36. (A) Scheme of hydroxyphenyl derivative of HA with attached RGD peptide sequence. (B) SEM image of HA-PH-RGD hydrogel structure. (C) Gelation kinetics of HA-PH-RGD crosslinked with 0.04 U/ml of HRP and 0.165 mM H_2O_2. (D) The influence of HA-PH-RGD swelling on the elastic modulus. Scale bar: 100 µm. 189x128mm (300 x 300 DPI).

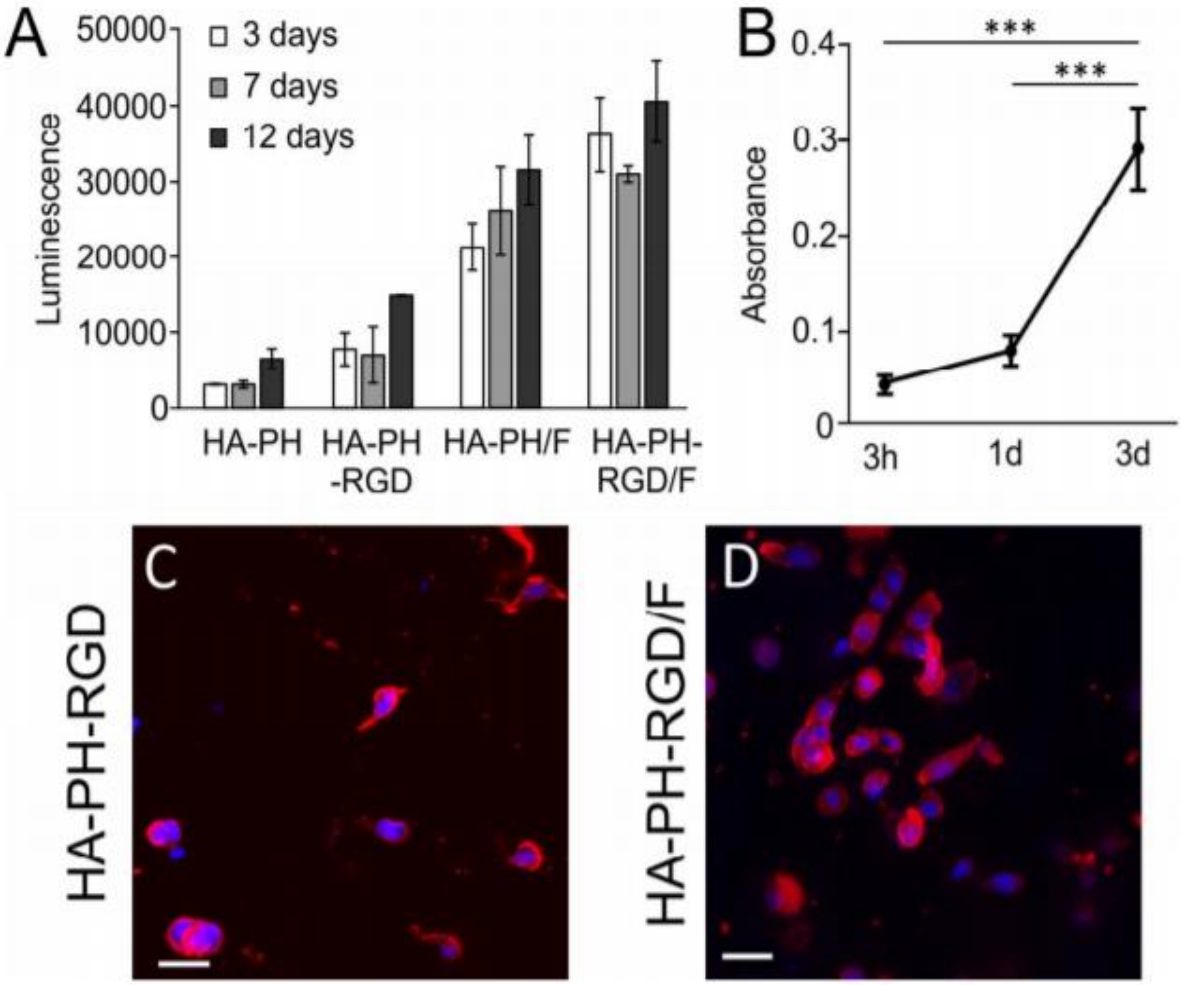

Figure 37. (A) Proliferation of hWJ-MSCs in HA-PH hydrogels on different adhesive substrates (RGD peptide, F = fibrinogen) measured by ATP luminescence. (B) Proliferation of hWJ-MSCs in 3D culture of HA-PH-RGD/F hydrogel measured by WST-1 assay. ***p < 0.001, (n = 3). (C, D) morphology of hWJ-MSCs in 3D culture in HA-PH-RGD and HA-PH-RGD/F hydrogel after 1 day of cultivation stained for phalloidin (red) and DAPI (blue). Scale bar: 25 µm. 129x102mm (300 x 300 DPI)

4.2.3.3. Evaluation of ingrowth of neurofilaments and blood vessels into HA-PH-RGD hydrogels in acute SCI lesions

Two methods of hydrogel application in an acute SCI lesion were compared - implantation of *in vitro* crosslinked HA-PH-RGD hydrogel and injection of HA-PH-RGD together with crosslinking agents to form a hydrogel *in situ*. Both the implanted as well as the injected hydrogels occupied the lesion cavity along with a high population of endogenous cells. dense ingrowth of neurofilaments (Figure 38A) and blood vessels (Figure 38B) into the hydrogel-treated lesion was observed throughout the whole implant after half a month and persisted with no considerable changes 2 months post application.

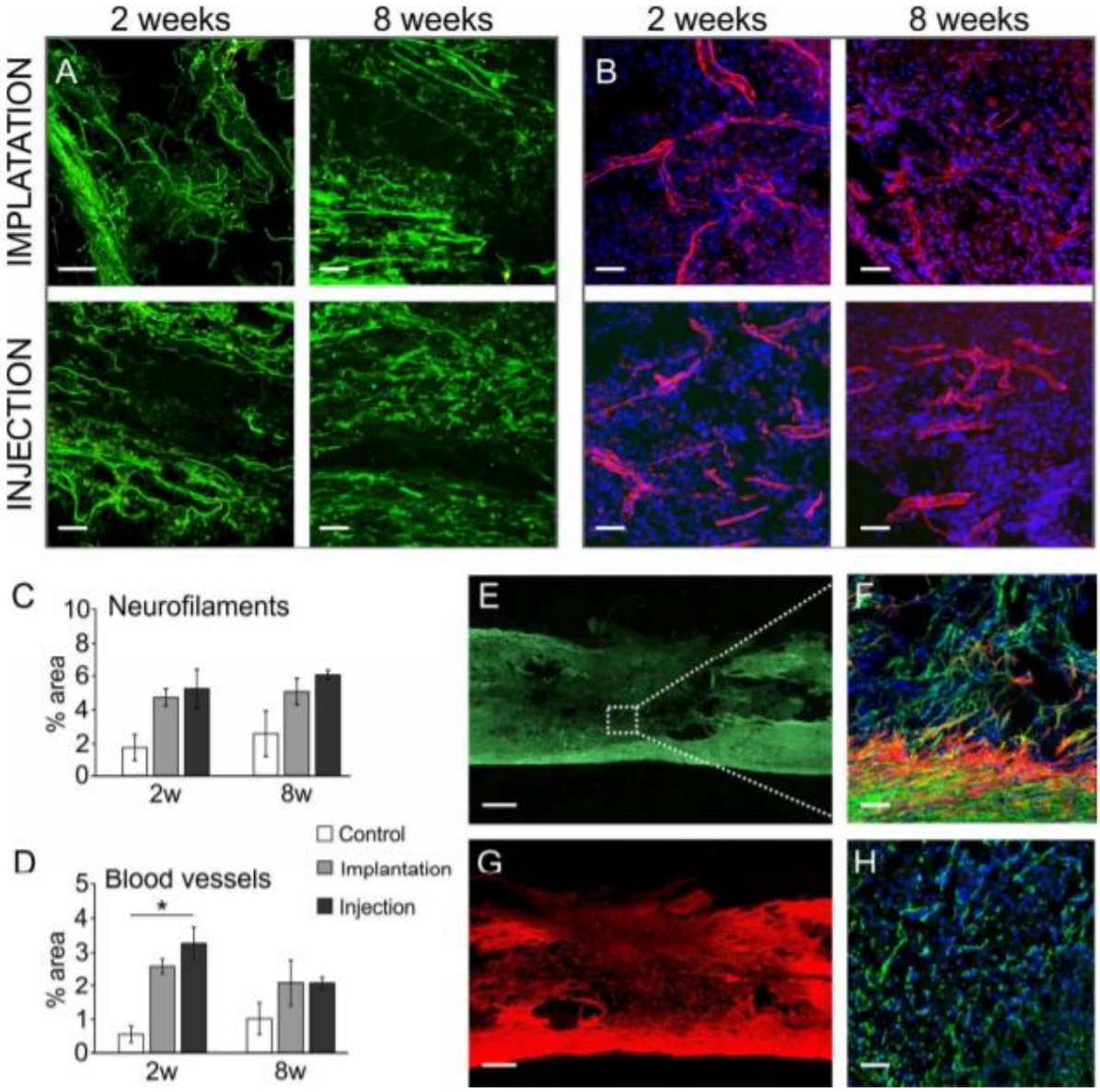

Figure 38. Representative images of longitudinal sections of the spinal cord lesion 2 and 8 weeks after the acute HA-PH-RGD hydrogel injection or implantation into the hemisection cavity: Staining for (A) neurofilaments (NF-160, green) and (B) blood vessels (RECA, red; DAPI, blue). Quantitative analysis of the ingrowth of (C) neurofilaments and (D) blood vessels into the lesion area 2 and 8 weeks after the injection or implantation of HA-PH-RGD hydrogel. The values are expressed as the percentage of (C) NF160 or (D) RECA positive area from the total lesion area. (n = 3), *p < 0.05. (E) Immunofluorescent staining for neurofilaments (NF160); the square in (E) is shown under the higher magnification inset in (F); (F) immunofluorescent staining for neurofilaments (NF-160, green), astrocytes (GFAP, red) and cell nuclei (DAPI, blue) and (G) immunofluorescent staining for astrocytes (GFAP) 2 weeks after HA-PH-RGD injection. (E) Immunofluorescent staining for growth associated protein 43 (GAP43, green) and cell nuclei (DAPI, blue) 8 weeks after HA-PH-RGD hydrogel implantation. Scale bar: 500 µm (E, G), 50 µm (A, B, F, H). 187x187mm (300 x 300 DPI).

On carrying out quantitative analysis, higher density of neurofilaments (Figure 38C) and blood vessels (Figure 38D) was noted in both hydrogel groups compared to the control lesion. Irrespective of which hydrogel introduction technique was used, i.e., implantation or injection, no variations were found between the two groups at any time point. Figures 38F, G then depicted migrating astrocytes (staining for GFAP) and Figure 38H newly formed axonal growth cones

(staining for GAP43) invading the hydrogel treated lesion. The results thus obtained indicate that hydrogel injection into the lesion and its subsequent crosslinking *in situ* is not harmful to the surrounding tissue and represents a non-invasive and effective way of hydrogel delivery resulting in tissue repair.

4.2.3.4. Histological evaluation of HA-PH-RGD hydrogels in subacute SCI lesion

Evaluation of the tissue response to subacute injection of HA-PH-RGD, HA-PH-RGD/F and HA-PH-RGD/F combined with hWJ-MSCs was done 2 months after injection. Both HA-PH-RGD and HA-PH-RGD/F hydrogels enhanced neurofilament infiltration density in the lesion (Figure 39). In comparison, the control untreated lesion did not see as much progress. This increase in neurofilament density was magnified by the introduction of hWJ-MSCs (Figure 39G). immunohistochemistry of the HA-PH-RGD/F is not shown here as the immunohistochemical results of HA-PH-RGD/F did not significantly differ from the results obtained with HA-PH-RGD.

Immunofluorescence staining for GFAP (Figure 40) made it possible to view astrocytes that were shown to migrate from the lesion border to the lesion area treated by hydrogel. This indicates the development of a permissive environment promoting glial cell infiltration (Figure 40D, F). On quantitative evaluation of GFAP staining density around the lesion to evaluate the density of glial scar, no notable differences between the control and hydrogel treated groups was observed (Figure 40G). The extent of blood vessel infiltration into the hydrogel treated lesion was higher compared to the control lesion (Figure 41).

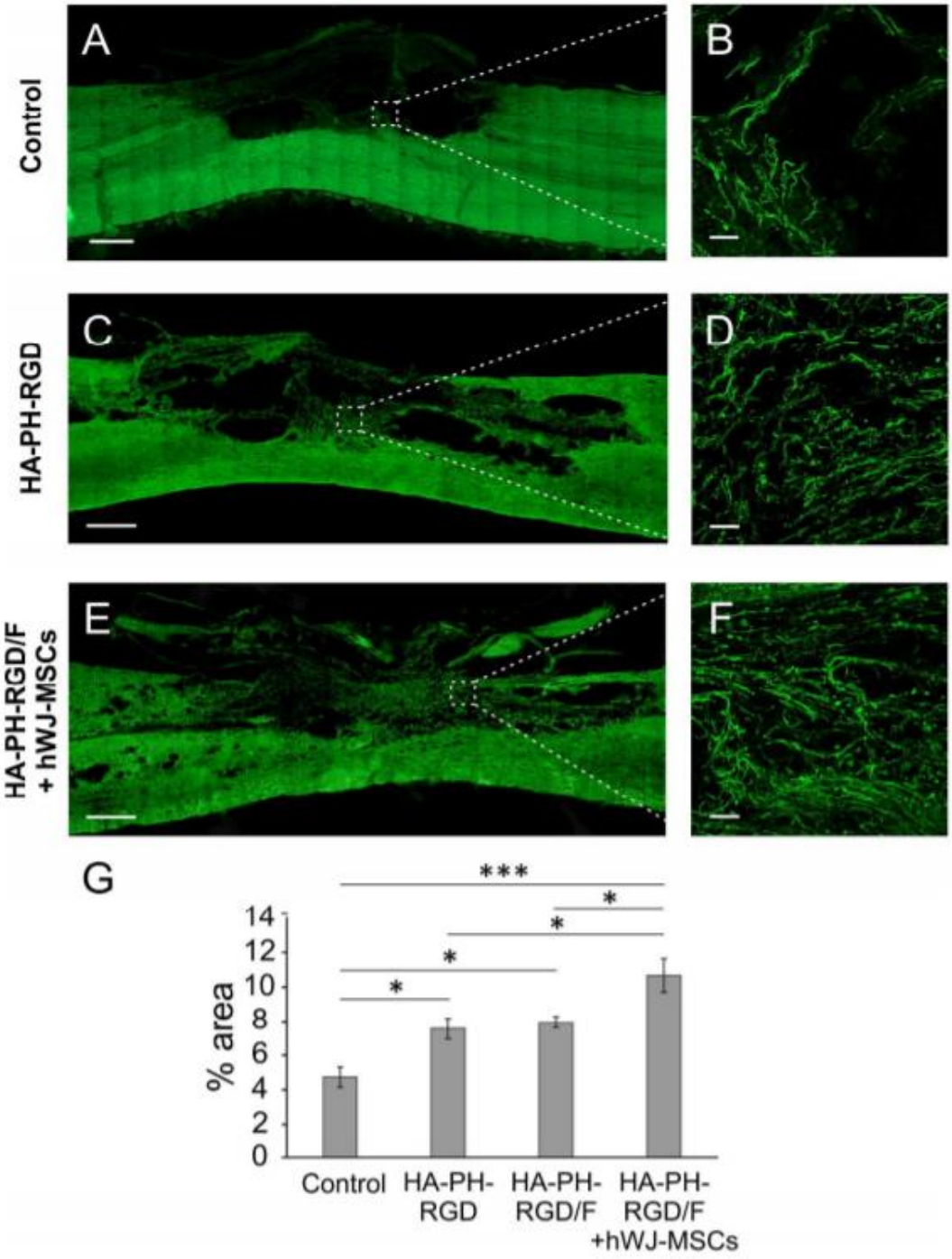

Figure 39. Representative images of longitudinal sections of the spinal cord lesion in (A, B) controls and at 8 weeks after subacute injection of (C, D) HA-PH-RGD and (E, F) HA-PH-RGD/F hydrogels combined with hWJ-MSCs stained for neurofilaments (NF-160). Squares (A, C, E) are also shown under higher magnification insets (B, D, F). (G) Quantitative analysis of axonal ingrowth is expressed as the percentage of NF160 positive area out of the total lesion area (n = 6). *p < 0.05, ***p < 0.001. Scale bar: 500 µm (A, C, E), 50 µm (B, D, F). 194x261mm (300 x 300 DPI).

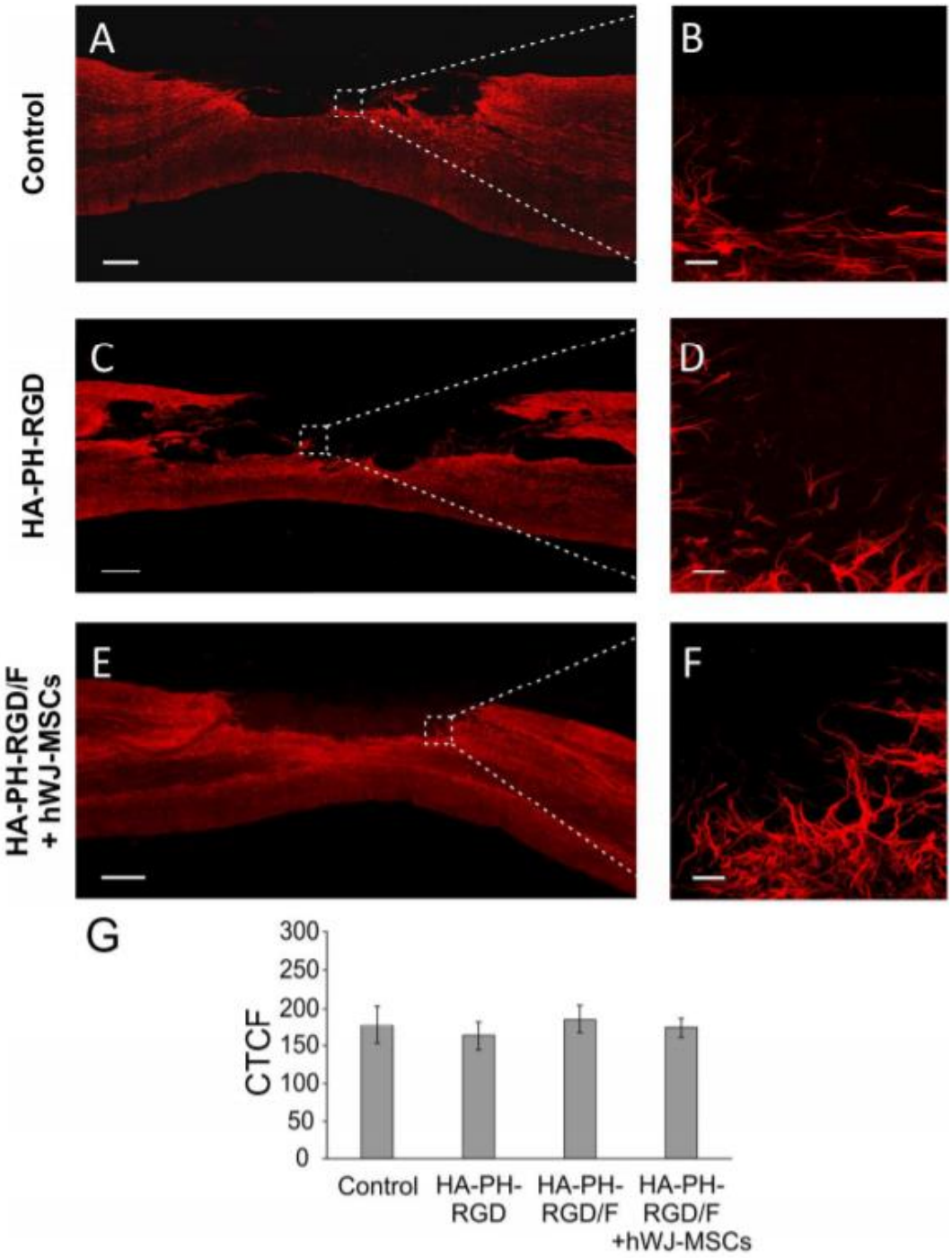

Figure 40. Representative images of longitudinal sections of the spinal cord lesion in (A, B) control and at 8 weeks after subacute injection of (C, D) HA-PH-RGD and (E, F) HA-PH-RGD/F hydrogels combined with hWJMSCs stained for astrocytes (GFAP). Squares (A, C, E) are also shown under the higher magnification insets (B, D, F). (G) Quantitative analysis of glial scar density around the lesion was expressed as corrected total fluorescence (CTCF) of GFAP staining (n = 6). Scale bar: 500 µm (A, C, E), 50 µm (B, D, F). 183x241mm (300 x 300 DPI).

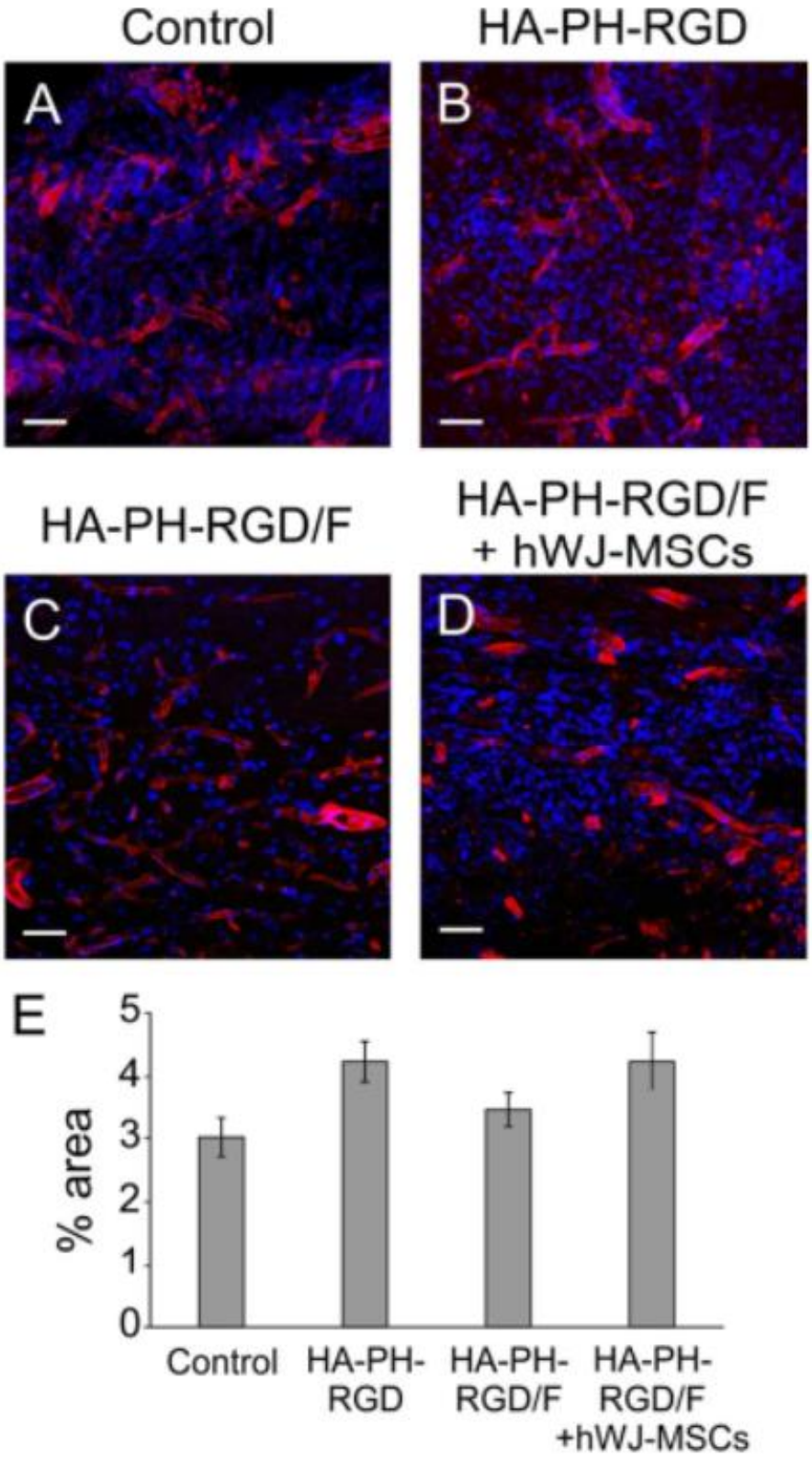

Figure 41. Representative images of longitudinal sections of the spinal cord lesion in (A) control and at 8 weeks after subacute injection of (B) HA-PH-RGD, (C) HA-PH-RGD/F hydrogels and (D) HA-PH-RGD/F combined with hWJ-MSCs stained for blood vessels (RECA, red) and DAPI (blue). (E) Quantitative analysis of blood vessel ingrowth is expressed as the percentage of RECA positive area out of the total lesion area (n = 6). Scale bar: 50 µm. 83x149mm (300 x 300 DPI).

Migration of e M1 and M2 macrophages into the hydrogel treated lesion was verified by ED1 staining, specific for microglia/macrophages combined with CD206 staining specific for M2 macrophages (Figure 42A-D). Quantification to calculate the M1/M2 ratio was not done.

oligodendrocytes were absent in the control lesion; however, Figure 42E-H demonstrates their presence in the area of hydrogel treated lesions. Testing on the basis of staining for the human mitochondria marker (MTCO2) was used for detection of human MSCs in the host tissue. At 2 months post cell application, the spinal cord tissue did not have any hWJ-MSCs (not shown).

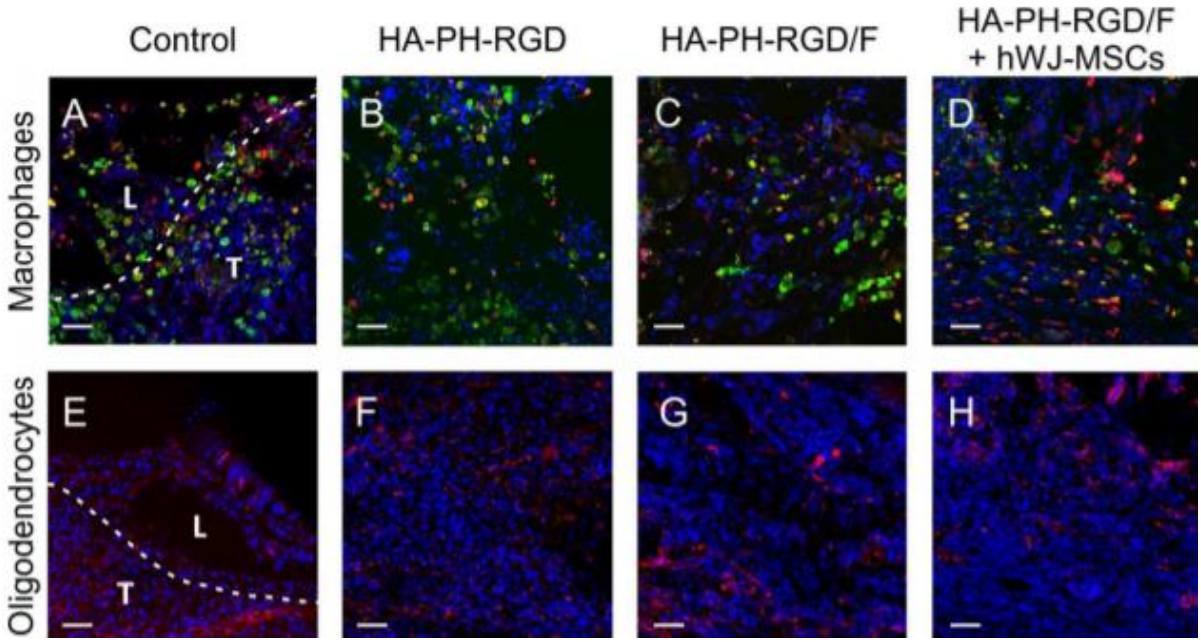

Figure 42. Representative images of longitudinal sections of the spinal cord lesion in (A, E) control and at 8 weeks after subacute injection of (B, F) HA-PH-RGD, (C, G) HA-PH-RGD/F and (D, H) HA-PH-RGD/F hydrogel combined with hWJ-MSCs. (A-D) M1 macrophages (ED1, green) and M2 macrophages (CD206, red), (E-H) oligodendrocytes (MOSP, red) and (A-H) DAPI (blue). The dotted lines in (A, E) outline the border of the tissue (T) and the lesion area (L). Other images are taken from the center of the lesion. Scale bar: 50 µm. 177x93mm (300 x 300 DPI).

4.2.3.5. Gene expression analysis in subacute SCI lesions

Two months post injection of the three hydrogel types (HA-PH-RGD, HA-PH-RGD/F and HA-PH-RGD/F combined with hWJ-MSCs), variations and modifications in mRNA expression of specific genes were analyzed (Figure 43). Decreased expression of genes related to macrophages (Irf5, Cd86), inflammation (Ccl3) or glial scar formation (Gfap, Ptprz1) was noted in the lesions with injected HA-PH-RGD and HA-PH-RGD/F hydrogels. However, the changes were not significant. Significant downregulation was then found for the expression of Gap43 when compared to the untreated control lesion. Contrarily, the expression of Gap43 was

significantly increased when HA-PH-RGD/F was combined with hWJ-MSCs. Along these lines, the combination with hWJ-MSCs led to a significant upregulation of both M1 (Irf5, Cd86) and M2 macrophages markers (Mrc1).

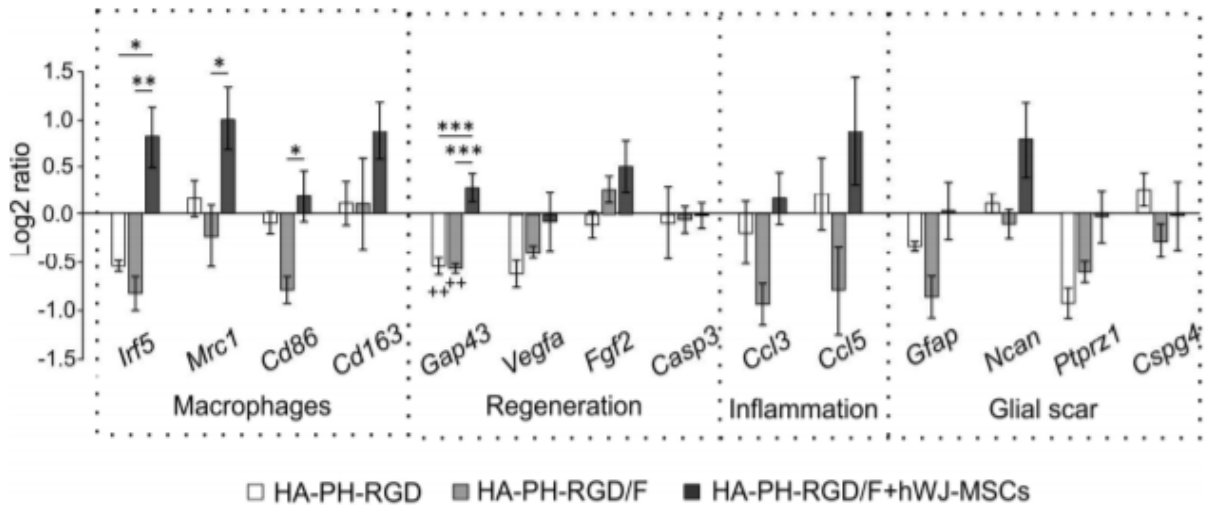

Figure 43. Analysis of mRNA gene expression of selected genes involved in reparative processes following spinal cord injury treated with HA-PH-RGD, HA-PH-RGD/F and HA-PH-RGD/F hydrogels combined with hWJMSCs. The graph shows the log2-fold changes in gene expression over the control lesion with saline. Significance is calculated between ΔCt values. ++p < 0.01: versus control lesion, *p < 0.05, **p < 0.01, ***p < 0.001, (n = 5). 193x80mm (300 x 300 DPI).

4.2.3.6. Analysis of locomotor functions in subacute SCI lesions

The TSE Motion 8.5.11 was used to study the effect of the hydrogel treatment on animal locomotor functions. Aspects of the study included knee and ankle angles and hind limb retraction and protraction (distance on the x axis of the metatarsophalangeal joint in relation to the iliac crest). At time points of 5 and 8 weeks, negligible statistical variations were seen between the control and hydrogel treated animals (not shown).

4.2.3.7. Discussion

Hyaluronic acid (HA) is a vital structural component of the ECM and plays an important role in regulating tissue regeneration because it acts as a signaling molecule via some specific HA receptors (Litwiniuk M. at al., 2016, Knopf-Marques H. at al., 2016). HA is very commonly used as biomaterial in clinical settings as it possesses significant biocompatibility, non-immunogenicity and biodegradability. HA-based substrates have previously been used *in vitro* for neural stem cell cultures and also *in vivo* in neural tissue engineering activities (Seidlits S.K. at al., 2010). They can be used either by themselves or as carriers for cell delivery to enhance cell retention and integration (Mothe A.J. at al., 2013, Raynald, Li Y., 2016, Liang Y., 2013, Li L.M., 2017). Injectable HA-based hydrogels have also been developed for localized intrathecal delivery of bioactive molecules to SCI (Fuhrmann T., 2015, Gupta D., 2006). The most significant benefit of using this material is that it can be manufactured in a reproducible manner under GMP (Good Manufacture Practice) conditions, which are required to allow the transfer of its production from bench-to-bedside to clinical practice.

Since native HA does not harbor the properties of forming a gel or supporting cell adhesion, the HA has to be modified chemically according to the demands. An enzymatic crosslinking reaction initiated by horseradish peroxidase and hydrogen peroxide was used to form the hydrogel in our study. Optimization of the concentration of non-toxic cross-linking agents was done to set mechanical properties comparable to native spinal cord tissue and to get the optimal time of gelation for material application into the site of the defect. This also made it possible to create cell-laden hydrogel under physiological conditions.

hydroxyphenyl derivative of HA, i.e. HA-PH, is one of the materials showing positive abilities of forming covalently cross-linked hydrogels. By inducting the enzyme horseradish peroxidase hydrogen peroxide (H_2O_2) *in situ* under physiological conditions, the cross-linking and subsequent gel formation in this HA-PH derivative can be triggered without any adverse consequences affecting the encapsulated cells (Kučera L., 2015). Previously, the chondrogenic potential of HA-PH derivative based on hydrogel has been demonstrated *in vitro* as well as *in vivo* in cartilage defects (Dvorakova J., 2014, Kučera L., 2015). For our current experiments, an HA-PH derivative bearing a newly developed 3-(4-hydroxyphenyl) propionic acid - L-lysine – aminohexanoic acid - L-glycine - L-arginine - L-glycine - L-aspartic acid (HA-PH-RGD) sequence was used to functionalize the HA-PH, improve cells adhesion and migration into implants. This increased its affinity for several integrin receptors and also supported cell spreading, cytoskeletal organization and cell proliferation (Mackova H., 2016). However, one of the important vital factors for successful cell adhesion considered ligand density, which in the

case of used HA-PH-RGD derivative, is limited due to the degree of substitution of PH-RGD oligopeptide. A hydrogel containing 20 mg/ml of the newly designed HA-PH-RGD conjugate with a degree of substitution of 2.5 % achieved a concentration of RGD sequence of 1 μmol per ml of hydrogel. *In vitro* experiments confirmed that the presence of the RGD motive in the HA-PH hydrogel structure improved its cell affinity to a certain degree. Hence, to assist cell encapsulation, the bioadhesive properties of the hydrogels were multiplied.

Fibrinogen offers cellular adhesive domains and has been previously proven to be a natural additive to enhance cell survival, growth and proliferation (Karoubi G., 2009, Zapotocky V., 2017). Therefore, the combination of HA-PH-RGD with fibrinogen (HA-PH-RGD/F) was created to enhance the adhesive abilities of hWJ-MSCs. The HA-PH-RGD/F thus created contains integrin binding sites, such as RGD, and is commonly used as a promising additive to enhance cell survival, growth and proliferation (Karoubi G., 2009, Zapotocky V., 2017). Since blood plasma is rich in fibrinogen, it is highly feasible to extract the required fibrinogen from the blood plasma of the patient for autologous use.

Contrarily, the addition of fibrinogen to HA-PH-RGD hydrogel had no effect on the assessed tissue repair parameters in subacute SCI. However, on exposure to *in vivo* conditions of the SCI lesion, endogenous protein-rich extracellular fluid entered the hydrogel. The endogenous proteins mentioned constituted fibronectin as well. In combination with endogenous cell infiltration and degradation of the hydrogel implant, they may overlap the potential benefit of fibrinogen in the HA-PH-RGD/F hydrogel.

A week after the subacute SCI lesion was induced, HA-PH-RGD, HA-PH-RGD/F and HA-PH-RGD/F combined with hWJ-MSCs were injected into the lesion for subsequent evaluation of the repair potential of HA based hydrogels. The results were compared with control injection of saline. Even though the tissue was removed during hemisection induction, the lesion cavity did not remain empty and was commonly occupied by debris and connective tissue, that enabled vascularization with compromised axonal infiltration. However, after injection of both HA-PH-RGD and HA-PH- RGD/F, the density of NF-positive fibers in the lesion cavity significantly increased, and this effect was further enhanced when the HA-PH-RGD/F was combined with hWJ-MSCs.

Ironically, it was noted that although mRNA expression of the Gap43 gene responsible for axonal growth had reduced, robust axonal ingrowth into HA-PH-RGD and HA-PH-RGD/F was still observed via histological analysis. In the group harboring hWJ-MSCs, Gap43 was, however, upregulated. This gene is therefore considered as a crucial component of an effective regenerative response in the nervous system.

Our findings suggest that in earlier times post injury, axonal ingrowth into HA-PH-RGD and HA-PH-RGD/F may be halted. In the group containing hWJ-MSCs this ingrowth, however, was continued. Hence, NF160 staining of the HA-PH-RGD and HA-PH-RGD/F hydrogel groups carried out at 2 months demonstrated already matured sprouting neurons. Moreover, the expression of both M1 and M2 macrophage/microglia markers increased when HA-PH-RGD/F was combined with hWJ-MSCs. All these findings are in accordance with the fact that tissue repair processes facilitated by stem cells treatment involve orchestrated activation of different macrophage phenotype (Gensel J.C., 2015).

Over the 2-month time period, hWJ-MSCs slowly died in spite of being treated with a combination of three immunosuppressant agents. The effect of the stem cells was proven using immunohistochemical and qPCR analysis. The results were in accordance with the widely proposed hypothesis that transplanted cells release trophic factors that provide long-lasting neurotrophic and immunomodulatory effects (Urdzikova L.M., 2014, Petrenko Y., 2017, Assinck P. at al., 2017).

In contrast to the improvement in tissue repair parameters, no significant improvement in locomotor functions was observed in animals treated with either hydrogel alone or in combination with hWJ-MSCs. While it is unlikely that HA scaffolds alone could lead to behavioral restoration without additional treatment, the combination of hydrogels with various stem cells may have beneficial effects on the repair of the injured spinal cord by providing trophic support (Kubinova S. and Sykova E., 2012, Pego A.P. at al., 2012, Shrestha B., 2014). However, the number of transplanted cells is an important factor which significantly affects the behavioral outcome after SCI. In our earlier studies, we calculated that 1.5 million cells in a single intrathecal application (unpublished data) is an effective hWJ-MSCs dose and it is sufficient to bring functional improvement after SCI contusion. This higher dose of transplanted cells is thought to increase the number of surviving cells as well as behavioral outcome. In the current study, however, we focused mainly on establishing the applicability of the HA-PH-RGD hydrogel for neural tissue repair and as a cell carrier per se. Following this, the quantity of transplanted cells was maintained at ~ 3 x 10^4. The number of cells was limited by the size of the lesion and the hydrogel volume (~ 5 µl) and did not exceed the level at which the functional locomotor improvement could be achieved. application of a combination of hydrogels with stem cells through direct cell injection into the lesion site or by intrathecal application is proposed to prevail over the limitation of the number of cells that can be implanted with the hydrogel.

Since spinal cord hemisection is the least invasive and destructive SCI model and it simultaneously allows filling the lesion cavity with the material and provides the possibility of a

clear analysis of the endogenous infiltration into the implant, we used this model in our study (Tukmachev D. at al., 2016, Kubinova S. at al., 2015, Kubinova S. at al., 2011). On the other hand, hemisection is a case of partial lesions with a high rate of spontaneous recovery and a high risk of inconsistencies in the injuries from one animal to another, which might lead to misinterpretation of the behavioural evaluation (Fouad K. at al., 2013).

Thus, although there are several scaffolds that can support axonal growth and spouting after SCI, there are few of those which are able to achieve significant functional recovery, due to the reduced regeneration of long-tract axons through sites of SCI. Designing and developing materials suitable for bridging the lesion must be accompanied by efforts to modify the extrinsic and intrinsic factors limiting regrowth after injury, which represents the current challenge of how to overcome the inhibitory properties of the axon–scar environment. Combinatorial therapies will probably be essential to achieve such functional connectivity (Chew D.J., 2012).

In conclusion, we have developed and characterized injectable HA-PH-RGD based hydrogel which represents a suitable material for further combinatorial therapies in neural tissue engineering. The injected HA-PH-RGD hydrogels bridge the SCI lesion cavity, support vascularization and also increase axonal sprouting into the lesion. Combining the hydrogels with hWJ-MSCs assisted in these activities. In spite of the significant improvements of neuroregenerative processes, it is still imperative to find additional treatments that would further stimulate axonal reconnection to best functional SCI restoration.

5. GENERAL DISCUSSION

Using stem cells for SCI treatment is modern promising method with high potential in the future. However, the major factor determining the success of the stem cells transplantation is delivery technique. Therefore, development and improvement of targeting cell delivery techniques are necessary for enhancing the efficacy of SCI treatment. Combination of magnetic nanomaterials conjugated with stem cells and focused magnetic field to guide cells migration and trap them in the lesion site has high potential for further development and introduction in practical therapy. Retention of cells at lesion site, engraftment efficacy and functional recovery were significantly enhanced when SPION-labelled stem cells delivery was magnetically guided to target organ/tissue/location (Landazuri N. et al., 2013; Vandergrif A.C. et al., 2014; Cheng K. et al., 2014, Pislaru S.V. et al., 2006, Polyak B. et al., 2008, Riegler J. et al., 2013, Panseri S. et al., 2012, Kamei G. et al., 2013, Yanai A. et al., 2012). However, only few attempts were performed for magnetic delivery of stem cells to SCI lesion site (Nishida K. et al., 2006; Vanecek V. et al., 2012; Hamasaki T. et al., 2007).

The main drawback in the application of magnetic delivery is poor focusing ability. In this study we designed new magnetic system which allows to focus magnetic field strongly in the spinal cord lesion site (Figure 12, 14) – trapping area. MSCs labelled by the poly-L-lysine-coated SPIONs were efficiently attracted by a magnet and concentrated in magnetic field focusing area *in vitro* as well as at the lesion site *in vivo* after injection intrathecally at the L5–L6 level after only 2 hours of exposition. Therefore, the application of our magnetic system demonstrates the potential benefits of fast and efficient stem cells delivery into SCI lesion. The proposed strategy can be used for stem cells-based treatments of not only traumatic SCIs, but also for non-traumatic SCI or neurodegenerative diseases (Sykova E. at al., 2006, Forostyak S. at al., 2013).

Other significant task which has to be solved in SCI treatment is replacement of the lesion cavity by implantation of matrix to support further tissue regeneration. This matrix can represent syntethic polymer or native extracellular matrix (ECM) and must provide supportive substrates for replacing lost tissue and re-establishing damaged connections (Kubinova S. and Sykova E., 2012, Assuncao-Silva R.C. at al., 2015). Scaffolds composed of native ECM represent structures very similar to uninjured host tissue with natural three-dimensional structure, biological activity promoting cell adhesion and proliferation, and biodegradability (Crapo P.M. at al., 2012). Currently, ECM scaffolds are being widely used for various tissue reconstructions, including

heart valves, blood vessels, etc, but only few studies addressing for the repair of SCI (Zhang X.Y. at al., 2011, Li C. at al., 2012, Liu J. at al., 2012).

ECM hydrogels prepared by decellularization of porcine spinal cord (SC-ECM) and porcine urinary bladder (UB-ECM) provide a supportive environment for the *in vitro* neural cell growth (Medberry C.J. at al., 2013, DeQuach J.A. at al., 2011). However, experimentally, it is unknown whether these materials can be successfully used for SCI repair, either alone or in combination with various types of cells. We examined the effects of injectable SC-ECM and UB-ECM hydrogels in the acute model of SCI. Despite the lack of a native three-dimensional ultrastructure intrinsic for source tissue, ECM hydrogels retain their biological activity and possess mechanical properties similar to that of soft neural tissue, with the advantage of injectability and *in situ* polymerization, which offer minimally invasive delivery techniques and facilitate the possibility of clinical translation. When injected into the SCI, both hydrogel types were well integrated into the surrounding tissue, and supported massive cell infiltration and neovascularization. Macrophages were the predominantly infiltrating cells within the grafts that participated in the ECM degradation. Degradation of ECM scaffolds is essential for the constructive tissue remodelling process by which a degradable biomaterial serves as a temporary inductive niche, which is gradually replaced by functional tissue as opposed to scar tissue (Badylak S.F. at al., 2009, Tottey S. at al., 2011, Valentin J.E. at al., 2009). Moreover, degradation of ECM scaffolds stimulates the release of matricryptic molecules which possess a variety of bioactive properties such as antimicrobial activity, angiogenic effects, as well as the recruitment of endogenous stem and progenitor cells (Valentin J.E. at al., 2009). Implantation of ECM hydrogels with seeded stem cells may partly prevent the massive scaffold contraction within the lesion cavity. However, the inflammatory milieu of the acute lesion together with the massive infiltration of macrophages did not support cell survival. Higher *in vivo* cell survival rate could be achieved by increasing the number of implanted cells.

Some synthetic hydrogels (SIKVAV (Ser-Ile-Lys-Val-Ala-Val)-modified highly superporous poly(2-hydroxyethyl methacrylate) hydrogel with oriented pores) possess a moderate modulus of elasticity, which has been shown to promote good bridging, tissue infiltration and abundant axonal ingrowth (Kubinova S. et al., 2010). SIKVAV sequence is a synthetic peptide from active regions of the chain A of basement membrane laminin, which promotes cell adhesion and neural outgrowth by the binding of transmembrane integrin receptors (Tashiro K. et al., 1989). Moreover, synthetic nature of implant attenuates fast scaffold degradation and provide stable matrix for cells filling. Other significant findings include the observation that the oriented pores of the hydrogel directed axonal growth in the cranio-caudal

and caudo-cranial direction. Such aligned ingrowth enabled easier evaluation of the amount and the length of axons into the scaffold.

According to our experience with hydrogel bridging in experimental SCI, we noticed that new axons do grow inside most scaffolds during the first weeks but, when evaluated at later time points, the number of axons seems to be rather inadequate with respect to the earlier results. Only few studies throw light on the time-related dynamics of the tissue infiltration of these scaffolds. Therefore, we estimated the time-dependent dynamics of ingrowth of connective tissue, axons and blood vessels inside the implanted scaffold hydrogel with or without seeded stem cells. SIKVAV-HEMA-based hydrogel scaffold environment supported the ingrowth of connective tissue, blood vessels and axons. Axonal infiltration into the scaffold was a slow and gradual process as compared to the much faster connective tissue ingrowth. Axons slowly and gradually infiltrated the hydrogel within the first month, after which the numbers became stable. One reason could be the spatial limitation in the hydrogel pores, due to the connective tissue infiltration. Deficiency of nutrients and growth factors can however be another plausible cause.

Progressive infiltration of the connective tissue into the hydrogel pores continues only for the first week, after which it plateaus for the next 2 months. On the contrary, the axons continue to grow into the hydrogel pores even at a time of one month after the implantation. This is not facilitated by the presence of MSCs inside the hydrogel pores. However, using genetically engineered MSCs, that over-express some of the growth factors like BDNF and VEGF, instead of simple MSCs, it may be possible to stimulate axonal ingrowth and improve tissue repair (Stewart A.N. et al., 2017). Inclusion of some other supportive cells such as Schwann cells may also improve neuroregenerative effects alongside the MSCs (Yang E.Z. et al., 2017). Thus, it is safe to assume that modified MSCs may promote their positive effect on the neuronal repair after SCI.

The physical and chemical properties of the scaffold dictate its inner architecture and structure, which is vital part of the micro-environmental milieu. In one of previous studies, was found that the web-like architecture of the hydrogel, together with the HPMA-based backbone promotes the ingrowth of new axons despite promoting the adhesion of fewer MSCs compared to HEMA-based hydrogels (Hejcl A. et al., 2013). The results of these studies yielded points to the fact that the effect of MSCs seeded on hydrogels is less important than the inner milieu of the hydrogel, influenced by the chemical backbone and the architecture of the scaffold.

Despite benefits of HEMA-SIKVAV hydrogel on axonal regeneration and functional outcome (Tysseling-Mattiace V.M. et al., 2008; Tysseling V.M. et al., 2010) it is still not the

solution to the problem how to bring for long-term survival and promotion of axons in the hydrogel scaffolds.

Hyaluronic acid (HA) is a vital structural component of the ECM and plays an important role in regulating tissue regeneration because it acts as a signaling molecule via some specific HA receptors (Litwiniuk M. at al., 2016, Knopf-Marques H. at al., 2016). HA is very commonly used as biomaterial in the clinical settings as it possesses significant biocompatibility, non-immunogenicity, and biodegradability. HA based substrates have previously been used *in vitro* for neural stem cell cultures and also *in vivo* in neural tissue engineering activities (Seidlits S.K. at al., 2010). They can be used either by themselves or as carriers for cell delivery to enhance cell retention and integration (Mothe A.J. at al., 2013, Raynald, Li Y., 2016, Liang Y., 2013, Li L.M., 2017). Injectable HA-based hydrogels were also developed for localized intrathecal delivery of bioactive molecules into the SCI (Fuhrmann T., 2015, Gupta D., 2006). The most significant benefit of using this material is that it can be manufactured in a reproducible manner under GMP (Good Manufacture Practice) conditions, which are required to allow the transfer of its production from bench-to-bedside in clinical practice.

Since native HA can't form a gel or support cell adhesion, it has to be modified chemically by addition of hydroxyphenyl (PH) groups. An enzymatic crosslink reaction initiated by horseradish peroxidase and hydrogen peroxide was used to form the hydrogel and set mechanical properties comparable to the native spinal cord tissue under physiological conditions (Kučera L., 2015). In our study, the HA-PH derivative bearing the newly developed 3-(4-hydroxyphenyl) propionic acid - L-lysine – aminohexanoic acid - L-glycine - L-arginine - L-glycine - L-aspartic acid (HA-PH-RGD) sequence was used to improve cells adhesion and migration into implants. RGD increased affinity for several integrin receptors and also supported cell spreading, cytoskeletal organization and cell proliferation (Mackova H., 2016, Karoubi G., 2009, Zapotocky V., 2017).

Fibrinogen offers cellular adhesive domains and has been previously proved as a natural additive to enhance cell survival, growth and proliferation (Karoubi G., 2009, Zapotocky V., 2017). Therefore, a combination of HA-PH-RGD with fibrinogen (HA-PH-RGD/F) enhanced the adhesive abilities of the hWJ-MSCs. Contrarily, the addition of fibrinogen had no effect on the assessed tissue repair parameters in subacute SCI that may be explained by overlapping endogenous integrins (i.e. fibronectin) from extracellular fluid entered the hydrogel. Injection of both HA-PHRGD and HA-PH-RGD/F hydrogels similarly promoted axonal ingrowth into the lesion and this effect was further enhanced when the HA-PH-RGD/F was combined with hWJ-

MSCs. On the other hand, no effect was found on locomotor recovery or the blood vessel ingrowth and density of glial scar around the lesion.

Thus, although there are several scaffolds that can support axonal growth and spouting after SCI, there are few of those which are able to achieve significant functional recovery, due to the reduced regeneration of long-tract axons through sites of SCI. Designing and developing materials suitable for bridging the lesion must be accompanied with efforts to modify the extrinsic and intrinsic factors limiting regrowth after injury which represents the current challenge of how to overcome the inhibitory properties of the axon–scar environment. Combinatorial therapies will probably be essential to achieve such functional connectivity (Chew D.J., 2012).

In conclusion, we have developed and characterized injectable HA-PH-RGD based hydrogel, which represents a suitable material for further combinatorial therapies in neural tissue engineering. The injected HA-PH-RGD hydrogels bridge the SCI lesion cavity, support vascularization and also increase axonal sprouting into the lesion. Combining the hydrogels with hWJ-MSCs assisted in these activities. In spite of the significant improvements of neuroregeneration processes, it is still imperative to find additional treatments that would further stimulate axonal reconnection to best functional SCI restoration.

6. CONCLUSIONS

1. A non-invasive magnetic system was designed and used to accumulate mesenchymal stem cells labelled with superparamagnetic iron oxide nanoparticles precisely at a specific site of a SCI lesion. This system allowed to reach a significantly higher concentration of SPION-labelled stem cells to the vicinity of the lesion site.

2. Two types of ECM hydrogels derived from decellularized porcine spinal cord and urinary bladder tissues were evaluated as scaffolds for SCI repair. Both ECM hydrogels showed significant immunomodulatory and neuroregenerative effects and provided a substrate for tissue bridging after SCI.

3. Connective tissue and blood vessels quickly infiltrate the SIKVAV-HEMA scaffold within the first week, however, axons showed a rather gradual infiltration over the first month, and this was not facilitated by the presence of MSCs inside the hydrogel pores.

4. An injectable HA-PH-RGD derivative hydrogel was developed and characterized. Injection of HA-PH-RGD hydrogels bridged the lesion cavity, supported vascularization and increased axonal sprouting into the lesion, which was further improved by its combination with hWJ-MSC.

7. SUMMARY

Restoration of lost neuronal function after spinal cord injury (SCI) still remains a big challenge for current medicine. One important repair strategy is bridging the SCI lesion with a supportive and stimulatory milieu that would enable axonal rewiring. Extracellular matrix (ECM)-derived hydrogels may serve as scaffold and provide infiltration of blood vessels and neurites. Treatment of SCI utilizing stem cell transplantation also represents a promising therapy. Hydrogel scaffolds which bridge the lesion, together with stem cell therapy represent a promising approach for spinal cord injury (SCI) repair. However, current conventional treatments are limited by inefficient delivery strategies of cells into the injured tissue. Therefore, the aim of this study was to develop new techniques for SCI treatment on the basis of addressing stem cell delivery via magnetic field or transplantation with injectable extracellular matrix hydrogels as a milieu for neuroregeneration *in vivo*.

We designed a magnetic system and used it to accumulate stem cells labelled with superparamagnetic iron oxide nanoparticles (SPION) at a specific site of a SCI lesion. The magnetic system allowed rapid guidance of the SPION-labelled cells precisely to the lesion location. Histological analysis of cell distribution throughout the cerebrospinal channel showed a good correlation with the calculated distribution of magnetic forces exerted onto the transplanted cells.

Natural and synthetic ECM: decellularized porcine spinal cord (SC) and urinary bladder (UB), superporous hydrogel, modification of hydroxyphenyl derivative of hyaluronic acid (HA-PH) with the integrin binding peptide RGD were evaluated for their neuroregenerative properties in a rat model of SCI. Hydrogels were injected or transplanted into the spinal cord hemisection cavity with or without stem cells. Histological analysis and gene expression analysis were performed after implantation.

All hydrogels supported neovascularization and axonal ingrowth into the lesion. No significant differences in tissue infiltration were found between effects of SC-ECM and UB-ECM, as well as between the plain hydrogels and seeded with stem cells hydrogels. However, injection of HA-PH-RGD/Fibrinogen with Wharton's jelly-derived human mesenchymal stem cells (hWJ-MSCs) enhanced only axonal ingrowth.

In conclusion, the combination of injectable hydrogel scaffolds and technique of noninvasive magnetic delivery of labelled stem cells seems to be promising strategy for SCI treatment due to improved cell survival, inhibition of systematic inflammation, enhanced engraftment and providing *in vivo*-like neural regeneration.

SOUHRN

Poranění míchy (SCI) je velice vážné trauma, které vede k významné mortalitě a morbiditě. Léčba SCI byla vždy léčbou nejobtížnější, nicméně využití transplantace kmenových buněk představuje slibnou terapii. Další důležitou reparační strategií je přemostění léze SCI podpůrným a stimulačním prostředím, které by umožnilo axonální přepojení. Nedávno bylo zjištěno, že injikovatelná extracelulární matrix (ECM) odvozená z hydrogelů má neurotrofický potenciál in vitro. Cílem této studie bylo proto vytvořit nové techniky pro léčbu SCI s využitím řešení, které spočívá v transportu kmenových buněk magnetickým polem nebo transplantaci využívající injikovatelné hydrogely na bázi extracelulární matrix jako prostředí pro neuroregeneraci *in vivo*.

Byl navržen neinvazivní magnetický systém, který byl následně použit k akumulaci kmenových buněk značených superparamagnetickými nanočásticemi oxidu železa (SPION) na specifickém místě léze SCI. Magnetický systém navíc umožnil rychlé navádění buněk značených SPION přesně na místo léze. Histologická analýza distribuce buněk v celém mozkomíšním kanálu prokázala dobrou korelaci s vypočítanou distribucí magnetických sil působících na transplantované buňky.

Decelularizované tkáně prasečí míchy (SC) a močového měchýře (UB) a superporézní hydrogel s orientovanou porozitou a modifikací hydroxyfenylderivátu kyseliny hyaluronové (HA-PH) s peptidem RGD vázajícím se na integrin jako skafoldové hydrogely byly hodnoceny z hlediska jejich neuroregenerativních vlastností na potkaním modelu SCI. Hydrogely s kmenovými buňkami nebo bez kmenových buněk byly injikovány nebo transplantovány do dutiny míšní hemisekce. Po injekci byla provedena histologická analýza a analýza genové exprese.

Všechny typy hydrogelů se integrovaly do léze a stimulovaly neovaskularizaci a axonální vrůstání do léze. Mezi SC-ECM a UB-ECM nebyly zjištěny žádné významné rozdíly. Nebyl zjištěn žádný rozdíl v infiltraci tkání mezi prostými hydrogely a hydrogely s nasazenými kmenovými buňkami. Subakutní injekce HA-PH-RGD/fibrinogenu v kombinaci s lidskými mezenchymálními kmenovými buňkami získanými z Whartonova želé (hWJ-MSC) však zesílila pouze axonální vrůstání do lézeю

Závěrem lze konstatovat, že kombinovaná aplikace injikovatelných hydrogelových skafoldů a technika neinvazivního magnetického transportu jsou klíčovými faktory pro zlepšení přežití buněk, jejich přihojení, neurální regeneraci podobnou *in vivo* a inhibici systematického zánětu.

8. LITERATURE REFERENCES

1. Acheson A, Conover JC, Fandl JP, DeChiara TM, Russell M, Thadani A, Squinto SP, Yancopoulos GD, Lindsay RM (1995) A BDNF autocrine loop in adult sensory neurons prevents cell death. Nature 374(6521):450–453.
2. Adam Young D, Bajaj V, Christman KL (2014) Award winner for outstanding research in the PhD category, Society for Biomaterials annual meeting and exposition, Denver, Colorado: Decellularized adipose matrix hydrogels stimulate in vivo neovascularization and adipose formation. Journal of biomedical materials research Part A 102:1641-1651.
3. Advances in replacement organs and tissue engineering. Technical Insights, Frost & Sullivan. 2008; Stem cell biology and cell technologies. Ed. by: Pal'cev MP. M.: Medicina, 2009:456.
4. Al Kindi A, Ge Y, Shum-Tim D, Chiu RCJ (2008) Cellular cardiomyoplasty: routes of cell delivery and retention. Front Biosci 13:2421–2434.
5. Al-Bagdadi FA, Barona HM, Martinez-Ceballos E, Yao JS (2019) Ultrastructure Morphological Characterization of Different Passages of Rat Dental Follicle Stem Cells at *In vitro* Culture. Microsc Ultrastruct 7(2):57–64.
6. Allen SJ, Watson JJ, Shoemark DK, Barua NU, Patel NK (2013) GDNF, NGF and BDNF as therapeutic options for neurodegeneration. Pharmacol Ther 138(2):155–175.
7. Allen SJ, Dawbarn D (2006) Clinical relevance of the neurotrophins and their receptors. Clinical Science 110(2):175–191.
8. Althaus HH (2004) Remyelination in multiple sclerosis: a new role for neurotrophins? Progress in Brain Research 146:415–432.
9. Amr SM, Gouda A, Koptan WT, Galal AA, Abdel-Fattah DS, Rashed LA (2014) Bridging defects in chronic spinal cord injury using peripheral nerve grafts combined with a chitosan-laminin scaffold and enhancing regeneration through them by cotransplantation with bone-marrow-derived mesenchymal stem cells: case series of 14 patients. J Spinal Cord Med 37:54–71.
10. Andrews MR, Czvitkovich S, Dassie E, Vogelaar CF, Faissner A, Blits B (2009) Alpha9 integrin promotes neurite outgrowth on tenascin-C and enhances sensory axon regeneration. J Neurosci 29:5546–5557.
11. Antonic A, Sena ES, Lees JS, Wills TE, Skeers P, Batchelor PE, Macleod MR, Howells DW (2013) Stem Cell Transplantation in Traumatic Spinal Cord Injury: A Systematic Review and Meta-Analysis of Animal Studies. PLoS Biol 11(12).

12. Assinck P, Duncan GJ, Plemel JR (2017) Myelinogenic Plasticity of Oligodendrocyte Precursor Cells following Spinal Cord Contusion Injury. J Neurosci 37(36):8635-8654.
13. Assuncao-Silva RC, Gomes ED, Sousa N, Silva NA, Salgado AJ (2015) Hydrogels and Cell Based Therapies in Spinal Cord Injury Regeneration. Stem Cells Int 2015:948040.
14. Atala A, Lanza R, Thompson J, Nerem R (2008) Principles of regenerative medicine. Academic Press is an imprint of Elsevier, First edition.
15. Babic M, Horak D, Trchova M, Jendelova P, Glogarova K, Lesny P, Herynek V, Hajek M, Sykova E (2008) Poly(N,N-dimethylacrylamide)-coated maghemite nanoparticles for stem cell labeling. Bioconjug Chem 19:740-750.
16. Badylak SF (2014) Decellularized allogeneic and xenogeneic tissue as a bioscaffold for regenerative medicine: factors that influence the host response. Annals of biomedical engineering 42:1517-1527.
17. Badylak SF, Freytes DO, Gilbert TW (2009) Extracellular matrix as a biological scaffold material: Structure and function. Acta biomaterialia; 5:1-13.
18. Badylak SF, Gilbert TW (2008) Immune response to biologic scaffold materials. Seminars in immunology 20:109-116.
19. Bakshi A, Hunter C, Swanger S, Lepore A, Fischer I (2004) Minimally invasive delivery of stem cells for spinal cord injury: advantages of the lumbar puncture technique. J Neurosurg: Spine 1:330–337.
20. Bartus K, James ND, Didangelos A, Bosch KD, Verhaagen J, Yáñez-Muñoz RJ, Rogers JH, Schneider BL, Muir EM, Bradbury EJ (2014) Large-scale chondroitin sulfate proteoglycan digestion with chondroitinase gene therapy leads to reduced pathology and modulates macrophage phenotype following spinal cord contusion injury. J Neurosci 34(14):4822–3486.
21. Basso DM, Beattie MS, Bresnahan JC (1995) A sensitive and reliable locomotor rating scale for open field testing in rats. J Neurotrauma 12:1.
22. Batchelor PE, Skeers P, Antonic A, Wills TE, Howells DW, Macleod MR, Sena ES (2013) Systematic Review and Meta-Analysis of Therapeutic Hypothermia in Animal Models of Spinal Cord Injury. 8(8):e71317.
23. Benton RL, Maddie MA, Gruenthal MJ, Hagg T, Whittemore SR (2009) Neutralizing endogenous VEGF following traumatic spinal cord injury modulates microvascular plasticity but not tissue sparing or functional recovery. Curr Neurovasc Res 6(2):124–131.

24. Benzel EC (2005) Spine surgery: techniques, complication avoidance, and management, 2nd ed. Elsevier Churchill Livingstone 2205p.
25. Bjorklund A, Stenevi U, Dunnett SB, Iversen SD (1981) Functional reactivation of the deafferented neostriatum by nigral transplants. Nature 289(5797):497.
26. Blinder SM (2011) Magnetic Field of a Cylindrical Bar Magnet Wolfram Demonstrations Project. http://demonstrations.wolfram.com /MagneticFieldOfACylindricalBarMagnet/ C178.
27. Boido MD, Garbossa S, Vercelli A (2011) Early graft of neural precursors in spinal cord compression reduces glial cyst and improves function. J Neurosurg Spine 15(1):97–106.
28. Borgens RB, Liu-Snyder P (2012) Understanding secondary injury. Q Rev Biol 87(2):89–127.
29. Bradbury EJ, Carter LM (2011) Manipulating the glial scar: chondroitinase ABC as a therapy for spinal cord injury. Brain Res Bull 84(4-5):306–316.
30. Brown BN, Ratner BD, Goodman SB, Amar S, Badylak SF (2012) Macrophage polarization: an opportunity for improved outcomes in biomaterials and regenerative medicine. Biomaterials 33:3792.
31. Brown RA (2013) In the beginning there were soft collagen-cell gels: towards better 3D connective tissue models? Exp Cell Res 319:2460.
32. Cafferty WB, Duffy P, Huebner E, Strittmatter SM (2010) MAG and OMgp synergize with Nogo-A to restrict axonal growth and neurological recovery after spinal cord trauma. J Neurosci 30(20):6825–6837.
33. Cao Q, Xu XM, Devries WH, Enzmann GU, Ping P, Tsoulfas P, Wood PM, Bunge MB (2005) Functional recovery in traumatic spinal cord injury after transplanta-tion of multineurotrophin–expressing glial–restricted precursor cells. J Neurosci 25(30):6947–6957.
34. Chao T, Gupta R (2012) Dose and duration of nerve growth factor (NGF) administration determine the extent of behavioral recovery following peripheral nerve injury in the rat. Exp Neurol 234:5–7.
35. Cheah M, Andrews MR, Chew DJ, Moloney EB, Verhaagen J, Fassler R (2016) Expression of an activated integrin promotes longdistance sensory axon regeneration in the spinal cord. J Neurosci 36:7283–7297.
36. Chen J, Chu YF, Chen JM, Li BC (2010) Synergistic effects of NGF, CNTF and GDNF on functional recovery following sciatic nerve injury in rats. Adv Med Sci 55(1):32–42.

37. Chen M, Xiang Z, Cai J (2013) The anti-apoptotic and neuro-protective effects of human umbilical cord blood mesenchymal stem cells (hUCB-MSCs) on acute optic nerve injury is transient. Brain Res 26:63–75.

38. Chen X, Katakowski M, Ki Y (2002) Human bone marrow stromal cell cultures conditioned by traumatic brain tissue extracts: growth factor production. Journal of Neuroscience Research 69(5):687-691.

39. Chen CT, Foo NH, Liu WS (2008) Chen Infusion of human umbilical cord blood cells ameliorates hind limb dysfunction in experimental spinal cord injury through antiinflammatory, vasculogenic and neurotrophic mechanisms. Pediatr Neonatol 49(3):77–83.

40. Cheng K, Shen D, Hensley MT, Middleton R, Sun B, Liu W, De Couto G, Marban E (2014) Magnetic antibody-linked nanomatchmakers for therapeutic cell targeting. Nat Commun 5:4880.

41. Cheng H, Liu X, Hua R (2014) Clinical observation of umbilical cord mesenchymal stem cell transplantation in treatment for sequelae of thoracolumbar spinal cord injury. J Transl Med 12:253.

42. Chi GF, Kim MR, Kim DW, Jiang MH, Son Y (2010) Schwann cells differentiated from spheroid-forming cells of rat subcutaneous fat tissue myelinate axons in the spinal cord injury. Exp Neurol 222(2):304-317.

43. Choi JS, Kim HY, Cha JH, Choi JY, Park SI, Jeong CH, Jeun SS, Lee MY (2007) Upregulation of vascular endothelial growth factor receptors Flt-1 and Flk-1 following acute spinal cord contusion in rats. J Histochem Cytochem 55:821–830.

44. Chopp M, Li Y (2002) Treatment of neural injury with marrow stromal cells. Lancet Neurology 1(2):92-100.

45. Christensen PB, Wermuth L, Hinge HH, Bømers K (1990) Clinical course and long-term prognosis of acute transverse myelopathy. Acta Neurol Scand 81:431–435.

46. Chuah MI, Teague R (1999) Basic fibroblast growth factor in the primary olfactory pathway: mitogenic effect on ensheathing cells. Neuroscience 88(4):1043–1050.

47. Chuah MI, Cossins J, Woodhall E, Tennent R, Nash G, West AK (2000) Glial growth factor 2 induces proliferation and structural changes in ensheathing cells. 857(1–2):265–274.

48. Cizkova D, Novotna I, Slovinska L, Vanicky I, Jergova S, Rosocha J, Radonak J (2011) Repetitive intrathecal catheter delivery of bone marrow mesenchymal stromal cells

improves functional recovery in a rat model of contusive spinal cord injury. J Neurotrauma 28:1951–1961.

49. Cloud BA, Ball BG, Chen BK, Knight AM, Hakim JS, Ortiz AM, Windebank AJ (2012) Hemisection spinal cord injury in rat: the value of intraoperative somatosensory evoked potential monitoring. J Neurosci Methods 211:179.

50. Crapo PM, Medberry CJ, Reing JE, Tottey S, van der Merwe Y, Jones KE et al. (2012) Biologic scaffolds composed of central nervous system extracellular matrix. Biomaterials 33:3539-3547.

51. Crapo PM, Tottey S, Slivka PF, Badylak SF (2014) Effects of biologic scaffolds on human stem cells and implications for CNS tissue engineering. Tissue Eng Part A 20:313.

52. Cummings BJ, Uchida N, Tamaki SJ, Salazar DL, Hooshmand M, Summers R, Gage FH, Anderson AJ (2005) Human neural stem cells differentiate and promote locomotor recovery in spinal cord–injured mice. Proc Natl Acad Sci U S A 102(39):14069–14074.

53. Dagci T, Armagan G, Konyaliogli S, Yalcina A (2009) Alterations in the expression of the apurinic/apyrimidinic endonuclease-1/redox factor-1 (APE/ref-1) and DNA damage in the caudal region of acute and chronic spinal cord injured rats treated by embryonic neural stem cells. Physiol Res 58(3):427–434.

54. Danisovic L, Varga I, Polák S, Ulicná M, Hlavacková L, Böhmer D, Vojtassák J (2009) Comparison of in vitro chondrogenic potential of human mesenchymal stem cells derived from bone marrow and adipose tissue. Gen Physiol Biophys 28(1):56-62.

55. Dasari VR, Veeravalli KK, Tsung AJ, Gondi CS, Gujrati M, Dinh DH, Rao JS (2009) Neuronal apoptosis is inhibited by cord blood stem cells after spinal cord injury. J Neurotrauma 26(11):2057–2069.

56. Davies S, Illis LS, Raisman G (1995) Perspective regeneration axonal long-distance text. Paraplegia 33(l):10-17.

57. Deda H, Inci MC, Kürekçi AE, Kayihan K, Ozgün E, Ustünsoy GE, Kocabay S (2008) Treatment of chronic spinal cord injured patients with autologous bone marrow-derived hematopoietic stem cell transplantation: 1-year follow-up. Cytotherapy 10(6):565–574.

58. Deng LX, Deng P, Ruan Y, Xu ZC, Liu NK, Wen X et al. (2013) A novel growth-promoting pathway formed by GDNFoverexpressing Schwann cells promotes propriospinal axonal regeneration, synapse formation, and partial recovery of function after spinal cord injury. J Neurosci 33:5655–5667.

59. Deng XY, Zhou RP, Lu KW, Jin DD (2010) Lithium chloride combined with human umbilical cord blood mesenchymal stem cell transplantation for treatment of spinal cord injury in rats. Nan Fang Yi Ke Da Xue Xue Bao 30(11):2436–2439.

60. DeQuach JA, Yuan SH, Goldstein LS, Christman KL (2011) Decellularized porcine brain matrix for cell culture and tissue engineering scaffolds. Tissue Eng Part A 17:2583-2592.

61. Deumens R, Koopmans GC, Honig WM, Hamers FP, Maquet V, Jerome R et al. (2006) Olfactory ensheathing cells, olfactory nerve fibroblasts and biomatrices to promote long-distance axon regrowth and functional recovery in the dorsally hemisected adult rat spinal cord. Exp Neurol 200:89–103.

62. Deumens R, Koopmans GC, Honig WM, Maquet V, Jerome R, Steinbusch HW et al. (2006) Limitations in transplantation of astrogliabiomatrix bridges to stimulate corticospinal axon regrowth across large spinal lesion gaps. Neurosci Lett 400:208–212.

63. Ditunno JF, Little JW, Tessler A, Burns AS (2004) Spinal shock revisited: a four-phase model. Spinal Cord 42:383–395.

64. Donega V, Nijboer CH, van Tilborg G, Dijkhuizen RM, Kavelaars A, Heijnen CJ (2014) Intranasally administered mesenchymal stem cells promote a regenerative niche for repair of neonatal ischemic brain injury. Exp Neurol 261C: 53–64.

65. Duncan ID, Hoffman RL (1997) Schwann cell invasion of the central nervous system of the myelin mutants. J Anat 190(1):35-49.

66. Ek CJ, Habgood MD, Callaway JK, Dennis R, Dziegielewska KM, Johansson PA, Potter A, Wheaton B, Saunders NR (2010) Spatio-Temporal Progression of Grey and White Matter Damage Following Contusion Injury in Rat Spinal Cord PLoS ONE 5(8):1–16.

67. Epsztejn-Litman S, Eiges R (2010) Genetic manipulation of human embryonic stem cells**.** Methods Mol Biol 584:387-411.

68. Erdogan B, Bavbek M, Sahin IF, Caner H, Ozen O, Denkbas EB, Altinors MN (2010) Fetal allogeneic umbilical cord cell transplantation improves motor function in spinal cord injured rats. Turk Neurosurg 20(3):286–294.

69. Eves FJ, Rivera N (2010) Prevention of urinary tract infections in persons with spinal cord injury in home health care. Home Healthc Nurse 28(4):230–241.

70. Fan L, Du F, Cheng BC, Peng H, Liu SQ (2008) Migration and distribution of bone marrow stromal cells in injured spinal cord with different transplantation techniques. Chin J Traumatol 11:94–97.

71. Fehlings MG, Nguyen DH (2010) Immunoglobulin G: a potential treatment to attenuate neuroinflammation following spinal cord injury. J Clin Immunol 30:109–112.

72. Fitch MT, Doller C, Combs CK, Landreth GE, Silver J (1999) Cellular and molecular mechanisms of glial scarring and progressive cavitation: in vivo and in vitro analysis of inflammationinduced secondary injury after CNS trauma. J Neurosci 19(19):8182–8198.

73. Forostyak S, Jendelova P, Sykova E (2013) The role of mesenchymal stromal cells in spinal cord injury, regenerative medicine and possible clinical applications. Biochimie 95:2257-2270.

74. Fouad K, Hurd C, Magnuson DS (2013) Functional testing in animal models of spinal cord injury: not as straight forward as one would think. Front Integr Neurosci 7:85.

75. Franklin RJ, Barnett SC (1997) Do olfactory glia have advantages over Schwann cells for CNS repair? J Neurosci Res 50(5):665-672.

76. Frantz S (2012) Embryonic stem cell pioneer Geron exits field, cuts losses. Nat Biotechnol 30:12–13.

77. Freeman RS, Burch RL, Crowder RJ, Lomb DJ, Schoell MC, Straub JA, Xie L (2004) NGF deprivation-induced gene expression: after ten years, where do we stand? NGF and Related Molecules in Health and Disease. Progress in Brain Research 146:111–126.

78. Freund V, Frossard N (2004) Expression of nerve growth factor in the airways and its possible role in asthma. Progress in Brain Research 146:335–346.

79. Furuya T, Hashimoto M, Koda M, Okawa A, Murata A, Takahashi K, Yamashita T, Yamazaki M (2009) Treatment of rat spinal cord injury with a Rho-kinase inhibitor and bone marrow stromal cell transplantation. Brain Res 1295:192–202.

80. Gao XR, Xu HJ, Wang LF, Liu CB, Yu F (2017) Mesenchymal stem cell transplantation carried in SVVYGLR modified self-assembling peptide promoted cardiac repair and angiogenesis after myocardial infarction. Biochem Biophys Res Commun 491:112–118.

81. Gavet O, Pines J (2010) Progressive Activation of CyclinB1-Cdk1 Coordinates Entry to Mitosis. Developmental Cell 18(4) :533–543.

82. Geller HM, Fawcett JW (2002) Building a bridge: engineering spinal cord repair. Exp Neurol 174:125–136.

83. Glaser J, Gonzalez R, Sadr E, Keirstead HS (2006) Neutralization of the chemokine CXCL10 reduces apoptosis and increases axon sprouting after spinal cord injury. J Neurosci Res 84:724–734.

84. Goldshmit HS (2009) Treatment of acute spinal cord injury by omental transposition: a new approach. J Am Coll Surg 208(2):289–292.

85. Goldshmit Y, Galea MP, Wise G, Bartlett PF, Turnley AM (2004) Axonal regeneration and lack of astrocytic gliosis in EphA4-deficient mice. J Neurosci 24(45):10064–10073.

86. Goldshmit Y, Spanevello MD, Tajouri S, Li L, Rogers F, Pearse M, Galea M, Bartlett PF, Boyd AW, Turnley AM (2011) EphA4 blockers promote axonal regeneration and functional recovery following spinal cord injury in mice. PLoS One 6(9):e24636.

87. Gorrie CA, Hayward I, Cameron N, Kailainathan G, Nandapalan N, Sutharsan R, Wang J, Mackay–Sim A, Waite PM (2010) Effects of human OEC–derived cell transplants in rodent spinal cord contusion injury. Brain Res 1337:8–20.

88. Gronthos S, Brahim J, Li W, Fisher LW, Cherman N, Boyde A, DenBesten P, Robey PG, Shi S (2002) Stem cell properties of human dental pulp stem cells. J Dent Res 81(8):531–535.

89. Gunther MI, Weidner N, Muller R, Blesch A (2015) Cell-seeded alginate hydrogel scaffolds promote directed linear axonal regeneration in the injured rat spinal cord. Acta Biomater 27:140–150.

90. Häfeli UO, Gilmour K, Zhou A, Lee S, Hayden ME (2006) Modeling of magnetic bandages for drug targeting: Button vs. Halbach arrays. J Magn Magn Mater 311:323–329.

91. Hama A, Sagen J (2012) Combination Drug Therapy for Pain following Chronic Spinal Cord Injury. Pain Res Treat 2012:840486.

92. Hamasaki T, Tanaka N, Kamei N, Ishida O, Yanada S, Nakanishi K, Nishida K, Oishi Y, Kawamata S, Sakai N, Ochi M (2007) Magnetically labeled neural progenitor cells, which are localized by magnetic force, promote axon growth in organotypic cocultures. Spine 32:2300–2309.

93. Han YF, Sun TJ, Han YQ, Tao R, Chai JK, Yin HN, Xu G, Liu J (2013) Preparation of microencapsulated VEGF gene-modified human umbilical cord mesenchymal stem cells and in vitro. Eur Rev Med Pharmacol Sci 17(2):217–223.

94. Hao P, Liang Z, Piao H, Ji X, Wang Y, Liu Y et al. (2014) Conditioned medium of human adipose-derived mesenchymal stem cells mediates protection in neurons following glutamate excitotoxicity by regulating energy metabolism and GAP-43 expression. Metab Brain Dis 29:193–205.

95. Hejcl A, Lesny P, Pradny M, Michalek J, Jendelova P, Stulik J, et al. (2008) Biocompatible hydrogels in spinal cord injury repair. Physiol Res 57(3):121–132.

96. Hejcl A, Lesny P, Pradny M, Sedy J, Zamecnik J, Jendelova P et al. (2009) Macroporous hydrogels based on 2-hydroxyethyl methacrylate. Part 6: 3D hydrogels with positive and negative surface charges and polyelectrolyte complexes in spinal cord injury repair. J Mater Sci Mater Med 20:1571–1577.

97. Hejcl A, Ruzicka J, Kapcalova M, Turnovcova K, Krumbholcova E, Pradny M, et al. (2013) Adjusting the chemical and physical properties of hydrogels leads to improved stem cell survival and tissue ingrowth in spinal cord injury reconstruction: a comparative study of four methacrylate hydrogels. Stem Cells Dev 22:2794–2805.

98. Hejcl A, Sedy J, Kapcalova M, Toro DA, Amemori T, Lesny P, et al. (2010) HPMA-RGD hydrogels seeded with mesenchymal stem cells improve functional outcome in chronic spinal cord injury. Stem Cells Dev 19:1535–1546.

99. Hejcl A, Urdzikova L, Sedy J, Lesny P, Pradny M, Michalek J, et al. (2008) Acute and delayed implantation of positively charged 2-hydroxyethyl methacrylate scaffolds in spinal cord injury in the rat. J Neurosurg Spine 8:67–73.

100. Hejčl AJ, Sameš P, Syková M (2015) Experimental treatment of spinal cord injuries. Cesk Slov Neurol N 78(111):377–393.

101. Higginson JR, Barnett SC (2011) The culture of olfactory ensheathing cells (OECs)-a distinct glial cell type. Exp Neurol 229(1):2–9.

102. Hill CE, Proschel C, Noble M, Mayer–Proschel M, Gensel JC, Beattie MS, Bresnahan JC (2004) Acute transplantation of glial–restricted precursor cells into spinal cord contusion injuries: survival, differentiation, and effects on lesion environment and axonal regeneration. Exp Neu-rol 190(2):289–310.

103. Horák D, Hradil H, Lapčíková M, Šlouf M (2008) Superporous poly(2-hydroxyethyl methacrylate) based scaffolds: preparation and characterization. Polymer 49:2046–2054.

104. Horak D, Kroupova J, Slouf M, Dvorak P (2004) Poly(2-hydroxyethyl methacrylate)-based slabs as a mouse embryonic stem cell support. Biomaterials 25:5249–5260.

105. Hou Y, Ryu CH, Jun JA, Kim SM, Jeong CH, Jeun SS (2014) IL-8 enhances the angiogenic potential of human bone marrow mesenchymal stem cells by increasing vascular endothelial growth factor. Cell Biol Int 38:1050–1059.

106. Huang EJ, Reichardt LF (2001) Neurotrophins: roles in neuronal development and function. Annual Review of Neuroscience 24:677–736.

107. Hu J-G, Fu S-L, Wang Y-X, Li Y, Jiang X-Y, Wang X-F, Qiu M-S, Lu P-H, Xu X-M (2008) Platelet-derived growth factor-AA mediates oligodendrocyte lineage

differentiation through activation of extracellular signal-regulated kinase signaling pathway. Neuroscience 151(1):138-147.

108. Fu SL, Hu JG, Li Y, Wang YX, Jin JQ, Xui XM, Lu PH (2007) A simplified method for generating oligodendrocyte progenitor cells from neural precursor cells isolated from the E16 rat spinal cord. Acta Neurobiol Exp (Wars) 67(4):367-377.

109. Hwang DH, Kim BG, Kim EJ, Lee SI, Joo IS, Suh-Kim H, Sohn S, Kim SU (2009) Transplantation of human neural stem cells transduced with Olig2 transcription factor improves locomotor recovery and enhances myelination in the white matter of rat spinal cord following contusive injury. BMC Neurosci 22(10):1–17.

110. Ichim TE, Solano F, Lara F, Paris E, Ugalde F, Rodriguez JP, Minev B, Bogin V, Ramos F, Woods EJ, Murphy MP, Patel AN, Harman RJ, Riordan NH (2010) Feasibility of combination allogeneic stem cell therapy for spinal cord injury: a case report. Int Arch Med 3:30–40.

111. Iida T, Nakagawa M, Asano T, Fukushima C, Tachi K (2006) Free vascularized lateral femoral cutaneous nerve graft with anterolateral thigh flap for reconstruction of facial nerve defects. J Reconstr Microsurg 22:343–348.

112. Inskip JA, Ramer LM, Ramer MS, Krassioukov AV (2009) Autonomic assessment of animals with spinal cord injury: tools, techniques and translation. Spinal Cord 47(1):2–35.

113. Ishizaka S, Hayashi K, Otsuka M, Fukuda S, Tsunoda K, Ushijima R, Kitagawa N, Suyama K, Nagata I (2012) Syringomyelia and arahnoid cysts associated with spinal arachnoiditis following subarachnoid hemorrage. Neurol Med Chir (Tokyo) 52(9):686–690.

114. Jarocha D, Milczarek O, Kawecki Z, Wendrychowicz A, Kwiatkowski S, Majk M (2014) Preliminary study of autologous bone marrow nucleated cells transplantation in children with spinal cord injury. Stem Cells Transl Med 3(3):395–404.

115. Jimenez Hamann MC, Tator CH, Shoichet MS (2005) Injectable intrathecal delivery system for localized administration of EGF and FGF-2 to the injured rat spinal cord. Experimental Neurology 194:106–119.

116. Jin MC, Medress ZA, Azad T D, Doulames VM, Veeravagu A (2019) Stem cell therapies for acute spinal cord injury in humans: a review. Neurosurgical Focus FOC 46(3):E10.

117. Jones LL, Margolis RU, Tuszynski MH (2003) The chondroitin sulfate proteoglycans neurocan, brevican, phosphacan, and versican are differentially regulated following spinal cord injury. Exp. Neurol 182(2):399–411.

118. Kalincik T, Jozefcikova K, Sutharsan R, Mackay-Sim A, Carrive P, Waite PM (2010) Selected changes in spinal cord morphology after T4 transection and olfactory ensheathing cell transplantation. Auton Neurosci 158(1-2):31–38.

119. Kamei G, Kobayashi T, Ohkawa S, Kongcharoensombat W, Adachi N, Takazawa K, Shibuya H, Deie M, Hattori K, Goldberg JL, Ochi M (2013) Articular cartilage repair with magnetic mesenchymal stem cells. Am J Sports Med 41:1255–1264.

120. Kaner T, Karadag T, Cirak B, Erken HA, Karabulut A, Kiroglu Y, Akkaya S, Acar F, Oskun E, Genc O, Colakoglu N (2010) The effects of human umbilical cord blood transplantation in rats with experimentally induced spinal cord injury. J Neurosurg Spine 13(4):543–551.

121. Karamouzian S, Nematollahi–Mahani SN, Nakhaee N, Eskandary H (2012) Clinical safety and primary efficacy of bone marrow mesenchymal cell transplantation in subacute spinal cord injured patients. Clin Neurol Neurosurg 114(7):935–939.

122. Kawano H, Kimura-Kuroda J, Komuta Y, Yoshioka N, Li HP, Kawamura K, Li Y, Raisman G (2012) Role of the lesion scar in the response to damage and repair of the central nervous system. Cell Tissue Res 349:169–171.

123. Keirstead HS (2005) Stem cells for the treatment of myelin loss. Trends Neurosci 28(12):677–683.

124. Kerkis I, Ambrosio CE, Kerkis A, Martins DS, Zucconi E, Fonseca SA, Cabral RM, Maranduba CM, Gaiad TP, Morini AC, Vieira NM, Brolio MP, Sant'Anna OA, Miglino MA, Zatz M (2008) Early transplantation of human immature dental pulp stem cells from baby teeth to golden retriever muscular dystrophy (GRMD) dogs: Local or systemic? J Transl Med 6(35):1–13.

125. Key B, Treloar HB, Wangerek L, Ford MD, Nurcombe V (1996) Expression and localization of FGF–1 in the developing rat olfactory system. J Comp Neurol 366(2):197–206.

126. King NM, Perrin J (2014) Ethical issues in stem cell research and therapy. Stem Cell Res Ther 5(4):85.

127. Kim KN, Oh SH, Lee KH, Yoon DH (2006) Effect of human mesenchymal stem cell transplantation combined with growth factor infusion in the repair of injured spinal cord. Acta Neurochir Suppl 99:133–136.

128. Kirschstein R, Skieboll LR (2001) Stem cells: Scientific Progress and Future Research Directions, National Institute of health, Washington DC.

129. Kleinsmith LJ, Pierce GB Jr (1964) Multipotentiality of Single Embryonal Carcinoma Cells. Cancer Res 1964 24:1544-1551.

130. Ko HY, Ditunno JF, Jr, Graziani V, Little JW (1999) The pattern of reflex recovery during spinal shock. Spinal Cord 37:402–409.

131. Kubinová S, Syková E (2010) Nanotechnologies in regenerative medicine. Minim Invasive Ther Allied Technol 19(3):144-156.

132. Kubinová S, Syková E (2010) Nanotechnology for treatment of stroke and spinal cord injury. Nanomedicine (Lond) 5(1):99-108.

133. Kubinova S, Sykova E (2012) Biomaterials combined with cell therapy for treatment of spinal cord injury. Regen Med 7:207-224.

134. Kubinova S, Horak D, Hejcl A, Plichta Z, Kotek J, Proks V, et al. (2015) SIKVAV-modified highly superporous PHEMA scaffolds with oriented pores for spinal cord injury repair. J Tissue Eng Regen Med 9:1298–1309.

135. Kubinova S, Horak D, Kozubenko N, Vanecek V, Proks V, Price J, et al. (2010) The use of superporous Ac-CGGASIKVAVS-OH-modified PHEMA scaffolds to promote cell adhesion and the differentiation of human fetal neural precursors. Biomaterials 31:5966–5975.

136. Kubinova S, Horak D, Hejcl A, Plichta Z, Kotek J, Sykova E (2011) Highly superporous cholesterol-modified poly(2-hydroxyethyl methacrylate) scaffolds for spinal cord injury repair. Journal of biomedical materials research 99:618.

137. Kubinova S, Horak D, Hejcl A, Plichta Z, Kotek J, Proks V, Forostyak S, Sykova E (2013) SIKVAV-modified highly superporous PHEMA scaffolds with oriented pores for spinal cord injury repair. J Tissue Eng Regen Med 19(9): 2481.

138. Kullander K, Croll SD, Zimmer M, Pan L, McClain J, Hughes V, Zabski S, DeChiara TM, Klein R, Yancopoulos GD, Gale NW (2001) Ephrin-B3 is the midline barrier that prevents corticospinal tract axons from recrossing, allowing for unilateral motor control. Genes Dev 15(7):877–888.

139. Kumar P, Choonara YE, Modi G, Naidoo D, Pillay V (2015) Multifunctional therapeutic delivery strategies for effective neuro-regeneration following traumatic spinal cord injury. Curr Pharm Des 21:1517.

140. Landazuri N, Tong S, Suo J, Joseph G, Weiss D, Sutcliffe DJ, Giddens DP, Bao G, Taylor RW (2013) Magnetic targeting of human mesenchymal stem cells with internalized superparamagnetic iron oxide nanoparticles. Small 9:4017–4026.

141. Lavoie JR, Rosu-Myles M (2013) Uncovering the secretes of mesenchymal stem cells. Biochimie 95:2212–2221.

142. Lee JW, Jergova S, Furmanski O, Gajavelli S, Sagen J (2012) Predifferentiated GABAergic neural precursor transplants for alleviation of dysesthetic central pain following excitotoxic spinal cord injury. Front Physiol 31(3):167–179.

143. Li C, Zhang X, Cao R, Yu B, Liang H, Zhou M, et al. 2012 Allografts of the acellular sciatic nerve and brain-derived neurotrophic factor repair spinal cord injury in adult rats. PLoS One 7:e42813.

144. Li N, Sarojini H, An J, Wang E (2010) Prosaposin in the secretome of marrow stroma-derived neural progenitor cells protects neural cells from apoptotic death. J Neurochem 112:1527–1538.

145. Li Y, Lepski G (2013) Cell Transplantation for Spinal Cord Injury: A Systematic Review. Biomed Res Int 786475:1–32.

146. Li Y, Chen J, Chen XG, Gautam SC, Xu YX, Katakowski M, Zhang LJ, Lu M, Janakiraman N, Chopp M (2002) Human marrow stromal cell therapy for stroke in rat: neurotrophins and functional recovery. Neurology 59(4):514-523.

147. Liu J, Han D, Wang Z, Xue M, Zhu L, Yan H, Zheng X, Guo Z, Wang H (2013) Clinical analysis of the treatment of spinal cord injury with umbilical cord mesenchymal stem cells. Cytotherapy 15:185–191.

148. Liu J, Chen J, Liu B, Yang C, Xie D, Zheng X, et al. (2012) Acellular spinal cord scaffold seeded with mesenchymal stem cells promotes long-distance axon regeneration and functional recovery in spinal cord injured rats. Journal of the neurological sciences 325:127-136.

149. Liu WM, Wu JY, Li FC, Chen QX (2011) Ion channel blockers and spinal cord injury. J Neurosci Res 89(6):791–801.

150. Loy DN, Darnall JB, Burke DA, Onifer SM, Whittemore SR (2002) Temporal progression of angiogenesis and basal lamina deposition after contusive spinal cord injury in the adult rat. J Comp Neurol 445(4):308–324.

151. Lukovic D, Stojkovic M, Moreno-Manzano V, Jendelova P, Sykova E, Bhattacharya SS, Erceg S (2015) Concise review: reactive astrocytes and stem cells in spinal cord injury: good guys or bad guys? Stem Cells 33(4):1036-1041.

152. Lunov O, Syrovets T, Buchele B, Jiang X, Rocker C, Tron K, Nienhaus GU, Walther P, Mailander V, Landfester K, Simmet T (2010) The effect of carboxydextran-coated superparamagnetic iron oxide nanoparticles on c-Jun N-terminal kinase-mediated apoptosis in human macrophages. Biomaterials 31:5063–5071.

153. Lunov O, Syrovets T, Rocker C, Tron K, Nienhaus GU, Rasche V, Mailander V, Landfester K, Simmet T (2010) Lysosomal degradation of the carboxydextran shell of coated superparamagnetic iron oxide nanoparticles and the fate of professional phagocytes. Biomaterials 31:9015–9022.

154. Macaya D, Spector M (2012) Injectable hydrogel materials for spinal cord regeneration: a review. Biomed Mater 7:012001.

155. Marin O, Plump AS, Flames N, Sanchez- Camacho C, Tessier-Lavigne M, Rubenstein JL (2003) Directional guidance of interneuron migration to the cerebral cortex relies on subcortical Slit1/2-independent repulsion and cortical attraction. Development 130:1889–1901.

156. Matsuyama D, Watanabe M, Suyama K, Kuroiwa M, Mochida J (2014) Endoplasmic reticulum stress response in the rat contusive spinal cord injury model - susceptibility in specific cell types. Spinal Cord 52:9–16.

157. McDonaldn JW (2004) Repairing the damaged spinal cord: from stem cells to activity-based restoration therapies. Clin Neurosurg 51:207–227.

158. Medberry CJ, Crapo PM, Siu BF, Carruthers CA, Wolf MT, Nagarkar SP, Agrawal V, Jones KE, Kelly J, Johnson SA, Velankar SS, Watkins SC, Modo M, Badylak SF (2013) Hydrogels derived from central nervous system extracellular matrix. Biomaterials 34 :1033.

159. Meng XT, Li C, Dong ZY, Liu JM, Li W, Liu Y, Xue H, Chen D (2008) Co-transplantation of bFGF-expressing amniotic epithelial cells and neural stem cells promotes functional recovery in spinal cord-injured rats. Cell Biol Int 32(12):1546–1558.

160. Miragall F, Kadmon G, Husmann M, Schachner M (1988) Expression of cell adhesion molecules in the olfactory system of the adult mouse: presence of the embryonic form of N–CAM. Dev Biol 129(2):516–531.

161. Miranda TA, Vicente JM, Marcon RM, Cristante AF, Morya E, Valle AC (2012) Time-related effects of general functional training in spinal cord-injured rats. Clinics (Sao Paulo) 67(7):799–804.

162. Mitsui T, Fischer I, Shumsky JS, Murray M (2005) Transplants of fibroblasts expressing BDNF and NT3 promote recovery of bladder and hindlimb function following spinal contusion injury in rats. Exp Neurol 194(2):410–431.

163. Monfils MH, Driscoll I, Vavrek R, Kolb B, Fouad K (2008) FGF-2-induced functional improvement from neonatal motor cortex injury via corticospinal projections. Exp Brain Res 185(3):453–460.

164. Morsczeck C, Moehl C, Götz W, Heredia A, Schäffer TE, Eckstein N, Sippel C, Hoffmann KH (2005) In vitro differentiation of human dental follicle cells with dexamethasone and insulin. Cell Biol Int 29(7):567–575.

165. Murrell W, Féron F, Wetzig A, Cameron N, Splatt K, Bellette B, Bianco J, Perry C, Lee G, Mackay-Sim A (2005) Multipotent stem cells from adult olfactory mucosa. Dev Dyn 233(2):496–515.

166. Nadvornik P, Zlatos J, Chrastina J (2014) Pathophysiological view of the possible restoration of movement after spinal cord transverse injury. Bratisl Lek Listy 115(2):113–115.

167. Nagoshi N, Okano H (2017) Applications of induced pluripotent stem cell technologies in spinal cord injury. J Neurochem 141(6):848-860.

168. Nakayama KH, Lee CC, Batchelder CA, Tarantal AF (2013) Tissue specificity of decellularized rhesus monkey kidney and lung scaffolds. PLoS One 8:e64134.

169. Narayana PA, Grill RJ, Chacko T, Vang R (2004) Endogenous recovery of injured spinal cord: longitudinal in vivo magnetic resonance imaging. J Neurosci Res 78:749–759.

170. Neuhuber B, Himes BT, Shumsky JS, Gallo G, Fischer I (2005) Axon growth and recovery of function supported by human bone marrow stromal cells in the injured spinal cord exhibit donor variations. Brain Res 1035:73–85.

171. Ning G, Tang L, Wu Q, Li Y, Li Y, Zhang C, Feng S (2013) Human umbilical cord blood stem cells for spinal cord injury: early transplantation results in better local angiogenesis. Regen Med 8(3):271–281.

172. Nishida K, Tanaka N, Nakanishi K, Kamei N, Hamasaki T, Yanada S, Mochizuki Y, Ochi M (2006) Magnetic targeting of bone marrow stromal cells into spinal cord: through cerebrospinal fluid. NeuroReport 17:1269–1272.

173. Nomura H, Baladie B, Katayama Y, Morshead CM, Shoichet MS, Tator CH (2008) Delayed implantation of intramedullary chitosan channels containing nerve grafts

promotes extensive axonal regeneration after spinal cord injury. Neurosurgery 63:127–41.

174. Nomura T, Göritz C, Catchpole T, Henkemeyer M, Frisén J. (2010) EphB signaling controls lineage plasticity of adult neural stem cell niche cells. Cell Stem Cell 7(6):730-743.

175. Nosrat IV, Widenfalk J, Olson L, Nosrat CA (2001) Dental pulp cells produce neurotrophic factors, interact with trigeminal neurons in vitro, and rescue motoneurons after spinal cord injury. Dev Biol 238(1):120–132.

176. Novotna B, Jendelova P, Kapcalova M, Rossner P, Turnovcova K, Bagryantseva Y, Babic M, Horak D, Sykova E (2012) Oxidative damage to biological macromolecules in human bone marrow mesenchymal stromal cells labeled with various types of iron oxide nanoparticles. Toxicol Lett 210:53–63.

177. Oliveira E, Assuncao-Silva RC, Ziv-Polat O, Gomes ED, Teixeira FG, Silva NA, et al. (2017) Influence of different ECM-like hydrogels on neurite outgrowth induced by adipose tissue-derived stem cells. Stem Cells Int 2017:6319129.

178. Oudega M, Xu XM (2006) Schwann cell transplantation for repair of the adult spinal cord. J Neurotrauma 23(3–4):453–467.

179. Oyinbo CA (2011) Secondary injury mechanisms in traumatic spinal cord injury: a nugget of this multiply cascade. Acta Neurobiol Exp 71:281–299.

180. Panseri S, Cunha C, D'Alessandro T, Sandri M, Russo A, Giavaresi G, Marcacci M, Hung CT, Tampieri A (2012) Magnetic hydroxyapatite bone substitutes to enhance tissue regeneration: evaluation in vitro using osteoblast-like cells and in vivo in a bone defect. PLoS One 7:e38710.

181. Papa S, Vismara I, Mariani A, Barilani M, Rimondo S, De Paola M, et al. (2018) Mesenchymal stem cells encapsulated into biomimetic hydrogel scaffold gradually release CCL2 chemokine in situ preserving cytoarchitecture and promoting functional recovery in spinal cord injury. J Control Release 278:49–56.

182. Papanagiotou P (2012) Spinal epidural hematoma. Radiologe 52(5):451–454.

183. Park DH, Lee JH, Borlongan CV, San-berg PR, Chung YG, Cho TH (2011) Transplantation of umbilical cord blood stem cells for treating spinal cord injury. Stem Cell Rev 7:181–194.

184. Park DY, Mayle RE, Smith RL, Corcoran-Schwartz I, Kharazi AI, Cheng I (2013) Combined Transplantation of Human Neuronal and Mesenchymal Stem Cells following Spinal Cord Injury. Global Spine Journal 3(1):1–6.

185. Pego AP, Kubinova S, Cizkova D, Vanicky I, Mar FM, Sousa MM, et al. (2012) Regenerative medicine for the treatment of spinal cord injury: more than just promises? Journal of cellular and molecular medicine 16:2564-2582.

186. Pfeifer K, Vroemen M, Blesch A, Weidner N (2004) Adult neural progenitor cells provide a permissive guiding substrate for corticospinal axon growth following spinal cord injury. Eur J Neurosci 20(7):1695–1704.

187. Pislaru SV, Harbuzariu A, Agarwal G, Witt T, Gulati R, Sandhu NP, Mueske C, Kalra M, Simari RD, Sandhu GS (2006) Magnetic forces enable rapid endothelialization of synthetic vascular grafts. Circulation 114:314–318.

188. Pizzi MA, Crowe MJ (2006) Transplantation of fibroblasts that overexpress matrix metalloproteinase-3 into the site of spinal cord injury in rats. J Neurotrauma 23(12):1750–1765.

189. Pluchino S, Quattrini A, Brambilla E, Gritti A, Salani G, Dina G, Galli R, Del Carro U, et al. (2003) Injection of adult neurospheres induces recovery in a chronic model of multiple sclerosis. Nature 422:688–694.

190. Polyak B, Fishbein I, Chorny M, Alferiev I, Williams D, Yellen B, Friedman G, Levy RJ (2008) High field gradient targeting of magnetic nanoparticle-loaded endothelial cells to the surfaces of steel stents. Proc Natl Acad Sci U.S.A. 105:698–703.

191. Qu J, Zhang H (2017) Roles of mesenchymal stem cells in spinal cord injury. Stem Cells Int 2017:5251313.

192. Ra JC, Shin IS, Kim SH, et al. (2011) Safety of intravenous infusion of human adipose tissue-derived mesenchymal stem cells in animals and humans. Stem Cells Dev 20(8):1297-1308.

193. Ramon-Cueto A, Plant GW, Avila J, Bunge MB (1998) Long-distance axonal regeneration in the transected adult rat spinal cord is promoted by olfactory ensheathing glia transplants. J Neurosci 18(10):3803–3815.

194. Reing JE, Zhang L, Myers-Irvin J, Cordero KE, Freytes DO, Heber-Katz E, et al. (2009) Degradation products of extracellular matrix affect cell migration and proliferation. Tissue engineering Part A 15:605-614.

195. Ren Z, Chen X, Yang J, Kress BT, Tong J, Liu H, Takano T, Zhao Y, Nedergaard M (2013) Improved axonal regeneration after spinal cord injury in mice with conditional deletion of ephrin B2 under the GFAP promoter. Neuroscience 241:89–99.

196. Repin VS, Rzhaninova AA, Shamenkov DA (2002) Embryonic stem cells: fundamental biology and medicine. M Remeteks 184.

197. Ricks CB, Shin SS, Becker C, Grandhi R (2014) Extracellular matrices, artificial neural scaffolds and the promise of neural regeneration. Neural Regen Res 9:1573.

198. Riegler J, Liew A, Hynes SO, Ortega D, O'Brien T, Day RM, Richards T, Sharif F, Pankhurst QA, Lythgoe MF (2013) Superparamagnetic iron oxide nanoparticle targeting of MSCs in vascular injury. Biomaterials 34:1987–1994.

199. Rodrigues LP, Iglesias D, Nicola FC, Stef-fens D, Valentim L, Witczak A, Zanatta G, Achaval M, Pranke P, Netto CA (2012) Transplantation of mononuclear cells from human umbilical cord blood promotes functional recovery after traumatic spinal cord injury in Wistar rats. Braz J Med Biol Res 45(1):49–57.

200. Ronaghi M, Erceg S, Moreno-Manzano V, Stojkovic M (2010) Challenges of stem cell therapy for spinal cord injury: human embryonic stem cells, endogenous neural stem cells, or induced 251 pluripotent stem cells? Stem Cells 28(1):93–99.

201. Rossignol S, Schwab M, Schwartz M, Fehlings MG (2007) Spinal cord injury: time to move? J Neurosci 27(44):11782–11792.

202. Ruzicka J, Romanyuk N, Hejcl A, Vetrik M, Hruby M, Cocks G, et al. (2013) Treating spinal cord injury in rats with a combination of human fetal neural stem cells and hydrogels modified with serotonin. Acta Neurobiol Exp 73:102–15.

203. Satti HS, Waheed A, Ahmed P, Ahmed K, Akram Z, Aziz T (2016) Autologous mesenchymal stromal cell transplantation for spinal cord injury: A Phase I pilot study. Cytotherapy 18:518–522.

204. Schwab ME, Bartholdi D (1996) Degeneration and regeneration of axons in the lesioned spinal cord. Physiol Rev 76:319-370.

205. Shang AJ, Hong SQ, Xu Q, Wang HY, Yang Y, Wang ZF, Xu BN, Jiang XD, Xu RX (2011) NT-3-secreting human umbilical cord mesenchymal stromal cell transplantation for the treatment of acute spinal cord injury in rats. Brain Res 1391:102–113.

206. Shao A, Tu S, Lu J, Zhang J (2019) Crosstalk between stem cell and spinal cord injury: pathophysiology and treatment strategies. Stem Cell Res Ther 10:238.

207. Sheth RN, Manzano G, Li X, Levi AD (2008) Transplantation of human bone marrow-derived stromal cells into the contused spinal cord of nude rats. J Neurosurg Spine 8(2)153–162.

208. Sicari BM, Dziki JL, Siu BF, Medberry CJ, Dearth CL, Badylak SF (2014) The promotion of a constructive macrophage phenotype by solubilized extracellular matrix. Biomaterials 35:8605.

209. Siebert JR, Eade AM, Osterhout DJ (2015) Biomaterial Approaches to Enhancing Neurorestoration after Spinal Cord Injury: Strategies for Overcoming Inherent Biological Obstacles. Biomed Res Int 752572.

210. Simard JM, Popovich PG, Tsymbalyuk O, Caridi J, Gullapalli RP, Kilbourne MJ, Gerzanich V (2013) MRI evidence that glibenclamide reduces acute lesion expansion in a rat model of spinal cord injury. Spinal Cord 51:823–827.

211. Simard JM, Popovich PG, Tsymbalyuk O, Gerzanich V (2012) Spinal cord injury with unilateral versus bilateral primary hemorrhage-effects of glibenclamide. Exp Neurol 233(2):829–835.

212. Simard JM, Gerzanich V (2012) When replication teaches more than the original experiment - the saga of the unknown unknown. Exp Neurol 233(2): 623–624.

213. Slivka PF, Dearth CL, Keane TJ, Meng FW, Medberry CJ, Riggio RT, Reing JE, Badylak SF (2014) Fractionation of an ECM hydrogel into structural and soluble components reveals distinctive roles in regulating macrophage behavior. Biomater SciUk 2:1521.

214. Smith JA, Park S, Krause JS, Banik NL (2013) Oxidative stress, DNA damage, and the telomeric complex as therapeutic targets in acute neurodegeneration. Neurochem Int 62(5):764–775.

215. Sosa I, Reyes O, Kuffler DP (2005) Immunosuppressants: neuroprotection and promoting neurological recovery following peripheral nerve and spinal cord lesions. Exp Neurol 195:7.

216. Soubeyrand M, Laemmel E, Dubory A, Vicaut E, Court C, Duranteau J (2012) Real-time and spatial quantification using contrastenhanced ultrasonography of spinal cord perfusion during experimental spinal cord injury. Spine (Phila Pa 1976) 37(22):1376–1382.

217. Stem cell technology: current applications and future directions. BCC Research. New York, 2008.

218. Stewart AN, Matyas JJ, Welchko RM, Goldsmith AD, Zeiler SE, Hochgeschwender U, et al. (2017) SDF-1 overexpression by mesenchymal stem cells enhances GAP-43-positive axonal growth following spinal cord injury. Restor Neurol Neurosci 35:395–411.

219. Sun W, Sun C, Lin H, Zhao H, Wang J, Ma H, Chen B, Xiao Z, Dai J (2009) The effect of collagen-binding NGF-beta on the promotion of sciatic nerve regeneration in a rat sciatic nerve crush injury model. Biomaterials. 30(27):4649–4656.

220. Syková E, Homola A, Mazanec R, Lachmann H, Konrádová SL, Kobylka P, Pádr R, Neuwirth J, Komrska V, Vávra V, Stulík J, Bojar M (2006) Autologous bone marrow transplantation in patients with subacute and chronic spinal cord injury. Cell Transplant 15(8-9):675-687.

221. Sykova E, Cizkova D, Kubinova S (2021) Mesenchymal Stem Cells in Treatment of Spinal Cord Injury and Amyotrophic Lateral Sclerosis. Front Cell Dev Biol 6(9):695900.

222. Sykova E, Forostyak S (2013) Stem cells in regenerative medicine. Laser Ther 22(2):87–92.

223. Sykova E, Jendelova P, et al. (2006) Bone marrow stem cells and polymer hydrogels-two strategies for spinal cord injury repair. Cell Mol Neurobiol 26(7–8):1113–1129.

224. Sykova E, Jendelova P *(*2007) *In vivo* tracking of stem cells in brain and spinal cord injury. II Program of Brain Research (161):367383.

225. Sykova E, Jendelova P (2007) Migration, fate and *in vivo* imaging of adult stem cells in the CNS. Cell Death and Differentiation 14(7):1336-1342.

226. Tashiro K, Sephel GC, Weeks B, Sasaki M, Martin GR, Kleinman HK (1989) A synthetic peptide containing the IKVAV sequence from the A chain of laminin mediates cell attachment, migration, and neurite outgrowth. J Biol Chem 264:16174–16182.

227. Tester NJ, Howland DR (2008) Chondroitinase ABC improves basic and skilled locomotion in spinal cord injured cats. Exp Neurol 209:483-496.

228. Torres-Espin A, Santos D, Gonzalez-Perez F, del Valle J, Navarro X (2014) Neurite-J: an image-J plug-in for axonal growth analysis in organotypic cultures. Journal of neuroscience methods 236:26.

229. Totoiu MO, Keirstead HS (2005) Spinal cord injury is accompanied by chronic progressive demyelination. J Comp Neurol 486(4):373–383.

230. Tottey S, Corselli M, Jeffries EM, Londono R, Peault B, Badylak SF (2011) Extracellular matrix degradation products and low-oxygen conditions enhance the regenerative potential of perivascular stem cells. Tissue Eng Part A 17:37.

231. Tu J, Liao J, Stoodley MA, Cunningham AM (2011) Reaction of endogenous progenitor cells in a rat model of posttraumatic syringomyelia. J Neurosurg Spine 14(5):573–582.

232. Tuszynski MH, Blesch A (2004) Nerve growth factor: from animal models of cholinergic neuronal degeneration to gene therapy in Alzheimer's disease. Progress in Brain Research 146:441–49.

233. Tyler JY, Xu XM, Cheng JX (2013) Nanomedicine for treating spinal cord injury. Nanoscale 5:8821–8836.

234. Tysseling VM, Sahni V, Pashuck ET, Birch D, Hebert A, Czeisler C, et al. (2010) Self-assembling peptide amphiphile promotes plasticity of serotonergic fibers following spinal cord injury. J Neurosci Res 88:3161–3170.

235. Tysseling-Mattiace VM, Sahni V, Niece KL, Birch D, Czeisler C, Fehlings MG, et al. (2008) Self-assembling nanofibers inhibit glial scar formation and promote axon elongation after spinal cord injury. J Neurosci 28:3814–3823.

236. Urdzikova L, Jendelova P, Glogarova K, Burian M, Hajek M, Sykova E (2006) Transplantation of bone marrow stem cells as well as mobilization by granulocyte-colony stimulating factor promotes recovery after spinal cord injury in rats. Journal of neurotrauma 23:1379-1391.

237. Valentin JE, Stewart-Akers AM, Gilbert TW, Badylak SF (2009) Macrophage participation in the degradation and remodeling of extracellular matrix scaffolds. Tissue Eng Part A 15:1687.

238. Vandergriff AC, Hensley TM, Henry ET, Shen DL, Anthony S, Zhang JY, Cheng K (2014) Magnetic targeting of cardiosphere-derived stem cells with ferumoxytol nanoparticles for treating rats with myocardial infarction. Biomaterials 35:8528–8539.

239. Vanecek V, Zablotskii V, Forostyak S, Ruzicka J, Herynek V, Babic M, Jendelova P, Kubinova S, Dejneka A, Sykova E (2012) Highly efficient magnetic targeting of mesenchymal stem cells in spinal cord injury. Int J Nanomed 7:3719–3730.

240. Vanicky I, Urdzikova L, Saganova K, Cizkova D, Galik J (2001) A simple and reproducible model of spinal cord injury induced by epidural balloon inflation in the rat. Journal of neurotrauma 18:1399-1407.

241. Varma AK, Das A, Wallace G, Barry J, Vertegel AA, Ray SK, Banik NL (2013) Spinal cord injury: a review of current therapy, future treatments, and basic science frontiers. Neurochem Res 38(5):895–905.

242. Vinay S, Khan SK, Braybrooke JR (2011) Lumbar vertebral haemangioma causing pathological fracture, epidural haemorrhage, and cord compression: a case report and review of literature. The Journal of Spinal Cord Medicine 34(3):335–339.

243. Vroemen M, Aigner L, Winkler J, Weidner N (2003) Adult neural progenitor cell grafts survive after acute spinal cord injury and integrate along axonal pathways. Eur J Neurosci 18(4):743–751.

244. Wang C, Poon S, Murali S, Koo CY, Bell TJ, Hinkley SF, et al. (2014) Engineering a vascular endothelial growth factor 165-binding heparan sulfate for vascular therapy. Biomaterials 35:6776–6786.

245. Wang KC, Kim JA, Sivasankaran R, Segal R, He Z (2002) p75 interacts with the Nogo receptor as a co-receptor for Nogo, MAG and OMgp. Nature 420(6911):74–78.

246. Wang ZY, Liu WG, Muharram A, Wu ZY, Lin JH (2014) Neuroprotective Effects of Autophagy Induced by Rapamycin in Rat Acute Spinal Cord Injury Model. Neuroimmunomodulation 21(5) 257–267.

247. Weissman IL (2000) Translating stem and progenitor cell biology to the clinic: barriers and opportunities. Science 287:1442–1446.

248. Wolf MT, Daly KA, Brennan-Pierce EP, Johnson SA, Carruthers CA, D'Amore A, Nagarkar SP, Velankar SS, Badylak SF (2012) A hydrogel derived from decellularized dermal extracellular matrix. Biomaterials 33:7028.

249. Woodhall E, West AK, Chuah MI (2001) Cultured olfactory ensheathing cells express nerve growth factor, brain–derived neurotrophic factor, glia cell line–derived neurotrophic factor and their receptors. Brain Res Mol Brain Res 88(1–2):203–213.

250. Wright KT, Masri WE, Osman A, Chowdhury J, Johnson WE (2011) Concise review: Bone marrow for the treatment of spinal cord injury: mechanisms and clinical applications. Stem Cells 29(2):169–178.

251. Wu SF, Suzuki Y, Kitada M, Kataoka K, Kitaura M, Chou H, Nishimura Y, Ide C (2002) New method for transplantation of neurosphere cells into injured spinal cord through cerebrospinal fluid in rat. Neurosci Lett 318:81–84.

252. Xue H, Zhang XY, Liu JM, Song Y, Li YF, Chen D (2013) Development of a chemically extracted acellular muscle scaffold seeded with amniotic epithelial cells to promote spinal cord repair. Journal of biomedical materials research 101:145-156.

253. Yanai A, Hafeli UO, Metcalfe AL, Soema P, Addo L, Gregory-Evans CY, Po K, Shan X, Moritz OL, Gregory-Evans K (2012) Focused magnetic stem cell targeting to the retina using superparamagnetic iron oxide nanoparticles. Cell Transplant 21:1137–1148.

254. Yang EZ, Zhang GW, Xu JG, Chen S, Wang H, Cao LL, et al. (2017) Multichannel polymer scaffold seeded with activated Schwann cells and bone mesenchymal stem cells improves axonal regeneration and functional recovery after rat spinal cord injury. Acta Pharmacol Sin 38:623–637.

255. Young W (2014) Spinal cord regeneration. Cell Transplant 23(4):573–611.

256. Zablotskii V, Pastor JM, Larumbe S, Pérez-Landazábal JI, Recarte V, Gómez-Polo C (2010) AIP Conf Proc 1311:152–157.

257. Zhang H, Vutskits L, Pepper MS, Kiss JZ (2003) VEGF is a chemoattractant for FGF-2–stimulated neural progenitors. The Journal of Cell Biology 163(6):1375–1384.

258. Zhang W, Yan Q, Zeng YS, Zhang XB, Xiong Y, Wang JM, Chen SJ, Li Y, Bruce IC, Wu W (2010) Implantation of adult bone marrow-derived mesenchymal stem cells transfected with the neurotrophin-3 gene and pretreated with retinoic acid in completely transected spinal cord. Brain Res 1359:256–271.

259. Zhang XY, Xue H, Liu JM, Chen D (2011) Chemically extracted acellular muscle: a new potential scaffold for spinal cord injury repair. Journal of biomedical materials research 100:578-587.

260. Zheng B, Ho C, Li S, Keirstead H, Steward O, Tessier-Lavigne M (2003) Lack of enhanced spinal regeneration in Nogo-deficient mice. Neuron 38:213–224.

9. LIST OF AUTHOR'S PUBLICATIONS

Original scientific works in extenso, which are the basis of the dissertation (with impact factor):

1. Tukmachev D, Lunov O, Zablotskii V, Dejneka A, Babic M, Syková E, Kubinová Š (2015) An effective strategy of magnetic stem cell delivery for spinal cord injury therapy. Nanoscale 7(9):3954-3958. **(IF 7.4)**

2. Tukmachev D, Forostyak S, Koci Z, Zaviskova K, Vackova I, Vyborny K, Sandvig I, Sandvig A, Medberry CJ, Badylak SF, Sykova E, Kubinova S (2016) Injectable Extracellular Matrix Hydrogels as Scaffolds for Spinal Cord Injury Repair. Tissue Eng Part A 22(3-4):306-317. **(IF 4.45)**

3. Hejčl A, Růžička J, Proks V, Mackova H, Kubinova S, Tukmachev D, Jiří C, Horák D, Jendelová P (2018) Dynamics of tissue ingrowth in SIKVAV-modified highly superporous PHEMA scaffolds with oriented pores after bridging a spinal cord transection. Materials in Medicine 29(7):89. **(IF 2.45)**

4. Zaviskova K, Tukmachev D, Dubisova J, Vackova I, Hejcl A, Bystronova J, Pravda M, Scigalkova I, Sulakova R, Velebny V, Wolfova L, Kubinova S (2018) Injectable hydroxyphenyl derivative of hyaluronic acid hydrogel modified with RGD as scaffold for spinal cord injury repair. J Biomed Mater Res A 106(4):1129-1140. **(IF 3.23)**